

# **MOLECULAR REGULATION OF SKELETAL MUSCLE MYOSIN HEAVY CHAIN ISOFORMS**

**DAVID M. BROWN (BSc, Hons)**

Thesis submitted to The University of Nottingham for the degree of Doctor of  
Philosophy, September 2014

Division of Nutritional Sciences  
School of Biosciences  
University of Nottingham  
Sutton Bonington Campus  
Leicestershire  
England

*“Science is a way of thinking much more than it is a  
body of knowledge”*

Carl Sagan



## ABSTRACT

Research investigating the regulation of muscle fibre type has traditionally been conducted *in vivo*, analyzing global changes at a whole muscle level. Broadly, this thesis aimed to explore more “molecular” approaches, utilizing *in vitro* cell biology and molecular biology to understand the expression and regulation of myosin heavy chain (MyHC) isoforms as an indicator of muscle fibre composition. Improving our understanding of the fundamental biology controlling MyHC isoform expression is important since these proteins are key determinants of the contractile and metabolic characteristics of the muscle fibre; influencing locomotion, metabolism and age related musculoskeletal diseases (Schiaffino and Reggiani 2011). Furthermore, establishing whether muscle fibre type research can be conducted using molecular and cell biology-based approaches, may encourage more extensive work to be conducted by such methods and advance our molecular understanding of muscle fibre type regulation.

The mRNA expression profile of six MyHC isoform genes during C2C12 myogenesis was elucidated to reveal that the C2C12 cell line mimics developing fast-twitch muscle fibres. Specifically, MyHC mRNA isoforms were expressed in a distinct temporal pattern as two distinct cohorts. MyHC emb, neo and type I expression was up-regulated during early differentiation (day 1/2) and their expression was subsequently down-regulated after 4 to 6 days in culture ( $p<0.001$ ). MyHC IIA, IIX and IIB, on the other hand, were expressed later in differentiation and their expression continued to increase to day 8 ( $p<0.001$ ). These results provide important information for future

research conducted using this cell line and suggest that the C2C12 cell line may be a good model for studying MyHC regulation *in vitro*.

The dynamic plasticity of MyHC isoform gene expression was then compared between C2C12 muscle cells and fully differentiated adult muscle. Exposure of adult muscle to the beta-adrenergic agonist, Ractopamine, induced dynamic transitions in MyHC isoform expression, from the IIA/IIX isoforms to increased IIB isoform expression ( $p < 0.05$  for all genes). Interestingly, an acute exposure of C2C12 muscle cells to Ractopamine was capable of inducing an exclusive and rapid induction of the MyHC IIB isoform gene expression during myogenesis ( $p < 0.001$ ). This work highlights that MyHC isoform expression is malleable in the C2C12 muscle cells during myogenesis and suggests that the C2C12 cell line is a useful model for studying MyHC gene regulation. Furthermore, this work reports a role for beta-adrenergic signaling in the transcriptional regulation of MyHC IIB during two developmental distinct stages of muscle growth.

Additional characterization of the C2C12 cell line revealed a dramatic restructuring of metabolic gene expression during the switch from proliferating to fully differentiated C2C12 muscle cells. Specifically, the changes in metabolic gene expression suggest that post-mitotic muscle cells might redirect glucose carbons into ATP generating pathways and away from macromolecule biosynthesis. In addition, post-mitotic muscle cells exhibited increased glycolytic gene expression and reduced oxidative gene expression ( $p < 0.01$  for all genes). These transitions in metabolic gene expression during myogenesis provide important information worthy of consideration when utilizing the C2C12 cell for muscle biology research. Furthermore, this work suggests a

potential role for very specific metabolic profiles to support, or even regulate, distinct stages of myogenic differentiation.

Finally, the C2C12 cell line was utilized as a host environment for a molecular-based approach to understand the role of the promoter sequence in regulating the species-differential induction of the MyHC IIB gene during myogenesis. Herein, a 3bp miss-match in the CArG-Ebox region (at -74bp, -68bp and -48bp) of the proximal MyHC IIB promoter was identified that dictates the differential expression of MyHC IIB in pigs and humans. This work demonstrates a molecular mechanism regulating a major physiological difference in the muscle phenotype between pigs and humans. The successful use of the C2C12 cell line as a MyHC IIB expressing environment shows that the C2C12 cell line is a useful tool for molecular and cell biology approaches to explore the regulation of MyHC isoforms. The genomic mechanism identified herein provides important information for understanding the pig as a model of human muscle biology research.

In summary, this thesis reports novel information regarding the regulation of MyHC isoform expression, using molecular and cell biology techniques. The use of molecular-based approaches may help further elucidate mechanisms regulating MyHC genes. An improved understanding of the regulation of MyHC isoforms is important given their critical role in dictating the contractile and metabolic characteristics of the muscle fibre.

## **ACKNOWLEDGEMENTS**

I'd like to start by thanking my supervisors, Dr John Brameld and Dr Tim Parr, for giving me the opportunity to conduct my PhD under your supervision on this BBSRC-CASE studentship. It has been a fantastic few years. Your guidance and support have enabled me to learn and develop the attributes to become a scientist, to which I am forever grateful. Working under your supervision has further boosted my enthusiasm for a career in scientific research, so thank you very much. In addition, thank you for the amazing travel and networking opportunities that have arisen due to your generosity, encouragement and organization. In particular, thank you for supporting my attendance to international conferences in Italy, America, and Austria, a collaboration meeting in China and a 6-month industrial placement at Pfizer Animal Health in Michigan, USA.

I'd like to say a huge thank you to the technicians, Zoe Daniel, Cathy Wells and Kirsty Jewell, for training me in molecular and cell biology techniques. In addition, thank you for always being there for me - your knowledge, support and sense of humour was fundamental to the completion of my projects.

Thank you to all my friends in the postgrad office for making such a fun and friendly environment to "work" in. I've had such a great time with all of you and I appreciate all your support.

I would like to thank David Thompson, Camille Daniel, Tracey Williams and Scott Brown for organizing my placement at Pfizer Animal Health (Michigan,

USA). It was due to your hard work and organization that this placement was possible so I am very grateful for what turned out to be such a wonderful life experience. I would also like to thank the Pfizer Biomolecular Technologies Lab members, Troy, Doug, Eric, Tom, Janet, Chris and Greg, for such an amazing time in their lab during my 6-month placement at Pfizer Animal Health. You all taught me so much and really made me feel like part of the team. This experience was incredibly valuable for my future in scientific research, so thank you all very much. I would also like to thank my friends, Jake, Brooks, Jenn and Matt for making my stay in America so fun filled and sending me home with lots of great memories.

I'd like to say a big thank you to Zoe, Trevor and Leslie for letting me stay in their lovely home for the latter half of my PhD and providing such a friendly environment to live and work.

I'd like to thank my girlfriend, Rabea Loczenski, for all your support and encouragement in the run up to finishing my PhD. Your positive attitude has been so energizing during the last few months of writing, so thank you for everything.

Finally, I'd like to say a huge thank you to my family for their endless support and encouragement throughout my PhD. Thank you for always being there and for listening to me ramble on about "science".

## LIST OF PUBLICATIONS

Some of the work reported in this thesis has been presented elsewhere:

Brown, D.M., Parr, T. and Brameld, J.M. (2012) Myosin heavy chain mRNA isoforms are expressed in two distinct cohorts during C2C12 myogenesis. *J Muscle Res Cell Motil* 32(6), 383-390

Brown, D.M., Brameld, J.M. and Parr, T. (2014) Expression of the Myosin Heavy Chain IIB Gene in Porcine Skeletal Muscle: The Role of the CArG-box Promoter Response element. (In Press, *PLoS ONE*)

## TABLE OF CONTENTS

<b>1. INTRODUCTION</b>	<b>1</b>
1.1 Skeletal muscle	2
1.2 Myogenesis: the formation of muscle fibres	2
1.3 Muscle fibre heterogeneity	4
1.4 The muscle sarcomere and the myosin heavy chain isoforms	8
1.5 Myosin heavy chain	10
1.6 Contraction of the sarcomere	10
1.7 Myosin heavy chain isoforms and contractile kinetics	12
1.8 The Myosin heavy chain gene family	13
1.9 Myosin heavy chain isoform expression	15
1.10 Species-differential expression of myosin heavy chain IIB	17
1.11 Postnatal transitions in myosin heavy chain expression	20
1.12 Molecular regulation of myosin heavy chain expression	22
1.13 Regulation of the slow myosin heavy chain isoforms	23
1.14 Regulation of the fast myosin heavy chain isoforms	25
1.15 Bi-directional promoters in myosin heavy chain gene clusters	28
1.16 Intronic miRNA's in myosin heavy chain gene regulation	29
1.17 Myosin heavy chain promoter response elements	30
1.18 Summary and objectives of this thesis	32
 <b>2. MATERIALS AND METHODS</b>	 <b>36</b>
2.1 CELL CULTURE	37
2.1.1 Overview	37
2.1.2 Culturing C2C12 cells	37
2.1.3 Passaging cells	38
2.1.4 Counting cells	38
2.1.5 Freezing cells	39
2.1.6 Measuring myotube diameters	39
2.1.7 Lowry assay - measurement of total protein content	41
2.1.8 Creatine kinase assay: marker of differentiation	42
2.1.9 DNA assay: marker of cell number	42
2.2 GENE EXPRESSION ANALYSIS	43
2.2.1 Overview	43
2.2.2 RNA extraction from cells	43
2.2.3 RNA extraction from porcine skeletal muscle	44
2.2.4 RNA integrity check	45
2.2.5 cDNA synthesis (Using Promega reagents)	45
2.2.6 cDNA synthesis (using Roche reagents)	46
2.2.7 Quantitative RT-PCR	47
2.2.8 Testing primers used for quantitative RT-PCR	48
2.2.9 Oligreen quantification of total cDNA	50
2.3 SDS-PAGE OF MYOSIN HEAVY CHAIN ISOFORMS	51
2.3.1 Overview	51

2.3.2 <i>Myosin heavy chain protein extraction</i>	51
2.3.3 <i>Sample preparation</i>	51
2.3.4 <i>SDS-PAGE gel composition</i>	52
2.3.5 <i>SDS-PAGE</i>	53
2.3.6 <i>Fixing and staining gels</i>	53
2.4 MOLECULAR BIOLOGY METHODS	54
2.4.1 <i>Overview</i>	54
2.4.2 <i>Experimental design summary</i>	54
2.4.3 <i>Extraction of genomic DNA from tissue and blood</i>	54
2.4.4 <i>Identification of the MyHC IIB promoter</i>	56
2.4.5 <i>PCR of the MyHC IIB promoter from genomic DNA</i>	56
2.4.6 <i>Spin column purification of PCR amplicons</i>	60
2.4.7 <i>Restriction endonuclease digestion</i>	61
2.4.8 <i>Gel purification of promoter and host plasmid</i>	64
2.4.9 <i>Ligation of the promoter into the host plasmid</i>	65
2.4.10 <i>Transformation of JM109 competent E-coli</i>	67
2.4.11 <i>Colony selection for plasmid expansion</i>	68
2.4.12 <i>Small scale plasmid extraction</i>	69
2.4.13 <i>Confirming successful cloning</i>	70
2.4.14 <i>DNA sequencing</i>	71
2.4.15 <i>The Sanger DNA sequencing method</i>	72
2.4.16 <i>Large-scale, endotoxin-free plasmid preparations</i>	76
2.4.17 <i>Five prime deletion of the MyHC IIB promoters</i>	77
2.4.18 <i>Pig-human chimeric promoter constructs</i>	77
2.4.19 <i>Site directed mutagenesis by PCR</i>	80
2.4.20 <i>Site directed mutagenesis of MyHC IIB promoter</i>	82
2.4.21 <i>Electrophoretic mobility shift assay (EMSA)</i>	83
2.4.22 <i>Producing double stranded EMSA probes</i>	84
2.4.23 <i>C2C12 nuclear protein extracts</i>	85
2.4.24 <i>EMSA binding reactions</i>	86
2.4.25 <i>Detection of protein-DNA complexes</i>	86
2.4.26 <i>Transfection of C2C12 myoblasts</i>	90
2.4.27 <i>Cloning murine MyoD cDNA</i>	93
2.4.28 <i>Generating a pDsRed-Express-N1 vehicle transfection control - Klenow Large Polymerase blunt-ending</i>	95



<b>3. CHARACTERIZATION OF THE C2C12 CELL LINE FOR MYOSIN HEAVY CHAIN STUDIES</b>	<b>97</b>
3.1 CHARACTERIZING C2C12 MYOGENESIS AND THE ENDOGENOUS TRANSITIONS IN MYOSIN HEAVY CHAIN ISOFORM EXPRESSION	98
3.1.1 INTRODUCTION	98
3.1.2 MATERIALS AND METHODS	99
3.1.2.1 <i>Cell culture</i>	99
3.1.2.2 <i>Cell harvest</i>	99
3.1.2.3 <i>DNA, Creatine Kinase and protein quantification assay</i>	100
3.1.2.4 <i>Quantitative RT-PCR</i>	100
3.1.2.5 <i>Mouse MyHC primer test</i>	101
3.1.2.6 <i>Statistical analysis</i>	102
3.1.3 RESULTS	103
3.1.3.1 <i>Proliferation</i>	103
3.1.3.2 <i>Differentiation</i>	104
3.1.3.3 <i>Myoblast fusion to form myotubes</i>	106
3.1.3.4 <i>RNA yield from proliferating myoblasts and differentiating myotubes</i>	107
3.1.3.5 <i>Myogenic regulatory factor (MRF) mRNA expression</i>	108
3.1.3.6 <i>Myosin Heavy Chain mRNA expression</i>	110
3.1.3.7 <i>Myosin Heavy Chain I promoter activity in C2C12's</i>	111
3.1.4 DISCUSSION	113
3.2 TRANSITIONS IN METABOLIC GENE EXPRESSION DURING C2C12 MYOGENESIS – ASSOCIATION WITH MYOSIN HEAVY CHAIN GENE EXPRESSION	121
3.2.1 INTRODUCTION	121
3.2.2 MATERIALS AND METHODS	124
3.2.2.1 <i>Cell culture</i>	124
3.2.2.2 <i>Cell harvest and RNA analysis</i>	124
3.2.2.3 <i>Oligonucleotide primers</i>	124
3.2.2.4 <i>Statistical analysis</i>	126
3.2.3 RESULTS	127
3.2.3.1 <i>Glycolytic enzyme gene expression</i>	127
3.2.3.2 <i>Mitochondrial enzyme gene expression</i>	128
3.2.3.3 <i>G6PDH gene expression: nucleotide biosynthesis pathway</i>	129
3.2.3.4 <i>PHGDH, PSAT1 and PSPH: The serine biosynthesis pathway</i>	129
3.2.3.5 <i>Pyruvate kinase 1/2 splice variant switching</i>	130
3.2.3.6 <i>Gene expression of enzymes involved in gluconeogenesis</i>	131
3.2.3.7 <i>Summary of the metabolic gene expression</i>	132
3.2.4 DISCUSSION	134

<b>4. BETA-ADRENERGIC SIGNALLING AND MYOSIN HEAVY CHAIN IIB GENE EXPRESSION</b>	<b>140</b>
4.1 BETA-ADRENERGIC AGONIST, RACTOPAMINE, INDUCES EXPRESSION OF THE MYOSIN HEAVY CHAIN IIB GENE IN GROWING PIGS	141
4.1.1 INTRODUCTION	141
4.1.2 MATERIALS AND METHODS	144
4.1.2.1 <i>Experimental design</i>	144
4.1.2.2 <i>Time course of drug administration</i>	144
4.1.2.3 <i>Animal growth and tissue collection</i>	145
4.1.2.4 <i>Total RNA extraction and cDNA synthesis</i>	145
4.1.2.5 <i>Quantitative-RT-PCR</i>	145
4.1.2.6 <i>Myosin heavy chain primers</i>	146
4.1.2.7 <i>Other oligonucleotide primers</i>	147
4.1.2.8 <i>SDS-PAGE separation of MyHC isoforms</i>	148
4.1.2.9 <i>Statistical analysis</i>	149
4.1.3 RESULTS	150
4.1.3.1 <i>Growth performance</i>	151
4.1.3.2 <i>Myosin heavy chain mRNA expression</i>	152
4.1.3.3 <i>Myosin heavy chain protein expression</i>	154
4.1.3.4 <i>Metabolic gene expression</i>	155
4.1.3.5 <i>Correlation between metabolic and MyHC expression</i>	156
4.1.3.6 <i>PGC-1<math>\alpha</math> and RIP-140 mRNA expression</i>	159
4.1.3.7 <i>Myogenic regulatory factor expression</i>	160
4.1.3.8 <i>Six1 and Eya1 mRNA expression</i>	161
4.1.3.9 <i>Summary of in vivo findings</i>	162
4.2 BETA-ADRENERGIC AGONIST, RACTOPAMINE, ACTS DIRECTLY ON MUSCLE CELLS TO ACCELERATE THE INDUCTION OF THE MYOSIN HEAVY CHAIN IIB GENE DURING C2C12 MYOGENESIS	163
4.2.1 INTRODUCTION	163
4.2.2 MATERIALS AND METHODS	166
4.2.2.1 <i>Overview</i>	166
4.2.2.2 <i>Cell culture</i>	166
4.2.2.3 <i>Treatments</i>	166
4.2.2.4 <i>Cell harvest for growth assays</i>	167
4.2.2.5 <i>Cell harvest for RNA extraction</i>	167
4.2.2.6 <i>cDNA synthesis and Quantitative-RT-PCR</i>	168
4.2.2.7 <i>Quantitative-RT-PCR primers</i>	168
4.2.2.8 <i>Porcine 1kb MyHC IIB promoter-reporter</i>	169
4.2.2.9 <i>Statistical analysis</i>	170
4.2.3 RESULTS	171
4.2.3.1 <i>Light microscopy</i>	171

4.2.3.2 Proliferation, differentiation and protein accretion	172
4.2.3.3 Myogenic regulatory factor expression	173
4.2.3.4 Myosin heavy chain mRNA expression	174
4.2.3.5 Metabolic gene expression	176
4.2.3.6 Beta-adrenergic receptor 2 ( $\text{Ad}\beta 2$ ) mRNA expression	177
4.2.3.7 <i>Six1</i> and <i>Eya1</i> mRNA expression	178
4.2.3.8 Porcine MyHC IIB promoter activation	179
4.2.3.9 Porcine 1kb MyHC IIB promoter lacks cAMP response elements (CRE)	181
4.2.4 DISCUSSION	183
4.2.4.1 Ractopamine induces differential regulation of MyHC isoforms in vivo compared to in vitro	183
4.2.4.2 Ractopamine altered in vivo but not in vitro metabolic gene expression	186
4.2.4.3 Ractopamine increased <i>Six1</i> and <i>Eya1</i> mRNA expression in fusing muscle cells only	187
4.2.4.4 Increased MyHC IIB mRNA expression was independent of changes in cellular differentiation, growth and myogenic gene expression	189
4.2.4.5 Conclusion	191

## 5. REGULATION OF THE MYOSIN HEAVY CHAIN IIB GENE IN PORCINE SKELETAL MUSCLE 192

5.1 TRANSCRIPTIONAL REGULATION OF THE MYOSIN HEAVY CHAIN IIB GENE IN PORCINE SKELETAL MUSCLE: A COMPARISON OF PIG AND HUMAN GENE PROMOTER ACTIVITIES	193
5.1.1 INTRODUCTION	193
5.1.2 MATERIALS AND METHODS	196
5.1.2.1 Cloning	196
5.1.2.2 Electrophoretic mobility shift assay	197
5.1.2.3 Cell culture and transfections	198
5.1.2.4 dbcAMP on myotube diameters	199
5.1.2.5 Statistical analysis	199
5.1.3 RESULTS	200
5.1.3.1 The pig and human MyHC IIB promoter sequence	200
5.1.3.2 Pig and human MyHC IIB promoter activity	201
5.1.3.3 MyoD activates the pig and human MyHC IIB promoter	203
5.1.3.4 Five prime deletion of the pig and human MyHC IIB promoter	204
5.1.3.5 Chimeric MyHC IIB promoters	205
5.1.3.6 Site directed mutagenesis of the human MyHC IIB promoter	207

5.1.3.7 Site directed mutagenesis (round 2) of the human MyHC IIB promoter	209
5.1.3.8 Electrophoretic mobility shift assay of the CArG/Ebox region	211
5.1.3.9 Removal of the CArG-box region from pig and human MyHC IIB promoters	212
5.1.3.10 Summary of genomic differences	214
5.1.3.11 Induction of MyHC IIB promoter with cAMP	215
5.1.4 DISCUSSION	217
<b>6. CONCLUSIONS AND FUTURE WORK</b>	223
6.1 FINAL CONCLUSIONS AND DIRECTIONS FOR FUTURE WORK	224
6.1.1 Characterization and exploration of MyHC isoform gene expression	225
6.1.2 Metabolic gene expression of proliferating and differentiated C2C12 cells	227
6.1.3 Regulation of the MyHC IIB gene in porcine skeletal muscle	229
6.1.4 Final summary of novel findings from this thesis	232
<b>7. REFERENCES</b>	233

## LIST OF FIGURES

**Figure 1.1** A schematic diagram detailing the process of myogenesis, from Jang et al. (2013)

**Figure 1.2** Muscle fibre type characteristics, from Gundersen (2011)

**Figure 1.3** Each skeletal muscle fibre contains a collection of myofibrils, which contain the sarcomere structures

**Figure 1.4** A schematic diagram of the muscle sarcomere and a respective comparison to an electron microscope image of a sarcomere within a myofibril, from Schiaffino and Reggiani (2011)

**Figure 1.5** A schematic to illustrate the process of sarcomere contractions, facilitated by the actin-myosin interactions in the presence of calcium and ATP

**Figure 1.6** A diagram illustrating the myosin heavy chain gene family, their respective protein names and the distribution of expression, from Schiaffino and Reggiani (2011).

**Figure 1.7** Schematic depiction of the MyHC bi-directional promoters

**Figure 1.8** Characterized response elements that play a critical role in MyHC promoter activity (from Allen et al. 2001)

**Figure 2.1** Representative images of myotube diameter analysis using Q-Capture Pro (version 7).

**Figure 2.2** Example outputs from the Roche LightCycler380.

**Figure 2.3** Examples of melt curve analysis outputs to assess the number of amplicons produced in a Q-RT-PCR reaction.

**Figure 2.4** Schematic representation of engineering restriction sites onto a PCR amplicon.

**Figure 2.5** Schematic representation of the PCR amplicon including the restriction sites and poly-A tail

**Figure 2.6** Example of a 1kb PCR product checked by agarose gel electrophoresis

**Figure 2.7** Schematic representation of the cloning protocol

**Figure 2.8** Migration patterns of plasmid DNA by agarose gel electrophoresis

**Figure 2.9** Relative quantities of the plasmid and promoter DNA estimated by gel electrophoresis

**Figure 2.10** Diagram illustrating the MyHC IIB promoter ligated upstream of the ZsGreen gene to generate a fluorescence promoter-reporter plasmid

**Figure 2.11** Antibiotic selection marker that ensures antibiotic resistance of JM109 cells containing intact copies of the plasmid

**Figure 2.12** Example gel for detecting differences in plasmid length

**Figure 2.13** Examples of the time-lapse view of the DNA sequencing capillary

**Figure 2.14** Example of the DNA chromatogram (analysed using Sequencher) signal and sequence generation

**Figure 2.15** Pig and Human MyHC IIB promoter sequences located in the correct orientation within the multiple cloning site of the pZsGreenI-I.

**Figure 2.16** Schematic diagram detailing the chimeric promoter constructs containing combinations of the pig and human MyHC IIB promoters.

**Figure 2.17** Alignment of the proximal pig and human MyHC IIB promoter showing the location of the HindIII chimeric junction

**Figure 2.18** The effect of the 2bp mutation introduced to the pig and human 1kb MyHC IIB promoter activity in C2C12 myotubes

**Figure 2.19** Schematic diagram (from Phusion SDM protocol, Thermo Scientific) showing the principle of the mutagenesis PCR protocol

**Figure 2.20** Alignment of the proximal pig and human MyHC IIB promoters.

**Figure 2.21** The probe sequence used in the EMSA experiment, spanning the 3 base pair mismatches in the CArG/E-box region

**Figure 2.22** Schematic diagram illustrating the overlapping un-labeled pig and human competitor probes relative to the biotin-labeled pig MyHC IIB 62bp probe

**Figure 2.23** Control EMSA (using manufacturer supplied controls) showing successful protein-DNA interactions and competitive binding of unlabeled probes

**Figure 2.24** Light microscopy image of the C2C12 myoblasts immediately prior to transfection

**Figure 2.25** Evidence for co-uptake of pDsRed-express-NI and with pZsGreen1-NI

**Figure 2.26** Full-length amino acid sequence for murine MyoD

**Figure 2.27** Full-length murine Myod cDNA in the pDsRed-Express-NI plasmid

**Figure 2.28** Schematic illustrating the removal of the CMV promoter from the pDsRed-Express-NI plasmid for use as a vehicle transfection control

**Figure 3.1** Horizontal agarose gel (1.5%) electrophoretic separation of MyHC PCR amplicons

**Figure 3.2** (A) DNA content and (B) creatine kinase activity (corrected for DNA content) during C2C12 proliferation and differentiation

**Figure 3.3** Light microscopy images of C2C12 cells during proliferation and differentiation

**Figure 3.4** (A) Hoechst stained C2C12 myoblasts show that myoblasts contain a single nucleus per cell and (B) ZsGreen expressing C2C12 myotubes highlights that myotubes contain multiple nuclei

**Figure 3.5** RNA yield from C2C12's during proliferation and differentiation represented (A) per well of 6-well plates or (B) relative to DNA content

**Figure 3.6** (A) MyoD (B) myf5 and (C) myogenin mRNA expression during C2C12 proliferation and differentiation

**Figure 3.7** (A) MyHC emb (B) neo (C) type I (D) type IIa (E) type IIx and (F) type IIb mRNA expression during C2C12 proliferation and differentiation

**Figure 3.8** Visualization of mouse 1kb MyHC I promoter activity using a ZsGreen reporter plasmid in C2C12 muscle cells

**Figure 3.9** Representative light microscopy images of the two cohorts of C2C12 cells used for gene expression analysis of proliferating cells and fully differentiated myotubes

**Figure 3.10** Hexokinase-2 (Hk2), Phosphofructokinase (PFK<sub>m</sub>) and Enolase 3 gene expression in proliferating myoblasts compared to differentiated myotubes

**Figure 3.11** Citrate synthase (CS), Isocitrate dehydrogenase (IDH2) and Malate dehydrogenase-2 (MDH2) gene expression in proliferating myoblasts compared to differentiated myotubes

**Figure 3.12** Glucose-6-phosphate dehydrogenase (G6PDH) gene expression in proliferating myoblasts compared to differentiated myotubes

**Figure 3.13** 3-phosphoglycerate dehydrogenase (PHGDH), Phosphoserine aminotransferase-1 (PSAT1) and phosphoserine phosphatase (PSPH) gene expression in proliferating myoblasts compared to differentiated myotubes

**Figure 3.14** (A) Total pyruvate kinase muscle type (Pkm) gene expression in proliferating myoblasts compared to differentiated myotubes. (B) Expression of Pkm splice variants, Pkm1 and Pkm2, relative to total Pkm (Tot.Pkm) in myoblasts compared to myotubes

**Figure 3.15** Pyruvate carboxylase (Pc), Phosphoenolpyruvate carboxykinase-2 (PEPCK2) and Malate dehydrogenase-1 (MDH-1) gene expression in proliferating myoblasts compared to differentiated myotubes

**Figure 3.16** Summary of metabolic gene expression in myotubes relative to myoblasts

**Figure 4.1** Gel electrophoretic separation of the porcine MyHC isoform amplicons produced by Q-RT-PCR

**Figure 4.2** Starting body weight and final carcass weight of non-treated pigs and pigs treated with Ractopamine or Reporcin for 1, 3, 7, 13 or 27 days

**Figure 4.3** Muscle weights (absolute and relative to carcass weight) of non-treated pigs and pigs treated with Ractopamine or Reporcin for 1, 3, 7, 13 or 27 days

**Figure 4.4** Myosin heavy chain (MyHC) mRNA isoform expression in the LD muscle of non-treated pigs and pigs treated with Ractopamine or Reporcin for 1, 3, 7, 13 or 27 days

**Figure 4.5** Representative images of SDS-PAGE separation of myosin heavy chain protein isoforms

**Figure 4.6** Enolase 3 and IDH2 mRNA expression in the LD muscle of non-treated pigs and pigs treated with Ractopamine or Reporcin for 1, 3, 7, 13 or 27 days

**Figure 4.7** Correlation between MyHC isoform and Enolase 3 mRNA expression

**Figure 4.8** Correlation between MyHC isoform and IDH2 gene expression

**Figure 4.9** PGC-1a and RIP140 mRNA expression in the LD muscle of non-treated pigs and pigs treated with Ractopamine or Reporcin for 1, 3, 7, 13 or 27 days

**Figure 4.10** MyoD and Myogenin mRNA expression in the LD muscle of non-treated pigs and pigs treated with Ractopamine or Reporcin for 1, 3, 7, 13 or 27 days



**Figure 4.11** Six1 and Eya1 mRNA expression in the LD muscle of non-treated pigs and pigs treated with Ractopamine or Reporcin for 1, 3, 7, 13 or 27 days

**Figure 4.12** Figure (and description) taken from Ryall et al. (2010) showing relative mRNA expression of the Beta-1 and Beta-2 adrenergic receptors during early myogenic differentiation of C2C12 myoblasts

**Figure 4.13** Predicted effects of Ractopamine treatment on type II MyHC mRNA induction during C2C12 myogenesis

**Figure 4.14** Representative light microscopy (phase contrast) images of C2C12 cells at days 0, 2 and 4 during differentiation

**Figure 4.15** DNA content, creatine kinase activity and protein:DNA ratio following 48 hours Ractopamine treatment finishing at either day 2 or 4

**Figure 4.16** mRNA expression of Myogenin and MyoD following 48 hours Ractopamine treatment finishing at either day 2 or 4

**Figure 4.17** mRNA expression of MyHC isoforms (embryonic, neonatal, I, IIA, IIX and IIB) following 48 hours Ractopamine treatment finishing at either day 2 or 4

**Figure 4.18** Beta-adrenergic receptor 2 ( $\text{Adr}\beta 2$ ) mRNA expression following 48 hours Ractopamine treatment finishing at either day 2 or 4

**Figure 4.19** mRNA expression of Six1 and Eya1 following 48 hours Ractopamine treatment finishing at either day 2 or 4

**Figure 4.20** Porcine 1kb myosin heavy chain IIB promoter activity in C2C12 myotubes following 4 days of treatment with Ractopamine or dbcAMP during differentiation

**Figure 4.21** Transcription factor search for CREB/ATF consensus binding sites in the pig and mouse (1kb) MyHC IIB promoters

**Figure 5.1** Alignment of ~1kb of the pig and human MyHC IIB promoters

**Figure 5.2** 1kb pig and human MyHC IIB promoter activity in day 6 differentiated C2C12 myotubes

**Figure 5.3** 1kb pig and human MyHC IIB promoter activity in response to (mouse) MyoD over expression in C2C12 myotubes

**Figure 5.4** Equivalent 5' deletion analysis of the pig and human MyHC IIB promoters in C2C12 myotubes

**Figure 5.5** Activity of Pig-human and human-pig (5' to 3') chimeric MyHC IIB promoters in C2C12 myotubes

**Figure 5.6** Mutagenesis of the human 1kb MyHC IIB promoter

**Figure 5.7** Mutagenesis of the human 1kb MyHC IIB promoter continued

**Figure 5.8** Competitive electrophoretic mobility shift assay to determine protein-DNA interactions within the MyHC IIB promoter

**Figure 5.9** Effect of removing the CArG-box region from the pig and human MyHC IIB promoters

**Figure 5.10** Alignment of the proximal pig and human MyHC IIB promoter

**Figure 5.11** Pig and human MyHC IIB promoter activity in response to 4 and 5 days exposure to 1mM dbcAMP treatment

## **LIST OF TABLES**

**Table 2.1** Composition of Reagent 1 for the Lowry assay

**Table 2.2** Composition of Reagent 2 for the Lowry assay

**Table 2.3** SDS-PAGE gel composition for separating rat MyHC isoforms

**Table 2.4** SDS-PAGE gel composition for separating sheep MyHC isoforms

**Table 2.5** Thermal cycling parameters for amplification of the 1kb pig and human MyHC IIB promoters.

**Table 2.6** Oligonucleotide primer sequences for all cloning

**Table 2.7** Components and quantities of the Applied Biosystems BigDyeFast sequencing PCR

**Table 2.8** Applied Biosystems BigDyeFast thermal cycling parameters for sequencing PCR

**Table 2.9** Components and quantities for site directed mutagenesis PCR using Q5 polymerase

**Table 2.10** Thermal cycling parameters for site directed mutagenesis PCR

**Table 2.11** Sense and anti-sense sequences of oligonucleotides used to generate double stranded EMSA probes

**Table 2.12** Excitation and emission settings for measuring ZsGreen and DsRed fluorescence from cell culture plates using the Typhoon Trio+ (GE healthcare)

**Table 2.13** Oligonucleotide primer sequences for amplifying full-length open reading frame murine MyoD cDNA and associated sequencing primers

**Table 2.14** Components and quantities for the Klenow Large Polymerase reaction

**Table 3.1** Forward and reverse primers for the mouse MyHC and MRF genes

**Table 3.2** Crossing point values for Q-PCR analysis of myogenic regulatory factors

**Table 3.3** Crossing point values for Q-PCR analysis of murine MyHC isoforms

**Table 3.4** Oligonucleotide sequences used for Q-RT-PCR analysis of mouse metabolic genes

**Table 4.1** Oligonucleotide sequences for measuring porcine myosin heavy chain isoforms (from Wimmers et. 2008)

**Table 4.2** Oligonucleotide sequences for measuring gene expression in porcine muscle

**Table 4.3** Crossing point values for Q-PCR analysis of porcine MyHC isoforms

**Table 4.4** Oligonucleotide primer sets for Q-PCR analysis of gene expression in mouse C2C12 cells

**Table 4.5** Relative gene expression following 48 hours Ractopamine (1 $\mu$ M) treatment in C2C12 cells finishing at either day 2 or 4

## LIST OF ABBREVIATIONS

ADP – Adenosine diphosphate  
ATP – Adenosine triphosphate  
cAMP - Cyclic adenosine monophosphate  
cDNA – Complimentary deoxyribonucleic acid  
CK – Creatine kinase  
CO<sub>2</sub> – Carbon dioxide  
Cs – Citrate synthase  
dbcAMP - Dibutyryl-Cyclic adenosine monophosphate  
DMEM - Dulbecco's modified eagle medium  
DMSO - dimethyl sulfoxide  
DNA - deoxyribonucleic acid  
dNTP - deoxyribonucleic acid triphosphates  
Emb – Embryonic  
EMSA – Electrophoretic mobility shift assay  
ERR $\alpha$  - Estrogen-related receptor alpha  
EYA1 – Eyes absent 1  
FBS – Fetal bovine serum  
G6PDH – Glucose-6-phosphate dehydrogenase  
HK2 – Hexokinase-2  
HS – Horse serum  
IDH2 / ICDH2 - Isocitrate dehydrogenase 2  
IU – International units  
kb - Kilobase  
kDa – Kilo daltons  
LD – Longissimus dorsi  
MDH1 – Malate dehydrogenase  
miRNA – Micro ribonucleic acid  
MRF – Myogenic regulatory factor  
mRNA - Messenger ribonucleic acid  
MyHC – Myosin heavy chain  
Neo – Neonatal  
NFAT - Nuclear factor- activated T cell  
O<sub>2</sub> - Oxygen  
PBS – Phosphate buffered saline  
Pc – Pyruvate carboxylase  
PCR – Polymerase chain reaction  
PEPCK2 – Phosphoenolpyruvate carboxykinase 2  
PFK $\mu$  – Phosphofructokinase, muscle type  
PGC-1 $\alpha$  - Peroxisome proliferator-activated receptor gamma coactivator 1-a  
PHGDH – 3-Phosphoglycerate dehydrogenase  
P<sub>i</sub> - Inorganic phosphate  
Pkm – Pyruvate kinase, muscle type  
PPAR $\delta$  - Peroxisome proliferator-activated receptor delta  
PS – Penicillin Streptomycin

PSAT1 – Phosphoserine aminotransferase 1  
PSPH – Phosphoserine phosphatase  
Q-RT-PCR – Quantitative reverse transcriptase polymerase chain reactions  
RIP140 - receptor-interacting protein 140  
RNA – Ribonucleic acid  
RT-PCR – Reverse transcriptase polymerase chain reaction  
SD – Standard deviation  
SDH – succinate dehydrogenase  
SDS-PAGE - sodium doecyl sulphate polyacrylamide gel electrophoresis  
SEM – Standard error of the mean  
SIX1 – Sine Oculis Homeobox 1  
SRF – Serum response factor  
TSS – Transcription start site

# 1

## INTRODUCTION

---

## 1. INTRODUCTION

### *1.1 Skeletal muscle*

Skeletal muscle is composed of a heterogeneous population of muscle fibres, with varying contractile and metabolic characteristics, and is fundamental to the locomotive capabilities of all mammals. Furthermore, skeletal muscle permits activities such as breathing and eating, making it an essential tissue for life. In addition to its mechanical roles, skeletal muscle is a metabolically active tissue that both stores and utilizes considerable quantities of energy; it is therefore considered to be a key contributor to whole body metabolism. Taken together, skeletal muscle is a multifunctional tissue that is critical to the survival of all mammals, making it the subject of considerable scientific interest for over a century (Schiaffino and Reggiani 2011).

### *1.2 Myogenesis: the formation of muscle fibres*

Skeletal muscle is a collection of multinucleated muscle fibres formed by a process called myogenesis, the regulation of which has been extensively reviewed (see Bentzinger et al. (2012) for an up to date review). Briefly, precursor cells become committed to the myogenic lineage (denoted as myoblasts) before undergoing several rounds of proliferation. Myoblasts then terminally exit the cell cycle, align and fuse together to form multinucleated myotubes. Ultimately, the myotubes mature to form the muscle fibres. See Figure 1.1 for a schematic representation of myogenesis. This process of myogenesis is critical to the formation of muscle fibres during development but also a fundamental aspect of muscle regeneration in adult muscle, with



resident muscle precursors showing the capacity to fuse to existing muscle fibres to aid repair of hypertrophic growth (Bentzinger et al. 2012).

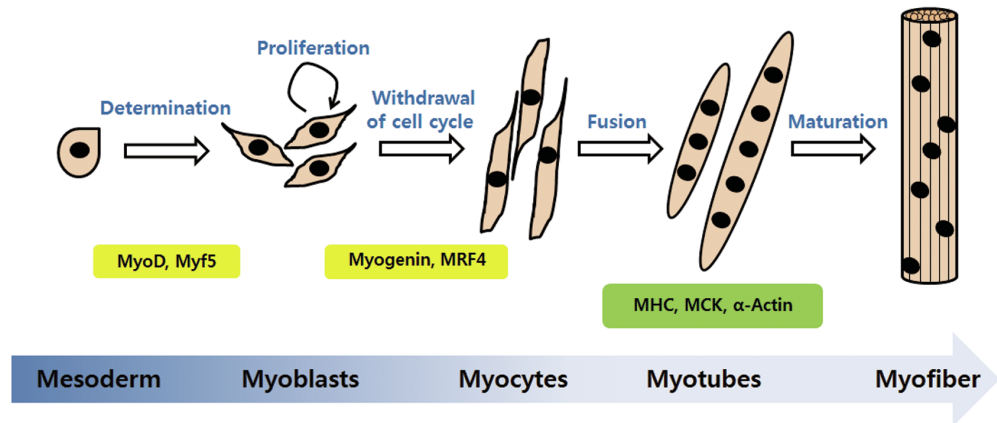


**Figure 1.1** A schematic, from Jang et al. (2013), detailing the process of myogenesis; mesodermal cells undergo determination to the myogenic lineage, forming myoblasts, which proliferate to expand cell number. On induction of differentiation, the myoblasts exit the cell cycle and fuse to form multinuclear myotubes and ultimately mature into myofibres.

The regulation of myogenesis is well characterized (Bentzinger et al. 2012) and highly regulated by a family of basic helix-loop-helix transcription factors called myogenic regulatory factors (MRF's), consisting of MyoD, Myf-5 and myogenin (Sabourin and Rudnicki 2000; Bentzinger et al. 2012). Expression profiles of the MRF genes are temporally distinct and display a hierarchical induction during myogenesis. The central role of MyoD in committing a cell to a myogenic fate was originally highlighted by forced expression of MyoD in non-muscle cells, which was capable of inducing muscle specific gene expression and fusion of non-muscle cells into myotubes (Davis et al. 1987). Interestingly, Myf-5 shows reciprocal redundancy to MyoD *in vivo*, as removal of the MyoD or Myf-5 gene from mice results in relatively normal muscle development due to compensation by the remaining MyoD or Myf-5 factor (Braun et al. 1992; Rudnicki et al. 1992). However, removal of both MyoD

and Myf-5 from mice results in neonatal lethality due to the complete lack of skeletal muscle formation (Rudnicki et al 1993), emphasizing that either MyoD or Myf-5 is required for the commitment of precursor cells to the myogenic program. Myogenin, on the other hand, is fundamental to the fusion and differentiation of committed myoblasts into myotubes, as demonstrated by the lack of differentiated myofibres but the presence of un-fused myoblasts in myogenin knockout mice (Nabeshima et al. 1993; Hasty et al. 1993). Thus, MyoD and Myf-5 are typically involved in the early stages of myoblast commitment, whereas myogenin is involved in the fusion and differentiation of myoblasts into myotubes. However, mice lacking both MyoD and Myf-5 display a lack of myogenin expression (Rudnicki et al 1993), highlighting the hierarchical nature of the MRF network, with MyoD or Myf-5 being required for the activation of Myogenin expression. The complex network of interactions between the MRF's to regulate myogenesis is fundamental to the formation of multinuclear muscle fibres and the induction in expression of the necessary components that constitute the mature, physiologically functional muscle fibre (Sabourin et al. 1999; Bentzinger et al. 2012).

### *1.3 Muscle fibre heterogeneity*





Adult skeletal muscle is comprised of a heterogeneous population of muscle fibres displaying a broad range of contractile and metabolic characteristics, which remain malleable throughout adult life. It is this heterogeneity in muscle fibre characteristics, within a given muscle, that allows skeletal muscle to perform a huge variation in contractile functions, from isometric postural support to explosive sprinting. The vast heterogeneity and plasticity of muscle

fibre phenotype has therefore been of significant interest to the scientific community due to its broad application to exercise physiology, ageing and sarcopenia, cancer cachexia, skeletal myopathies, metabolic disorders, and even livestock production.

Differences in skeletal muscle phenotype have long been reported since the late 19<sup>th</sup> century (Ranvier 1874), with differences in phenotype originally identified by differences in muscle colour (red and white). Further characterization in the early 20<sup>th</sup> century split red and white muscle phenotypes into two distinct groups; the fast- and slow- twitch muscles with a glycolytic and oxidative metabolism, respectively (Needham 1926). In 1967 it was discovered that myosin ATPase activity of the myosin heavy chain molecule linked the contractile and metabolic characteristics of muscle fibres (Barany 1967). A more extensive examination of muscle fibre types began, combining physiological, histochemical and biochemical properties of muscle fibres. The pivotal work of Brooke and Kaiser (1970) devised a method to stain transverse cross sections (~10µM thick) of frozen muscle to visualize differences in myofibrillar ATPase (mATPase) activity between muscle fibres, transforming muscle biology research. Typically, cross sections are stained for mATPase following a pre-incubation in an acidic (pH 4.3-4.6) or alkaline (pH 10.2-10.6) environment. An acidic pre-incubation inhibits the activity mATPase in fast fibres, thus only staining slow fibres and an alkaline pre-incubation inhibits the activity of mATPase in slow fibres, staining only the fast fibres. This method categorized muscle fibres into a slow-twitch (type I) fibre type and two fast-twitch (type IIA and IIB) fibre types. Further biochemical analyses, combining mATPase staining with staining for metabolic enzyme activity, such as

succinate dehydrogenase (SDH), revealed that the metabolic profile is closely correlated with the mATPase within muscle fibres (Burke et al. 1971). Thus, fibre types were commonly categorized as slow-twitch oxidative (type I), fast-twitch oxidative-glycolytic (type IIA) and fast-twitch glycolytic (type IIB). However, the introduction of antibodies raised against components that constitute the contractile machinery of the muscle fibre, revealed there might be more than three muscle fibre types. Specifically, antibodies raised against myosin heavy chain (MyHC) isoforms highlighted four distinct fibre types expressing type I, IIA, IIX or IIB MyHC isoforms (Schiaffino et al. 1989), which now form the labeling system for characterizing muscle fibre types. Furthermore, using *in situ* riboprobe hybridization against MyHC isoform transcripts revealed that the classically labeled type IIB fibre type actually consisted of two sub-populations expressing either IIX, IIB or both IIX and IIB MyHC isoforms (Lefaucheur et al. 1998). Thus, type IIX muscle fibres have been erroneously labeled as type IIB muscle fibres in much of the early muscle fibre type literature. Furthermore, MyHC analysis in human skeletal muscle revealed that classically labeled IIB fibres in fact express a gene homologous to the rat type IIX MyHC isoform and actually lack expression of the MyHC IIB gene (Smerdu et al. 1994), despite the human genome containing a gene encoding the MyHC IIB gene (Weiss, Schiaffino & Leinwand, 1999). Molecular analysis of MyHC isoform expression in single fibres has also lead to the discovery that muscle fibre phenotypes do not fit exactly into discrete fibre types, often expressing multiple MyHC isoforms (Lefaucheur et al. 1998; Stephenson 2001), and thus display a continuum of characteristics. However, MyHC is the molecular motor of the muscle sarcomere and closely correlates

with the contractile and metabolic characteristics of the muscle fibre plus it is differentially expressed in physiologically diverse muscle fibre types, thus making it an excellent marker of muscle fibre type (Schiaffino and Reggiani 2011; Gundersen 2011). Furthermore, global expression of MyHC isoforms in muscle tissue homogenate gives an average indication of phenotype across the sample. The figure below details the characteristics correlating with MyHC isoform expression (Gundersen 2011). Briefly, physiological characteristics generally follow a sequential order with the corresponding MyHC isoform expressed in the order of type I > IIA > IIX > IIB (oxidative to glycolytic, slow to fast, small to large, high to low endurance; see Figure 1.2 below for example).

MyHC type	Twitch duration	Shortening velocity	Cross-sectional area	Metabolism	Endurance	Energy efficiency	
I		Slow	Small		High	High	
IIa							
IIx							
IIb	Fast	Fast	Large	Glycolytic	Low	Low	

**Figure 1.2** This Figure, from Gundersen (2011), shows the physiological characteristics of the four adult muscle fibre types, classified by their expression of myosin heavy chain isoform (I, IIA, IIX, IIB).

As it stands, measuring MyHC isoform expression as an indicator of muscle fibre type is likely a gross over-simplification, as there are many components of the muscle sarcomere that display fibre type specific expression, but it is currently considered the best and most convenient marker of muscle fibre composition (Schiaffino and Reggiani 2011). However, MyHC is a key component of the muscle sarcomere and is actively (not just passively) involved in directly influencing the physiology of the muscle fibre. Thus, it is

not only a useful “biomarker” of muscle fibre type but of physiological interest to the scientific community as an influential component of the muscle fibre phenotype.

#### *1.4 The muscle sarcomere and the myosin heavy chain isoforms*

Skeletal muscle fibres consist of a collection of myofibrils which contain the major contractile components, the sarcomere, which permits contraction of the muscle (see Figure 1.3).

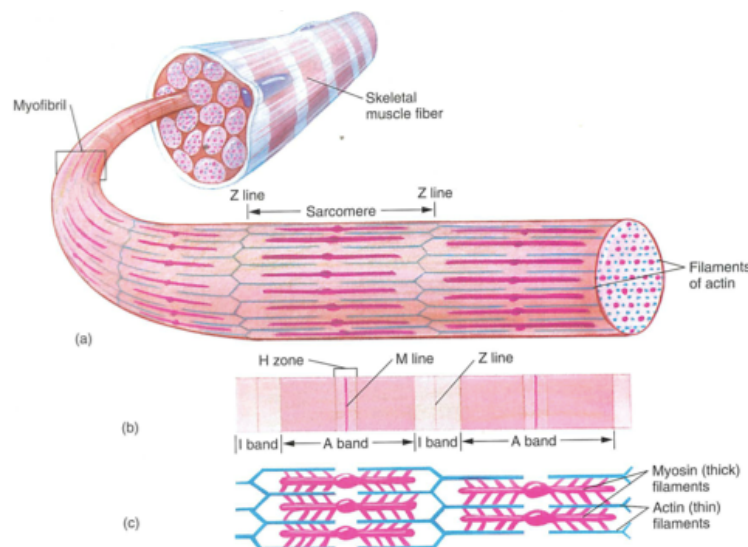


**Figure 1.3** Each skeletal muscle fibre contains a collection of myofibrils, which contain the sarcomere structures (diagram from Powers and Howley 2007).

The sarcomere is a highly ordered molecular structure that forms the contractile machinery of the muscle fibre (Schiaffino and Reggiani 2011). Information regarding the molecular structures and functions of the sarcomere described herein, can be obtained from an excellent review by Schiaffino and Reggiani (2011) unless otherwise stated. The sarcomeres are aligned in a parallel, back-to-back, alignment to form the myofibrils, generating the characteristic striated pattern of muscle fibres (see Figure 1.4 below).

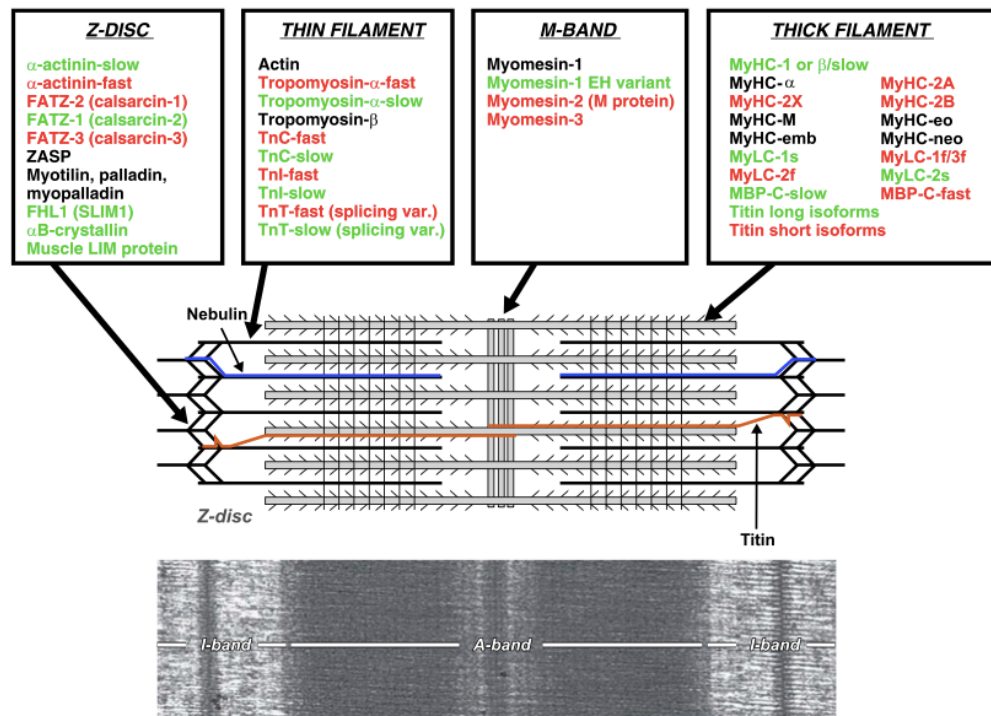


**Figure 1.4** Schematic diagram of the muscle sarcomere and a respective comparison to an electron microscope image of a sarcomere within a myofibril (Schiaffino and Reggiani 2011). The sarcomere is annotated with its key components; labels in red or green denote selective expression in fast and slow muscle fibres respectively.

The cytoskeletal sarcomeric structures, comprising the Z-disc and M-band, align perpendicular to the direction of the myofibril, and provide a structural scaffold for the contractile machinery. The myosin (thick) and actin (thin) filaments form the “major” components of the sarcomeric contractile machinery, which run longitudinal to the myofibrils and transverse to the Z-disc and M-disc sarcomeric structures (see Figure 1.4). The interaction between the myosin and actin filaments largely determines the contractile function of the sarcomere; hence they are commonly denoted as the “major” contractile components. Also of critical importance to the contraction of the sarcomere is the troponin-tropomyosin complex attached to the actin filament. This complex interacts with calcium (the chemical signal that induces muscle contraction) to expose the myosin binding sites on the actin filaments,

permitting actin-myosin interactions and thus allowing sarcomeric contraction. Many of the components constituting the sarcomere exist as multiple isoforms, resulting in functionally diverse sarcomeres, which reside in fast and slow contracting muscle fibres (as shown in Figure 1.4 with “fast” and “slow” specific isoforms indicated by red and green text, respectively). Although many components of the sarcomere exist as multiple isoforms that elicit phenotype-specific expression, i.e. in fast and slow muscle fibres, it is predominantly the myosin heavy chain (MyHC) isoforms that actively dictate the diverse magnitude of actin-myosin force generation.

### *1.5 Myosin heavy chain*

The MyHC molecule is a large, 200kDa, elongated protein consisting of two globular “head” domains (~840 amino acid) and a long alpha-helical coiled “tail” domain (~1,100 amino acid). The myosin tails align together to create the “thick” myosin filament, which comprises hundreds of myosin heads, each containing the ATP- and actin- binding sites necessary to facilitate the mechanical movements of the myosin molecule, which in turn regulate the contraction of the sarcomere. The myosin “molecular motors” directly interact with the actin filaments causing the sarcomeres to shorten, by sliding the myosin and actin filaments across one another in opposing directions.

### *1.6 Contraction of the sarcomere*

The mechanism of contraction of the muscle sarcomere is essentially a repetitive interaction of the myosin heads with the actin filaments, resulting in a shortening of the sarcomeric structure, and has been well reviewed elsewhere



(Schiaffino and Reggiani 2011). The arrival of an action potential at the muscle fibre results in depolarization and a rapid release of calcium. Calcium binds the troponin-tropomyosin complex, which subsequently exposes the myosin binding sites on the actin filament, permitting actin-myosin interactions in the presence of Adenosine Triphosphate (ATP). The myosin head rapidly hydrolyzes ATP into Adenosine Diphosphate (ADP) and inorganic phosphate ( $P_i$ ), which induces an elevation in the myosin lever arm, followed by binding of the myosin head to the actin filament (see Figure 1.5 for schematic representation of sarcomere contraction). Subsequent release of  $P_i$  from the myosin head causes a structural change to the myosin molecule inducing the “power stroke”, transmitting force against the actin filament and displacing the thick (myosin) and thin (actin) filaments in opposing directions, resulting in contraction of the sarcomere. Following the power stroke, ADP is released, firmly associating the myosin head to the actin filament. Binding of ATP to myosin subsequently causes disassociation of the myosin head from the actin filament and induces a conformational change in the lever arm of the myosin molecule, causing a “reverse stroke” of the myosin head whilst unattached to the actin filament. In the presence of ATP and calcium, this process repeats itself in a cyclic fashion to induce actin-myosin filament sliding, causing a mass shortening of the muscle fibre and ultimately a muscle contraction.

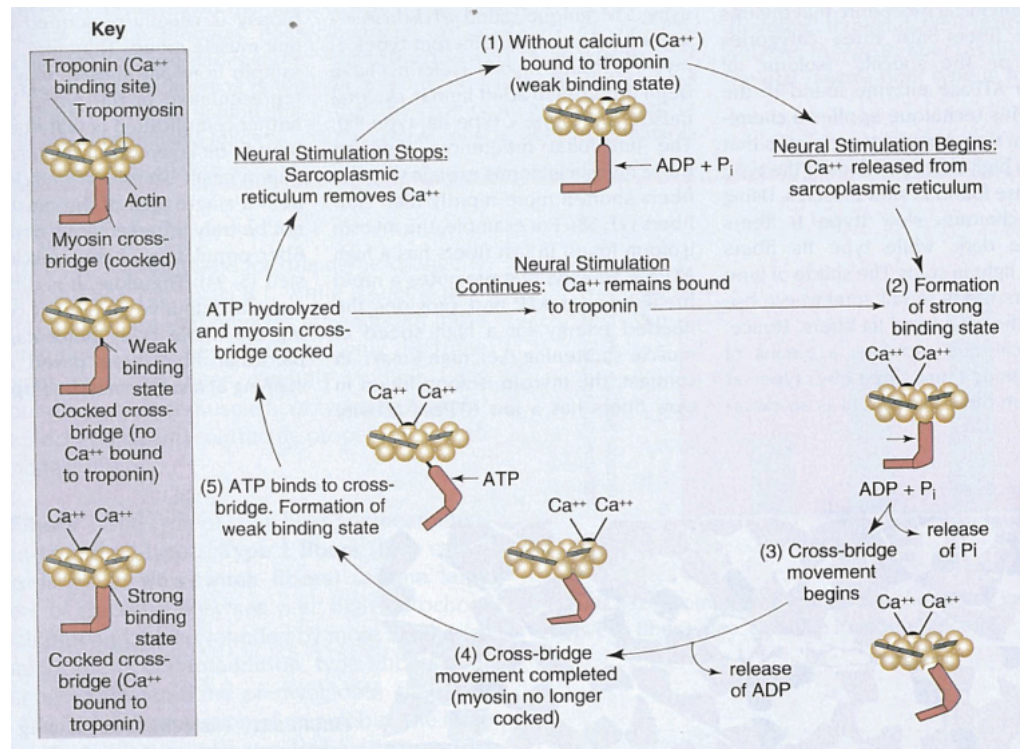


**Figure 1.5** A schematic to illustrate the process of sarcomere contractions, facilitated by the actin-myosin interactions in the presence of calcium and ATP (Diagram from Powers and Howley 2007).

### *1.7 Myosin heavy chain isoforms and contractile kinetics*

The kinetics of the aforementioned actin-myosin interaction to induce contraction of the sarcomere is largely determined by the specific MyHC isoform expressed, resulting in a diverse range of contractile speeds. Thus, MyHC isoforms in adult muscle are commonly referred to as slow and fast MyHC's as they have a strong physiological effect on the contractile phenotype of the muscle. Differences in the kinetics of the MyHC isoforms are due to disparity in their rate of ATP hydrolysis and ADP dissociation (Schiaffino and Reggiani 2011). The rate of ATP hydrolysis influences the rate of actin-myosin binding, thus influencing the speed of the sarcomere contraction. For instance, in rabbit skeletal muscle, differences in the rate of

ATP hydrolysis between MyHC's are very disparate, with fast MyHC isoforms eliciting up to 20-30-fold faster ATP hydrolysis compared to slow (type I) MyHC (Weiss and Leinwand 1996). These differences in ATPase activity of the fast and slow MyHC's results in vastly different contractile characteristics between "fast" and "slow" muscles. The rate of ADP dissociation is also critical to the speed of contraction; influencing the speed of detachment of the myosin head from the actin filament, thus increasing the time taken to re-start the cycle of sarcomere contraction (Schiaffino and Reggiani 2011). The fast type II MyHC isoforms are typically more responsive, with ADP dissociation occurring quickly, enabling a shorter delay between sarcomere contractions. Taken together, the MyHC isoform is a critical determinant of the contractile capacity of a muscle fibre (Schiaffino and Reggiani 2011).

### *1.8 The Myosin heavy chain gene family*

In total, there are 11 highly conserved mammalian sarcomeric MyHC genes (*MYH*), each encoding an individual isoform (Figure 1.6). It is suggested that the mammalian MyHC gene family arose from multiple replications of a single ancestral MyHC gene (Stedman et al 1990, Moore et al 1993). As a result, sarcomeric MyHC genes are highly conserved, sharing 78-98% amino acid identity, between isoforms and across multiple species (Weiss and Leinwand 1996). This originally lead to speculation that MyHC genes were highly redundant, given the level of gene duplication, but it is now clear that multiple MyHC isoforms provide functionally diverse contractile characteristics (Weiss and Leinwand 1996). The MyHC gene is typically around 30kb in length,

containing 40 or 41 exons, with a similar intron-exon organization (Weiss and Leinwand 1996).

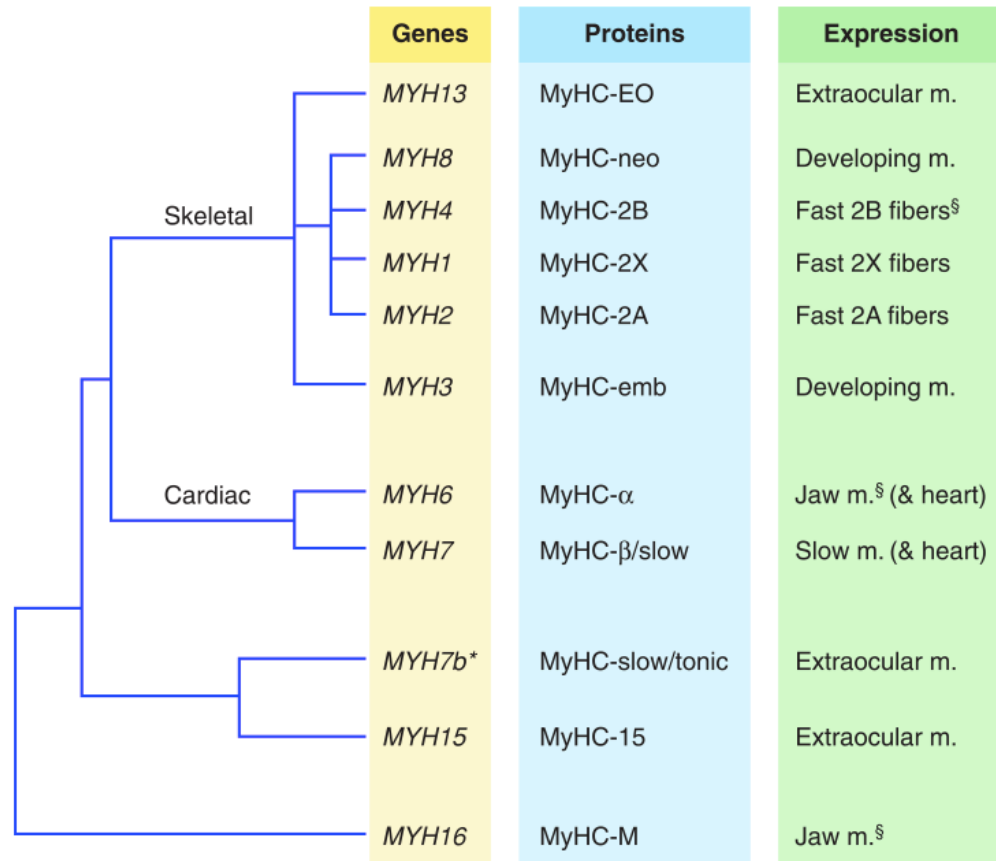


**Figure 1.6** A diagram illustrating the myosin heavy chain gene family, their respective protein names and the distribution of expression (Schiaffino and Reggiani 2011).

The MyHC genes are mostly distributed between two clusters on two separate chromosomes (Weiss and Leinwand 1996; Schiaffino and Reggiani 2011), with one cluster containing the isoforms expressed in cardiac muscle (MyHC- $\alpha$  and MyHC- $\beta$ ) and the other containing three isoforms expressed in adult skeletal muscle (MyHC-IIA, MyHC-IIX, and MyHC-IIB), two developmental isoforms (MyHC-emb and MyHC-neo) and one isoform exclusively expressed in the extraocular muscles (MyHC-EO; see Figure 1.6).

In addition, three highly specialized MyHC isoforms have recently been identified (MyHC-slow tonic, MyHC-15 and MyHC-M) which are specifically expressed in some head and neck muscles.

### *1.9 Myosin heavy chain isoform expression*

MyHC genes are induced during the differentiation of myogenic cells to form physiologically functional multinuclear myofibres. The induction of the MyHC genes during *in vivo* development has been well characterized (Lyons et al. 1990; Weydert et al. 1987; Agbulut et al. 2003). Prior to birth, it is predominantly only the embryonic (emb) and neonatal (neo) MyHC isoforms that are expressed in skeletal muscle (Weydert et al. 1987), with some studies showing low levels of the adult type I MyHC isoform (Lyons et al. 1990). Postnatally, however, the adult MyHC isoforms are selective induced, possibly due to the introduction of contractile activity present after birth (Agbulut et al. 2003; Cerny and Bandman 1986). A comprehensive analysis of MyHC isoform protein expression in postnatal development of mouse muscle highlights distinct differences in the induction of MyHC isoforms in fast and slow muscles (Agbulut et al. 2003). In slow muscles (e.g. the soleus), the MyHC emb, neo and type I isoforms are expressed first, and then the type I isoform progressively predominates with a concomitant reduction in expression of the emb and neo isoforms. In contrast, fast muscles (e.g. the extensor digitorum longus) show a gradual replacement of the emb neo and type I isoforms with fast type IIA, IIX and IIB isoforms (Agbulut et al. 2003). It is generally well accepted that postnatal transitions occur *in vivo* due to the introduction of neural stimulation, mechanical load and circulating hormones

(Schiaffino and Reggiani 2011). Attempts to explore the induction of MyHC isoforms during development were extended to *in vitro* experiments, exploring MyHC isoform induction during myogenesis (Silberstein et al. 1986; Weydert et al. 1987; Miller 1990). However, these attempts were somewhat limited by the use of relatively non-specific antibodies against MyHC isoforms and did not completely elucidate the developmental induction profiles of MyHC isoforms during myogenesis. They did however show that developmental MyHC isoforms were induced earlier during myogenic differentiation than the adult isoforms, which were induced later, suggesting there were “early” and “late” expressed MyHC isoforms during myogenesis (Silberstein et al. 1986; Miller 1990). This also suggests that early developmental transitions in MyHC isoform expression might occur independent of neural innervation, mechanical load and circulating hormones, in contrast to what is commonly reported. The specific MyHC isoforms within each of these “early” and “late” cohorts are yet to be identified during myogenesis. Elucidation of the specific expression profiles all skeletal muscle MyHC isoforms during myogenesis was therefore an objective of this thesis. Such characterization would be conducted on the commonly used C2C12 cell line to provide important information for scientists using this cell line for muscle biology research. It is clear from *in vivo* characterization studies that fast and slow muscles show a differential induction of the MyHC isoforms during postnatal development in mice (Agbulut et al. 2003), and these transitions are considered as an effect of the postnatal introduction of specific motor unit firing patterns and introduction of circulating hormones, such as thyroid hormone (Schiaffino and Reggiani 2011). It is unknown whether C2C12 muscle cells mimic the development of

fast or slow muscles with regard to the expression of MyHC isoforms. Such information is of importance for scientists using the C2C12 cell line for muscle biology research, with particular relevance to muscle fibre type, metabolism or growth (hypertrophy and atrophy). In addition, the majority of work conducted on elucidating the regulation of muscle fibre type is routinely conducted using histochemical and immunochemical methods on whole muscle from *in vivo* experiments. Characterization of the expression profiles of the MyHC isoforms during C2C12 differentiation could elucidate whether this cell line could be utilized for *in vitro* experiments examining the molecular regulation of the contractile components that constitute the muscle fibre.

#### *1.10 Species-differential expression of myosin heavy chain IIB*

Although the MyHC isoforms are evolutionary conserved genes with very high homology and similar functionality between species, the MyHC IIB isoform displays a very noticeable species-specific expression in skeletal muscle. Despite all mammals carrying the gene (MYH4) encoding MyHC IIB, extensive characterization has revealed a striking divide between large and small mammals with regard to MyHC IIB expression. Most small mammals such as mice (Pellegrino et al. 2003), rats (Pellegrino et al. 2003), rabbits (Wada et al. 1995; Pellegrino et al. 2003), and guinea pigs (Gorza 1990; Tonge et al., 2010) express MyHC IIB but most larger mammals such as cows (Chikuni et al. 2004), sheep (Hemmings et al. 2009) horses (Rivero et al. 1999), goats (Arguello et al. 2001), cats (Talmadge et al. 1996; Lucas et al. 2000), dogs (Toniolo et al. 2007), baboons (Lucas et al. 2000) and humans (Smerdu et al., 1994, Pellegrino et al. 2003) do not express MyHC IIB.

Originally it was proposed that the powerfully fast contractile speeds of the MyHC IIB isoform would be incompatible with the mechanics of muscles from large mammals (Hill 1950). From an evolutionary perspective, small mammals tend to be preyed upon by larger mammals, therefore the muscles surrounding the short limbs of small mammals would be required to contract quickly and forcefully to provide whole body locomotion rates similar to that of large mammals, permitting predator-prey competition and subsequently allowing survival of both mammal groups (Hill 1950). Larger muscles/limbs confer mechanical advantages over smaller muscles and thus don't require such extreme contractile characteristics in order to provide equivalent locomotion rates compared to small mammals. Interestingly, despite these hypotheses, domesticated pigs present an anomaly amongst the large mammals as they express very high levels of MyHC IIB (Lefaucheur et al. 1998; Gunawan et al. 2007), a phenotype likely exacerbated by the intensive selection pressure for enhanced muscle growth in these animals (Ruusunen and Puolanne 2004; Lefaucheur et al. 2004). The contractile properties of MyHC IIB fibres from pig skeletal muscle also exhibit comparable shortening velocity to that of small mammals, such as rats and rabbits, suggesting that the mechanical constraints imposed by larger muscles are in fact still compatible with the MyHC IIB isoform. The mechanism(s) dictating the differential expression of the MyHC IIB isoform between different species are yet to be explored. Elucidating the molecular mechanisms controlling the expression of the MyHC IIB isoform between species would improve our understanding of the fundamental biology controlling species diversity in muscle physiology. Of particular interest would be the mechanisms dictating the expression of MyHC



IIB in pig skeletal muscle since expression of this isoform is very unusual amongst large mammals. Furthermore, pigs are physiologically similar to humans and are therefore increasingly being considered as a good animal model for studying a range of human diseases (Luo et al. 2012). Differences in the expression of MyHC IIB, and the fast-glycolytic muscle phenotype associated with expression of this gene, between pigs and humans presents a major limitation of the pig as a model for human muscle biology research. Thus, an understanding of mechanisms controlling the differential expression of MyHC IIB between pigs and humans would improve our understanding of the pig as a model for human skeletal muscle biology research. Furthermore, it would elucidate the fundamental biology controlling expression of MyHC IIB in a large mammal. Work conducted in this thesis set out to explore the molecular mechanisms controlling the expression of the MyHC IIB gene in porcine skeletal muscle. Two potential mechanisms exist in controlling the transcriptional expression of MyHC IIB in pigs; 1) a genomic difference in the MYH4 promoter dictates strong transcriptional activity, leading to MyHC IIB expression, or 2) specific transcriptional regulators or co-regulators exist in abundance to induce high level transcription of MyHC IIB. Since the list of regulatory factors likely controlling transcriptional expression of MyHC IIB is far from complete, the former suggested mechanism was explored in this thesis, examining the role of the MyHC IIB promoter sequence in dictating species-specific expression of MyHC IIB in pig skeletal muscle.

### *1.11 Postnatal transitions in myosin heavy chain isoform expression*

Although the initial induction of the MyHC isoforms is determined during early muscle fibre formation and that clusters of MyHC isoforms typically display muscle-type specific expression (i.e. in fast and slow muscles), dynamic plasticity in the expression of MyHC isoforms remains malleable throughout adult life. Transitions in MyHC isoform expression in adult skeletal muscle can be induced by a variety of stimuli, such as neural/electrical activity (Buller et al. 1960; Gambke et al. 1983; Ausoni et al. 1990), hormones (Russell et al. 1988; Hughes et al. 1993; Gambke et al. 1983), ageing (Klitgaard et al. 1990) and mechanical load (Loughna et al. 1990; Caiozzo et al. 1996). The seminal work of Buller et al. (1960) showed that swapping the neural input of slow and fast muscles resulted in a change in muscle phenotype according to the new nerve supply. This work highlighted that the pattern of neural stimulation has a fundamental role in regulating muscle phenotype in the adult animal. More recent work has utilized different frequencies of electrical stimulation to mimic neural activity of fast and slow muscles to show that differences in muscle contractile activity can reprogram muscle fibre type and specifically alter MyHC isoform expression (Ausoni et al. 1990). Fast muscles, such as the EDL, can be electrically stimulated to become “slower” muscles (based on MyHC isoform expression) and slow muscles, such as the soleus, can be electrically stimulated to become “faster” muscles (Ausoni et al. 1990). Importantly, it is suggested that innervation, and thus neural activity, is required for the expression of slow type I MyHC isoforms, whereas induction of the fast type II MyHC isoforms can occur independent of neural innervation, as demonstrated by denervation in rats (Gambke et al. 1983). In

support of the somewhat extreme experimental conditions employed by authors using electrical stimulation and neural re-innervation, experiments conducted using endurance and resistance exercise training have confirmed that physiological levels of muscle activity *in vivo* are capable of inducing alterations in MyHC isoform expression (Demirel et al. 1999; Andersen and Aagaard 2000) and that the plasticity in expression of MyHC isoforms remain malleable through to elderly ages (Konopka et al. 2011).

Forced disuse or reduced activity of skeletal muscle also demonstrates the role of neural input and muscle contractile activity on MyHC isoform expression. For instance, just four days of hindlimb suspension in rats can induce *de novo* expression of the MyHC IIB transcription (Loughna et al. 1990), suggesting that the lack of neural/contractile stimuli can induce a transition in expression of contractile machinery constituting the muscle fibre. In addition, rats exposed to a microgravity environment (spaceflight) for 14 days have shown a switch from slow to fast MyHC isoforms in the postural load-bearing muscle, the soleus (Caiozzo et al. 1996). Thus, muscle activity and inactivity are potent regulators of MyHC isoforms in adult skeletal muscle. A huge body of work exists to support this notion that neural input and muscle contractile activity regulate postnatal expression of MyHC isoforms and has been aptly named “excitation-transcription coupling” (Gundersen et al. 2011).

In addition to neural and activity dependent regulation of MyHC isoform expression, circulating hormones can be influential to MyHC isoform expression in postnatal muscle. Perhaps the most commonly reported hormone involved in fibre type regulation is thyroid hormone, which is capable of specifically inducing the fast MyHC IIB isoform (Russell et al. 1988; Hughes

et al. 1993). Circulating thyroid hormone increases rapidly at birth and is likely responsible, at least in part, for the postnatal induction of the MyHC IIB isoform in developing muscle (Gambke et al. 1983; Russell et al. 1988). Furthermore, a hyperthyroid state (increased circulating thyroid hormone levels) is capable of inducing alterations in MyHC isoform in neonatal, young and old rats (Russell et al. 1988; Larsson et al. 1995), suggesting thyroid hormone can influence muscle fibre composition throughout the lifespan of an animal.

### *1.12 Molecular regulation of myosin heavy chain isoform expression*

Expression of the MyHC genes display remarkably dynamic plasticity evidenced by coordinated transition in isoform expression, with single isoforms demonstrating an ability to replace one another, generally in a sequential manner I<IIA<IIX<IIB (Schiaffino and Reggiano 2011; Gundersen 2011). This plasticity in expression of the MyHC genes in response to a variety of stimuli has lead scientists to explore the molecular regulation of such coordinated and dynamic transitions in MyHC isoform expression. Of significant interest are the mechanisms capable of “sensing” external/physiological stimuli and subsequently altering MyHC isoform expression according to the demands placed upon the muscle. In addition, the precise mechanisms by which multiple isoforms are regulated in transitional manner are also of particular interest. Gundersen (2011) provides an excellent current review on the molecular mechanisms involved in “translating” the external/physiological stimuli to molecular changes in expression of the contractile components of the muscle fibre, often termed “excitation-

transcription coupling”. The mechanisms regulating the co-ordinated transition in MyHC isoforms remain less well understood but research has identified three main mechanisms by which co-ordinated regulation of the MyHC isoforms probably occur, along with many more mechanisms identified for regulating individual isoforms (Schiaffino and Reggiano 2011). Briefly, the three mechanisms include 1) transcriptional regulatory factors influencing gene expression, by activation or repression, of MyHC genes, 2) miRNA embedded within the introns of MyHC genes that subsequently influence expression of other MyHC isoforms, and 3) bi-directional promoters co-regulating sequentially located MyHC isoform genes using antisense RNA mediated inhibition of neighboring isoforms. In addition, a fourth mechanism may exist and relates to how sequence variation in promoter response elements of the MyHC isoform promoters influence the selective binding of transcriptional regulatory factors and subsequently influence MyHC isoform gene expression. However, such work requires extending to identify the role of sequence variation between MyHC promoters in regulating the coordinated regulation of multiple MyHC isoforms.

### *1.13 Regulation of the slow myosin heavy chain isoforms*

The regulation of the slow-twitch oxidative muscle fibre phenotype has been thoroughly examined with several well established mechanisms of regulation being reported. A transcriptional co-regulator, peroxisome proliferator-activated receptor gamma co-activator 1 alpha (PGC1- $\alpha$ ), and two nuclear receptors, peroxisome proliferator-activated receptor delta (PPAR $\delta$ ) and estrogen receptor-related receptor gamma (ERR $\gamma$ ), have been identified as

“master regulators” of a slow muscle phenotype (Lin et al. 2002; Narker et al. 2011; Wang et al. 2004). Transgenic mice over-expressing PGC1- $\alpha$ , exclusively in skeletal muscle, display an increase in expression of type I MyHC, with a concomitant increase in mitochondrial biogenesis and increased expression of oxidative enzymes. In addition, a repressive counterpart to PGC1- $\alpha$ , RIP140 (nuclear receptor interacting protein; NRIP1), causes the opposing effects, namely a reduction in type I MyHC expression and reduced oxidative enzyme expression (Seth et al. 2007). Thus, the ratio of PGC1- $\alpha$  to RIP140 may be critical in determining the “activity” of transcription factors inducing expression of the type I MyHC isoform and an oxidative muscle fibre phenotype. It is suggested that these transcriptional co-regulators (PGC1- $\alpha$  and RIP140) interact with nuclear receptors such NFAT, MEF2, and PPAR transcription factors to influence transcriptional activity of “slow” muscle target genes (Lin et al. 2002; Seth et al. 2007).

Expression of the nuclear receptor, ERR $\gamma$ , is highly abundant in mammalian skeletal muscle and exclusively accumulates in the type I muscle fibres. Forced over-expression of this factor in mouse skeletal muscle identified it as a “master regulator” of a slow muscle phenotype, displaying a striking coordinated induction of slow, type I and IIA MyHC isoforms (with a modest concomitant reduction in MyHC IIB) and increased the expression of enzymes involved in oxidative metabolism (Narker et al. 2011). Similar results have been obtained by generating a transgenic mouse over-expressing the nuclear receptor, PPAR $\delta$  (Wang et al. 2004). Expression of PPAR $\delta$  is highly abundant in skeletal muscle (compared to the other PPAR $\alpha$  and PPAR $\gamma$  isoforms) and is selectively expressed in slow-twitch muscles, indicating a role in fibre type

specification. Over-expression of PPAR $\delta$  in transgenic mice induced a switch to a slow muscle fibre type (expressing more type I fibres), increased mitochondrial biogenesis and increased expression of enzymes involved in oxidative metabolism (Wang et al. 2004).

#### *1.14 Regulation of the fast myosin heavy chain isoforms*

Relative to the mechanisms discovered that regulate the slow MyHC isoforms (or a slow muscle phenotype), transcriptional mechanisms regulating the fast contractile MyHC isoforms (IIA, IIX and IIB) remain poorly understood. Indeed, only a few studies exist in this area and most of which are yet to be repeated or confirmed by others.

Grifone et al. (2004) reported that the transcription factor Sine Oculis Homeobox 1 (SIX1) and a transcriptional co-activator Eyes Absent 1 (EYA1) are co-expressed in the nuclei of fast twitch (IIX and IIB) muscle fibres in mice. They demonstrate that SIX1 and EYA1 act synergistically when over-expressed in slow muscle fibres to replace type I and IIA MyHC isoforms with type IIX and IIB isoforms. In addition to the MyHC transitions induced by the co-operative actions of SIX1 and EYA1, they also induce a coupled switch in metabolic gene expression towards a more glycolytic expression profile, demonstrating that SIX1 and EYA1 can coordinately regulate a fast-glycolytic muscle fibre type.

The myogenic regulatory factors MyoD and Myogenin, have been shown to preferentially accumulate in fast and slow muscle respectively (Voytik *et al.*, 1993; Hughes *et al.*, 1993; Ekmark *et al.*, 2007). However, MyoD remains the only factor to be explored in terms of its role in muscle fibre type regulation

and has been shown to induce specific activation of the MyHC IIB promoter (Wheeler et al. 1999; Allen et al. 2001; Ekmark et al. 2007). Interestingly, myogenic regulatory factors bind E-box response elements, that are present on all MyHC gene promoters, and it remains unknown how these factors, such as MyoD, can elicit specificity in terms of transcriptional induction of MyHC isoforms. Ekmark et al. (2007) however, did highlight that MyoD induced activation of the fast MyHC genes is dependent on de-phosphorylation of MyoD, which is regulated by neural input or contractile activity. Other mechanisms regulating the actions of the myogenic regulatory factors on MyHC gene regulation warrant exploration, as information in this field remains sparse.

Various stimuli that cause muscle hypertrophy, such as IGF-I signaling, myostatin signaling, and beta-adrenergic signaling, have been shown to induce fast MyHC isoform expression, although the mechanisms regulating these effects remain poorly understood. IGF-1 can induce a MyHC IIB promoter-reporter construct in C2C12 muscle cells (Shanely et al. 2009). However, IGF-I appeared to accelerate differentiation, which could subsequently induce an early expression of all MyHC genes, suggesting a potentially indirect and perhaps non-isoform specific induction of the MyHC IIB gene by IGF-I signaling.

Myostatin, a TGF-beta family member, has been shown to be a fundamental negative regulator of myogenesis and muscle growth (Thomas et al. 2000; Langley et al. 2002). Myostatin knockout mice display profound muscle hypertrophy and hyperplasia with increased IIB muscle fibres and specific hypertrophy of type IIB fibres (Matsakas et al. 2010). Hence it is plausible that



molecular signals driving muscle hypertrophy may also regulate MyHC isoform expression towards the fast type II isoforms. However, the mechanisms regulating the increased abundance of IIB fibres in myostatin knockout animals remain elusive.

Beta-adrenergic signaling also presents a potent anabolic effect in muscle (Ryall et al. 2002; 2004; Kline et al. 2007) and is associated with a transition from the slow to fast MyHC isoforms in a variety of species (Baker et al. 2006; Bricout et al. 2004; Depreux et al. 2002; Oishi et al. 2002; Gunawan et al. 2007). The mode of action of beta-adrenergic signaling on muscle growth and MyHC isoform regulation remains poorly understood and was therefore explored in this thesis. Specifically, transitions in MyHC isoform expression in response to beta-adrenergic stimulation were examined across a broad time course to fully characterize the dynamic plasticity in transitions of these isoforms in adult muscle. Interestingly, the role of beta-adrenergic signaling during myogenesis remains relatively unexplored in comparison to the volume of work conducted *in vivo* and was therefore a focus of this thesis. Ryall et al. (2010) recently highlighted a substantial yet acute up-regulation of beta-adrenergic receptor mRNA expression specifically during early myogenic fusion, suggesting a potential role for beta-adrenergic signaling during myogenesis. Moreover, the majority of studies examining alterations in MyHC isoform expression in response to beta-adrenergic signaling have been conducted in adult muscle and not during myogenesis. Therefore this thesis aimed to extend this work in myoblasts undergoing differentiation to assess the role of beta-adrenergic signaling on myogenesis and the initial induction of MyHC isoform gene expression during myoblast differentiation.

### 1.15 Bi-directional promoters in myosin heavy chain gene clusters

A *cis* acting mechanism has been identified that implicates bidirectional promoters, located between MyHC genes, which coordinately regulate expression of multiple MyHC isoforms under a single promoter (Pandorf et al. 2006; Haddad et al. 2008; Rinaldi et al. 2008; see Figure 1.7).

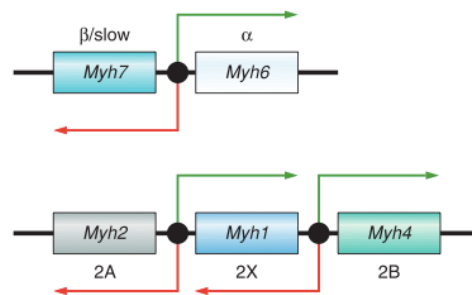


**Figure 1.7** Schematic depiction of the MyHC bi-directional promoters from a recent review by Schiaffino and Reggiano (2011).

The majority of MyHC genes are located as two clusters on separate chromosomes and are organized in a sequential pattern (i.e. slow to fast isoforms), separated by non-protein coding DNA. Several reports have highlighted a concomitant up-regulation of an upstream MyHC antisense transcript following induction of its nearest downstream sense transcript (Pandorf et al. 2006; Haddad et al. 2008; Rinaldi et al. 2008). It is postulated that the generation of an upstream antisense transcript can regulate expression of the corresponding upstream MyHC isoform gene(s), thus coordinating the sequential transitions in expression often exhibited by MyHC isoforms. Rinaldi et al. (2008) demonstrated that a down-regulation of the MyHC IIB sense transcript in response to resistance exercise produces a concomitant down-regulation of the IIX antisense, which the authors proposed was

responsible for permitting the subsequent up-regulation of the IIX MyHC isoform transcript. Identification of a bidirectional promoter in the cardiac MyHC gene cluster has also been identified and was shown to be responsive to thyroid hormone during neonatal rat development (Haddad et al. 2008). The authors implicate this bidirectional promoter in causing an increase in alpha MyHC sense transcript and a concomitant increase in beta-MyHC antisense transcript, which subsequently causes a down-regulation of beta-MyHC gene expression. Taken together, it would appear that intergenic bidirectional promoters might provide a putative *cis* acting mechanism that coordinately regulates MyHC isoforms located in the same cluster (Pandorf et al. 2006; Haddad et al. 2008; Rinaldi et al. 2008). However, these results have all been produced from the same laboratory and are yet to be replicated by others, at least in the available literature. Furthermore, mechanisms of MyHC antisense regulation of neighboring MyHC genes remain to be elucidated.

#### *1.16 Intronic miRNA's in myosin heavy chain gene regulation*

Recent reports have illustrated that MyHC genes do not only encode their respective contractile protein, but also contain intronic sequences encoding miRNA's involved in the complex regulation of MyHC isoform expression (Rooij et al. 2008; 2009). Specifically, miR-208b and miR-499, encoded by an intronic region of the MyHC-beta (type I) and MyHC-7b (slow-tonic) respectively, are exclusively expressed in slow muscles (Rooij et al. 2009). A double knockout of both miR-208b and miR-499 in mice resulted in a transition from slow to fast MyHC isoform expression, reducing slow and increasing fast MyHC isoform expression (Rooij et al. 2009). In contrast,

forced over-expression of miR-499 caused a transition from fast to slow MyHC isoform expression, confirming the role of miR208b and miR-499 in regulating a slow muscle fibre phenotype. The identification of intronic miRNA in MyHC genes has exposed another level of complexity in the regulation of MyHC expression, a field that will likely continue to expand rapidly (Rooij et al. 2008).

#### *1.17 Myosin heavy chain promoter response elements*

Analysis of the promoter region upstream of the MyHC genes has revealed insights into regulatory mechanisms controlling the expression of these genes, both *in vitro* and *in vivo* (Takeda et al. 1992; Wheeler et al. 1999; Allen et al. 2001; 2005). In particular, comparisons of proximal promoter sequence variation amongst the three fast MyHC promoters (IIA, IIX and IIB) from mice has shown several highly conserved regions (AT-2, CArG-box and E-box) that serve a regulatory role in controlling individual MyHC isoform gene expression (Allen et al. 2001; see Figure 1.8 below).

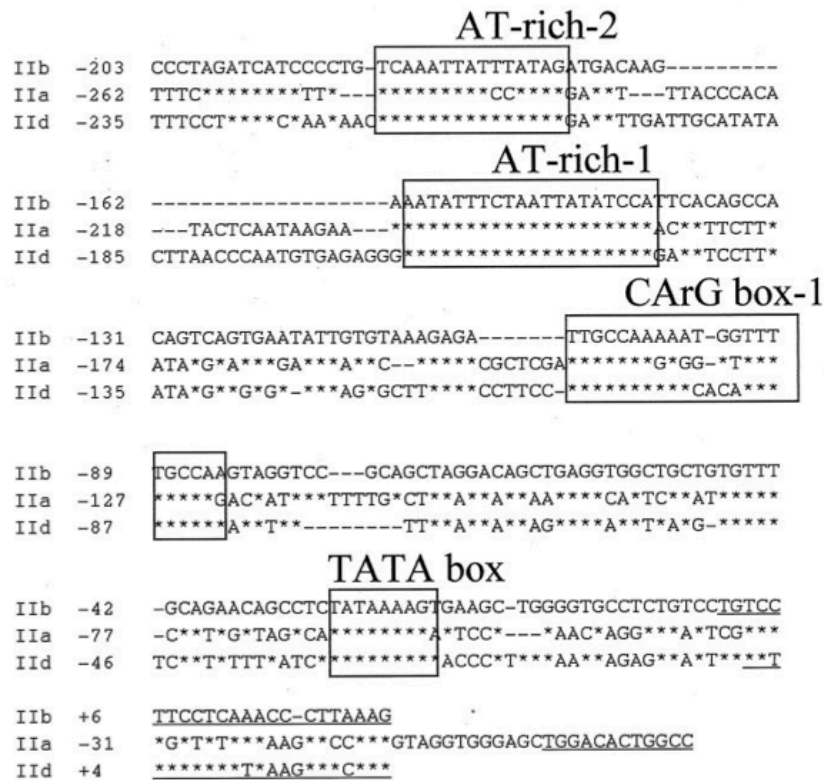


**Figure 1.8** Characterized response elements that play a critical role in MyHC promoter activity (from Allen et al. 2001)

Furthermore, it has been reported that the subtle sequence differences in these highly conserved regions (AT-2 and CARg-box) between the IIA, IIX and IIB MyHC promoters confers a specific regulatory control of the corresponding promoter activity (Allen et al. 2005). The AT-2 and CARg-box regions have been thoroughly examined in the context of the mouse MyHC IIB promoter, with reports showing that the AT-2 region interacts with MEF2 and Oct1 proteins, and the CARg-box interacts with SRF (Allen et al. 2005; Lackich et al. 1998). However, such work needs to be continued to elucidate how promoter sequence variation, between MyHC isoform promoters, permits coordinated regulation of multiple MyHC isoforms. For instance, Allen et al. (2005) show that sequence variation within the CARg-box response element between the MyHC IIB and IIX promoters determine whether this site is bound

by activating or repressing transcriptional regulatory factors, respectively. Thus, sequence variation within conserved response elements may exist as a mechanism to allow differential regulation of different MyHC isoforms. With this in mind, there is significant variation in sequence amongst the same MyHC promoters from different species and this may therefore confer differential expression profiles of MyHC genes between species. Therefore, studying MyHC promoters from a variety of different species and attempting to elucidate signaling pathways altering activity of MyHC promoters at the molecular level would continue to advance the field of muscle fibre type regulation.

#### *1.18 Summary and objectives of this thesis*

It is clear that our understanding of skeletal muscle biology and muscle fibre type has increased tremendously over the last century and continued advances in analytical methods will likely see our understanding improve further over the coming years. In particular, further advancements in the use of molecular and cell biology is beginning to advance our understanding of the mechanistic biology that underpins the regulation of specific components of the muscle fibre. Research investigating the regulation of muscle fibre type has traditionally been conducted *in vivo*, analyzing global changes at a whole muscle level. Broadly, this thesis aimed to explore more “molecular” approaches, utilizing *in vitro* cell biology and molecular biology to understand the expression and regulation of myosin heavy chain (MyHC) isoforms as an indicator of muscle fibre composition. Given the critical role of specific MyHC isoforms to dictate the contractile and metabolic characteristics of skeletal

muscle fibres, an understanding of the mechanisms regulating these genes is of broad importance.

The *in vitro* work within this thesis was conducted using the mouse C2C12 skeletal muscle cell line, probably the most commonly used muscle cell line in muscle biology labs across the world. Since muscle fibre type research is typically conducted *in vivo*, very little is known about the use of a cell line for studying fibre “type”. A few studies conducted in the late 1980’s attempted to examine the expression of MyHC isoforms during myogenesis in cultured muscle cells (Silberstein et al. 1986; Weydert et al. 1987; Miller 1990). However, these studies used relatively non-specific antibodies and therefore did not fully elucidate MyHC isoform expression profiles during myogenesis. To better understand whether the C2C12 cell line is a suitable *in vitro* model for studying MyHC regulation as an indicator of muscle fibre composition, endogenous expression of the MyHC isoforms must first be characterized. This body of work was the first objective of this thesis and set out to establish if the C2C12 cell line can be used to study the regulation of MyHC isoforms *in vitro*. Moreover, this work specifically intended to provide a detailed characterization of MyHC expression during C2C12 myogenesis, permit an understanding of the C2C12 cell as a representative model for studying MyHC expression and ultimately to provide a foundation of knowledge to support future experiments to be conducted in this thesis and by others. In addition to the MyHC isoform expression profiles, other important characteristics of the C2C12 cell line were established, including metabolic gene expression and markers of proliferation and differentiation, to fully understand how the C2C12 cell line can be utilized in future experiments.

In addition to characterizing the endogenous expression of MyHC isoforms in the C2C12 cell line, it was important to validate whether regulation of MyHC isoform expression *in vitro* would mimic the regulation in adult muscle *in vivo*. Therefore, this thesis aimed to examine whether the dynamic plasticity of MyHC isoform gene expression *in vivo* could be mimicked in the C2C12 cell line. To test this, the beta-adrenergic agonist Ractopamine, a potent stimulator of dynamic transitions in MyHC isoform gene expression (Baker et al. 2006; Bricout et al. 2004; Depreux et al. 2002; Oishi et al. 2002; Gunawan et al. 2007), was utilized both *in vivo* and *in vitro*. Furthermore, this work would elucidate whether a role for beta-adrenergic signaling in regulating MyHC isoform expression during early myogenesis exists, something that currently remains unknown.

Finally, this thesis attempted to utilize the C2C12 cell line as a host environment for a “molecular” based approach to understand a physiological difference in muscle fibre phenotype between two large mammals, the pig and the human. The molecular mechanisms regulating the species-differential expression of the MyHC IIB isoform, which is partly attributable to the vastly different muscle physiology displayed between these two mammals, was explored *in vitro* using the C2C12 cell line as a common MyHC IIB expressing environment. In particular, this body of work would establish the role of sequence variations between the pig and human MyHC IIB promoters in controlling the strength of promoter induction during myogenesis. Such work therefore aimed to elucidate why pigs have a very unique muscle fibre physiology amongst large mammals and this work would follow a molecular and cell biology based approach.



In summary, this thesis intended to conduct the following body of work:

1. Characterize the C2C12 cell line to...
  - a. Establish the endogenous MyHC isoform expression and determine whether the C2C12 cell line can be utilized for research into the molecular mechanisms regulating MyHC isoform expression.
  - b. Provide a useful foundation of knowledge, including biomarkers of myogenesis, MyHC expression profiles and metabolic gene expression, to underpin future experiments to be conducted in this thesis, and by others.
2. Validate whether the C2C12 cell line can mimic the plasticity of MyHC isoform expression profiles that occur *in vivo* when exposed to a known regulator of muscle fibre type transitions (Beta-adrenergic agonist, Ractopamine). Furthermore, such work should elucidate whether beta-adrenergic signaling has a direct role in MyHC isoform regulation during myogenesis.
3. Examine whether the C2C12 cell line can be used as a host environment for molecular based approaches to understand the regulation of MyHC isoforms. Specifically, this work will aim to elucidate the molecular mechanisms controlling the species-differential expression of MyHC IIB between pigs and humans.

It was hypothesized that the C2C12 skeletal muscle cell line would provide an interesting and valid *in vitro* tool for studying the molecular regulation of myosin heavy chain isoforms as an indicator of muscle fibre composition.

# 2

## MATERIALS AND METHODS

---

## 2. MATERIALS AND METHODS

### 2.1 CELL CULTURE

#### *2.1.1 Overview*

*In vitro* experiments were conducted using the C2C12 cell line. C2C12 cells are an immortalized muscle cell line from the mouse hind limb, sub-cultured to retain differentiation potential following prolonged cultivation (Yaffe 1968). Due to these characteristics, this cell line is commonly used for *in vitro* muscle biology research.

#### *2.1.2 Culturing C2C12 cells*

C2C12 myoblasts were cultured in growth medium (Dulbecco's modified eagle medium (DMEM; Sigma Aldrich, Poole, UK), 10% fetal bovine serum (FBS; Invitrogen, Paisley, UK), 1% penicillin and streptomycin (P/S; Invitrogen, Paisley, UK)). In order to prevent C2C12 myoblasts exiting the cell cycle, myoblasts were maintained at sub confluence (<70% confluent) to allow expansion by serial passaging. C2C12 myoblasts were encouraged to differentiate at near confluence by replacing the medium with a low serum differentiation medium (DMEM, 2% horse serum (Invitrogen, Paisley, UK) and 1% P/S) and cultured for up to 8 days. Myoblasts would fuse to form multinuclear myotubes within 4-8 days of differentiation. Culture medium was changed every 48 hours to remove harmful waste products, maintain a suitable pH and replenish nutrients required for growth.

### *2.1.3 Passaging cells*

If left to grow, proliferating C2C12 myoblasts would proliferate to cover the entire surface of a T75 cell culture flask. If C2C12 myoblasts reach this confluent state, they exit the cell cycle and terminally differentiate. To maintain C2C12 myoblasts in a proliferative state, cells were transferred to a new flask at a lower density to continue growth (passaged). Briefly, cell culture medium was removed from proliferating myoblasts (less than 70% confluent) and cells were washed with warm PBS (10ml). Cells were dislodged by incubating with Trypsin-EDTA (2ml; warm) at 37°C for ~5 minutes. Trypsin-EDTA was neutralized by the addition of DMEM containing 10% fetal bovine serum (8ml). The cell suspension was centrifuged at 1000rpm for 5 minutes and the cell pellet was re-suspended in 10ml of growth medium. Approximately 1/10<sup>th</sup> of the cells were transferred to a new T75 flask, providing 2 days of sub-confluent growth.

### *2.1.4 Counting cells*

Myoblasts in suspension were counted using a haemocytometer. Cell number per ml of culture medium was calculated (see formula below) to ascertain the volume of cell suspension required to provide the appropriate cell number for seeding cells into culture plates.

(Desired cell number / total cell number) X volume of cell suspension =  
volume required

### *2.1.5 Freezing cells*

C2C12 myoblasts were frozen in liquid nitrogen to be used in later experiments. Briefly, cells were dislodged from the culture flask and pelleted (as described above in “*passaging cells*”). Cells were re-suspended in freezing medium (fetal bovine serum with 10% DMSO) in cryovials and slowly frozen (using polystyrene insulation) at -80°C overnight before being transferred to liquid nitrogen.

### *2.1.6 Measuring myotube diameters*

Images of myotubes containing a ZsGreen fluorescence reporter (controlled by a differentiation specific promoter (MyHC IIB)) were analysed for myotube diameters using Q-Capture Pro (version 7). Images of myotubes were blind labelled for analysis, removing bias when analysing treated and non-treated myotube diameters. For each field of view, 10 myotube diameters were measured at 25%, 50% and 75% of the total myotube length (providing an average myotube diameter per myotube). Analysis of 5 fields of view per well (n=4 wells) of a 24-well plate was conducted to give an average myotube diameter for 200 myotubes per treatment. Examples of the image analysis software are shown below (Figure 2.1). Note that diameters were measured perpendicular to the myotube length (estimated by eye only). Myotube diameters were analysed on raw images captured using a fluorescence microscope and were initially measured as “number of pixels”. Myotube diameters (in number of pixels) were subsequently converted to  $\mu\text{m}$  by dividing the number of pixels covering  $1\mu\text{m}$  (1.96 pixels) on an image of a haemocytometer at the same magnification.

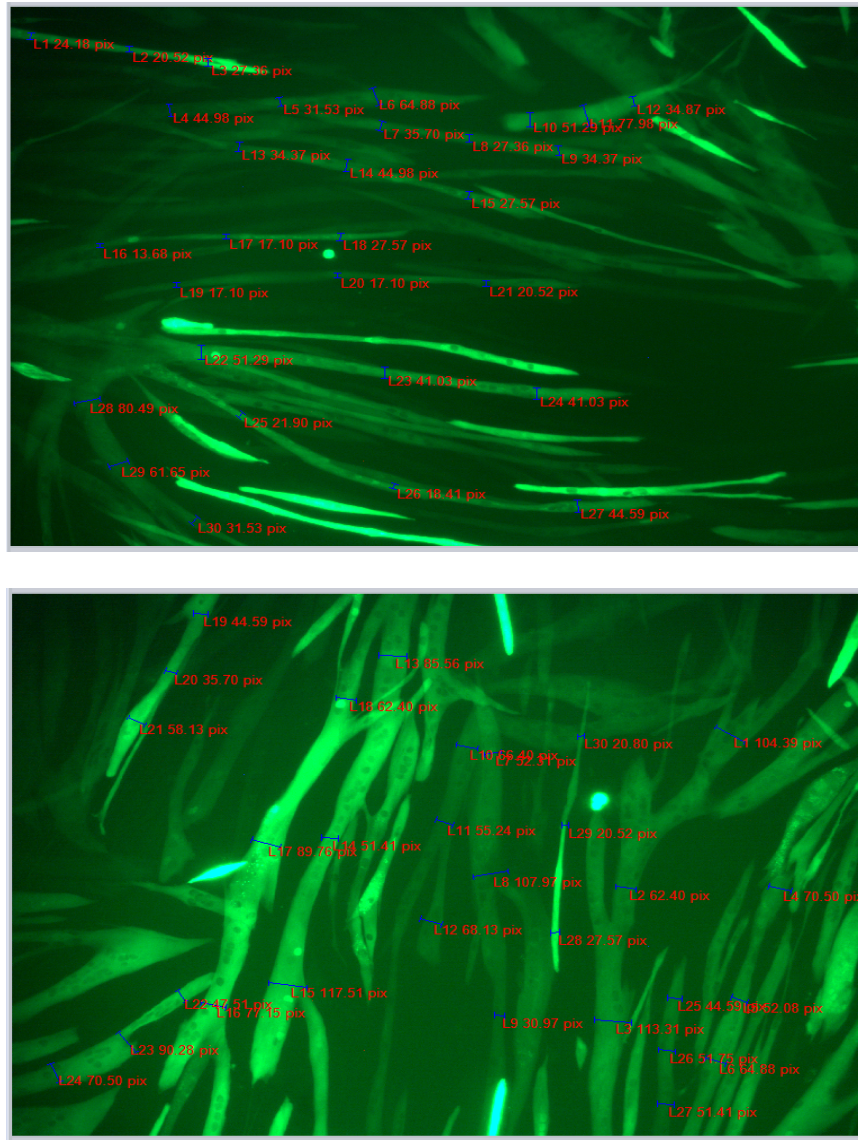


**Figure 2.1** Representative images of myotube diameter analysis using Q-Capture Pro (version 7). Blue lines indicate measurements at 25%, 50% and 75% of total myotube length for 10 myotubes per field of view. Red text is the myotube measurements in number of pixels.

### *2.1.7 Lowry assay - measurement of total protein content*

A Lowry assay was conducted to determine the total protein content of cells cultured in multi-well plates. Cells were washed in warm PBS, scraped into 500µl tri-sodium citrate (0.05 M; pH 6.8; 4°C) and frozen at -20°C until use. Fifteen microliters of each sample (quantity loaded was optimized to fit on the standard curve) was loaded onto a clear 96-well flat-bottomed plate and combined with 150µl of 0.1M NaOH and 35µl dH<sub>2</sub>O. Serial dilutions of a known concentration of bovine serum albumin (BSA; 0-60µg) were loaded onto the 96-well plate to generate a standard curve for quantifying protein concentration. Following the loading of samples and standards, 50µl of Reagent 1 (see Table 2.1) was added to each well and incubated at room temperature for 5 minutes. Subsequently, 50µl of Reagent 2 (see Table 2.2) was added to each well and incubated at room temperature for 20 minutes prior to measuring absorbance (optimal wavelength = 620nm; BioRad 680XR Microplate reader).

**Table 2.1** Composition of Lowry Reagent 1

	Volume required (ml)
2% Na <sub>2</sub> CO <sub>3</sub> in 0.1M NaOH	5
1% CuSO <sub>4</sub>	0.5
2% KNa tartrate	0.5

**Table 2.2** Composition of Lowry Reagent 2

	Volume required (ml)
Folin and cioculteaus phenol reagent	0.5
0.1M NaOH	5

#### *2.1.8 Creatine kinase assay: marker of myogenic differentiation*

Creatine kinase activity was assayed as a marker of myogenic differentiation using the CK kinetic assay kit (Thermo Electron Corporation, Fisher Scientific, Loughborough, UK). Others have shown that CK activity is reflective of differentiation status (Sharples et al. 2010). Cells were harvested as described above for the Lowry assay. Cells were lysed by sonication on ice (10 seconds at 10 amplitude microns). Ten microliters of each sample (lysed cells) was loaded onto a 96 well plate. Solution A and B, from the CK assay kit, were combined and 200µl of the combined solution were added promptly to each well. Absorbance was read at 340 nm at 37°C every 5 min for 30 min and rate was determined, indicating creatine kinase activity.

#### *2.1.9 DNA assay – marker of cell number*

DNA content of cultured cells was used as a marker of cell number. DNA in 50µl of lysed C2C12 cells was stained using Hoechst dye and assayed using a fluorescence platereader (excitation at 350 nm and emission at 460 nm; Fluostar Optima, BMG Labtech). Lysed cells (by previous sonication) were assayed in 1x TNE (100mM Tris, 1M NaCl, 10mM EDTA; pH 7.4) containing 1mg/ml Hoechst dye. A standard curve was generated using serial dilutions of calf thymus DNA (from 40µg/ml to 0.6µg/ml) and used to quantify DNA content in the lysed cells. DNA content was assayed following the measurement of creatine kinase activity from the same samples, as creatine kinase activity was sensitive to freeze thawing. This allowed for creatine kinase activity to be analysed relative to DNA content (cell number).



## 2.2 GENE EXPRESSION ANALYSIS

### *2.2.1 Overview*

To assess changes in gene expression, total RNA was extracted from the samples of interest, RNA was reverse transcribed to form cDNA, and specific transcripts of interest were amplified by Q-RT-PCR to quantify relative gene expression (using the standard curve method).

### *2.2.2 RNA extraction from cells*

Total RNA was extracted from cells using an RNA isolation kit (Roche High Pure Isolation Kit for RNA isolation). To lyse the cells and precipitate the RNA, 400µl of lysis-binding solution was added directly to the frozen cells, allowed to thaw, and then vortexed for 15 seconds. The 600µl sample was centrifuged through a spin column at 8000xg for 15 seconds (at room temperature for all centrifugations). The flow through was discarded after each step. RNA caught on the membrane of the spin column was treated with 10µl DNase I and 90µl of DNase-incubation buffer for 15 minutes at room temperature. 500µl of wash solutions I and II (containing ethanol to ensure the RNA was precipitated and thus remained in the spin-column membrane) were passed through the spin column via centrifugation at 8000xg for 15 seconds. A further 200µl of wash solution II was passed through the column via centrifugation at 13000xg for 2 minutes to ensure all contaminants were removed from the RNA on the spin-column membrane. Finally, the RNA was eluted in 50µl of RNase-free H<sub>2</sub>O into a fresh 1.5ml tube via centrifugation at 8000xg for 1 minute and stored at -80°C.

### 2.2.3 RNA extraction from porcine skeletal muscle

Due to the fibrous nature of skeletal muscle, a more robust method, compared to that used for cells, was required for RNA extractions from skeletal muscle. One hundred milligrams of crushed *Longissimus Dorsi* (LD) muscle tissue was homogenized in 1ml Trizol reagent (Invitrogen) and centrifuged at 12,000xg for 10 minutes at 4°C. The supernatant was transferred to a fresh tube, incubated at 20°C for 5 minutes before the addition of 200µl chloroform. The sample was shaken by hand, incubated at 20°C for 3 minutes before being centrifuged at 12,000xg for 15 minutes at 4°C. The colorless aqueous phase was transferred to a fresh tube, mixed with 250µl isopropanol and 250µl high salt precipitation solution (0.8M Sodium Citrate/ 1.2M NaCl), incubated for 10 minutes at 20°C and then centrifuged at 12,000xg for 10 minutes at 4°C. The supernatant was discarded, the RNA pellet was washed with 1ml 75% ethanol and then re-centrifuged at 7,500xg for 5 minutes at 4°C. The supernatant was removed, the RNA pellet was air-dried, re-suspended in 40µl water with 5µl DNase 10x buffer (Promega) and 5µl DNase (1U/µl; Promega) and incubated for 30 minutes at 37°C. Following incubation, 150µl water and 200ul Phenol/Chloroform/Isoamylalcohol were added to the DNase-treated RNA, mixed and centrifuged at 12,000xg for 5 minutes. The upper layer was transferred to a fresh tube with 15µl NaAc (3M) and 375ul ethanol and was precipitated at -80°C overnight. Following precipitation, the RNA was pelleted via centrifugation, washed in 75% ethanol and re-suspended in water as previously described above. RNA was stored at -80°C until used. RNA concentration was determined using a Nanodrop ND-1000 (Thermo Scientific,

Wilmington, USA) and concentrations were adjusted to 100ng/μl for cDNA synthesis.

#### *2.2.4 RNA integrity check*

As an indicator of RNA integrity, ribosomal RNA (18S and 28S) bands were visualised by agarose gel electrophoresis to ensure bands were intact and not degraded. Furthermore, RNA concentration and purity was checked using a Nanodrop® ND-1000 (Thermo Scientific, Wilmington, USA). A 260/280 ratio of ~2.0 was suggestive of pure RNA (with minimal contaminants).

#### *2.2.5 cDNA synthesis (Using Promega reagents)*

RNA concentration was quantified using a Nanodrop® ND-1000 (Thermo Scientific, Wilmington, USA) and concentrations were adjusted to 100ng/μl. First strand cDNA synthesis was carried out by combining 5μl of RNA (500ng) with 1μl of random primers (500μg/ml; Promega, Southampton, UK) and 9μl of RNase-free H<sub>2</sub>O (total volume 15μl) and incubated at 70°C for 5 minutes and then placed immediately on ice. On ice, 5μl Moloney Murine Leukemia Virus (MMLV) reverse transcriptase buffer (5X), 1μl of MMLV reverse transcriptase (200U/μl), 1.25μl of dNTP's (10mM each), 0.5μl RNasin (RNase inhibitor; 40U/μl; all Promega, Southampton, UK) and 2.25μl RNase-free H<sub>2</sub>O were added to each reaction (total volume 25μl), vortexed and incubated for 10 minutes at room temperature followed by 1 hour at 42°C. Following incubation, cDNA was diluted 4-fold by the addition of 75μl RNase-free H<sub>2</sub>O and stored at -20°C. All synthesized cDNA was tested by

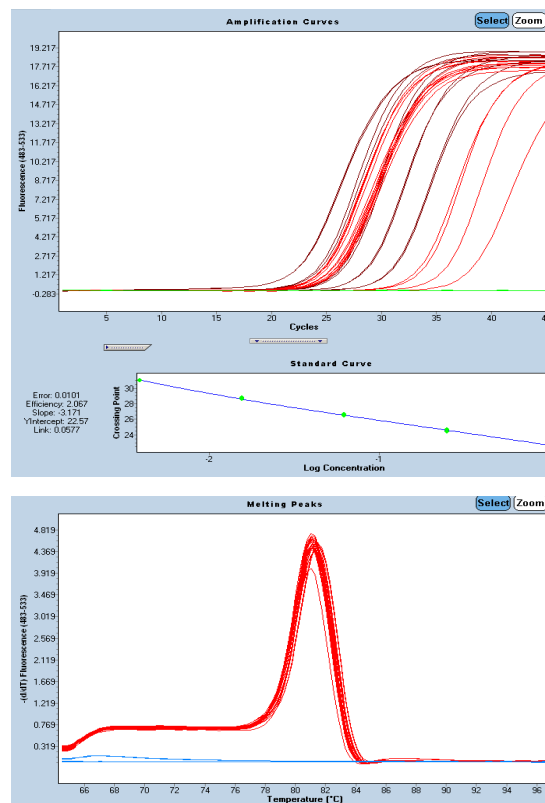
conducting a single Q-RT-PCR reaction using a validated primer set to ensure every sample contained cDNA.

#### *2.2.6 cDNA synthesis (using Roche reagents)*

Suppliers for cDNA synthesis reagents were changed for improved cost effectiveness but all experiments were conducted using reagents from only one supplier. First strand cDNA synthesis was carried out using a cDNA synthesis kit (Transcriptor First Strand cDNA Synthesis Kit, Roche, Burgess Hill, UK). In thin walled PCR tubes, 500ng total RNA was incubated in a total volume of 13µl with a final concentration of 60µM random hexamer primers at 65°C for 10 minutes. The reaction was immediately cooled on ice. Whilst on ice, Transcriptor Reverse Transcriptase Reaction Buffer (5X concentrated), Deoxynucleotide Mix (final concentration 1mM each), 10 U Transcriptor Reverse Transcriptase and 20 U Protector RNase Inhibitor were added to the initial reaction, to a final volume of 20µl. The reaction mixture was gently pipette mixed and incubated at 25°C for 10 minutes, 55°C for 30 minutes, 85°C for 5 minutes and then immediately placed on ice. The cDNA was diluted 5-fold to give 100µl “stock” cDNA for Q-RT-PCR and stored at -20°C until analysis. All synthesized cDNA was tested by conducting a single Q-RT-PCR reaction using a validated primer set to ensure every sample contained cDNA.

### *2.2.7 Quantitative RT-PCR*

Real time PCR was conducted on a Lightcycler 480® (Roche, Burgess Hill, UK) to assess the relative abundance of specific mRNA's. Reactions were carried out in triplicate on 384 well plates. Each well contained 5µl of cDNA with the following reagents: 7.5µl SYBR green master mix (Roche, Burgess Hill, UK), 0.45µl forward and reverse primers (10µM each; final concentration 0.3µM each) and 1.6µl RNase-free H<sub>2</sub>O (total volume of 15µl per well). Samples were pre-incubated at 95°C for 5 minutes followed by 45 PCR amplification cycles (de-naturation: 95°C for 10 seconds; annealing: 60°C for 15 seconds; elongation: 72°C for 15seconds). A standard curve was produced using serial dilutions (typically 1:8) of a pool of cDNA made from all samples to check the linearity and efficiency of the PCR reactions (see Figure 2.2). PCR efficiency was between 1.8 and 2.1 for all primers. Relative transcript abundance was determined using the standard curve and was corrected for the quantity of cDNA in each reaction.

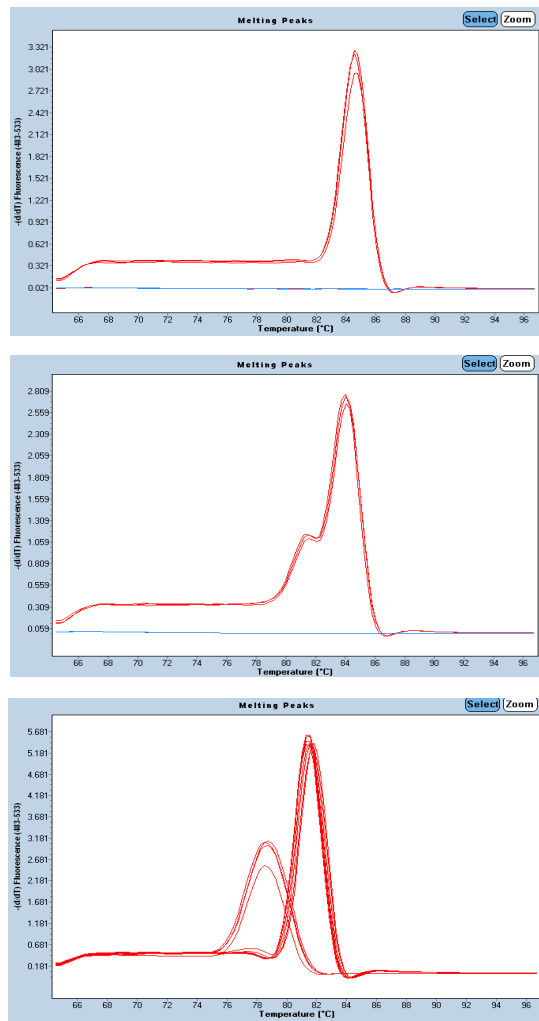


- Standard curve using serial dilutions (1:8) of pooled cDNA samples (brown lines)
- Sample cDNA expression curves are expressed within the range of the standards
- PCR linearity check (linear slope)
- Optimal gradient = 3.3
- Optimal efficiency = 2.0
- Melt curve analysis of samples in the above expression curves (one peak indicates only one amplicon was produced)

**Figure 2.2** Outputs from the Roche LightCycler380. Upper panel shows a standard curve, generated by using serial dilutions of the template cDNA in Q-PCR reaction. The standard curve generated confirms the reaction was efficient, producing a linear standard curve which subsequently permits quantification of relative mRNA abundance. The lower panel shows melt curve analysis of the samples used in the upper panel. Only one melt curve peak was produced indicating a single amplicon was generated in the PCR reaction.

### 2.2.8 Testing primers used for quantitative RT-PCR

Melt-curve analysis for all primer sets was conducted on cDNA (derived from the appropriate species) to ensure only one amplicon was being produced in the PCR reaction and that no primer-dimers were forming (see Figure 2.3). Amplicons were separated by horizontal agarose gel (1.5%) electrophoresis following Q-RT-PCR for all primers to ensure a) only one amplicon was being produced by the PCR reaction (i.e. no miss-amplified products or primer-dimers), b) that the amplicon produced was of the correct length, and c) that no amplicon was produced in the absence of template cDNA.



- Clean melt curve analysis
- Single peak indicates only one amplicon was produced

- Non-specific amplification
- Two melt curve peaks (indicates two amplicons have been produced)

- Primer-dimers in non-template control (smaller peak)

**Figure 2.3** Examples of melt curve analysis outputs to assess the number of amplicons produced in the Q-PCR reaction. The upper panel shows a single peak indicating only one amplicon was produced. The middle panel shows two peaks, which indicates some non-specific binding and the generation of two amplicons in the Q-PCR reaction. The lower panel shows a single peak for samples with cDNA and a different peak for the non-template controls, suggesting the formation of primer-dimers in the absences of cDNA template.

### *2.2.9 Oligreen quantification of total cDNA*

Due to the broad time course studied for cell culture work (from myoblasts to mature myotubes) quantifying mRNA transcript abundance relative to a housekeeper gene was not possible as unpublished data from this laboratory suggests that no housekeeper gene remains constant across the entire time course investigated. Thus, total cDNA concentration was determined and mRNA transcript abundance was corrected for total cDNA.

Total cDNA quantification was conducted on a Lightcycler 480® (Roche, Burgess Hill, UK) using Oligreen (Invitrogen, Paisley, UK), shown to specifically bind with single stranded DNA molecules (Rhinn et al. 2008). Reactions were carried out in triplicate on 384 well plates. 5µl Oligreen was added to 995µl 1x TE buffer to make the working Oligreen solution. Each well contained 5µl of cDNA plus 5µl Oligreen working solution. Fluorescence was quantified with increasing temperature (constant ramp rate of 0.11°C/s; up to 95°C). The fluorescence at 80°C was plotted against a standard curve, produced using serial dilutions of a pool of cDNA made from all samples, to determine the relative quantity of cDNA. Normalization using the oligreen method was also used for Q-RT-PCR conducted on cDNA derived from porcine skeletal muscle.



## 2.3 SDS-PAGE OF MYOSIN HEAVY CHAIN ISOFORMS

### *2.3.1 Overview*

The technique described herein was conducted in an attempt to separate porcine myosin heavy chain (MyHC) isoforms by SDS-PAGE (to quantify relative proportions of MyHC isoform expression). Unfortunately, separation of the porcine type II MyHC isoforms was not possible despite getting the method working successfully for other species, such as rat and sheep. The gel compositions presented herein successfully separated rat and sheep MyHC isoforms. A range of variations in these recipes was conducted (not shown).

Antibody approaches were not conducted as porcine specific antibodies do not exist and existing MyHC antibodies for other species have shown poor cross-reactivity between species.

### *2.3.2 Myosin heavy chain protein extraction*

One hundred milligrams of crushed muscle tissue was homogenized at 22,000 rpm in 5ml of extraction buffer (0.5M NaCl, 20mM NaPPi, 50mM Tris Base, 1mM EDTA and 1mM DTT). Samples were placed on ice for 10 minutes prior to centrifugation at 2,500xg (10 minutes at 4°C). The interphase (500µl) was transferred to a separate tube, mixed with 500µl of 87% glycerol and stored at -20°C. Protein concentration was determined by Lowry assay (previously described in this chapter).

### *2.3.3 Sample preparation*

Samples were adjusted to equal concentrations of protein, combined with an equal volume of Laemmli loading buffer (20% (v/v; 87%) glycerol, 125mM

Tris (pH 6.8), 4% (w/v) SDS, 0.02% (w/v) pyronin-Y and 10% (v/v)  $\beta$ -mercaptoethanol), incubated for 10 minutes at room temperature, followed by 10 minutes at 70°C. Two micrograms of protein was loaded per lane on 0.75mm thick SDS-PAGE gels (see section below for gel compositions).

#### 2.3.4 SDS-PAGE gel composition

A range of gel compositions was tested in an attempt to successfully separate all 4 porcine MyHC isoforms by SDS-PAGE. The two tables below show the optimal gel compositions for the separation of rat (Table 2.3) and sheep (Table 2.4) MyHC isoforms. Note that these gels were species-specific and would therefore exclusively separate rat or sheep MyHC isoforms (not both).

**Table 2.3** SDS-PAGE gel for separating rat MyHC isoforms

	Separating gel	Stacking gel
87% Glycerol (ul)	2015	750
49:1 Acrylamide (ul)	1000	250
2M Tris pH 8.8 (ul)	500	
700mM Tris pH 6.7 (ul)		250
50mM EDTA (ul)		200
1M Glycine (ul)	500	
40mg/ml SDS (ul)	500	250
dH <sub>2</sub> O (ul)	435	800
AMPS (100mg/ml) (ul)	50	25
TEMED (ul)	2.5	1.25
Total volume (ml):	5	2.5

**Table 2.4** SDS-PAGE gel composition for separating sheep MyHC isoforms

	Separating gel	Stacking gel
40% Acrylamide (ul)	980	245
2% Bis-Acrylamide (ul)	393	98
2 M Tris pH 8.8 (ul)	500	
1 M Tris pH 6.8 (ul)		175
1 M glycine (ul)	500	
100 mM EDTA (ul)		100
87% glycerol (ul)	1725	863
10% SDS (ul)	200	100
TEMED (ul)	2.5	1.25
AMPS (ul)	50	25
Total volume (ml):	4.4	1.6

### 2.3.5 SDS-PAGE

SDS-PAGE was conducted using Bio-Rad mini-gel tanks. The upper running buffer consisted of 100mM Tris, 150 mM glycine, 0.1% (w/v) SDS, and 10mM  $\beta$ -mercaptoethanol. The lower running buffer was half the concentration of the upper running buffer and did not contain  $\beta$ -mercaptoethanol. Gels were run at 70 volts for 30 hours at 4°C.

### 2.3.6 Fixing and staining gels

Following electrophoresis, gels were stained in fixing solution (30% (v/v) ethanol and 5% (v/v) acetic acid) for 30 minutes. After fixing, gels were stained for 30 minutes in 25% (v/v) isopropanol, 10% (v/v) acetic acid and 0.2% (w/v) Coomassie Blue R250. Gels were de-stained overnight in fixing solution. Images of the gels were obtained to assess MyHC band migration.

## 2.4 MOLECULAR BIOLOGY METHODS

### *2.4.1 Overview*

The methods described herein are a detailed description of the molecular biology techniques used to study the role of the myosin heavy chain (MyHC) IIB promoter sequence in dictating the expression of the MyHC IIB gene in porcine skeletal muscle (Chapter 5).

### *2.4.2 Experimental design summary*

Approximately 1kb of the pig and human myosin heavy chain IIB (MyHC IIB) promoters (-961bp to +32bp, relative to the TATA box) was generated by polymerase chain reaction (PCR), cloned into the pZsGreenI-I fluorescence-reporter plasmid (Clontech) and transfected into the C2C12 mouse myoblast cell line to assess relative promoter activities. Additional constructs were made to elucidate regions of regulatory control within the MyHC IIB promoters and are discussed in detail in the following sections.

### *2.4.3 Extraction of genomic DNA from tissue and blood*

Porcine genomic DNA (gDNA) was extracted from liver tissue using the Qiagen DNeasy kit using the manufacturers guidelines for use with animal tissue. Briefly, 15mg of frozen, crushed liver tissue was incubated in 180µl of ATL (lysis) buffer and 20µl proteinase-K at 56°C for 3 hours, vortexing every 30 minutes, to lyse cells and digest protein. DNA was precipitated by the addition of 200µl buffer AL and 200µl 100% ethanol and vortexed for 15 seconds. The mixture was transferred to a spin column, centrifuged at 6000xg for 1 minute and the flow through discarded. The DNA caught in the column

membrane was washed by the addition of wash buffer AW1, centrifuged at 6000g for 1 minute and flow through discarded. A second wash was performed by the addition of wash buffer AW2 to the column and centrifuged at 20,000xg for 3 minutes to remove any residual wash buffers. The spin column, containing the trapped DNA, was transferred to a 1.5ml tube, and the DNA was eluted by the addition of 100µl elution buffer AE and centrifugation at 6000xg for 1 minute. Extracted DNA was inspected for quantity and purity using a NanoDrop (Agilent Biosystems). Porcine DNA concentration from liver tissue was 355ng/µl and had a 260/280 reading of 1.86. This DNA was considered pure and ready for PCR applications.

Human DNA was extracted from anti-coagulated fresh whole blood using the Qiagen DNeasy kit according to the manufacturer's instructions for use with whole blood. In a 1.5ml tube, 20µl proteinase-K was combined with 50µl of anti-coagulated human blood and adjusted to a final volume of 220µl with phosphate buffered saline. Prior to the addition of ethanol, 200µl buffer AL was added to the blood, vortexed and incubated at 56°C for 10 minutes. Following this incubation, 200µl of 100% ethanol was added to the mixture, vortexed and then transferred to a spin column membrane for centrifugation at 6000xg for 1 minute. The flow through was discarded. The membrane, containing the DNA, was washed twice by the addition of 500µl of wash buffers AW1 and AW2 and centrifuged for 1 and 3 minutes respectively (at 6000xg and 20,000xg respectively). The spin column was transferred to a fresh 1.5ml tube. The DNA was eluted in 100µl elution buffer AE by centrifugation at 6000xg for 1 minute. Human DNA concentration from whole blood was

17ng/μl and had a 260/280 reading of 1.82. This DNA was considered pure and ready for PCR applications.

#### *2.4.4 Identification of the MyHC IIB promoter*

Using the current genome builds for pig (Sscrofa10) and human (GRCh37), accession numbers for the pig and human MyHC IIB gene (NM\_001123141.1 and ENSG00000264424.1, respectively) and subsequent screening of expressed sequence tags, enabled the identification of the first exon of the MyHC IIB gene for both species. The 3' oligonucleotide primer was designed to span into the first exon to ensure inclusion of the transcription start site. Both predicted start sites were approximately 25 base pairs downstream of a TATA-box, providing confidence in the location of the transcription start site. All base pair numbering is given relative to the TATA-box, as a discrepancy existed as to the precise location of the transcription start site between the two promoters.

#### *2.4.5 PCR of the MyHC IIB promoter from genomic DNA*

Oligonucleotides were designed complementary to the sense and anti-sense strand covering the genomic region of interest. Five-prime oligonucleotide modifications introduced restriction endonuclease sites and poly-A tails to the amplicon produced (Figure 2.4 and 2.5).

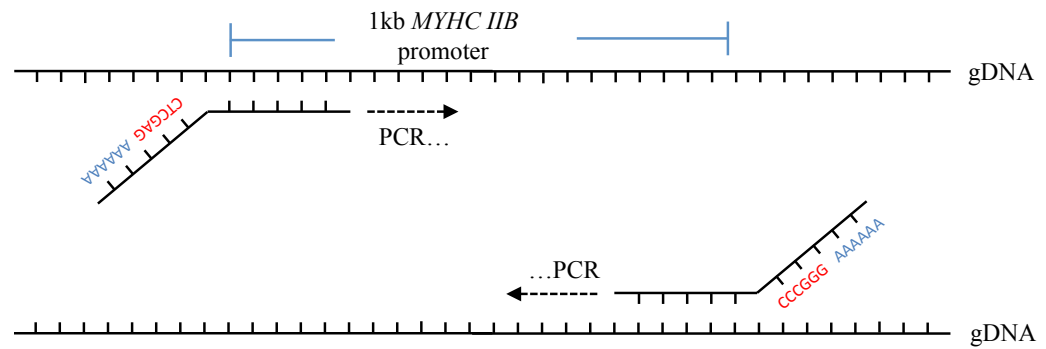


**Figure 2.4** Schematic detailing the engineering of restriction sites onto a PCR amplicon. Complementary primer sequences anneal to the template DNA whilst the additional sequence (restriction site and poly-A tail)

Complimentary regions of the primer anneal to the gDNA whilst the 5 prime additions remained non-annealed (as shown in Figure 2.4). The PCR amplicon produced contained the engineered restriction sites and poly-A tails introduced by the oligonucleotide 5 prime modifications (shown in Figure 2.5).

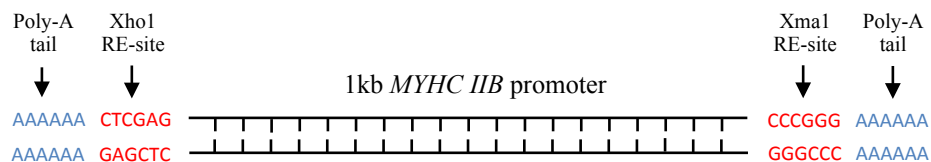


**Figure 2.5** Schematic representation of the PCR amplicon including the restriction sites and poly-A tail

Inclusion of these modifications allowed directional insertion of the MyHC IIB promoter to the host plasmid (pZsGreen1-1 plasmid; explained in detail below). The addition of a poly-A tail was included to improve the efficacy of the restriction endonucleases employed.

Amplification of the 1kb MyHC IIB promoter region was conducted using the Expand High Fidelity PCR System (Roche). In a final reaction volume of 50 $\mu$ l, 50ng of template gDNA was combined with 200 $\mu$ M of each dNTP, 300nM forward and reverse primers, 1x Expand High Fidelity PCR Buffer (with magnesium at 1.5mM) and 2.6U of Expand High Fidelity Enzyme Mix. The reaction was gently mixed by pipetting up and down followed by a brief centrifugation prior to incubation in a thermal cycler. Thermal cycling parameters were dependant on the length of the amplicon being produced and the oligonucleotide sequences employed. Thermal cycling parameters for the 1kb pig and human MyHC IIB promoters is detailed in Table 2.5. All primer sequences are displayed in Table 2.6.

**Table 2.5** Thermal cycling parameters for amplification of the 1kb pig and human MyHC IIB promoters.

	Temperature	Time	Cycles
Initial denaturation	94°C	2 minutes	X 1
Denaturation	94°C	15 seconds	X 10
Annealing	55°C	30 seconds	
Elongation	72°C	2 minutes	
Denaturation	94°C	15 seconds	X 20
Annealing	55°C	30 seconds	
Elongation	72°C	2 minutes + 5 seconds	
Final elongation	72°C	7 minutes	X 1
Cooling	4°C	$\infty$	X 1



**Table 2.6** Oligonucleotide primer sequences for all cloning

Oligonucleotide name	Sequence (5'-3')
Human_IIB_R	AAAAAACC CGGAGGAAGGATGGGAAAGAGG
Pig_IIB_R	AAAAAACC CGGAGGAAGGACAGGACAGAGGCAT
Human_IIB_67bp_F	AAAAAACTCGAGGCCAAGTAGGTTCCCAGCTAG
Pig_IIB_67bp_F	AAAAAACTCGAGGCCAAGTAGGTTCCCAGCTGG
Human+pig_IIB_113bp_F	AAAAAACTCGAGCCACAGTCAGTGAATATTGTGCA
Human_IIB_231bp_F	AAAAAACTCGAGCAGTGTTAGAAGCCCTGAATCC
Pig_IIB_231bp_F	AAAAAACTCGAGTAGCCTTAGAAGCCCTGAATCTC
Human_IIB_466bp_F	AAAAAACTCGAGTCCAGACTGTGGCTAGGAATG
Pig_IIB_466bp_F	AAAAAACTCGAGTCATCAGTATTTCTAAAATCCAGACC
Pig_961bp_(1kb)_F	AAAAAACTCGAGTAGGTGACACACTTAGCGTGGACA
Human_961bp_(1kb)_F	AAAAAACTCGAGCTTAGAGTAGGTATATTTCTGCCAT
Human_IIB_HindIII_F	CAGTGTTAGAAGC <u>TT</u> TGAATCCCCATC
Human_IIB_HindIII_R	TTTCTCCAGTTTGGCTGTTGCATC
Pig_IIB_HindIII_F	GCCTTAGAAGC <u>TT</u> TGAATCTCCATC
Pig_IIB_HindIII_R	TATTTCTCCAGCTTTGCTGTTCCATC
Human_IIB_AT3_SDM_F	CTATCAAATGCCT <u>CA</u> AAAAGAACCCTAGA
Human_IIB_AT3_SDM_R	GGGATGGGGATT CAGGGC
Human_IIB_midAT2-3_SDM_F	GAACCCTAGAT <u>G</u> ATCCTCTGTAAAT
Human_IIB_midAT2-3_SDM_R	TTTATAGGCATTTGATAGGGGATGG
Human_IIB_distAT2_SDM_F	CTAGATCATCCTCTGT <u>C</u> AAATTATTTATGGG
Human_IIB_distAT2_SDM_R	GGTTCTTTATAGGCATTTGATAGGGG
Human_IIB_proxAT2_SDM_F	CCTCTGTAAATTATTTA <u>T</u> AGGTGTCAAGAAATA
Human_IIB_proxAT2_SDM_R	ATGATCTAGGGTTCTTTATAGGCATT
Human_IIB_CArG_SDM_F	AGATTGCCAAAAA <u>A</u> GGTTTTGCCAAG
Human_IIB_CArG_SDM_R	CTTGCACAATATTCAGTACTGTGG
Human_IIB_EBOX2_SDM_F	TTCCCAGCT <u>G</u> GGACAGCT
Human_IIB_EBOX2_SDM_R	CCTACTTGGCAAAACCGTTTTTGGC
Human_IIB_T_removal_F	GCCAAGTAGGTTCCCAGCT
Human_IIB_T_removal_R	AAACCTTTTTTGGCAATCTCTTTGCAC
No-CArG_R	CTCTTTGCACAATATTCAGTACTGTG
No-CArG_Pig_IIB_F	AGTAGGTTCCCAGCTGGG
No-CArG_Human_IIB_F	AGTAGGTTCCCAGCTAGGAC
CMV-basic_F	AAAAAAAAGCTTGCAAATGGGCGGTAGGC
CMV-basic_R	AAAAAACC CGGGATCTGACGGTTCATAAACCAGC
MyoD_F	AAAAAAAAGATCTGCCACCATGGAGCTTCTATCGCCG
MyoD_R	AAAAAAAACCGGTGCTCAAAGCACCTGATAAATCGC

To confirm the length of the amplicon produced and that no (or minimal) non-specific binding and subsequent miss-amplification had occurred, an aliquot of the PCR reaction was checked on a horizontal agarose gel (see example below; Figure 2.6). A 6µl aliquot of the PCR reaction (including 1x loading buffer) was loaded into the well of a horizontal 1% agarose gel, separated by electrophoresis and visualised following 30 minutes staining with ethidium bromide.

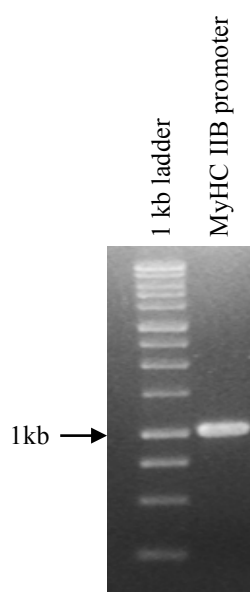


**Figure 2.6** The successful amplification of a 1kb PCR product was checked by agarose gel electrophoresis. The DNA was stained with ethidium bromide and visualised under UV light.

#### *2.4.6 Spin column purification of PCR amplicons*

If the PCR produced an amplicon of the correct length, the DNA was purified through a PCR purification column (PCR clean-up kit, Sigma Aldrich). The spin columns used herein effectively separated the large (wanted) DNA fragments from the small (unwanted) DNA fragments (<100bp), whilst also removing buffers and enzymes. The purified DNA could subsequently be used in downstream applications. Briefly, a spin column was prepared by applying

500µl of column preparation solution to the column membrane and centrifuging at 12,000xg for 30 seconds (flow through was discarded). Five volumes of binding solution was added to the PCR, mixed, transferred to the spin column and centrifuged at 12,000xg for 1 minute (flow through was discarded). The DNA trapped in the column membrane was washed by applying 500µl of wash buffer (containing ethanol) to the column and centrifuging at 12,000xg for 1 minute. The flow through was discarded and the spin column was centrifuged at 12,000xg for 2 minutes to remove residual wash buffer from the column. The column membrane was subsequently incubated with 50µl molecular grade water (Sigma Aldrich) at room temperature for 1 minute to re-dissolve the DNA and then centrifuged (12,000xg for 1 minute) to elute the DNA in a final volume of 50µl.

#### *2.4.7 Restriction endonuclease digestion*

The 1kb MyHC IIB promoters were engineered via PCR to contain Xho1 and Xma1 restriction sites at their 5' and 3' ends respectively. These restriction sites were unique (i.e. they did not appear elsewhere within the MyHC IIB promoters) and were appropriately located in the multiple cloning site (MCS) of the host plasmid (pZsGreenI-I). Both the MyHC IIB promoter and the host vector underwent a double restriction endonuclease digest reaction to create overhanging sticky ends to allow the directional insertion of the promoter into the host vector, upstream of the fluorescence reporter gene (ZsGreen; see Figure 2.7 below). The activity of Xho1 and Xma1 was 100% in NEB buffer 4, allowing both enzymes to be used in the same reaction (known as a double digest).

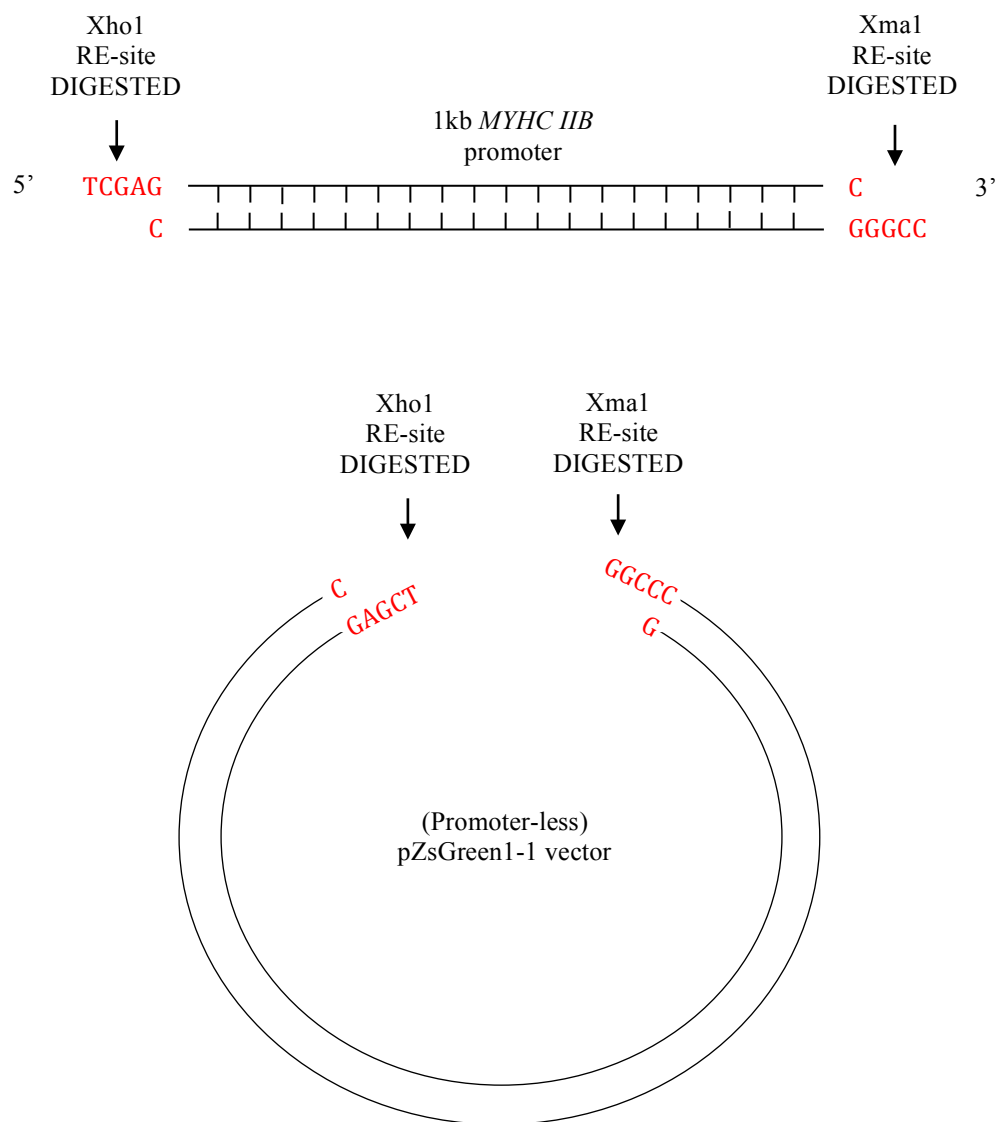


**Figure 2.7** Schematic representation of the cloning strategy employed herein. The generation of complementary overhanging sticky ends, by restriction digest, permitted directional insertion of the promoter into the host plasmid.

DNA was digested for approximately 3-4 hours at 37°C in a reaction volume of 50µl containing 1x NEB Buffer 4, ~10U of each Xho1 and Xma1 restriction endonucleases (New England Biolabs) and 5ug bovine serum albumin (BSA). Inclusion of BSA was necessary to stabilise the Xho1 and Xma1 enzymes during the reaction. Control digests were conducted to ensure each restriction endonuclease was capable of cutting plasmid DNA in separate reactions. The

successful digestion of plasmid DNA was confirmed by gel electrophoresis. Circular plasmid DNA appeared as multiple bands (supercoiled DNA) whereas linearized plasmid DNA appeared a single band, confirming the activity of the restriction endonuclease (see Figure 2.8 below).

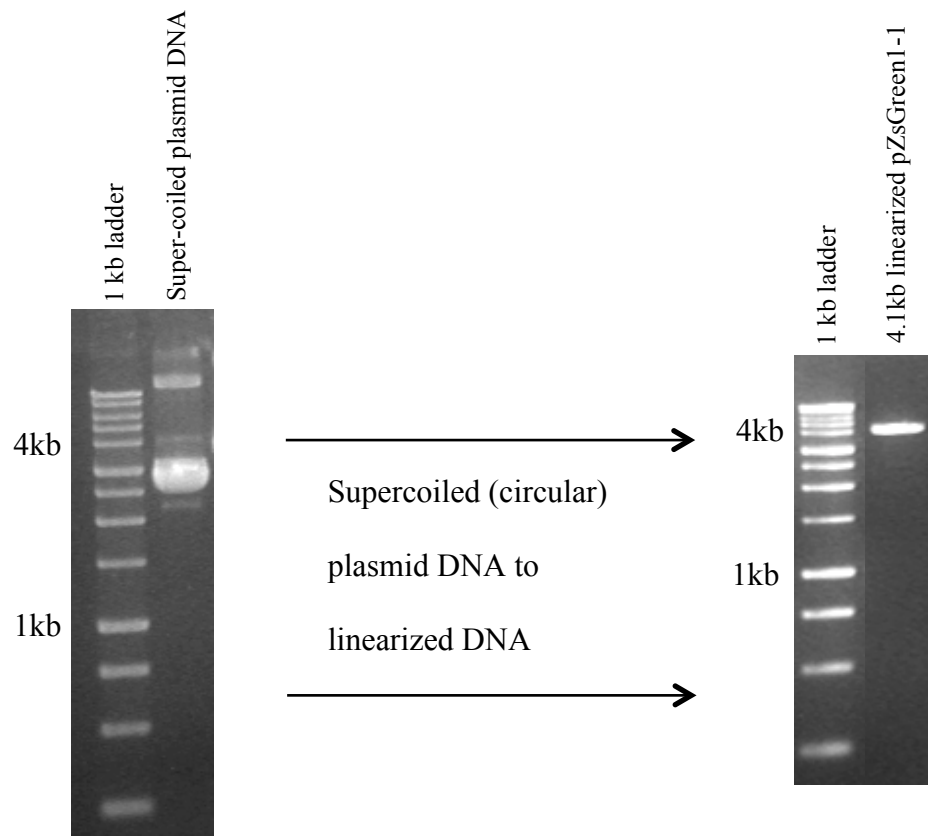


**Figure 2.8** Circular plasmid DNA migrates as multiple bands due to supercoiling (left gel). Linearized plasmid DNA, by a single restriction digest, migrates as a single band (right gel).

Following a 3-4 hour restriction endonuclease reaction, 20U of calf intestinal alkaline phosphatase (CIAP; Promega) was added to the plasmid reaction (but not to the promoters) and maintained at 37°C for an additional 30 minutes. Although the overhanging sticky ends were essentially non-cohesive, addition of CIAP removed the 5' phosphate group from the plasmid DNA to further

reduce the risk of plasmid re-ligation and thus reduce background, plasmid-only, colonies during cloning. CIAP was compatible with the NEB buffers being used herein.

#### *2.4.8 Gel purification of MyHC IIB promoter and host plasmid*

Following restriction endonuclease digest of plasmid and promoter DNA, removal of buffers, enzymes and most importantly, small fragments of digested DNA that could interfere with downstream ligation reactions, was conducted via agarose gel purification. The DNA mixture, containing 1x loading buffer and 1x SYBRgreen, was loaded onto a 1% agarose gel and separated by gel electrophoresis. Since SYBRgreen intercalates with double stranded DNA, the DNA bands, attaining to the correct length, could be visualised and excised on a transilluminator box using a sterile scalpel blade. Excising the band of the correct length from an agarose gel ensures that only the bands of interest are taken forward for downstream cloning applications. The DNA was then purified from the agarose gel using a gel extraction kit (Qiagen) according to the manufacturers guidelines. Briefly, the excised band was combined with 3 volumes Buffer QG and incubated at 50°C for 10 minutes (vortexing occasionally) to dissolve the agarose. To increase the yield of large DNA fragments (>4kb; the plasmid DNA used herein), 1 volume isopropanol was added to the solution and vortexed. The entire solution was then transferred to a spin column, centrifuged at 10,000xg for 1 minute and the flow through discarded. The spin column was washed by applying 750µl Buffer PE (containing ethanol), centrifugation at 10,000xg for 1 minute and discarding the flow through. The spin column was centrifuged for an

additional 2 minutes to removal any residual wash buffer. The column was transferred to a fresh 1.5ml tube, incubated with 50µl Elution Buffer (10mM Tris-Cl, pH 8.5) on the column membrane for 1 minute at room temperature and centrifuged for 1 minute at 10,000xg to elute the DNA.

#### *2.4.9 Ligation of the MyHC IIB promoter into the host plasmid*

Following the extraction and purification of the plasmid DNA and the MyHC IIB promoters, a small aliquot (5µl) was checked on a 1% agarose gel (see Figure 2.9) to a) ensure a single product of the correct length was present and b) to estimate the relative quantities of DNA present. An estimate of the relative quantity of DNA is required for optimal ligation efficiency (explained below).

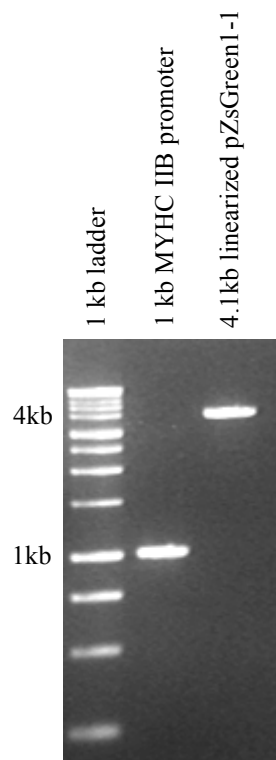


**Figure 2.9** Relative quantities of the plasmid and promoter DNA were estimated by gel electrophoresis.

The relative quantity of insert:plasmid DNA takes into account both the density of the DNA band and the length of the given DNA fragments. For example, the bands on the above gel image (Figure 2.9) are of a similar density but the insert DNA (MyHC IIB promoter) is 4x smaller than the plasmid. Thus, an equal volume of both insert and plasmid DNA would equate to a ratio of 4:1 (insert:plasmid). The optimal molar ratio of insert:plasmid DNA for ligations reactions is typically between 3:1 and 5:1. Therefore, 1µl of both the MyHC IIB promoter DNA and plasmid DNA (molar ratio of 4:1) were used in the ligation reaction for the products in the above example.

The ligation reaction was carried out in a volume of 10µl with 1x T4 DNA Ligase Buffer (Promega), 1.5U T4 DNA ligase (Promega) and an insert:plasmid DNA ratio of approximately 4:1. Reactions were conducted over night at 16°C and then stored at 4°C for approximately 6 hours prior to use. Negative ligation controls (containing only plasmid DNA with no insert DNA) were used to check for the relative occurrence of plasmid re-ligation.

Ligation of the MyHC IIB promoter into the MCS of the pZsGreenI-I plasmid resulted in the MyHC IIB promoter residing upstream of the ZsGreen fluorescence reporter gene as depicted below (Figure 2.10).



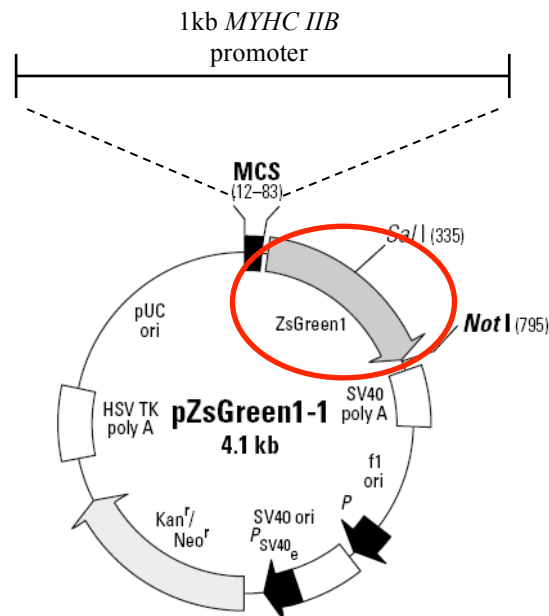


**Figure 2.10** The MyHC IIB promoter was ligated upstream of the ZsGreen gene to generate a fluorescence promoter-reporter plasmid. The ZsGreen gene is circled in red.

#### 2.4.10 Transformation of JM109 competent *E-coli*

Following the ligation reaction, some plasmids should now contain the MyHC IIB promoter. To amplify clonal copies of the MyHC IIB pZsGreenI-I plasmids, they were cloned in JM109 competent *E-coli* cells (Promega). Approximately 8µl of the ligation reaction was incubated with 50µl competent *E-coli* cells on ice for 30 minutes. This mixture of cells and DNA underwent a heat shock by submerging the mixture (in 14ml tubes) into water at 42°C for 45 seconds followed by 2 minutes on ice. This process essentially damages the cell wall, allowing plasmid DNA to randomly move into the cell. Following incubation on ice, 950µl of Super Optimal Broth with additional glucose (SOC) medium (Invitrogen) was added and the cells were cultured in suspension at 37°C whilst shaking at 200rpm for 1.5 hours. This allowed the

cells to recover and start producing the antibiotic resistance gene encoded by the plasmid back bone (see Figure 2.11).

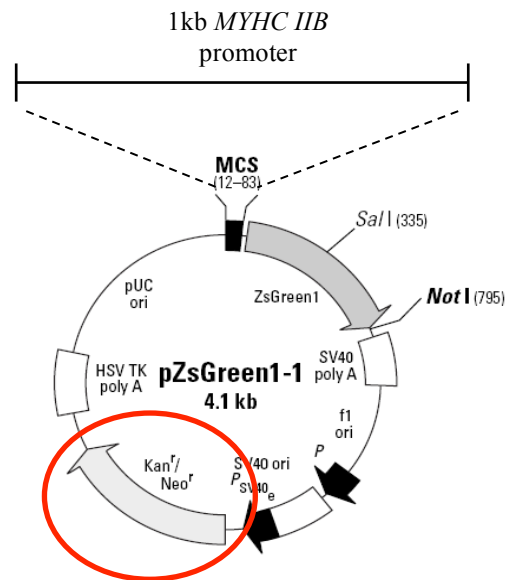


**Figure 2.11** The red circle indicates the antibiotic selection marker that ensures antibiotic resistance of JM109 cells containing intact copies of the plasmid.

Using kanamycin containing agar plates (50µg/ml), 50µl of the cultured competent cells were seeded and grown over-night under selection at 37°C. Only competent cells containing the kanamycin resistance gene (encoded by intact plasmids; shown in the diagram above) would survive and grow to form colonies.

#### 2.4.11 Colony selection for plasmid expansion

Growth of colonies would only occur if they contained circular plasmid DNA. The plasmid DNA in the cell will either contain no insert (i.e. it has self-ligated) or it will have the MyHC IIB promoter inserted. To estimate the

percentage of colonies on a plate that had the MyHC IIB inserted, the number of so called positive colonies were corrected for the number of colonies that had grown on the negative ligation control plate (that contained only plasmid DNA in the ligation reaction). For example, if 100 colonies appeared on the plasmid-with-insert ligation plate and 10 colonies appeared on the plasmid only (negative) ligation plate, it would stand that approximately 1 in 10 colonies may contain no insert. Using this information, a number of colonies could be selected to ensure that some of these colonies stood a reasonable chance of containing plasmid DNA with the MyHC IIB promoter inserted. Typically 5 to 10 colonies were selected for expansion. Colonies were picked for expansion by touching the colony with a sterile pipette tip, dropping the tip into 3ml LB medium containing 50µg/ml kanamycin and grown overnight at 37°C (whilst shaking at 200rpm). The medium would turn from clear to cloudy over-night indicating bacterial growth.

#### *2.4.12 Small-scale plasmid extraction*

The Sigma Plasmid Miniprep Kit (Sigma Aldrich) was used to extract small quantities of plasmid DNA from an overnight culture. Briefly, 3-5ml of overnight culture was pelleted by centrifugation at 3,000rpm for 5-10 minutes. Medium was removed (which should be clear post-centrifugation) and the pellet was re-suspended in 200µl cold (4°C) re-suspension solution containing RNase. Cells were lysed by the addition of 200µl lysis solution and mixed by inversion 6-8 times. The addition of 350µl of neutralization solution followed by gentle inversion (4-6 times) neutralized the lysis reaction to prevent permanent damage to plasmid DNA. Cell debris and chromosomal DNA

precipitated and were subsequently pelleted by centrifugation at 12,000xg for 10 minutes. A miniprep binding column was prepared by adding 500µl of column preparation solution to the column and centrifuging at 12,000xg for 30 seconds and discarding the flow through. The supernatant of the lysed cells was then transferred to the pre-prepared spin column and centrifuged at 12,000xg for 30 seconds and the flow through discarded. The column was washed by the addition of 750µl of wash solution (containing ethanol), centrifuging at 12,000xg for 30 seconds and discarding the flow through. Any residual wash buffers were removed from the column by centrifugation at 12,000xg for 2 minutes. To elute the plasmid DNA, the column membrane was incubated with 100µl molecular grade water for 1 minute prior to centrifuging at 12,000xg for 1 minute. The elute, containing approximately 200-300ng/µl, plasmid DNA was stored at -20°C.

#### *2.4.13 Confirming successful cloning*

To identify the successful ligation of the MyHC IIB promoter into the host plasmid, the relative size of the purified plasmid DNA was checked on a 1% agarose gel by electrophoretic separation. From the example below (Figure 2.12), it is clear that lanes 2 and 4 contain plasmid DNA that is approximately 1kb larger than that in lanes 1, 3 and 5, suggesting the insertion of a 1kb DNA fragment. To confirm the actual length of the plasmids potentially containing the 1kb MyHC IIB promoter, plasmid DNA was linearized by a single restriction endonuclease digest and re-checked on a 1% agarose gel against a DNA ladder.

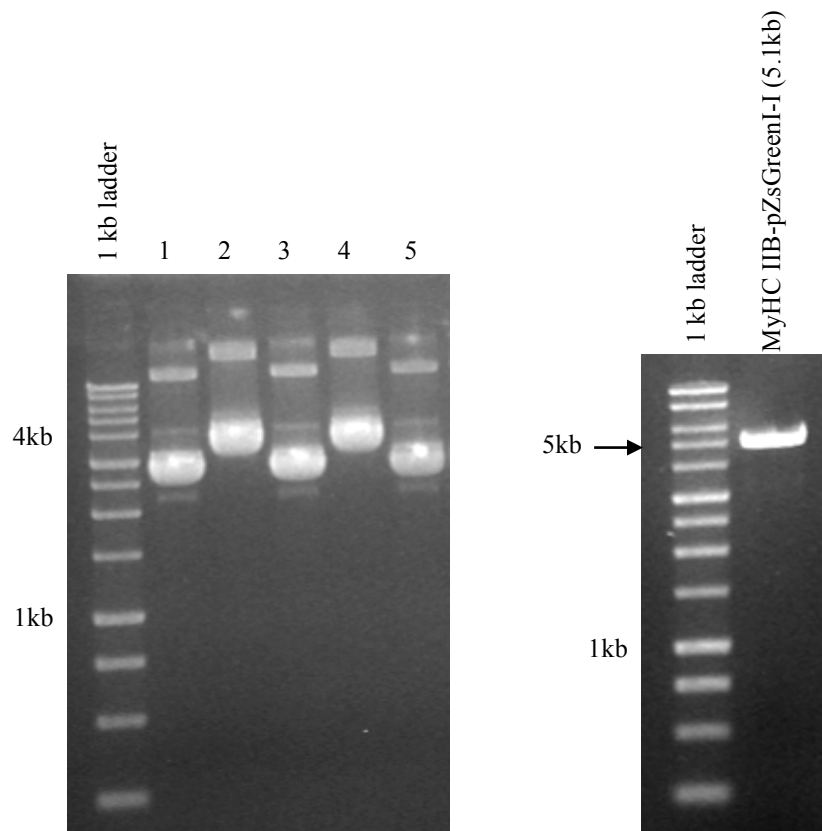


**Figure 2.12** Relative sizes of supercoiled plasmids were checked for differences in size, indicating the insertion of the MyHC IIB promoter (left gel). Plasmids were linearized to confirm the total length of the plasmids with the inserted MyHC IIB promoter (right gel).

#### 2.4.14 DNA sequencing

Plasmids were sequenced to confirm that the inserted 1kb fragment was a) the MyHC IIB promoter, b) contained no errors introduced by the PCR and c) was inserted in the correct orientation and location. Sequencing PCR was conducted using forward and reverse oligonucleotide primers complementary to plasmid DNA flanking the 5' and 3' regions of the multiple cloning site. Sequencing of MyoD cDNA was conducted in the same way (explained below).

#### *2.4.15 The Sanger DNA sequencing method*

Sequencing of DNA products was performed in house whilst on placement at Pfizer Animal Health (Michigan, USA) using the Sanger fluorescent terminal nucleotide capillary detection method. Template DNA was amplified by PCR (Applied Biosystems BigDyeFast) using a combination of normal unlabelled nucleotides (dNTP) and fluorescent-labelled terminating nucleotides to produce amplicons of varying lengths with fluorescent indicators of the final 3' nucleotide (PCR parameters are in Table 2.7 and 2.8). PCR amplicons were cleaned (to remove excess buffers and nucleotides) using the Zymo Research PCR clean up kit (ZR-96 DNA sequencing clean up kit). Briefly, 240µl sequencing binding buffer was added to the 20µl PCR reaction, gently pipette mixed, transferred to a spin column and centrifuged at 3000xg for 2 minutes. Without removing flow-through, 300µl sequencing wash buffer was added to the spin column and centrifuged at 3000xg for 5 minutes. The spin column was transferred to a fresh collecting tube. To elute the DNA, 35µl of molecular grade water (Sigma) was added directly to the spin column and centrifuged at 3000xg for 2 minutes. The eluted DNA amplicons (sequentially varying in length by a single base pair) were separated through a capillary (Applied Biosystems 3730 DNA Analyser) and the terminating fluorescent nucleotides were read to provide the DNA sequence. Example fluorescence images of the capillary are provided in Figure 2.13. Each fluorescent “bar” (per lane) indicates the nucleotide sequence (A = red, C = green, T = yellow, G = Blue). Chromatograms were trimmed to remove nucleotide readouts with low confidence (see Figure 2.14). Note that sequencing of only ~700bp was possible with this method as the fluorescence signal strength declines with

increasing amplicon length (see Figure 2.13). For DNA products longer than 700bp, forward sequencing primers were designed to amplify DNA every 500bp and sequenced amplicons were overlapped to generate the full-length sequence.

**Table 2.7** Components and quantities of the Applied Biosystems BigDyeFast sequencing PCR

Reagents	Volume per reaction (μl)
5x Applied Biosystems buffer	3.5
Water (molecular grade)	7.5
Template DNA (50-500ng)	5
1μM primer	3
Big Dye	1
<i>Total</i>	20

**Table 2.8** Applied Biosystems BigDyeFast thermal cycling parameters for sequencing PCR

Thermal cycle	Temperature	Duration
Initial denaturation	96°C	1 minute
Amplification (25 cycles)	96°C	10 seconds
	55°C	5 seconds
	60°C	1 minute 15 seconds
Hold	4°C	∞

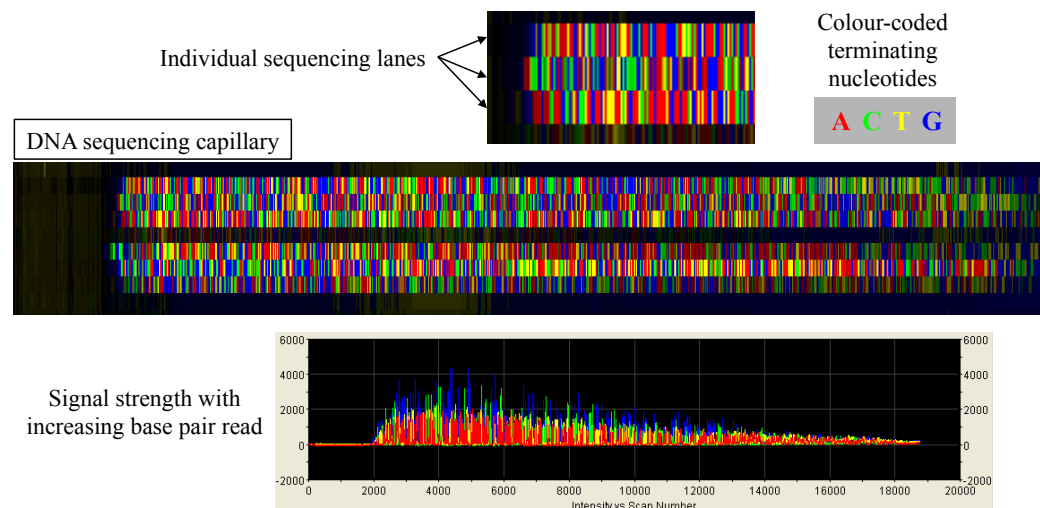


**Figure 2.13** Examples of the time-lapse view of the sequencing capillary. The image generated shows a coloured bar for each of the colour-coded terminating nucleotides on the end of the DNA products (with each product being a single base pair longer than the previous).

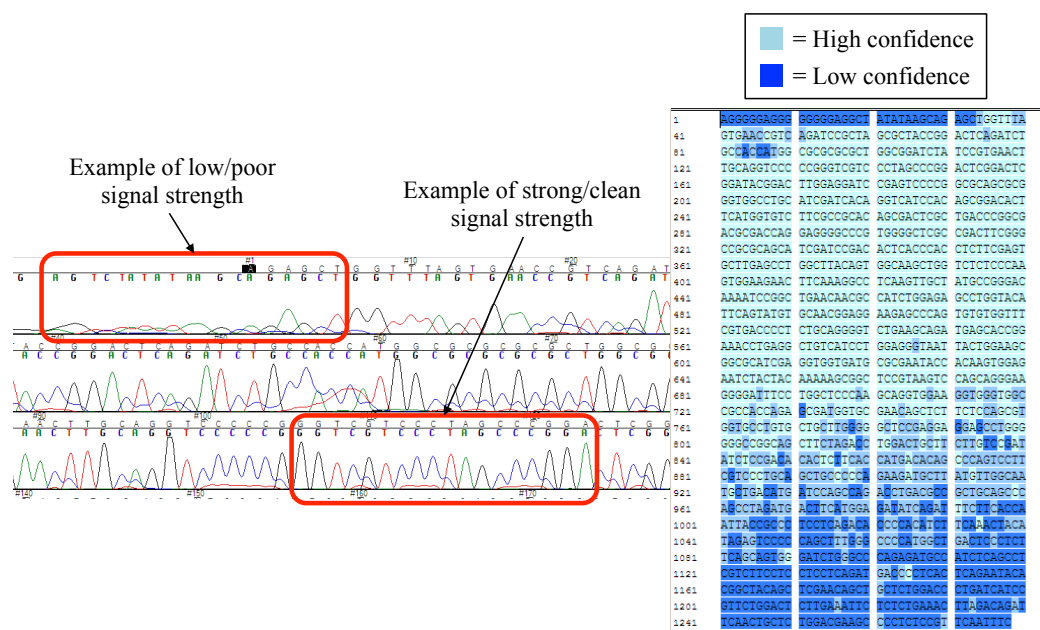


**Figure 2.14** Example of the DNA chromatogram (analysed using Sequencer) signal and sequence generation. Highlighted in red boxes are examples of poor base readout signals (small inconsistent peaks) and good base readout signal (clear defined and evenly separated peaks). The generated sequence shows bases with high and low confidence of correct base call (light blue shows high confidence and dark blue shows low confidence).



Sequencing data for the MyHC IIB promoters was cross-checked with their respective database sequence (from Ensembl or NCBI). Final versions of the pig and human MyHC IIB promoters are displayed below (Figure 2.15). The human DNA donor had a single nucleotide polymorphism (SNP) relative to the current human genome database (highlighted in red; C substituted for a T).

**Pig *MYHC IIB* -pZsGreen1-1**

CTGTGGATAACCGTATTACCGCCATGCATTAGTTATTACTAGCGCTACCGGACTCAGATCTCG  
AGTAGGTGACACACTTAGCGTGGACAGATTTGCTGTTACATTACAGCAGCAGCTGTGTCTGTGG  
CAAAACCACCAAAACCCAATTTACAAGCATCGTGGGCATATGTGATAGCCCCCTTATGTTCTC  
AACCACAAAGAGTCCTGTGGGTATCACATCTCTCCTCCCACCTTAAATAAAAAATACGTATTA  
CCCACCTCATTAGAGCTACTGCTAGTCATGAGGATTTGCCTGTGAACTAGGAATGCATATTGA  
TGCCTCCTTCCATCATTATGCGGTAGAAACACACATAGAACATCACACGGACTCCTGCAGTCC  
CCCCAGTGAAGCATGTGAGCTCAAGACAGCCACGGCAAGCTCTCCAGAAAAGGAAAAGAAGT  
GTTTCTATCTATTCTAAATCCCTTATGGCTCCCCACTGGTCTGTCACCATGGCTTAGCCCGA  
GAATCTGCCTAAACTTTCTCCTTCATGCTTAGTCTTTTAGACTTTAAAAAATCTATCATCAG  
TATTTCTAAAATCCAGACCCAGGCTAGGAGTTTTCTGCTTTAATACCAATCATGTTGTCAGAG  
CTAAAATCATCCCAGCTCCTCAATGGCCCTAAGCACTAACAAATCAATTAGTTCTCAACTCC  
TCGTGTCTGGCTCATTCTGTGCGACCAATTTTACAGGCAGGAGAGTAAGTGGGAACCTGGCTT  
TCAACTCAGTGATGAATGATGGAACAGCAAAGCTGGAGAAATAGCCTTAGAAGCCCTGAATCT  
CCATCCCTATCAAATGCCTCAAAAGAACCCTAGATGATCCTCTGTCAAATTATTTATAGGTGT  
CAAGAAATATTTCTAATTATATCCATTACAGCCACAGTCAGTGAATATTGTCAAAGAGATT  
GCCAAAAAAGGTTTGCCAAGTAGGTTCCAGCTGGGACAGCTGAGGTGGCTGCTGTGTTTGCA  
AAATGGTCTCTATAAAAGTGGAGCTGAGATGCCTCTGTCTGTCTCCTTCCCGGGATCCACC  
GGTGCACCACATGGCCAGTCCAAGCACGGCCTGACCAAGGAGATGACCATGAA

**Human *MYHC IIB* -pZsGreen1-1**

ATGCATTAGTTATTACTAGCGCTACCGGACTCAGATCTCGAGCTTAGAGTAGGTATATTTCCCT  
GCCATATTTCAGTAACAGCTGTGTATGTAGCAAAACCATCAAAGCCAATTTATGAGTATTATG  
GGCATATGTGATGGCCCATCCATCTTTTCAATCCACAGGGAGAATATCGTGGATAACCATGACT  
TTCTCCACCTTAAATAAAAAATATGGGTTCCACCTCATTAGAGCTATAGCTAGTCATGAG  
AGTCTGCCCATGAAGTAGGAATGCATGTTTGTGTCTCCTTCCATTATGCAGAGGAAACATGCA  
TGGAACATCACACAGCATCCTGTTGTTTCTCAGTGAAAACATACAAGCTGGAGATATCCATG  
GAAAGTCCTCCAGAAAAAGAACAGAAGTGTTTATATCTATTCTAAATCCCTTATGCCTCCCCC  
AGTGGTCCATCACCCTGCCTAATCTGAGAATTCACCTTTCACCTTCATATTTAGACTTTCAGA  
CTTTAAAGAATCTATCGCCAGTCTTTCTAAAATCCAGACTGTGGCTAGGAATGTTGTCTTAA  
AATCCATCGCTCACTGCTTCCAATCATAGTGTGAGGTCTAAAATTCATTCCAGACTCCTTAAT  
GGCTCTAAGAACCAACAAATTAATTAATCCTAAATTCCTCACATCAGACTCATTCTGTTGGAC  
CAATTTTATAGGCAGAGGAGTAAGTGGGAATCTGGCTTTGAATCTGTGATGAATGATGCAAC  
AGCCAAACTGGAGAAACAGTGTTAGAAGCCCTGAATCCCCATCCCCTATCAAATGCCTATAAA  
GAACCCTAGATCATCCTCTGTTAAATTATTTATGGGTGTCAAGAAATATTTCTAATTATATCC  
ATTCACAGCCACAGTCAGTGAATATTGTCAAAGAGATTGCCAAAAACGGTTTTGCCAAGTAG  
GTTCCAGCTAGGACAGCTGAGGTGGCTGCTGTGTTTGCAGAATGGTCTCTATAAAAGTGGAG  
CTGAGATGCCTCTTTCCCATCCTTCCCTCCCGGGATCCACCGGTGCGCCACCATGGCCAGTCCA  
AGCACGGCCTGACCAAGGAGATGACC

**Key:** Plasmid Insert (MyHC IIB promoter) Transfection Start Site  
PCR Primers RE-site (*XhoI* + *XmaI*) Single Nucleotide Polymorphism

**Figure 2.15** Pig and Human MyHC IIB promoter sequences located in the correct orientation within the multiple cloning site of the pZsGreen1-I. Annotations are described in the key.

#### *2.4.16 Large-scale, endotoxin-free plasmid preparations*

To conduct mammalian cell transfections using plasmids cloned in bacterial cells, the plasmid DNA was a) produced in a quantity large enough to perform the transfection procedure and b) removed of any contaminants that may damage mammalian cells and potentially inhibit transfection efficiency. In order to achieve this, a single colony containing the plasmid of interest was cultured in 3ml of LB medium containing the appropriate antibiotic for 6-8 hours. From this, 100µl of culture was transferred to 40ml of LB medium (with appropriate antibiotic) and cultured overnight at 37°C (200rpm shaking). A Sigma Endotoxin-free Plasmid MidiPrep Kit (Sigma Aldrich) was used to extract and purify plasmid DNA from large cultures. The majority of the procedure is similar to the plasmid miniprep extraction (see above; but on a larger scale) with the addition of an endotoxin removal step. Following lysis and neutralization of the cells, the lysate containing plasmid DNA was incubated on ice with 300µl of endotoxin removal solution for 5 minutes. The solution was then moved to a 37°C water bath for 5 minutes (the solution turned cloudy) and centrifuged at 3,000rpm for 5 minutes and the supernatant (free of endotoxins) was transferred to a fresh tube. This step was repeated. The remaining steps were as in the plasmid miniprep protocol. Plasmid DNA was eluted in 1ml of endotoxin-free water.

To further purify the plasmid DNA prior to transfection, an ethanol precipitation of the DNA was conducted using 0.1 volumes 3M Sodium Acetate and 2.5 volumes Ethanol, vortexing the entire solution and storing at -20°C overnight. The DNA was pelleted by centrifugation at 13,000rpm for 30 minutes (at 2°C). The supernatant was removed, the pellet was washed in 1 ml

70% Ethanol, re-pelleted by centrifugation at 13,000rpm for 10 minutes and the supernatant removed again. The pellet was air dried on the bench to allow ethanol to evaporate and then re-suspended in an appropriate volume of endotoxin-free water (typically 500µl) to give the desired concentration of plasmid DNA.

#### *2.4.17 Five prime deletion of the MyHC IIB promoters*

Equivalent 5' deletion of the pig and human MyHC IIB promoters was conducted to elucidate regions of regulatory control. Pig and human MyHC IIB promoters of varying lengths (-961bp, -466bp, -231bp, -113bp, -67bp; promoter lengths are relative to the TATA-box) were generated by PCR using the 1kb MyHC IIB-pZsGreenI-I plasmids as template DNA (<1ng). PCR primers were designed to introduce a 5' and 3' restriction site (Xho1 and Xma1, respectively) to clone the new shorter promoter into the pZsGreen1-1 vector (as described above). The PCR thermal cycle used during amplification of the 5' deletion promoters was the same as when creating the 1kb promoters (as described above).

#### *2.4.18 Pig-human chimeric promoter constructs*

Chimeric MyHC IIB promoters (containing combinations of both distal and proximal regions of the pig and human MyHC IIB promoters) were produced according to a similar design previously demonstrated by Harrison et al., (2011). A HindIII restriction site (2bp mutation; at -218bp and -217bp) was first introduced (by site directed mutagenesis PCR – explained below) to both the pig and human 1kb promoter. The sequence was mutated from AAGCCC

to AAGCTT (bold case indicate changes) and was situated such that it would disrupt the sequence of both the pig and human MyHC IIB promoters in the same way. The new HindIII restriction site and the 3' XmaI restriction site were digested and the two fragments (the proximal promoter and the remaining linear plasmid containing the distal promoter) were gel purified. The proximal promoters were subsequently ligated (as described above) to the linear plasmid containing the distal promoter of the opposing species, generating chimeric promoters (see Figure 2.16). For completeness, the proximal promoter regions were also swapped with a minimal CMV promoter (84bp) to test for potential regulatory regions in the 5' distal region (~750bp) of each promoter, independent of the proximal promoter (see Figure 2.16). The minimal CMV promoter was produced by PCR, using the pDsRed-Express-NI plasmid as template DNA, and cloned as described above (primer sequences in Table 2.6).

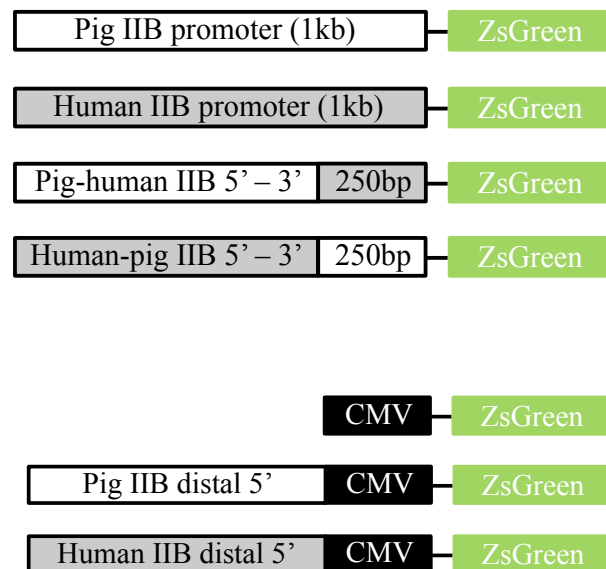


**Figure 2.16** Schematic diagram detailing the chimeric promoter constructs containing combinations of the pig and human MyHC IIB promoters. CMV is a minimal basal promoter (84bp), used herein to test for enhancer activity from the distal MyHC IIB promoters.

The location of the HindIII chimeric junction is displayed below (Figure 2.17). Swapping the proximal pig and human MyHC IIB promoters, downstream of the HindIII chimeric junction, effectively equated to 14bp changes in the proximal promoter region (highlighted in black below; Figure 2.17). The mutated promoter (2bp to generate HindIII restriction site) was used as a control and had no effect on the relative promoter activities of the pig and human 1kb MyHC IIB promoters (Figure 2.18).

				HindIII chimeric-junction		
Human	-261	ATGAATGATGCAACAGCCAAACTGGAGAAACAGTGTTC	AAGCCC	TGAATC	CCATCCC	-202
Pig	-259	ATGAATGATGGAAACAGCAAAGCTGGAGAAATAGCCTTC	AAGCCC	TGAATC	CCATCCC	-201
		*****	*****	**	*****	*****
			AT3		AT2	
Human	-201	TATCAATGCCTTA	AAAAGAACCCTAGATCATCCTCTGT	AAATTATTAT	GCGGTGTCAAG	-142
Pig	-200	TATCAATGCCTCA	AAAAGAACCCTAGATCATCCTCTGT	AAATTATTAT	GCGGTGTCAAG	-141
		*****	*****	*****	*****	*****
			AT1			
Human	-141	AAATATTTCTAATTATATCCATTACAGCCACAGTCAGTGAATATTGTGCAAAGAGATTG				-82
Pig	-140	AAATATTTCTAATTATATCCATTACAGCCACAGTCAGTGAATATTGTGCAAAGAGATTG				-81
		*****	*****	*****	*****	*****
			CARg-box	E-box2	E-Box1	
Human	-81	CCAAAAAGGTTTT	TGCCAAGTAGGTTCCAGCT	AGGACAGCTGAGGTGGCTGCTGTGTTT		-22
Pig	-80	CCAAAAAGGTTTT	TGCCAAGTAGGTTCCAGCT	GGACAGCTGAGGTGGCTGCTGTGTTT		-22
		*****	*****	*****	*****	*****
			TATA-box (+1)			
Human	-21	GC	CAATGGTCTCTATAAAAGTGAGCTGAGATGCCTCT	TTCC	CATCCTTCCT	+32
Pig	-21	GC	CAATGGTCTCTATAAAAGTGAGCTGAGATGCCTCT	GTCC	GTGCTTCCT	+32
		***	*****	*****	*****	*****

**Figure 2.17** Alignment of the proximal pig and human MyHC IIB promoter showing the location of the HindIII chimeric junction. Downstream of the chimeric junction, there are 14bp mismatches between the pig and human sequence (highlighted in black). Grey highlights indicate regions of known regulatory importance.

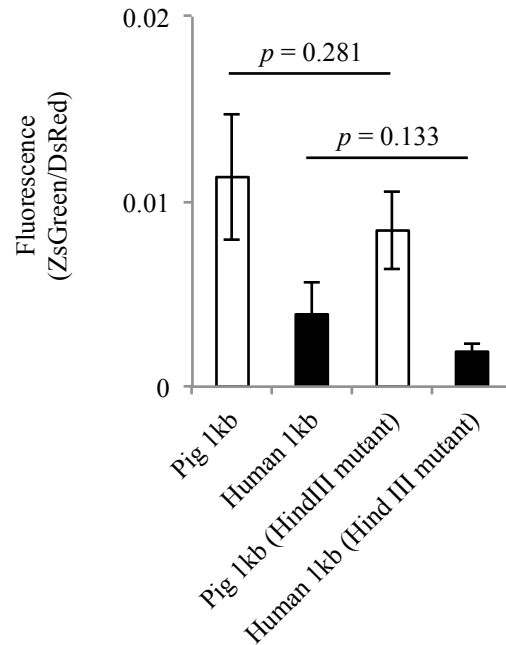


**Figure 2.18** The 2bp mutation introduced to the pig and human 1kb MyHC IIB promoters had no effect on the relative promoter activity in C2C12 myotubes (measured by fluorescence output).

#### 2.4.19 Site directed mutagenesis by PCR

Nucleotide substitutions within the promoter sequence were conducted by mutagenesis PCR, amplifying the entire plasmid but strategically forcing non-specific nucleotide annealing (within the primer) to create a mutated amplicon. Similarly, removal of nucleotides was conducted by omitting the relevant base pairs from the plasmid sequence being amplified. Nucleotide substitutions were typically located in the centre of the primer, with approximately 12 nucleotides on either side to ensure adequate annealing at the 5' and 3' ends. All primers for mutagenesis PCR were HPLC purified to minimise incorrect primer sequences. Primers were 5' phosphorylated to allow the linear PCR amplicon to be re-ligated into a circular plasmid for transformation in JM109 competent cells (as described above). A schematic diagram depicting the site

directed mutagenesis protocol is shown below (Figure 2.19). The image used is from the Phusion Site Directed Mutagenesis protocol (Thermo Scientific).

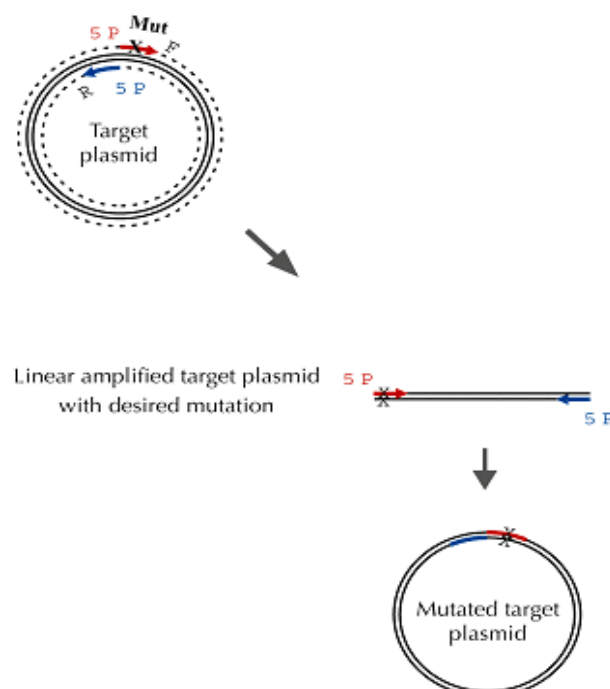


**Figure 2.19** Schematic diagram (from Phusion SDM protocol, Thermo Scientific) showing the principle of the mutagenesis PCR protocol employed herein.

The mutagenesis PCR was conducted using a high fidelity DNA polymerase (Q5, New England Biolabs) to amplify the entire plasmid with minimal PCR induced errors. The mutagenesis PCR was conducted in a 50µl volume (details in Table 2.9). Thermal cycling parameters for the Q5 polymerase is detailed in Table 2.10. Elongation times were based on a manufacturers recommendation of 30 seconds per 1kb of DNA to be amplified.

**Table 2.9** Components and quantities for site directed mutagenesis PCR using Q5 polymerase

Reagents	50µl reaction	Final concentration
5X reaction buffer	10µl	1X
10mM dNTP's	1µl	200µM
10µM Forward Primer	2.5µl	0.5µM
10µM Reverse Primer	2.5µl	0.5µM
Template DNA	-	50-500ng
Q5 polymerase	0.5µl	0.02U/µl
Nuclease-free water	Up to 50µl	-

**Table 2.10** Thermal cycling parameters for site directed mutagenesis PCR

Thermal cycle	Temperature	Duration
Initial denaturation	98°C	30 seconds
Amplification (30 cycles)	98°C	10 seconds
	50-72°C	30 seconds
	72°C	30 seconds/kb
Final extension	72°C	2 minutes
Hold	4°C	∞

#### 2.4.20 Site directed mutagenesis of MyHC IIB promoter

In order to study the role of sequence variation between the pig and human MyHC IIB promoters, site directed mutagenesis was conducted in the proximal human MyHC IIB promoter (making base pair alterations to match the equivalent pig sequence). Base pair substitutions were conducted at the locations specified in Figure 2.20 (highlighted in black), spread over two separate experiments. In addition to base pair substitutions, the CArG-box region (-63bp to -84bp; including the immediate 5' and 3' flanking region) was deleted from the pig and human 1kb MyHC IIB promoter (via mutagenesis PCR – simply occluding the amplification of the CArG-box region).





				HindIII chimeric-junction		
Human	-261	ATGAATGATGCAACAGCCAAACTGGAGAAACAGTGTAGAGCCCTGAATCCCCATCCCC	-202			
Pig	-259	ATGAATGATGGAACAGCAAAGCTGGAGAAATAGCCTTAGAGCCCTGAATCTCCATCCC-	-201			
		*****				
		AT3		AT2		
Human	-201	TATCAAATGCCTATAAAGAACCCTAGATCATCCTCTGTAAATTATTTATGGGTGTCAAG	-142			
Pig	-200	TATCAAATGCCTCAAAGAACCCTAGATGATCCTCTGTCAAATTATTTATAGGTGTCAAG	-141			
		*****				
		AT1				
Human	-141	AAATATTTCTAATTATATCCATTCACAGCCACAGTCAGTGAATATTGTGCAAAGAGATTG	-82			
Pig	-140	AAATATTTCTAATTATATCCATTCACAGCCACAGTCAGTGAATATTGTGCAAAGAGATTG	-81			
		*****				
		CArG-box		E-box2		E-Box1
Human	-81	CCAAAAACGGTTTGCCAAGTAGGTTCCAGCTAGGACAGCTGAGGTGGCTGCTGTGTTT	-22			
Pig	-80	CCAAAAAGGTTTGCCAAGTAGGTTCCAGCTAGGACAGCTGAGGTGGCTGCTGTGTTT	-22			
		*****				
		TATA-box (+1)				
Human	-21	GCAGAAATGGTCTCTATAAAAGTGGAGCTGAGATGCCTCTTTCCCATCCTTCCT	+32			
Pig	-21	GCAAAATGGTCTCTATAAAAGTGGAGCTGAGATGCCTCTGTCTGCTCCTTCCT	+32			
		***				

**Figure 2.21** The bold underline indicates the probe sequence used in the EMSA experiment, spanning the 3 base pair mismatches in the CArG/E-box region.

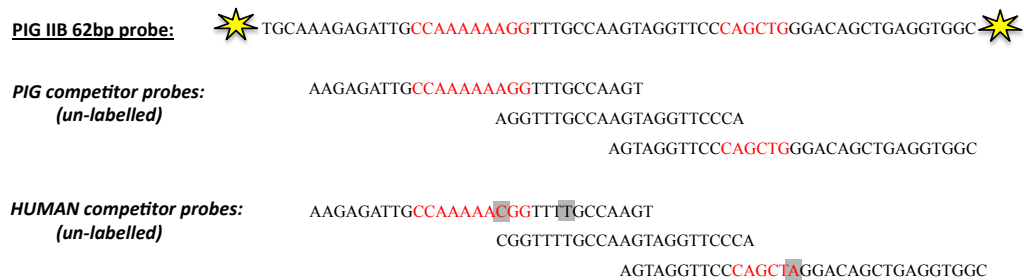


**Figure 2.22** Schematic diagram illustrating the overlapping un-labelled pig and human competitor probes relative to the biotin-labelled pig MyHC IIB 62bp probe (stars indicate biotin labelled probe). Red text indicates specific regions of interest (CArG-box and E-box). Grey boxes indicate base pair differences between the pig and human competitor probes. Only the sense probe strand is shown.

#### 2.4.22 Producing double stranded EMSA probes

Oligonucleotides, with 5' biotin labels, were synthesized and annealed to generate the double stranded probes used for EMSA experiments. Sense and antisense oligonucleotides (5µM each) were annealed in “annealing buffer” (10mM Tris-base (pH 8), 1mM EDTA, 50mM NaCl – in ultrapure water) by heating to 95°C for 5 minutes (in a hot block) and then slowly cooled to room

temperature over 90 minutes (by removing the metal hot block and leaving to cool on the bench), generating 5 $\mu$ M of each double stranded probe. Probes were diluted to the required concentrations on the day of use (concentrations noted below).

#### *2.4.23 C2C12 nuclear protein extracts*

C2C12 myotubes were removed from a T75 flask using the trypsin method (described above). Myotubes in suspension were pelleted at 500rpm for 5 minutes and re-suspended in cold PBS in a 1.5ml tube. Myotubes were then pelleted at 1000rpm for 3 minutes and the supernatant was removed. Myotube nuclear proteins were extracted using the NE-PER extraction kit (Thermo Scientific). Volumes of reagents used with the NE-PER kit are based on packed cell volume (day 4 myotubes from a T75 flask equated to a 100 $\mu$ l packed cell volume). The 100 $\mu$ l packed cell volume was combined with 1ml of CER I, mixed by vortexing for 15 seconds and then incubated on ice for 10 minutes to lyse cell membranes. Fifty-five micro litres of CER II was added to the lysed cells, vortexed for 5 seconds and incubated on ice for 1 minute. Lysed cells were then vortexed for 5 seconds followed by centrifugation at 16,000xg for 5 minutes. The supernatant, containing cytoplasmic proteins, was removed and stored at -80°C. The remaining pellet (containing myotube nuclei) was re-suspended in 500 $\mu$ l NER and incubated on ice for 40 minutes, vortexing for 15 seconds for every 10 minutes. Following incubation, lysed nuclei debris was pelleted by centrifugation at 16,000xg for 10 minutes. The supernatant (containing nuclear proteins) was stored at -80°C. Nuclear proteins

were stored in small aliquots to avoid freeze thawing, helping to maintain the integrity of nuclear proteins for use in downstream binding applications.

#### *2.4.24 EMSA binding reactions*

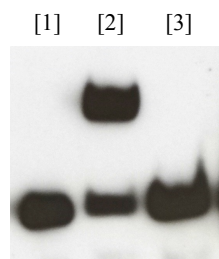
It was predicted that the response elements in the probe (CArG-box and E-box) would likely bind serum response factor (SRF) and/or myogenic regulatory factors (MRF), respectively. Therefore, the literature was searched for commonly used binding conditions for studying SRF or MRF DNA binding and the following predicted binding conditions were used herein. Protein-DNA binding conditions consisted of 50ng/ul Poly dI-dC, 5% glycerol, 0.05% NP-40, 50mM KCL, 1mM MgCl<sub>2</sub>, 1mM EDTA, 20fmol biotin-labeled probe, 4pmol un-labeled competitor probe and 3μl of C2C12 myotube nuclear extract (from NE-PER extraction kit, Thermo Scientific) in 1x binding buffer (LightShift Chemiluminescent EMSA kit, Thermo Scientific) in a total volume of 20μl. Protein-DNA binding reactions were incubated at room temperature for 20 minutes.

#### *2.4.25 Detection of protein-DNA complexes*

Protein-DNA complexes were separated by electrophoresis on a 6% non-denaturing polyacrylamide gel (Invitrogen, Novex) at 100V for 75 minutes (on ice) and transferred by electro-blotting to a Biodyne-B nylon membrane (Thermo Scientific) at 100V for 45 minutes. Protein-DNA complexes were cross-linked for 60 seconds (auto-crosslink) and biotin-labeled probes were detected using the LightShift Chemiluminescent EMSA detection module (Thermo Scientific) according to the manufacturer's instructions. Briefly, the

membrane was blocked in 20ml of blocking buffer for 15 minutes with gentle shaking. The blocking solution was then replaced with blocking buffer containing stabilized streptavidin-horseradish peroxidase conjugate (1:300 dilution) for a further 15 minutes with gentle shaking. The membrane was then washed for 5 minutes, five times, in 1x wash buffer (made in ultrapure water) with shaking. Following the wash steps, the membrane was transferred to 30ml of substrate equilibration solution for 5 minutes with gentle shaking. The membrane was transferred to a new container containing. A solution containing 6ml luminol/enhancer solution and 6ml stable peroxidase solution was gently poured onto the membrane and incubated for 5 minutes without shaking. The membrane was then dabbed on a paper towel for 3 seconds, transferred to a clear plastic sleeve, placed in a black-out cassette and exposed to x-ray film for approximately 5-10 seconds. Film was developed under dark conditions to visualise biotin labelled DNA probes.

A control EMSA (using manufacturer controls) was conducted to validate the method (see Figure 2.23). This experiment confirmed that protein-DNA interactions, electrophoretic separation of protein-DNA complexes and detection of biotin labelled probes on X-ray film was successfully conducted prior to attempting this method on experimental samples.



[1] Biotin-labeled EBNA DNA probe

[2] Biotin-labeled EBNA DNA probe + EBNA extract

[3] Biotin-labeled EBNA DNA probe + EBNA extract + 200-fold molar excess un-labeled EBNA probe

**Figure 2.23** Control EMSA (using manufacturer controls) shows successful protein-DNA interactions (lane 2) and competitive binding of unlabelled probes (lane 3).

**Table 2.11** Sense and anti-sense sequences of oligonucleotides used to generate double stranded EMSA probes

EMSA probe name	EMSA probe sequence (5' to 3')
Pig_MyHC-IIB_probe_sense	[biotin]TGCAAAAGAGATTGCCAAAAAAGGTTTGCCAAGTAGGTTCCCAGCTGGGACAGCTGAGGTGGC
Pig_MyHC-IIB_probe_anti-sense	[biotin]GCCACCTCAGCTGTCCAGCTGGGAACCTACTTGGCAAAACCTTTTTTTGGCAAATCTCTTTTGCA
Human_MyHC-IIB_CAR-G-competitor_sense	AAGAGATTGCCAAAAAACGGTTTTTGCCAAAGT
Human_MyHC-IIB_CAR-G-competitor_anti-sense	ACTTGGCAAAACCGTTTTTTGGCAAATCTCTT
Human_MyHC-IIB_mid-probe-competitor_sense	CGGTTTTTGCCAAAGTAGGTTCCCA
Human_MyHC-IIB_mid-probe-competitor_anti-sense	TGGGAACCTACTTTGGCAAAACCG
Human_MyHC-IIB_E-box2-competitor_sense	AGTAGGTTCCCAGCTAGGACAGCTGAGGTGGC
Human_MyHC-IIB_E-box2-competitor_anti-sense	GCCACCTCAGCTGTCTAGCTAGCTGGGAACCTACT
Pig_MyHC-IIB_CAR-G-competitor_sense	AAGAGATTGCCAAAAAAGGTTTGCCAAAGT
Pig_MyHC-IIB_CAR-G-competitor_anti-sense	ACTTGGCAAAACCTTTTTTTGGCAAATCTCTT
Pig_MyHC-IIB_mid-probe-competitor_sense	AGGTTTGCCAAAGTAGGTTCCCA
Pig_MyHC-IIB_mid-probe-competitor_anti-sense	TGGGAACCTACTTTGGCAAAACCT
Pig_MyHC-IIB_E-box2-competitor_sense	AGTAGGTTCCCAGCTGGGACAGCTGAGGTGGC
Pig_MyHC-IIB_E-box2-competitor_anti-sense	GCCACCTCAGCTGTCCAGCTGGGAACCTACT

#### 2.4.26 Transfection of C2C12 myoblasts

C2C12 myoblasts were seeded at approximately 30,000 cells per well of a 24-well plate and cultured for 30 hours in growth medium (10% FBS and 1% PS; 0.5ml per well) to reach approximately ~70% confluence. Myoblasts were considered to be in the log phase of proliferation at this phase (highlighted by the appearance of dividing cells – see light refractive cells below (indicated by black arrows; Figure 2.24)). Dividing cells elicit the best uptake of foreign plasmid DNA by lipid based transfection methods (according to manufacturer guidelines).

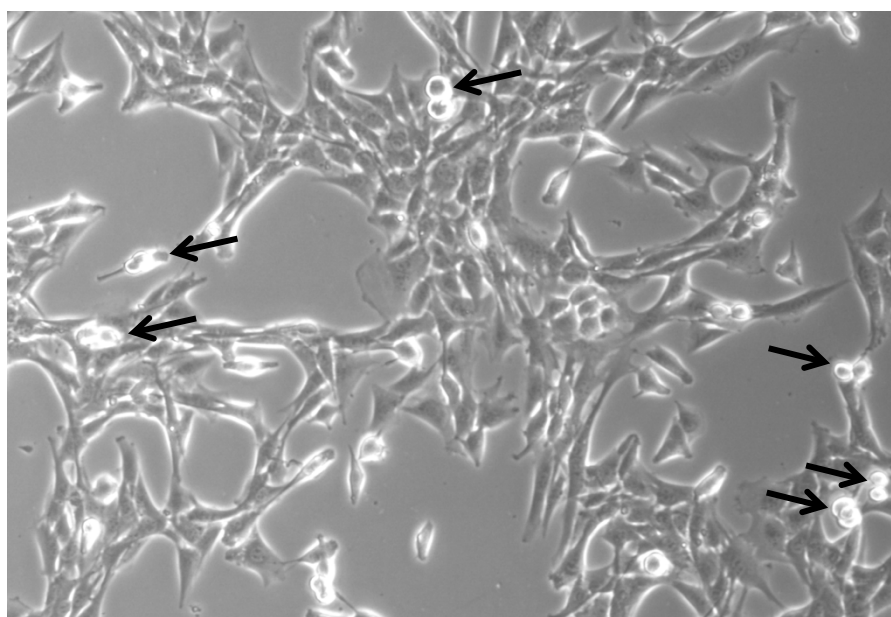


**Figure 2.24** Light microscopy image of the C2C12 myoblasts immediately prior to transfection (at ~70% confluence). Arrows indicate proliferating cells.

Cells were transfected using the lipid based transfection reagent, FugeneHD (Promega), at a ratio of 3:1 (FugeneHD:DNA). To compare the activity of the pig and human MyHC IIB promoters in C2C12 cells, 25µl of transfection complex containing 200ng of promoter-reporter plasmid and 100ng pDsRed-



Express-N1 (as a normalization control) was transfected into individual wells. A negative (pZsGreenI-I; 200ng per well) and a positive control (pZsGreenI-NI; 50ng per well) were included in transfection experiments to monitor the transfections conditions. The quantity of plasmid DNA used for transfections was optimized by a previous PhD student (Dr Mohd Nazmi Bin Abd Manap). When cells reached confluence, culture medium was switched to a differentiation medium (2% HS, 1% P/S) to encourage differentiation, and this medium was refreshed every 48 hours. Fluorescence output (as a marker of promoter activity) was measured on day 5 or 6 of differentiation using a Typhoon Trio+ (GE Healthcare). The excitation and emission settings for measuring ZsGreen and DsRed fluorescence from cell culture plates are displayed in the table below (Table 2.12).

**Table 2.12** Excitation and emission settings for measuring ZsGreen and DsRed fluorescence from cell culture plates using the Typhoon Trio+ (GE healthcare).

<b>Filter</b>	<b>Detected fluorescence</b>	<b>(nm)</b>	<b>Emission (nm)</b>	<b>PMT</b>	<b>Sensitivity setting</b>
1	ZsGreen	488	520	450	Medium
2	DsRed	532	580	600	Medium
<b>Additional notes:</b>		Focal plane = 3mm			
		Image quality = 100 micron			
		Scan time = 20 minutes per plate			

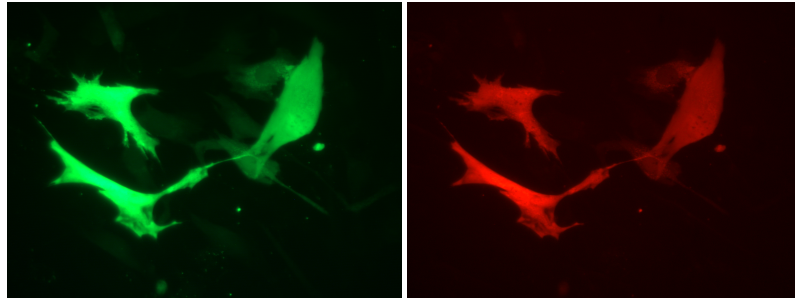


**Figure 2.25** Evidence for co-uptake of pDsRed-express-NI, with pZsGreen1-NI, for use as an internal transfection control (fluorescence images taken 48 hours post-transfection in C2C12 myoblasts).

ZsGreen fluorescence values (indicating promoter activity) were normalised against DsRed fluorescence values (from the same well) to correct for variation in transfection efficiency between wells ( $\text{ZsGreen} \div \text{DsRed}$ ). The fluorescence images in Figure 2.25 show co-uptake of the DsRed and ZsGreen plasmids validating the efficacy of DsRed as a co-transfection internal control for normalizing reporter gene fluorescence.

#### 2.4.27 Cloning murine MyoD cDNA

Full-length open reading frame murine MyoD cDNA (accession number: ENSMUST00000072514.1; amino acid sequence in Figure 2.26) was generated by RT-PCR for over-expression in C2C12 muscle cells. Firstly, RNA was extracted from C2C12 myoblasts as described previously in this chapter. First strand cDNA was synthesised (also described previously in this chapter) and the full-length MyoD transcript was amplified by RT-PCR using the primers in Table 2.13. The PCR was conducted as described previously in this Chapter (annealing temperature was 50°C).

```
MELLSPPLRDIDLTGPDGSLCSFETADDFYDDPCFDSPDLRFFEDLDPRLVH  
MGALLKPEEHAHFPTAVHGPFGAREDEHVRAPSGHHQAGRCLLWACKACKRK  
TTNADRRKAATMRERRRLSKVNEAFETLKRCTSSNPNQRLPKVEILRNAIRY  
IEGLQALLRDQDAAPPGAAAFYAPGPLPPGRGSEHYSGDS DASSPRSNCS DG  
MMDYSGPPSGPRRQNGYDTAYYSEAAARESRPGKSAAVSSLDCLSSIVERIST  
DSPAAPALLLADAPPESPPGPPEGASLS DTEQGTQTPSPDAAPQCPAGSNPN  
AIYQVL
```

**Figure 2.26** Full-length amino acid sequence for murine MyoD.

Following amplification of full-length MyoD cDNA, the 5' and 3' ends were cut by restriction digest and cloned upstream of CMV promoter in the pDsRed-Express-NI plasmid (as described previously in this chapter). Below is the sequence of the MyoD cDNA located within the multiple cloning site of the host plasmid (Figure 2.27). A Kozac sequence was engineered into the 5' end of the MyoD cDNA (by PCR) to maximise translation efficiency of the transcript produced. The downstream DsRed gene remained un-translated due to the inclusion of a translation stop codon at the end of the MyoD transcript, preventing the production of a MyoD-DsRed fusion protein.

**Table 2.13** Oligonucleotide primer sequences for amplifying full-length open reading frame murine MyoD cDNA and associated sequencing primers. Grey highlights indicate engineered nucleotides to introduce a Kozac sequence (forward primer) and in-frame additions (reverse primer). Underlined nucleotides indicate restriction sites used for cloning purposes (BglII and AgeI).

Primer name	Primer sequence
MyoD forward primer	AAAAAAAGATCTGCCACCATGGAGCTTCTATCGCCG
MyoD reverse primer	AAAAAAACCGGTGCTCAAAGCACCTGATAAATCGC
Mid-sequencing primer	GAGGCCTTCGAGACGCTC
5' flank sequencing primer	CATTGACGCAAATGGGCGGTAGG
3' flank sequencing primer	GGCCACGAGTTCGAGATCGAGG

ATTTCCAAGTCTCCACCCCATTTGACGTCAATGGGAGTTTGTTTTGGCACCAAAATCAACGGGA  
CTTTCCAAAATGTCGTAACAACCTCCGCCCATTTGACGCAAATGGGCGGTAGGCGTGTACGGTG  
GGAGGTCTATATAAGCAGAGCTGGTTTAGTGAACCGTCAGATCCGCTAGCGCTACCGGACTCA  
GATCTGCCACCATGGAGCTTCTATCGCCGCCACTCCGGGACATAGACTTGACAGGCCCCGACG  
GCTCTCTCTGCTCCTTTGAGACAGCAGACGACTTCTATGATGACCCGTGTTTCGACTCACCAG  
ACCTGCGCTTTTTTGGAGACCTGGACCCGCGCCTGGTGCACATGGGAGCCCTCCTGAAACCGG  
AGGAGCACGCACACTTCCCTACTGCGGTGCACCCAGGCCAGGCGCTCGTGAGGATGAGCATG  
TGCGCGCGCCAGCGGGCACCACCAGGCGGGTCTGCTGCTTGTGTGGGCTGCAAGGCGTGCA  
AGCGCAAGACCACCAACGCTGATCGCCGCAAGGCCGCCACCATGCGCGAGCGCCGCGCTGA  
GCAAAGTGAATGAGGCCTTCGAGACGCTCAAGCGCTGCACGTCCAGCAACCCGAACCAGCGGC  
TACCCAAGGTGGAGATCCTGCGCAACGCCATCCGCTACATCGAAGGTCTGCAGGCTCTGCTGC  
GCGACCAGGACGCGCGCCCCCTGGCGCCGCTGCCTTCTACGCACCTGGACCGCTGCCCCCAG  
GCCGTGGCAGCGAGCACTACAGTGGCGACTCAGATGCATCCAGCCCGCGCTCCAAGTCTCTG  
ATGGCATGATGGATTACAGCGGCCCCCAAGCGGCCCCCGGCGGCAGAAATGGCTACGACACCG  
CCTACTACAGTGAGGCGGCGCGAGTCCAGGCCAGGGAAGAGTGCGGCTGTGTGCGAGCCTCG  
ACTGCCTGTCCAGCATAGTGGAGCGCATCTCCACAGACAGCCCCGCTGCGCCTGCGCTGCTTT  
TGGCAGATGCACCACCAGAGTCGCCTCCGGGTCCGCCAGAGGGGGCATCCCTAAGCGACACAG  
AACAGGGAACCCAGACCCCGTCTCCCGACGCCGCCCTCAGTGTCTCTGCAGGCTCAAACCCCA  
ATGCGATTTATCAGGTGCTTTGAGCACCGGTGCCACCATGGCCTCCTCCGAGGACGTCATCA  
AGGAGTTCATGCGCTTCAAGGTGCGCATGGAGGGCTCCGTGAACGGCCACGAGTTCGAGATCG  
AGGGCGAGGGCGAGGGCCGCCCTACGAGGGCACCCAGACCGCCAAGCTGAAGGTGACCAAGG  
GCGGCCCCCTG

**Key:** MyoD sequence RE site (BglII + AgeI) Primers Plasmid  
engineered Kozak sequence

**Figure 2.27** Full-length murine MyoD cDNA in the pDsRed-Express-NI plasmid.

MyoD over-expression plasmids were transfected into proliferating myoblasts (at approximately 70% confluence) at a ratio of 1:1 with MyHC IIB promoter-reporter plasmids.

#### 2.4.28 Generating a pDsRed-Express-NI vehicle transfection control – Klenow Large Polymerase blunt-ending

Cells transfected with MyoD over-expression plasmids were compared against cells transfected with an equivalent quantity of non-functional, control plasmid DNA. The control plasmid DNA was generated by removing the CMV promoter from the MyoD host plasmid, pDsRed-Express-NI.

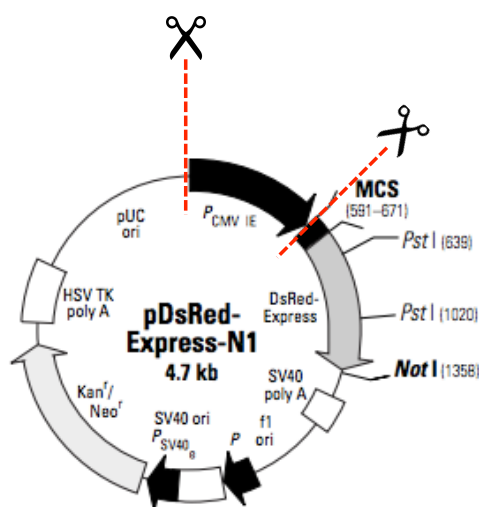


**Figure 2.28** Schematic illustrating the removal of the CMV promoter from the pDsRed-Express-NI plasmid for use as a vehicle transfection control in MyoD over-expression experiments

Restriction sites (AseI and XhoI) flanking the CMV promoter were digested and the linear plasmid, lacking the CMV promoter, was subsequently gel purified as described previously in this chapter. The digested restriction sites generated non-cohesive overhanging ends, making re-circularisation of the plasmid not possible. Therefore, the overhanging ends were converted to blunt ends using Klenow Large Polymerase (Promega) and the linear plasmid was blunt-end ligated. Purified linear plasmid (lacking the CMV promoter) was incubated as described in Table 2.14 at room temperature for 12 minutes. The

reaction was stopped by heating to 75°C for 10 minutes and the blunt-ended fragment was cleaned by conducting a PCR clean up procedure as previously described in this chapter. The blunt-ended linear plasmid was then re-ligated as described previously using T4 DNA ligase.

**Table 2.14** Components and quantities for the Klenow Large Polymerase reaction

Reagent	Volume (μl)	Final concentration
Klenow Buffer (10X)	4μl	1X
dNTP (500μM)	3.2μl	40μM
BSA (400μg/ml)	2μl	20μg/ml
Klenow Large Polymerase (5U/μl)	1μl	5U
Linearized plasmid	29.8μl	1-4μg
Total:	40μl	-

# 3

## CHARACTERIZATION OF THE C2C12 CELL LINE FOR MYOSIN HEAVY CHAIN STUDIES

---

*It was hypothesized that the C2C12 skeletal muscle cell line would exhibit dynamic alterations in expression of the myosin heavy chain isoform genes during myogenesis. Furthermore, it was hypothesized that the induction in expression of myosin heavy chain isoforms genes during myogenic differentiation would coincide with a restructuring of metabolic gene expression.*

### 3.1 CHARACTERIZING C2C12 MYOGENESIS AND THE ENDOGENOUS TRANSITIONS IN MYOSIN HEAVY CHAIN ISOFORM EXPRESSION

#### 3.1.1 INTRODUCTION

Measuring myosin heavy chain (MyHC) isoform expression currently offers the most suitable marker of muscle fibre composition as specific MyHC isoforms generally coincide with a well-defined set of contractile and metabolic properties (Delbono 2010). Adult skeletal muscle is composed of four major muscle fibre types (type I, IIa, IIx and IIb; Lefaucheur 2010) with two further isoforms, embryonic (emb) and neonatal (neo), which are generally only expressed during development or states of muscle regeneration (Harrison et al. 2011; D'Antona et al. 2006). Research investigating muscle fibre type transitions are typically studied *in vivo* with relatively few reports *in vitro*. Furthermore, the few studies which have explored transitions in expression of MyHC isoforms *in vitro* have been conducted using relatively non-specific antibodies. These antibodies typically detect several MyHC isoforms and thus are ineffective in elucidating the precise pattern of expression as myogenic cells differentiate and mature (Silberstein et al., 1986; Miller 1990). Thus this study attempted to produce a comprehensive analysis of the endogenous mRNA expression of all six specific MyHC isoforms and myogenic regulatory factors (MRF) during the proliferation and differentiation of the C2C12 mouse myoblast cell line (a commonly used cell line for muscle biology research). Understanding the typical characteristics of this cell line will provide important information to any scientist working with this cell line and also enables further *in vitro* research into the molecular mechanisms regulating transitions in MyHC isoform expression.



### 3.1.2 MATERIALS AND METHODS

*The materials and methods described here are a brief overview only. A more comprehensive explanation of the techniques described herein is detailed in the Materials and Methods Chapter.*

#### 3.1.2.1 Cell culture

C2C12 muscle cells were seeded at 100,000 cells per well of 6-well plates and grown in growth medium (DMEM, 10% FBS, 1% P/S). Cells were encouraged to differentiate at near confluence (day 0; 36-48hrs post seeding) by replacing the medium with a low serum differentiation medium (DMEM, 2% HS, 1% P/S) and cultured for 8 days to allow myoblasts to fuse to form mature myotubes. Medium was replenished every 48 hours.

#### 3.1.2.2 Cell harvest

Cells were harvested on days -1, 0, 1, 2, 4, 6 and 8. Immediately prior to harvesting cells, the culture medium was removed. Cells harvested for RNA were scraped directly into 200µl of RNase-free phosphate buffered saline (PBS), snap frozen on dry ice (solid CO<sub>2</sub>) and stored at -80°C until analysis. Cells harvested for DNA content and creatine kinase (CK) activity were washed with 1ml PBS and then scraped into 500µl tri-sodium citrate (4°C), placed on ice whilst the other samples were harvested and then stored at -20°C until use.

#### *3.1.2.3 DNA, Creatine Kinase and protein quantification assay*

Cells harvested for DNA content and CK activity were initially stored at -20°C. Cells were thawed slowly on ice followed by immediate lysis by sonication (Soniprep150, MSE, UK) on ice with amplitudes of 10 microns for 10 seconds (until the sample turned clear). Lysed cells were assayed for CK activity using a CK kinetic assay kit (Thermo Electron Corporation, Fisher Scientific, Loughborough, UK) on a 96-well absorbance platereader. Hoechst fluorescent dye was used to quantify DNA content in lysed cell samples using a 96-well fluorescence platereader assay (described in detail by Hurley et al. 2006). Total protein of the cell lysate was measured by the assay of Lowry.

#### *3.1.2.4 Quantitative RT-PCR*

Total RNA was extracted from cells using an RNA isolation kit (ROCHE High Pure Isolation Kit for RNA isolation) and stored at -80°C until use. RNA concentrations were adjusted to 100ng/μl and first strand cDNA was synthesised (using Promega reagents). Relative abundance of specific transcripts was determined by Q-RT-PCR using the standard curve method (conducted on a Roche Lightcycler480). Transcript abundance was normalized for total cDNA in the Q-RT-PCR reaction (using the oligreen method; Rhinn et al. 2008). A list of genes measured by Q-RT-PCR and their respective primer sets are displayed in Table 3.1.

Primer sequences for measuring MyHC I, IIA, IIX and neonatal isoforms were obtained from Zhou et al. (2010) and primer sequences for MyHC IIB and embryonic isoforms were from Da Costa et al. (2007). Primer sequences for

MyoD (ENSMUST00000072514), Myf-5 (ENSMUST00000000445) and Myogenin (ENSMUST00000027730) were previously designed and tested in-house (by Dr Zoe Daniel).

**Table 3.1** Forward and reverse primers for the mouse MyHC and MRF's genes

Gene	Forward primer	Reverse primer	Amplicon length
MyHC I	CTCAAGCTGCTCAGCAATCTATTT	GGAGCGCAAGTTTGTCTAAGT	152bp
MyHC IIa	AGGCGGCTGAGGAGCACGTA	GCGGCACAAGCAGCGTTGG	130bp
MyHC IIx	GAGGGACAGTTCATCGATAGCAA	GGGCCAACTTGTCATCTCTCAT	154bp
MyHC IIb	CAATCAGGAACCTTCGGAACAC	GTCCTGGCCTCTGAGAGCAT	80bp
MyHC emb	TCCGACAACGCCTACCAGTT	CCCGGATTCTCCGGTGAT	72bp
MyHC neo	CAGGAGCAGGAATGATGCTCTGAG	AGTTCCTCAAACCTTCAGCAGCCAA	113bp
Myogenin	CCCATGGTGCCCAAGTGAA	GCAGATTGTGGGCGTCTGTA	130bp
Myf5	CAGCCCCACCTCCAAGTG	GCAGCACATGCATTGATACATC	117bp
MyoD	CGTGGCAGCGAGCACTAC	TGTAATCCATCATGCCATCAGA	79bp

#### 3.1.2.5 Mouse MyHC primer test

Melt-curve analysis for each primer set was conducted on C2C12 derived cDNA. Due to the very similar sequences of the MyHC isoforms, Q-RT-PCR amplicons were separated by horizontal agarose gel (1.5%) electrophoresis to ensure the amplicons produced in the reaction were of the correct length (see Figure 3.1 for MyHC primer test), providing confidence that the correct isoforms were being measured.

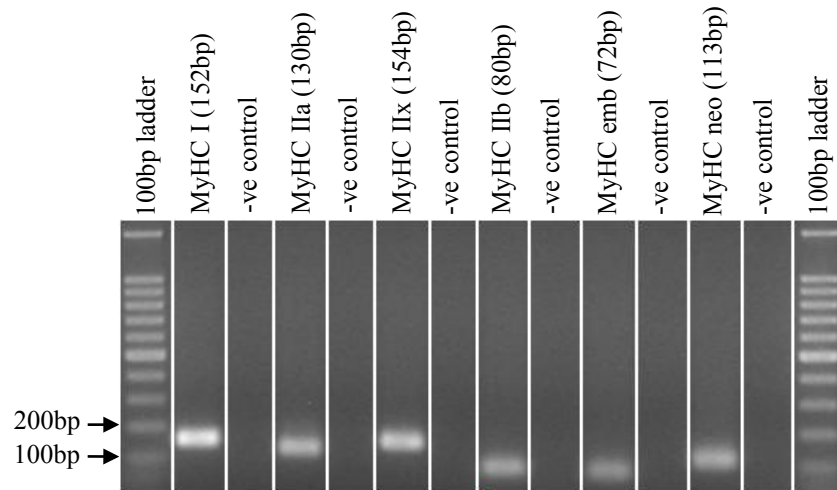


**Figure 3.1** Horizontal agarose gel (1.5%) electrophoretic separation of MyHC PCR amplicons to confirm primers are specific

#### *3.1.2.6 Statistical analysis*

All analyses were carried out on a single experiment with four biological repeats (separate wells) spread over two 6-well plates. Changes in mRNA transcript abundance, DNA content and CK activity across the time course were analysed by one-way analysis of variance. Tukey HSD post hoc analysis was used to determine differences between specific time points. Significance was accepted if  $p < 0.05$ . All statistical analyses were performed on SPSS statistical package version 16 (SPSS Inc., Chicago, IL, USA). Data in figures is displayed as mean  $\pm$  standard deviation (SD).

### 3.1.3 RESULTS

#### 3.1.3.1 Proliferation

DNA content was measured as a marker of cell proliferation, with an increase in DNA content suggesting an increase in cell number. As expected, DNA content changed significantly over the time course ( $p < 0.001$ ). DNA content increased rapidly from day -1 to day 0 (3.7-fold increase;  $p < 0.001$ ) as cells proliferated (Figure 3.2A). This coincided with a visual increase in cell number (Figure 3.2A; day -1 and day 0). DNA content increased slightly between day 0 and day 1 ( $p = 0.039$ ) when it began to plateau as cells started to differentiate (Figure 3.2A; Figure 3.3).

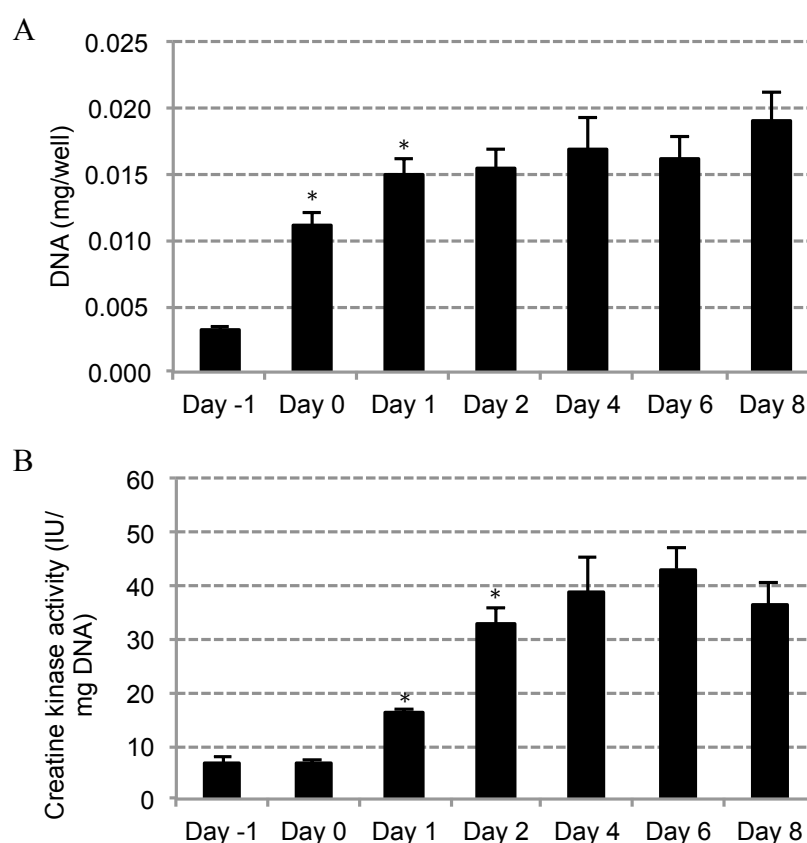


**Figure 3.2** (A) DNA content and (B) creatine kinase activity (corrected for DNA content) during C2C12 proliferation and differentiation (mean  $\pm$  SD;  $p < 0.001$ ). \* indicates significant difference from the previous timepoint ( $p < 0.05$ ).

### *3.1.3.2 Differentiation*

Creatine kinase (CK) activity (corrected for DNA content) was measured as a marker of muscle differentiation and changed significantly across the time course ( $p < 0.001$ ). CK activity was low in myoblasts and did not change between day -1 and day 0 ( $p = 1.0$ ), when cells were still proliferating (Figure 3.2B). This was confirmed visually by a lack of myotubes observed at days -1 and 0 (Figure 3.3). CK activity increased slightly on day 1 ( $p = 0.014$ ; Figure 3.2B), which coincided with the cells becoming confluent and beginning to fuse (Figure 3.3). As cells formed small, early stage myotubes (day 2; Figure 3.3) CK activity increased substantially (4.7-fold increase over day -1;  $p < 0.001$ ) and continued to increase to day 6 (6.3-fold increase over day -1;  $p < 0.001$ ; Figure 3.2B). Interestingly, CK activity peaked at day 6 and began to decline on day 8 (Figure 3.2B).

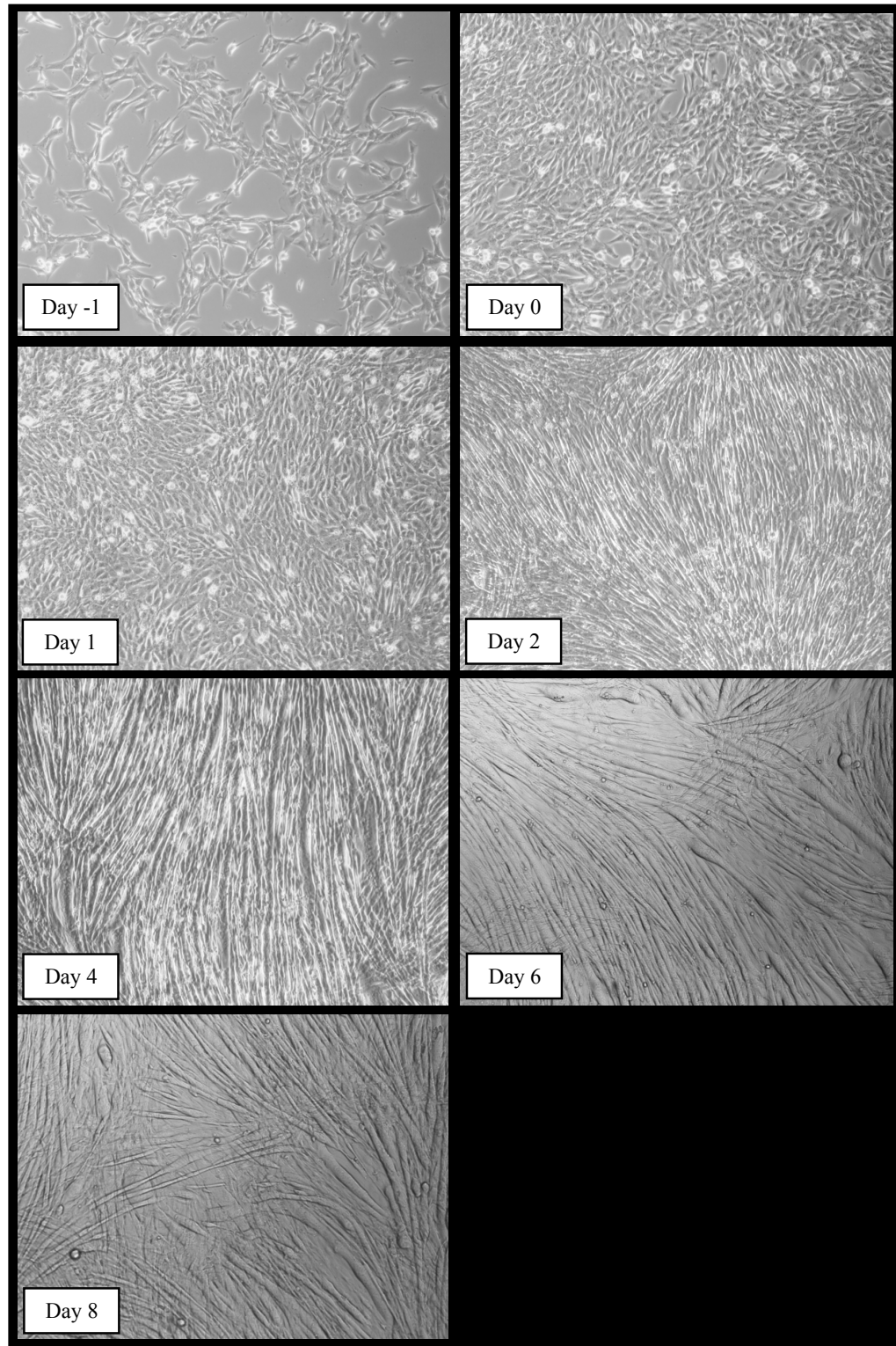


**Figure 3.3** Light microscopy images of C2C12 cells during proliferation and differentiation

### 3.1.3.3 Myoblast fusion to form myotubes

As highlighted in the pictures below, myoblasts in Figure 3.4A (stained with Hoechst dye) contain single nuclei (examples indicated by white arrows). In Figure 3.4B, myotubes expressing ZsGreen in the cytoplasmic regions show that individual myotubes contain several nuclei per cell (black circles; examples indicated by white arrows). Collectively, these images confirm the fusion of single nuclear myoblasts to form multinucleated myotubes during myogenesis.

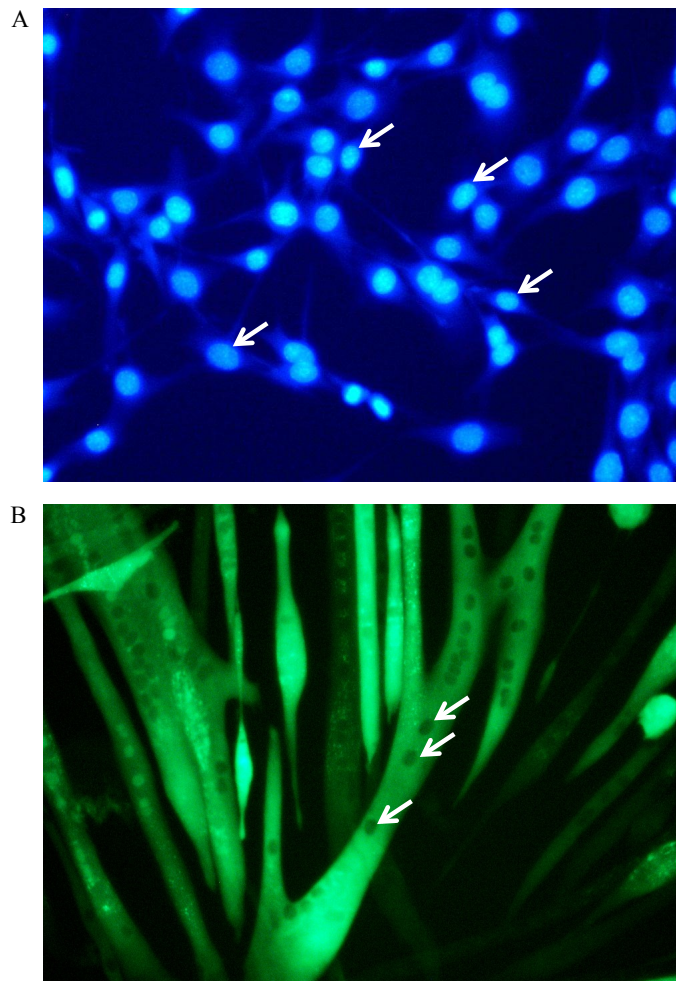


**Figure 3.4** (A) Hoechst stained C2C12 myoblasts show that myoblasts contain a single nuclei per cell (examples indicated by arrows). (B) ZsGreen expressing C2C12 myotubes highlights that myotubes contain multiple nuclei (black circles – examples indicated by arrows).



### 3.1.3.4 RNA yield from proliferating myoblasts and differentiating myotubes

Average RNA yield (per well) from C2C12's cultured in 6-well plates is presented below (Figure. 3.5). Crude RNA concentration from cultured cells shows total RNA yield increasing with differentiation. Interestingly, when RNA yield is corrected for total DNA (as a marker of cell number), relative RNA abundance displays a biphasic profile (Figure 3.5). The highest RNA:DNA ratio was exhibited by proliferating myoblasts. RNA:DNA ratio initially declined with myoblast fusion and then increased throughout differentiation.

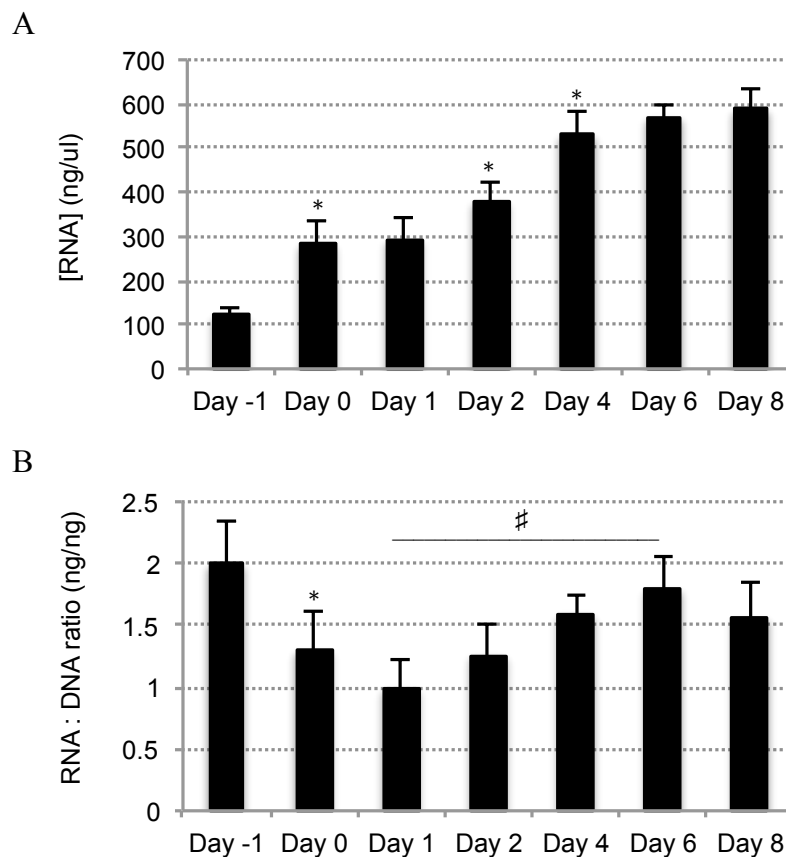


**Figure 3.5** RNA yield from C2C12's during proliferation and differentiation represented (A) per well of 6-well plates or (B) relative to DNA content. Data presented as mean  $\pm$  SD. \* indicates significant difference relative to the previous time point ( $p < 0.05$ ); # indicates a significant difference between day 1 and 6 ( $p < 0.01$ ).

#### 3.1.3.5 Myogenic regulatory factor (MRF) mRNA expression

MyoD mRNA expression did not change ( $p=0.189$ ) during the time course (Figure 3.6A). In contrast, Myf5 mRNA expression changed over the time course ( $p<0.001$ ), being high in myoblasts, with a similar level of expression from day -1 to day 1 (Figure 3.6B). On day 2, myf5 mRNA expression dramatically declined (to ~50% of the level of expression at days -1 to day1;  $p<0.001$ ) whereby it remained the same throughout differentiation (Figure 3.6B). There were also significant changes in expression of myogenin mRNA across the time course ( $p<0.001$ ). Figure 3.6C shows myogenin mRNA expression was low in myoblasts (day -1 and 0), increased substantially on days 1 (48.3-fold increase over day -1;  $p<0.001$ ) and 2 (70.8-fold increase over day -1;  $p<0.001$ ), but then declined on days 6 and 8 (approx. 35-fold increase over day -1;  $p<0.001$ ). The initial and substantial increase in myogenin mRNA expression at days 1 and 2 coincided with myotube formation being observed at day 2 (Figure 3.3).

Crossing point values during Q-PCR analysis of myogenic regulatory factors are displayed in Table 3.2.

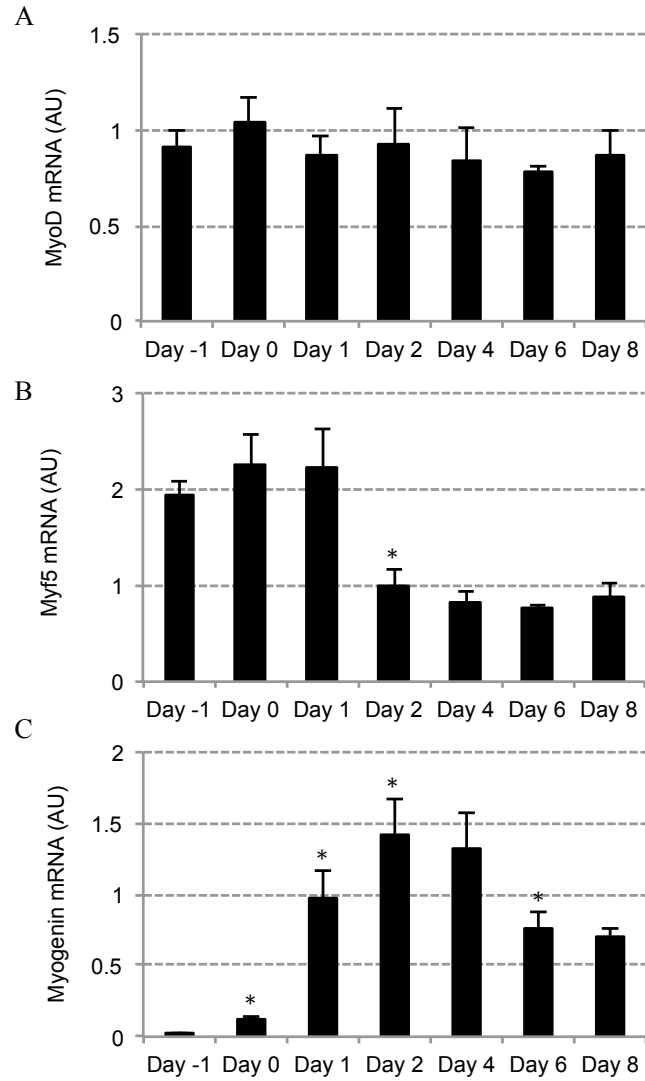


**Figure 3.6** (A) MyoD ( $p=0.189$ ) (B) myf5 ( $p<0.001$ ) and (C) myogenin ( $p<0.001$ ) mRNA expression during C2C12 proliferation and differentiation (mean  $\pm$  SD). \* indicates a significant difference relative to the previous time point ( $p < 0.05$ ).

**Table 3.2** Crossing point values for Q-PCR analysis of myogenic regulatory factors

	MyoD	Myogenin	Myf5
Day -1	27.9	31.8	27.0
Day 0	27.4	28.5	26.4
Day 1	27.8	25.3	26.5
Day 2	27.6	24.6	27.9
Day 4	27.8	24.7	28.2
Day 6	27.8	25.6	28.2
Day 8	27.8	25.8	28.2

### 3.1.3.6 Myosin Heavy Chain mRNA expression

Expression of all six myosin heavy chain (MyHC) mRNA isoforms changed significantly across the time course of differentiation (all  $p < 0.001$ ), but in two distinct cohorts. Expression of MyHC emb, neo and type I isoforms was low on day 1, increased dramatically at day 2 ( $p < 0.001$ ), peaked at days 2 or 4 and then declined to day 8 (Figure 3.7A, 3.7B and 3.7C). The fast, type II isoforms (IIa, IIx and IIb) were expressed in a distinctly different pattern to the emb, neo and type I isoforms, in that their expression appeared much later during differentiation and continued to increase to day 8 (Figure 3.7D, 3.7E and 3.7F). MyHC IIa and IIx expression first appeared at a low level on day 2 (Figure 3.7D and 3.7E), whereas MyHC IIb mRNA expression appeared later, on day 4 (Figure 3.7F).

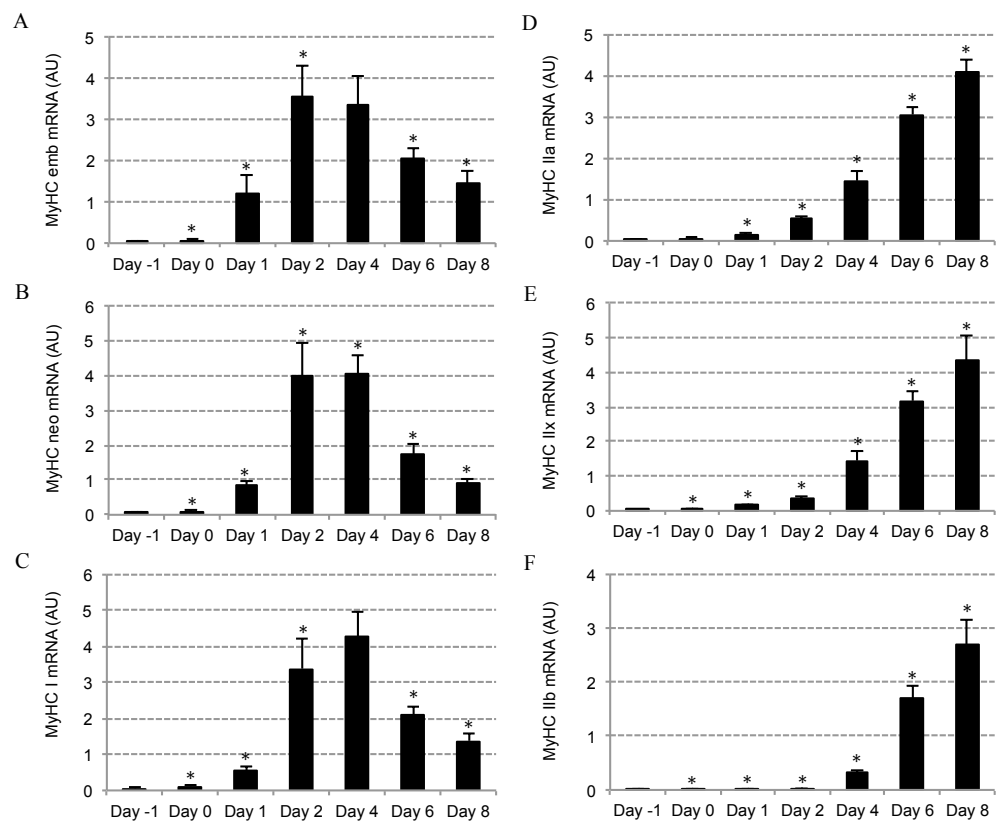


**Figure 3.7** (A) MyHC emb (B) neo (C) type I (D) type IIa (E) type IIx and (F) type IIb mRNA expression during C2C12 proliferation and differentiation (mean  $\pm$  SD;  $p < 0.001$ ). \* indicates a significant difference relative to the previous time point ( $p < 0.05$ ).

Assessment of the crossing point values during Q-PCR of the MyHC isoforms confirms that individual isoforms do exhibit differential expression profiles during differentiation (Table 3.3). Using crossing point values as an indicator absolute transcript abundance, these data show that fully differentiated C2C12 myotubes express an abundance of transcripts for type IIX and IIB MyHC isoform, with lower quantities of the emb, neo, type I and IIA MyHC isoforms.

**Table 3.3** Crossing point values for Q-PCR analysis of MyHC isoforms

	MyHC emb	MyHC neo	MyHC I	MyHC IIA	MyHC IIX	MyHC IIB*
Day -1	39.2	36.5	37.0	39.1	32.4	35.5
Day 0	38.2	35.8	36.0	37.2	31.1	33.7
Day 1	32.0	31.8	33.1	34.7	28.3	32.4
Day 2	29.9	29.3	30.0	32.4	26.8	31.5
Day 4	29.6	28.9	29.3	30.9	24.5	27.5
Day 6	30.6	30.3	30.5	29.9	23.3	24.9
Day 8	31.1	31.2	31.0	29.4	22.7	24.4

\* conducted on a different batch of cDNA

### 3.1.3.7 Myosin Heavy Chain I promoter activity in C2C12 cells

Transcripts for the type I MyHC isoform were present from day 1 in differentiation, which was surprisingly early as this was prior to myoblast fusion (Figure 3.3 and 3.7C). Therefore, a 1kb mouse MyHC I fluorescence promoter-reporter plasmid was constructed and transfected into C2C12 myoblasts to visually confirm the timing of MyHC I promoter activation. Indeed, MyHC I promoter activity was detected in myoblast cells, prior to fusion into myotubes (Figure 3.8). As differentiation proceeded to day 4, MyHC I promoter activity was restricted to myotubes.

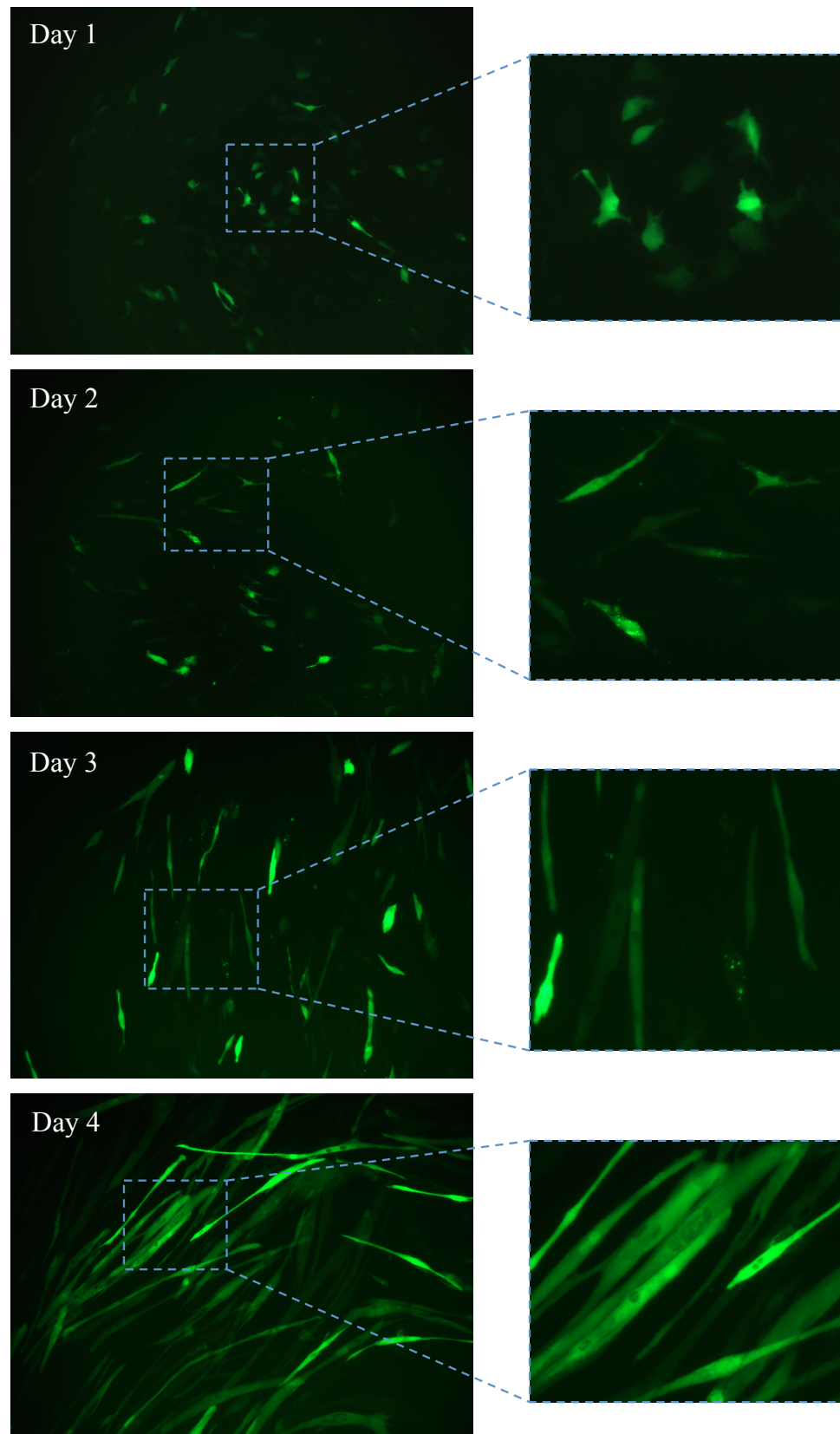


**Figure 3.8** Visualization of mouse 1kb MyHC I promoter activity using a ZsGreen reporter plasmid in C2C12 muscle cells. Note that the MyHC I promoter is active in myoblasts (day 1), prior to myotube formation. By day 4 of differentiation, MyHC I promoter activity was strong and restricted to differentiated myotubes.

### 3.1.4 DISCUSSION

Understanding the typical characteristics of a cell line is a prerequisite for any scientific intervention. Thus, this initial study set out to characterize the process of C2C12 myogenesis and in particular, the changes in relative mRNA expression of the MyHC isoforms and myogenic regulatory factors (MRFs) during differentiation.

Muscle differentiation (myogenesis) is associated with the activation of muscle specific genes (Sabourin and Rudnicki 2000) and is characterized by myoblasts fusing to form myotubes. The present study highlighted that C2C12 myoblasts fuse/differentiate to form multinuclear myotubes, supporting the wealth of literature detailing myogenesis. During muscle cell differentiation, genes encoding contractile proteins, such as the MyHC's, are activated (Sabourin et al. 1999). This study revealed, for the first time, that during *in vitro* C2C12 myogenesis, the activation of MyHC genes are not all activated at the same time nor in the same pattern and that potentially, a transition from emb, neo and type I to the fast, type II MyHC isoforms is occurring.

The results of the present study provide probably the most detailed account of the endogenous MyHC isoform expression during C2C12 myogenesis, with few previously published *in vitro* studies examining MyHC isoform transitions during myogenesis (Silberstein et al. 1986; Weydert et al. 1987; Miller 1990). Miller et al. (1990) conducted immunofluorescent staining of C2C12 cells and immunoblotting using monoclonal antibodies, R11D10 (against type I MyHC), F47 (against perinatal (also known as neonatal), type IIa and type IIb) and F59 (against all MyHC isoforms). The authors report that C2C12 myotubes differentiated for 7 days expressed predominantly type I and perinatal MyHC

isoforms. However, the use of antibodies that were not specific to individual isoforms does not enable an accurate elucidation of the expression patterns of specific MyHC isoforms. Furthermore, previous studies used antibodies raised against MyHC isoforms expressed in human muscle at fetal and neonatal stages of development (Silberstein et al. 1986). The fetal antibody (F1.652) detected MyHC in mouse fetal (gestation day 17), but not adult (4 months) muscle, whereas the neonatal antibody (N3.36) detected MyHC in mouse perinatal muscle (gestation day 19) and adult (4 months and 6 months) muscles, but not fetal muscle. Immunofluorescence studies in cell culture using these antibodies allowed the identification that transitions from “early” to “late” MyHC isoforms occur *in vitro*, but did not reveal the specific MyHC isoforms present in these “early” and “late” MyHC groups (Silberstein et al. 1986). For the first time, data presented herein shows that these two cohorts of MyHC isoforms consist of emb, neo and type I as “early” isoforms and fast IIa, IIx and IIb as “late” isoforms. In support of our findings, Weydert et al. (1987) reported that C2/7 mouse myotubes, cultured for 3 days, exhibit a sequential accumulation of embryonic, perinatal and adult IIb MyHC transcripts. We report a sequential pattern of accumulation of these mRNA isoforms during early differentiation (up to day 2 or 4) but in addition, we also report a transition from day 2 or 4 onwards in that embryonic and neonatal isoforms become down regulated as the adult IIa, IIx and IIb isoforms are up-regulated. Importantly, the transitions in MyHC isoforms expressed in C2C12 cells described here are in agreement with the pattern of transitions reported previously in mouse skeletal muscle during postnatal development *in vivo*, at both the mRNA (Weydert et al. 1987) and the protein (Agbulut et al. 2003)



levels, suggesting that the C2C12 muscle cell line is a good model for studying developmental myogenesis. Interestingly, the responses observed in the current study in C2C12 cells only matched the expression patterns of MyHC in fast muscles (EDL, plantaris and Gastrocnemius), but not slow (soleus) muscles (Agbulut et al. 2003). In fast muscle, MyHC protein expression began with emb, neo and type I isoforms, which were gradually replaced with the fast isoforms; whereas in the soleus (a slow muscle), emb and neo isoforms declined with development, but type I expression increased. The authors suggest that the postnatal transitions from emb, neo and type I MyHC to the fast MyHC isoforms in fast skeletal muscle is a result of the introduction of external/environmental stimuli such as innervation, contraction and circulating hormones. That the same pattern of transitions occurred *in vitro* in the current study (at the mRNA level), suggests that the driving factors inducing transitions from emb, neo and type I MyHC isoforms to the adult, fast MyHC isoforms can occur independent of innervation, although effects of spontaneous cellular contractions cannot be ruled out. In support of this, Weydert et al. (1987) reported that injection of beta-bungarotoxin (which destroys peripheral nerves) into mouse fetuses had no effect on the accumulation of perinatal and adult IIb MyHC isoform transcripts. However, the involvement of contraction mediated transitions in MyHC isoforms cannot be excluded, as sodium channel blockers that inhibit spontaneous myotube contraction, such as tetrodotoxin, were shown to reduce the appearance of neonatal MyHC expression *in vitro* (Cerny and Bandman 1986).

It is interesting to speculate, from the data presented herein, that the specific timing of MyHC mRNA isoform induction serves a developmental purpose

during myogenesis. For example, the embryonic, neonatal and type I MyHC isoforms may be induced prior to myoblast fusion to provide the structural components to form the immature myotube, but do not permit fast contractions that may damage the developing myotubes. The fast contracting, type II isoforms, on the other hand, are likely induced later in differentiation only once the myotubes are structurally capable of coping with a stronger contracting cellular machinery, thus limiting contraction induced cell damage during early myotube development.

The genes encoding the type II isoforms (IIa, IIx and IIb) are found in a gene cluster on chromosome 11 for mice in this sequential order from 5' to 3', which also includes the emb and neo isoforms (on either side of the fast isoform cluster). However, the gene encoding the type I isoform is located in a separate cluster on a different chromosome (14 for mice). It has been suggested that the clustered location of the MyHC genes is involved in their regulation (Luther et al. 1998; Pandorf et al. 2006; Giger et al. 2007; Rinaldi et al. 2008). Of particular interest, Pandorf et al. (2006) and Rinaldi et al. (2008) report that a bi-directional promoter in the intergenic regions of the type II MyHC genes produces sense RNA of the target gene whilst simultaneously producing antisense RNA of the upstream gene(s) (5' direction) and subsequently causes a down regulation of the upstream gene(s), although the mechanism of action remains elusive. This process would result in a coordinated pattern of expression, whereby up-regulating one isoform subsequently down-regulates its nearest 5' isoform. Although the naturally occurring antisense was not measured in the current study, the co-expression of the type II MyHC genes suggests that a bi-directional promoter may not be

involved in their regulation in this *in vitro* system. In addition, perhaps this mechanism of regulation may require a more physiological system, such as innervation, to function.

The down-regulation of the emb, neo and type I isoforms from day 4 or day 6 onwards and the continual increase in expression of the type II isoforms from day 4 through to day 8 suggests a transition in MyHC isoforms. This transition coincided with the visual observation of myotube hypertrophy and presents the question as to whether the molecular signals inducing myotube hypertrophy also initiate a transition towards the fast MyHC isoforms. It would seem logical for enlarging myofibres to express the necessary fast contractile machinery as well; particular as the largest myofibres *in vivo* typically express the faster MyHC isoforms (Lefaucheur 2010). Indeed, it has been reported that increased proportions of type IIb MyHC transcripts are associated with increased muscularity in pigs (Wimmers et al. 2008) and that increased rates of hypertrophy during development is likely to be driving a transition to increased MyHC IIb content rather than *vice versa* (Gunawan et al. 2007). Support for this notion comes from the observation that small myotubes express “early” fetal MyHC isoforms and large myotubes express “late” neonatal and adult MyHC isoforms (Silberstein et al. 1986), suggesting that MyHC transitions coincide with myotube hypertrophy. Interestingly, myostatin knockout mice display profound muscle hypertrophy and hyperplasia with subsequent alterations in muscle phenotype, namely a transition towards increased IIb fibres and hypertrophy of type IIb fibres (Matsakas et al. 2010). Hence it is plausible that molecular signals driving hypertrophy may also regulate MyHC isoform expression towards the fast type II isoforms. Of course, this may be

mediated via changes in contractility, since myotube hypertrophy may lead to spontaneous myotube contraction, which could in turn influence MyHC expression (Cerny and Bandman 1986).

Myogenin is a key signalling factor required for muscle cell differentiation (Nabeshima et al. 1993; Hasty et al. 1993). The pattern of myogenin mRNA expression in the current *in vitro* study was very similar to that reported in cultured L6 rat myoblasts (Wright et al. 1989) and during ovine fetal development *in vivo* (Fahey et al. 2005), all showing increasing myogenin mRNA as cells differentiate and declining myogenin mRNA as cells become well differentiated. This provides support for the validity of an *in vitro* muscle cell culture system to mimic the *in vivo* developmental myogenic program. Myf5 mRNA expression was high during myoblast proliferation and displayed a rapid down-regulation which coincided with myotube formation. This supports the notion that myf5 is a proliferative transcription factor during myogenesis (Kitzmann et al. 1998; Ustanina et al. 2007; Gayraud-Morel et al. 2007). MyoD and myogenin have been well documented to accumulate in fast and slow muscles, respectively (Voytik et al. 1993; Hughes et al. 1993; Elmark et al. 2007). Due to the differential accumulation in phenotypically different muscles, the ratio of MyoD to myogenin in skeletal muscle may contribute to muscle fibre type regulation. MyoD has been implicated in activating the fast, MyHC IIb gene (Wheeler et al. 1999; Allen et al. 2001; Harrison et al. 2011). Surprisingly, MyoD mRNA expression remained unchanged throughout myogenesis in C2C12 cells in the current study, which agrees with a previous study in numerous myogenic cell types (Miller 1990). It is interesting that the pattern of expression of MyHC IIb mRNA was not preceded by an up-

regulation of MyoD mRNA expression, as is the case during muscle fibre type transitions towards increasing MyHC IIb observed *in vivo* (Wheeler et al. 1999). There is evidence to suggest that MRF's may be post-transcriptionally regulated as long term changes in MyoD and myogenin at the mRNA level can occur without changes at the protein level (Alway et al. 2002). Thus, MRF's should be measured at the protein level to give a more valid indication of the quantity of "functional" MRF's present and to provide more viable data on their influence on MyHC isoform regulation. Furthermore, Elmark et al. (2007) reported that the phosphorylation status determines the effect of MyoD on MyHC IIb activation. Over-expression of MyoD in normally active mouse soleus muscle had little effect on fibre type composition, but over-expression of MyoD mutated at T115, making it resistant to phosphorylation, had profound effects on fibre type composition, increasing type II positive fibres from 50% to 85% (Elmark et al. 2007). The slow pattern electrical activity of the soleus appears to phosphorylate MyoD, impairing its activity as a MyHC IIb inducing transcription factor. The phosphorylation status of other MRF's and their subsequent role in myogenesis and MyHC expression has not been investigated. Due to the lack of nerve innervation in cell culture systems, contraction-induced phosphorylation of MRF's may be overlooked. Thus, studying MRF transcript and protein levels as well as phosphorylation status during myogenesis would be informative to elucidate their role, if any, on MyHC isoform expression during myogenesis. Furthermore, MRF's have been shown to physically interact with other transcription factors known to induce muscle specific gene expression, such as serum response factor (Groisman et

al. 1996), suggesting post-translational regulation of MRF's during myogenesis is an interesting avenue for further research.

In summary, this study reports a comprehensive analysis of MyHC and MRF mRNA expression during myogenesis of C2C12 mouse myoblasts. MyHC mRNA isoforms were expressed in a distinct temporal pattern as two distinct cohorts. MyHC emb, neo and type I expression was up-regulated during early differentiation and their expression was subsequently down-regulated after 4 to 6 days in culture. MyHC IIa, IIx and IIb, on the other hand, were expressed later in differentiation and their expression continued to increase to day 8. The C2C12 cell line therefore mimics the development of a fast muscle fibre type, and scientists utilizing this cell line for muscle biology research should take this into consideration. The MRF and MyHC mRNA expression observed during myogenesis of the C2C12 cell line closely matched the reported expression patterns during development *in vivo*. Thus, *in vitro* cell culture systems may be viable models for studying MyHC isoform transitions during development and of myogenic precursor (satellite) cells during adult muscle regeneration. However, the lack of stimuli from innervation, circulating hormones and stretch does expose a major limitation of *in vitro* experiments.

### 3.2 TRANSITIONS IN METABOLIC GENE EXPRESSION DURING C2C12 MYOGENESIS – ASSOCIATION WITH MYOSIN HEAVY CHAIN GENE EXPRESSION

#### 3.2.1 INTRODUCTION

The C2C12 cell line displayed a transition towards a predominantly fast contracting (type II) MyHC isoform profile during myogenic differentiation. The ATP consumption of a myofibre is largely determined by the MyHC isoform expression (Schiaffino and Reggiani 2011) and increases in the order of type I<IIA<IIX<IIB. Consequently, myofibres containing the fast, type II MyHC isoforms typically display a glycolytic phenotype (Lefaucheur 2010) in order to supply the necessary ATP required to permit forceful contractions of these fibres. Given that the rate of the rate of ATP hydrolysis by fast MyHC's is approximately 20-30-fold greater than that of type I MyHC's (Weiss and Leinwand 1996), it was hypothesized that mature C2C12 myotubes, transitioning to a predominantly type II MyHC expressing phenotype, would also display a very glycolytic phenotype in order to rapidly supply the high ATP requirements of these MyHC's. To assess the metabolic profile of cultured C2C12 myotubes, the metabolic gene expression profile of these cells was compared to proliferating C2C12 myoblasts. Given that mitotic cells typically display a very glycolytic metabolism (Gatenby and Gilles 2004; Lunt et al. 2011), they were considered an interesting reference/control to assess the relative metabolic gene expression profile displayed by fully differentiated muscle cells, expressing type II MyHC isoforms.

Cellular metabolism is a complex series of interconnecting chemical reactions that can be split into “catabolic” and “anabolic” metabolism. The main purposes of such chemical reactions are 1) to provide ATP for cellular function

(catabolic metabolism) and 2) to provide precursors for the biosynthesis of macromolecules to support cell growth and maintenance (anabolic metabolism). Catabolic metabolism can occur through glycolytic and/ or oxidative metabolic pathways. Glycolytic metabolism is considered relatively inefficient, producing just 2 ATP per glucose molecule, but can produce ATP very quickly and in the absence of oxygen. Oxidative metabolism, on the other hand, is very efficient; producing 36 ATP per glucose molecule but requires oxygen. These dynamic metabolic pathways present a very adaptive system, adjusting metabolism according to the energy requirements of the cell but also the oxidative and nutritional status of the cellular environment. In skeletal muscles, the ability to utilize glycolytic and oxidative metabolic pathways for ATP production permits the use of skeletal muscle for rapid, powerful force production (glycolytic) and slow, prolonged force production (oxidative). In addition to metabolism being essential to the provision of ATP for muscle contraction and other cellular functions, recent advances in cancer cell biology have highlighted a critical dependence on biosynthetic pathways (namely serine and nucleotide biosynthesis), stemming from glycolysis, to support the anabolic requirements of rapidly proliferating cells (Lunt et al. 2011; Possemato et al. 2011; Tong et al. 2009). Thus, cancer cells (and most highly proliferating cells) switch away from efficient ATP producing metabolic pathways (oxidative) and focus on the synthesis of anabolic precursors using biosynthetic pathways stemming from glycolysis (Lunt et al. 2011). It was therefore hypothesized that gene expression of enzymes in these pathways may be highly up-regulated in the proliferating C2C12 myoblasts and down-regulated in the differentiated myotubes. It was speculated that a dramatic



remodelling of metabolic gene expression would occur between the proliferating and fully differentiated C2C12 muscle cells, with the emphasis on maximising ATP production for the type II MyHC's expressed in differentiated myotubes.

Given the relatively un-physiological conditions of most muscle cell culture systems (supraphysiological concentrations of glucose, hard plastic culture surfaces, high oxygen concentrations and no neural innervation), a combined MyHC and metabolic gene expression profile of cultured C2C12 myotubes provides important information for understanding the C2C12 cell line as a model for skeletal muscle research.

### 3.2.2 MATERIALS AND METHODS

*The materials and methods described here are a brief overview only. A more comprehensive explanation of the techniques described herein is detailed in the Materials and Methods Chapter.*

#### 3.2.2.1 Cell culture

C2C12 mouse myoblasts were seeded at 50,000 cells per well of a 6-well plate. Myoblasts were cultured in growth medium (DMEM, 10% FBS, 1% P/S) until near confluent, at which point, cells were encouraged to differentiate by switching to a low serum differentiation medium (DMEM, 2% HS, 1% P/S) and cultured for 7 days. Culture medium was refreshed every 48 hours.

#### 3.2.2.2 Cell harvest and RNA analysis

Proliferating myoblasts (approximately 85% confluent; 24 hours post-seeding) and mature myotubes (following 7 days in differentiation medium) were harvested in 200µl ice-cold PBS for total RNA extraction and subsequent Q-RT-PCR analysis of metabolic gene expression. Details of RNA extraction, cDNA synthesis and Q-RT-PCR analysis were described in the Materials and Methods Chapter. Synthesis of cDNA for this experiment was conducted using the Roche Transcriptor First Strand cDNA Synthesis Kit.

#### 3.2.2.3 Oligonucleotide primers

Oligonucleotide primers were designed against the latest mouse genome build (GRCm38) using Primer Express. All primers sets were tested by melt-curve analysis (Lighcycler480, Roche). The transcripts measured herein were

selected to cover major metabolic pathways and muscle specific isoforms were selected where possible. Metabolic genes measured are listed in Table 3.4 with their accession number and primer sequences.

**Table 3.4** Oligonucleotide sequences used for Q-RT-PCR analysis of mouse metabolic genes

Gene	Forward primer	Reverse primer	Amplicon length
<b>Hexokinase-2</b> ( <i>ENSMUST00000000642</i> )	GAGCCTCGGTTTC TCTATTGG	ATACTGGTCAAC CTTCTGCACTTG	117 bp
<b>Phosphofructokinase, muscle type</b> ( <i>ENSMUST000000051226</i> )	CCGGCTCAGTGAG ACAAGGA	GGCACCTTCAGC AACAATGA	64 bp
<b>Enolase-3</b> ( <i>ENSSSCT00000019484</i> )	GCCTGCTCCTGAA GGTCAAC	TGCAAGTTTACA GGCCTGGAT	65 bp
<b>Glucose-6-phosphate dehydrogenase</b> ( <i>ENSMUST000000004327</i> )	CCCGCTCACGACT CACAGT	AGTGGCTTTAAA GAAGGGCTCACT	62 bp
<b>3-Phosphoglycerate dehydrogenase</b> ( <i>ENSMUST000000065793</i> )	CGTGAACCTGGTG AACGCTAAG	GTGGGAGGTGGT GACATTGAG	64 bp
<b>Phosphoserine aminotransferase 1</b> ( <i>ENSMUST000000025542</i> )	CGTGCTTCAGCAT CTACGTCAT	GCCCCGCCGTTG TTCT	61 bp
<b>Phosphoserine phosphatase</b> ( <i>ENSMUST000000031399</i> )	GGCATAAGGGAGC TGGTAAGC	GCCACCAGAGAT GAGGAACAC	66 bp
<b>Pyruvate carboxylase</b> ( <i>ENSMUST00000113825</i> )	CCAACTTCGCTCA CGTCTCA	GCGTTCTCATAG CCTACCTGCTT	66 bp
<b>Citrate synthase</b> ( <i>ENSMUST000000005826</i> )	GCTGCTGGTAACT GGACAGATG	GCCCTTTTGGCC CATTCTC	72 bp
<b>Isocitrate dehydrogenase 2</b> ( <i>ENSSSCT00000002075</i> )	TTGAGGCTGAGGC TGCTCAT	CCGGCCCTTCTG GTGTT	62 bp
<b>Malate dehydrogenase 1</b> ( <i>ENSMUST00000102874</i> )	GGAAAGGAAGTCG GTGTGTATGA	GCTGTTGCACAG TCGTGATGA	79 bp
<b>Malate dehydrogenase 2</b> ( <i>ENSMUST000000019323</i> )	CAGTCCAAAGAGA CGGAATGC	GGCCCTTTTCC CCAAGA	61 bp
<b>Phosphoenolpyruvate carboxykinase 2</b> ( <i>ENSMUST000000048781</i> )	GCAGAGCACATGC TGATTTTG	GGAAAGCAGCT GCCACGTA	70 bp
<b>Pyruvate kinase, muscle-1</b> ( <i>ENSMUST00000163694</i> )	GTTTAGCAGCAGC TTGATAGTTCTC	GCGGTACCTGGC CACTTG	68 bp
<b>Pyruvate kinase, muscle-2</b> ( <i>ENSMUST000000034834</i> )	GGCCAATGCAGTC CTGGAT	TCGAATAGCTGC AAGTGGTAGATG	144 bp
<b>Total Pyruvate kinase, muscle</b> ( <i>combined Pkm 1 and 2 above</i> )	GCGGTGGCTCTGG ATACAAA	GTGCCGCTGCCC TTGAT	62 bp

#### 3.2.2.4 *Statistical analysis*

Gene expression from a single experiment with three biological replicates (for myoblasts and myotubes) were analysed by one-way analysis of variance using GenStat. Data is displayed as mean  $\pm$  standard deviation. Significance was accepted if  $p < 0.05$ .

### 3.2.3 RESULTS

The two time points at which C2C12 cells were harvested are shown in the light microscopy images below (Figure 3.9). Myoblasts were sub-confluent, un-fused, and proliferating. Day 7 myotubes were fully differentiated.

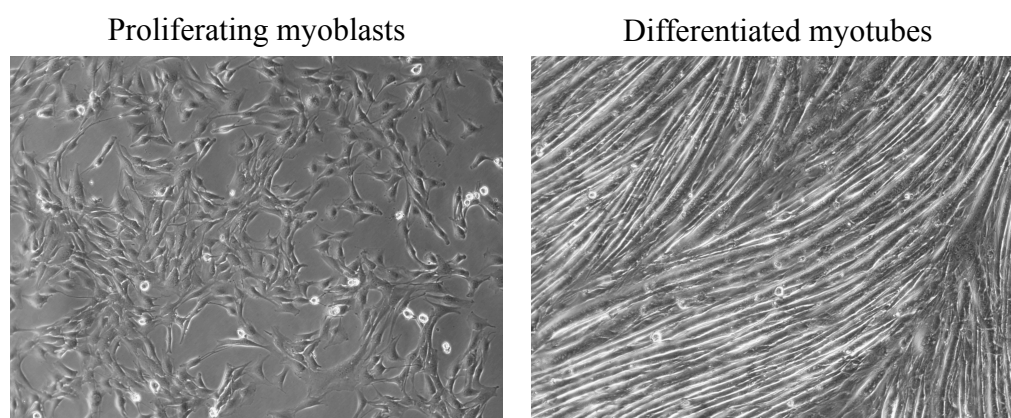


**Figure 3.9** Representative light microscopy images of the two cohorts of C2C12 cells used for gene expression analysis of proliferating cells and fully differentiated mature myotubes.

#### *3.2.3.1 Glycolytic enzyme gene expression*

In comparison to proliferating myoblasts, differentiated myotubes displayed increased mRNA expression of a selection of muscle-specific glycolytic enzymes (Hexokinase-2 (HK2), Phosphofructokinase-M (PFKm) and Enolase-3; Figure 3.10). Of the glycolytic genes measured herein, PFKm transcript abundance showed the largest disparity in expression levels between myoblasts and myotubes, with myotubes displaying an ~14-fold higher ( $p < 0.001$ ) expression level than proliferating myoblasts. Enolase-3 and HK2 mRNA expression was approximately 3-fold ( $p = 0.005$ ) and 2-fold ( $p = 0.001$ ) greater in myotubes compared to myoblasts, respectively.

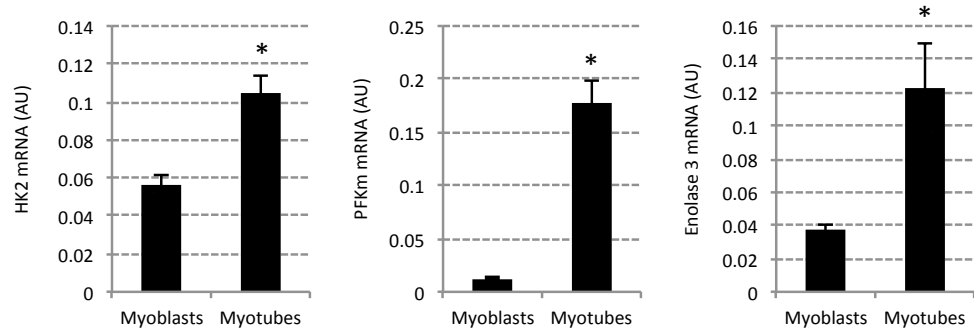


**Figure 3.10** Hexokinase-2 (Hk2), Phosphofructokinase (PFKm) and Enolase 3 gene expression (muscle specific glycolytic enzymes) in proliferating myoblasts compared to differentiated myotubes. Data is presented as mean  $\pm$  SD. \* indicates  $p < 0.01$ .

### 3.2.3.2 Mitochondrial enzyme gene expression

Gene expression of mitochondrial enzymes involved in the TCA cycle (Citrate Synthase (Cs), Isocitrate Dehydrogenase 2 (IDH2) and Malate Dehydrogenase 2 (MDH2)) were all approximately 2-fold lower ( $p = 0.002$ ,  $p < 0.001$ ,  $p < 0.001$ , respectively) in differentiated myotubes compared with proliferating myoblasts (Figure 3.11).

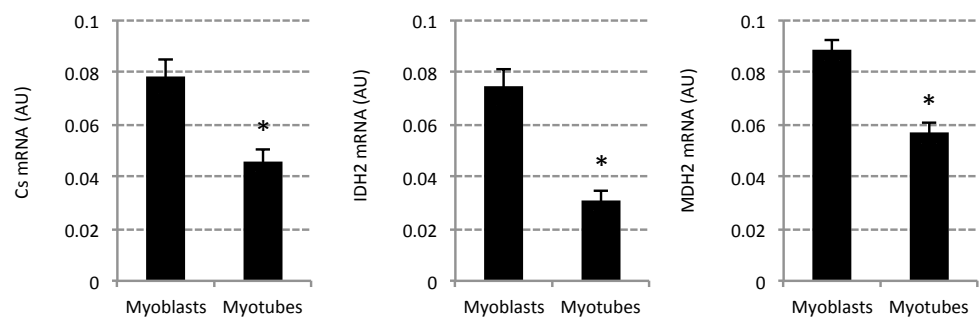


**Figure 3.11** Citrate synthase (CS), Isocitrate dehydrogenase (IDH2) and Malate dehydrogenase-2 (MDH2) gene expression in proliferating myoblasts compared to differentiated myotubes. Data is presented as mean  $\pm$  SD. \* indicates  $p < 0.01$ .

### 3.2.3.3 *G6PDH* gene expression: The nucleotide biosynthesis pathway

Glucose-6-Phosphate Dehydrogenase (G6PDH) is the committing enzyme of the pentose phosphate pathway. G6PDH mRNA expression was ~6-fold greater ( $p < 0.001$ ) in proliferating myoblasts compared to differentiated myotubes (Figure 3.12).

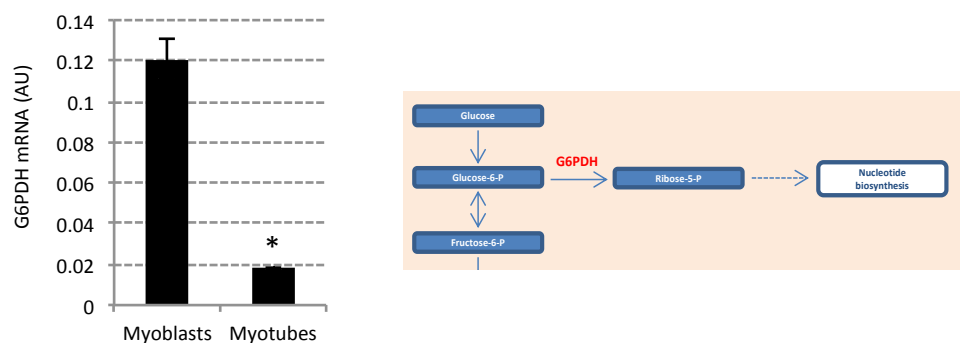


**Figure 3.12** Glucose-6-phosphate dehydrogenase (G6PDH) gene expression in proliferating myoblasts compared to differentiated myotubes. Data is presented as mean  $\pm$  SD. The image depicts the location of G6PDH initiating the nucleotide biosynthesis pathway. \* indicates  $p < 0.001$ .

### 3.2.3.4 *PHGDH*, *PSAT1* and *PSPH*: The serine biosynthesis pathway

Gene expression of enzymes involved in the serine biosynthesis pathway all displayed a greater level of expression in proliferating myoblasts compared to differentiated myotubes (Figure 3.13). The committing enzyme, 3-phosphoglycerate dehydrogenase (PHGDH), had the greatest difference in expression with levels ~3.5-fold greater ( $p < 0.001$ ) in myoblasts compared to myotubes. Phosphoserine aminotransferase-1 (PSAT1) and phosphoserine phosphatase (PSPH) mRNA expression levels were approximately 2-fold

greater ( $p = 0.002$ ,  $p < 0.001$ , respectively) in myoblasts compared to myotubes.

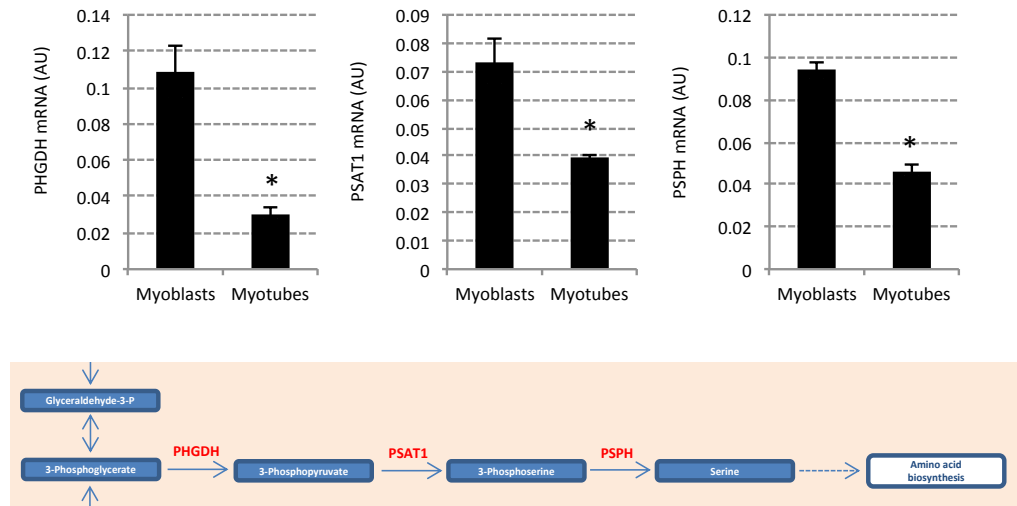


**Figure 3.13** 3-phosphoglycerate dehydrogenase (PHGDH), Phosphoserine aminotransferase-1 (PSAT1) and phosphoserine phosphatase (PSPH) gene expression in proliferating myoblasts compared to differentiated myotubes. Data is presented as mean  $\pm$  SD. The image depicts the location of these enzymes forming the serine biosynthesis pathway. \* indicates  $p < 0.01$ .

### 3.2.3.5 Pyruvate kinase 1/2 splice variant switching

Total pyruvate kinase (muscle type) mRNA expression was higher in proliferating myoblasts compared to fully differentiated myotubes (Figure 3.14A;  $p = 0.009$ ). Interestingly, when the Pkm splice variant transcripts, Pkm1 and 2, are normalized against total Pkm transcript expression, a switch in the relative proportions of Pkm splice variant expression occurs between myoblasts and myotubes (Figure 3.14B). In proliferating myoblasts, Pkm2 is the predominant mRNA isoform, with only low levels of Pkm1 mRNA expression ( $p < 0.001$ ). Fully differentiated myotubes, on the other hand, display an equal abundance of Pkm1 and 2 mRNA expression ( $p = 0.286$ ).



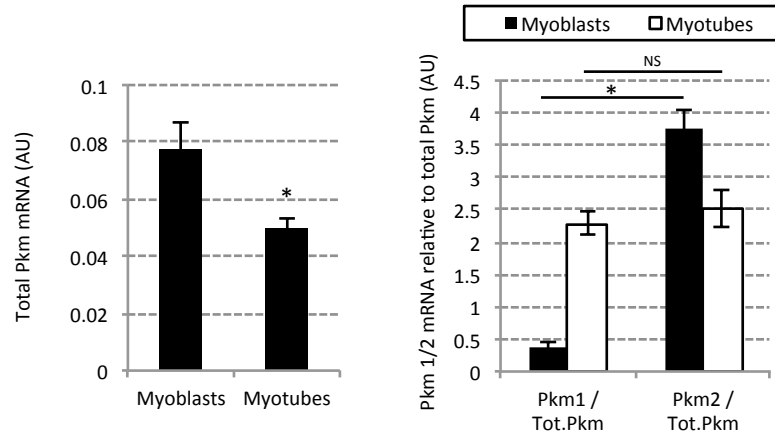


**Figure 3.14** (A) Total pyruvate kinase muscle type (Pkm) gene expression in proliferating myoblasts compared to differentiated myotubes. (B) Expression of Pkm splice variants, Pkm1 and Pkm2, relative to total Pkm (Tot.Pkm) in myoblasts compared to myotubes. Data is presented as mean  $\pm$  SD. \* indicates  $p < 0.01$ . NS = not significantly different.

### 3.2.3.6 Gene expression of enzymes involved in gluconeogenesis

Gene expression of enzymes involved in gluconeogenesis showed no common alteration in expression levels in proliferating versus differentiated C2C12 cells (Figure 3.15). Pyruvate carboxylase (Pc) mRNA expression was approximately 5-fold greater ( $p = 0.002$ ) in myotubes compared to myoblasts. Phosphoenolpyruvate carboxykinase-2 (PEPCK2; mitochondrial isoform) mRNA expression was approximately 2-fold lower ( $p = 0.008$ ) in myotubes compared to myoblasts. Malate dehydrogenase (MDH1; cytoplasmic isoform) mRNA expression was not different between myoblasts and myotubes ( $p = 0.276$ ).

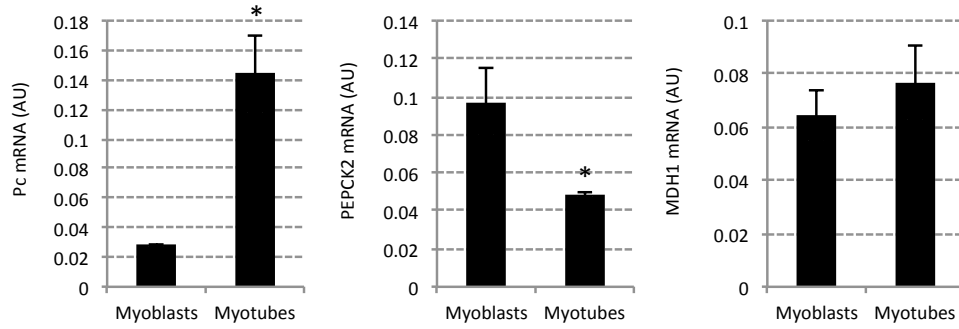


**Figure 3.15** Pyruvate carboxylase (Pc), Phosphoenolpyruvate carboxykinase-2 (PEPCK2) and Malate dehydrogenase-1 (MDH-1) gene expression in proliferating myoblasts compared to differentiated myotubes. Data is presented as mean  $\pm$  SD. \* indicates  $p < 0.01$ .

### 3.2.3.7 Summary of the metabolic gene expression

Below is a diagram summarising the metabolic profile of fully differentiated myotubes in comparison to proliferating myoblasts (Figure 3.16). Enzymes are highlighted in green and red to indicate whether mRNA expression of that enzyme was higher or lower (respectively) in myotubes relative to myoblasts. Briefly, the metabolic enzyme gene expression profile of differentiated myotubes displayed a reduced reliance on pathways associated with nucleotide and serine biosynthesis, reduced reliance on the TCA cycle and an increase in glycolytic enzyme gene expression, compared to proliferating myoblasts.

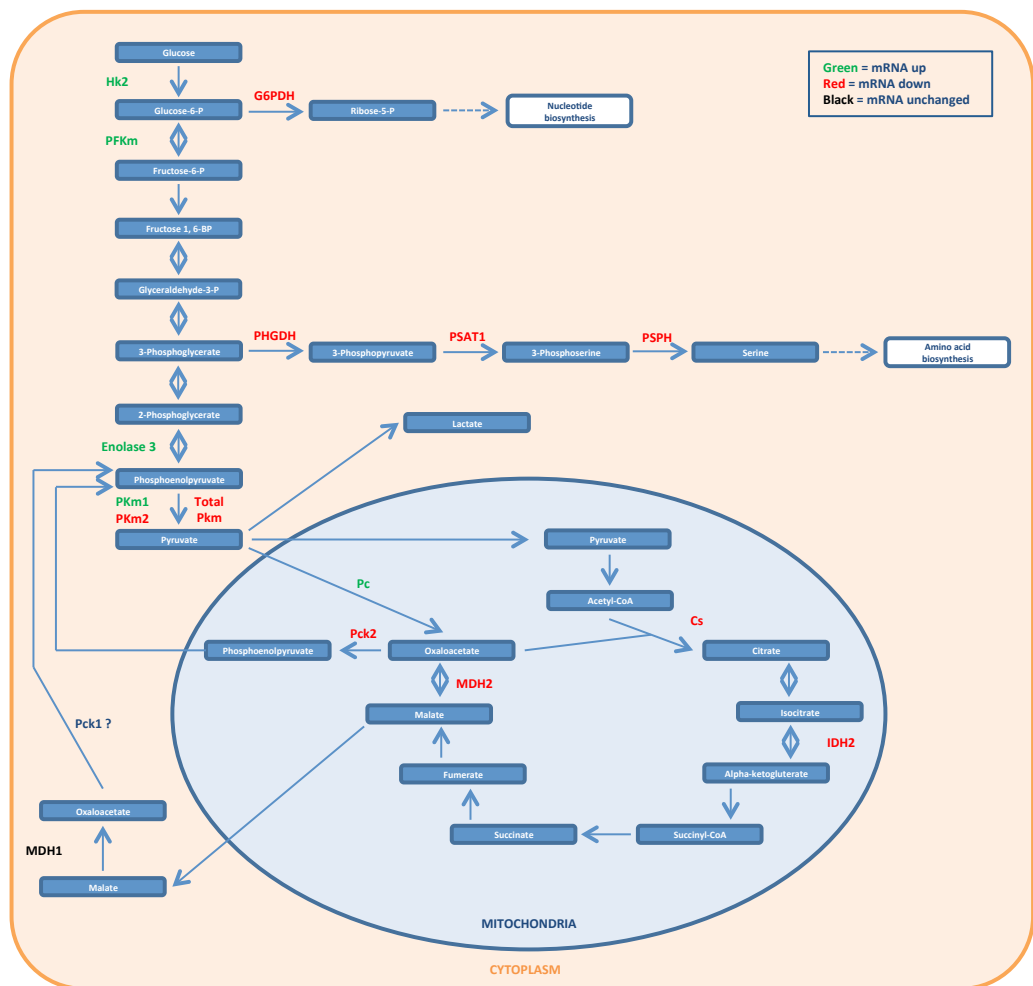


**Figure 3.16** Summary of metabolic gene expression in myotubes relative to myoblasts. Enzymes in green and red indicate whether gene expression of that enzyme was increased or decreased, respectively, in myotubes relative to myoblasts.

### 3.2.4 DISCUSSION

The metabolic gene expression profile of C2C12 myoblasts and myotubes were compared to assess whether fully differentiated myotubes, expressing type II MyHC isoforms, exhibit a concomitant glycolytic gene expression profile. Indeed, relative to myoblasts, myotubes displayed an increased mRNA abundance of glycolytic genes and a decreased mRNA expression of oxidative genes. However, myotubes also showed a decrease in expression of genes involved in macromolecule biosynthesis, with a concomitant switch in Pkm splice variant expression (from Pkm2 to Pkm1), suggesting myotubes may actually re-focus their metabolic profile to support ATP production and shunt glucose carbons away from biosynthetic pathways with cellular differentiation. Compared to proliferating C2C12 myoblasts, fully differentiated myotubes displayed increased expression of glycolytic genes and decreased expression of oxidative genes. Chung et al. (2010) also reported increased gene expression of a range of glycolytic enzymes (Enolase-3, PFKm and Hexokinase-1) with cardiomyocyte differentiation, supporting the data presented herein. It is important to note that Chung et al. (2010) also highlighted several examples of disparity in mRNA expression and corresponding enzyme activity, suggesting that the gene expression data presented herein should be interpreted cautiously to avoid misleading conclusions. Gene expression data does however provide information as to the transcriptional programming of the cell during different stages of myogenesis. It is interesting to speculate that transcriptional changes in metabolic gene expression during myogenic differentiation may be closely linked to mechanisms regulating transcription of genes encoding contractile components of the myotube, to ensure a co-ordinated “metabolic-contractile”

phenotype. For example, fast (type II MyHC) and slow (type I MyHC) muscles typically express a glycolytic and oxidative phenotype, respectively (Schiaffino and Reggiani 2011), suggesting that both contractile and metabolic components of muscles may be co-ordinately regulated. Hence, the mature C2C12 myotubes used herein may exhibit a glycolytic gene expression profile to support the ATP requirements of their fast (type II MyHC) contractile cellular machinery. Indeed, examples of so-called master regulators of skeletal muscle phenotype have been identified that show co-ordinated transcriptional control of contractile and metabolic components of muscle. For instance, transgenic mice over-expressing the transcriptional co-factors, PGC-1alpha or PPAR-delta, display a co-ordinated up-regulation of genes encoding slow-contracting components of muscle and genes encoding oxidative and mitochondrial enzymes (Lin et al., 2002; Wang et al., 2004). Such master transcriptional regulators of a fast contracting glycolytic muscle phenotype are yet to be identified.

The increased expression of glycolytic genes and decreased expression of oxidative genes in differentiated myotubes, compared to myoblasts, was somewhat unexpected given that rapidly proliferating cells typically display a very glycolytic phenotype (Gatenby and Gillies 2004) and that differentiation of C2C12 muscle cells or ES-derived cardiomyocytes generally exhibit a reduced glycolytic capacity, as demonstrated by a progressive reduction in lactate production (Leary et al. 1998; Chung et al. 2010). Furthermore, the “choice” displayed by fully differentiated myotubes to preferentially increase gene expression of glycolytic enzymes and concomitantly decrease gene expression of oxidative enzymes is confusing given that oxidative metabolism

is typically considered the more efficient mode of ATP production, compared to glycolysis (Lunt et al. 2011). It is possible, however, that the supraphysiological concentrations of glucose in the culture medium (25mM) could allow myotubes to generate greater quantities of ATP (more rapidly) via glycolysis, compared to oxidative metabolism (Pfeiffer et al. 2001). Given that the glucose concentration in the culture medium was the same for the proliferating and differentiated C2C12 cells, the appearance of GLUT4 transporters with myogenic differentiation likely causes increased transport of glucose into myotubes and may subsequently increase reliance on glucose metabolism (Shyh-Chang et al. 2013). Increased transport of glucose into myotubes and the subsequent increased abundance of intracellular glucose may therefore explain the increase in glycolytic gene expression in mature myotubes compared to proliferating myoblasts.

Interestingly, the increased glycolytic gene expression in differentiated myotubes (compared to myoblasts) was paralleled by a concomitant reduction in gene expression for enzymes involved in serine and nucleotide biosynthesis. Such a co-ordinated metabolic switch would suggest that myotubes increase glycolytic metabolism but importantly, may shunt glucose carbons away from biosynthetic pathways (stemming from glycolysis) and presumably into downstream ATP producing pathways (such as the TCA cycle). Chung et al. (2010) also demonstrated a major restructuring of glycolytic gene expression during cardiomyocyte differentiation and suggested that such changes occurred to support downstream ATP production by mitochondrial metabolism. Given the recent reports that serine and nucleotide biosynthetic pathways are critical for mitotic cell growth (Possemato et al. 2011; Tong et al. 2009), it is perhaps

unsurprising that these pathways are down-regulated in differentiated myotubes compared to proliferating myoblasts. Indeed, proliferating cancer cells are well documented to exhibit a glycolytic phenotype (Gatenby and Gilles 2004), but the majority of ATP produced in proliferating cancer cells is typically generated by oxidative metabolism, with an average of just 17% derived from glycolytic metabolism (Zu and Guppy 2004). This suggests that the glycolytic phenotype displayed by proliferating cells is not to rapidly generate ATP, but more likely to permit macromolecule biosynthesis to support mitotic cell growth (Lunt et al. 2011). Given that the myotubes used herein were terminally post-mitotic, it seems logical that they would switch their focus to ATP production and away from macromolecule biosynthesis. Furthermore, the rate of ATP hydrolysis by fast MyHC's is approximately 20-30-fold greater than that of type I MyHC's (Weiss and Leinwand 1996), supporting the notion that mature C2C12 myotubes, transitioning to a predominantly type II MyHC isoform profile, may switch their metabolic focus to maximise ATP production and thus support the energy requirements of their contractile machinery.

Pkm1 and Pkm2 splice variant mRNA expression displayed an interesting switch in proliferating versus differentiated C2C12 muscle cells and this presents a likely mechanism responsible for re-directing metabolism, away from macromolecule biosynthesis and towards ATP production in differentiated myotubes. The data presented herein shows that Pkm2 is the predominant Pkm splice variant expressed in proliferating myoblasts. Expression of the Pkm1 splice variant is increased in differentiated myotubes, with a concomitant reduction in the Pkm2 splice variant expression, causing an

equalling of the Pkm1:Pkm2 ratio with differentiation. David et al. (2010) also reported that C2C12 myoblasts almost exclusively express the Pkm2 splice variant and that differentiated C2C12 myotubes express approximately equal quantities of both Pkm1 and Pkm2. Further, Clower et al. (2010) reported a gradual replacement of the Pkm2 splice variant with the Pkm1 splice variant during C2C12 differentiation, strongly suggesting a role for specific Pkm splice variants during muscle cell differentiation. Pkm facilitates the final, non-reversible, step in glycolysis, converting phosphoenolpyruvate (PEP) to pyruvate. Recently, the Pkm2 splice variant has been implicated as a regulatory component controlling metabolic flux through to mitochondrial ATP production or re-directing glucose carbons into biosynthetic pathways stemming from glycolysis (Lyssiotis et al. 2012). The splice variant Pkm2 is less effective than Pkm1 at facilitating the conversion of PEP to pyruvate and its activity can be regulated by various metabolic inputs (Lyssiotis et al. 2012). Therefore, the ratio of Pkm2:Pkm1 is likely critical in controlling the metabolic fate of glucose carbons. A high ratio of Pkm2:Pkm1 is theorised to cause a “back-log” effect, re-directing glucose carbons to biosynthetic pathways (Lyssiotis et al. 2012). The induction of Pkm1 and a concomitant reduction in Pkm2 splice variant expression with myotube differentiation likely better facilitates the conversion of PEP to pyruvate for entry into the TCA cycle, thus reducing the “back-log” effect and shunting glucose carbons away from macromolecule biosynthesis and into ATP producing pathways (Shyh-Chang et al. 2013). The 5-fold increase in pyruvate carboxylase mRNA expression in differentiated versus proliferating C2C12 myoblasts (converting pyruvate to oxaloacetate for entry into the TCA cycle) supports this notion that



myotubes modify glycolytic gene expression to shunt glucose carbons into ATP producing pathways. The switching of Pkm splice variant expression presented herein may be responsible for re-structuring the “metabolic focus” of C2C12 muscle cells during myogenic differentiation.

In summary, cultured C2C12 myotubes show an increase in glycolytic gene expression and a reduction in oxidative gene expression, compared to proliferating myoblasts. Given the previously identified transition in MyHC mRNA isoforms during C2C12 myogenesis, from type I to type II MyHC isoforms, it is attractive to speculate that contractile and metabolic genes are co-ordinately regulated during myogenesis. However, the reduction in gene expression of enzymes involved in macromolecule biosynthesis and the switch in Pkm splice variant expression (from Pkm2 to Pkm1) strongly suggests that the restructuring of metabolic gene expression in C2C12 myotubes (compared to proliferating myoblasts) is likely to support ATP generation, instead of focusing on macromolecule biosynthesis. The progressive induction of contractile machinery during myogenic differentiation and the transition towards increased type II MyHC isoforms, is likely to increase the ATP requirements of the myotube, compared to proliferating myoblasts, thus requiring a dramatic remodelling of metabolism during myogenic differentiation. Cross talk between mechanisms regulating contractile and metabolic components of muscle cells is an interesting avenue for exploration given the importance of these components to display a coupled phenotype.

# 4

## BETA-ADRENERGIC SIGNALLING AND MYOSIN HEAVY CHAIN IIB GENE EXPRESSION

---

*It was hypothesized that cultured C2C12 skeletal muscle cells would exhibit alterations in myosin heavy chain gene expression in response to beta-adrenergic receptor stimulation and that these changes would mimic those seen in vivo.*

## 4.1 BETA-ADRENERGIC AGONIST, RACTOPAMINE, INDUCES EXPRESSION OF THE MYOSIN HEAVY CHAIN IIB GENE IN GROWING PIGS

### 4.1.1 INTRODUCTION

In the previous chapter, it was shown that MyHC isoforms are a dynamic group of genes, displaying a dramatic and coordinated transition in mRNA expression during myogenic differentiation. This chapter subsequently intended to determine whether the dramatic transitions in MyHC mRNA isoform expression during myogenic differentiation were restricted to myogenesis or whether chronic transitions in MyHC mRNA isoform expression could be induced in adult skeletal muscle *in vivo* (Chapter 4.1). Furthermore, the stimulus used to induce a transition in MyHC mRNA isoform expression *in vivo* was subsequently explored *in vitro* (Chapter 4.2) to allow comparisons between the two developmentally distinct muscle cell types.

Two growth-promoting agents, Ractopamine (a beta-adrenergic agonist) and Reporcin (recombinant growth hormone), were administered to growing pigs to assess their impact on MyHC mRNA isoform expression. Beta-adrenergic receptor stimulation in skeletal muscle has therapeutic potential for inducing muscle hypertrophy (Ryall et al. 2002; 2004; Kline et al. 2007), improving muscle force producing capacity (Ryall et al. 2002; 2004), enhancing muscle regeneration (Beitzel et al. 2004; 2007) and protecting against muscle wasting (Ryall et al. 2004; Kline et al. 2007). In addition to their effects on muscle growth, beta-adrenergic agonists typically induce a fast, glycolytic muscle fibre type *in vivo* (Baker et al. 2006; Bricout et al. 2004; Depreux et al. 2002;

Oishi et al. 2002; Gunawan et al. 2007). To fully characterize the dynamic plasticity of MyHC isoform gene expression in response to beta-adrenergic agonist (Ractopamine) administration *in vivo*, a time course of treatment, spanning 1 to 27 days, was conducted in adult pigs (aged ~6 months). In addition, intramuscular injection of growth hormone (Reporcin) was examined over the same 27-day time course to elucidate the effect of this “repartitioning agent” (Sillence 2004) on transitions towards a type II MyHC isoform expression. Muscle growth promoter agents were selected for these experiments since it has been shown the domestic selection for fast growing pigs, with a high lean:fat ratio, has likely inadvertently selected for a fast muscle phenotype, suggesting links between muscle hypertrophy (or lean deposition) with muscle fibre type composition (Wimmers et al. 2008). Improving the understanding of type II muscle fibre regulation may elucidate potential interventions to ameliorate the loss of type II muscle fibres in diseases such as sarcopenia (Evans 2010).

In addition to measuring changes in MyHC mRNA expression in response to Ractopamine and Reporcin treatment, several potential mediators of muscle fibre type transitions were monitored for associated changes. In particular, we measured mRNA expression of factors associated with altered MyHC isoform composition. *Sine Oculis*-related Homeobox 1 (*Six1*) and Eyes Absent 1 (*Eya1*) transcript abundance was measured as these factors have previously been implicated in driving a fast, glycolytic muscle fibre type in adult mice (Grifone et al. 2004). Transcriptional co-regulators associated with driving a slow MyHC isoform expression were also measured (PGC-1 $\alpha$  and RIP140; Lin et al. 2002; Seth et al. 2007). In addition, markers of cellular

differentiation (MyoD and myogenin) were monitored as a potential mechanism of altered MyHC isoform expression (Brown et al. 2012). This laboratory previously detected altered gene expression of Enolase 3 and IDH2 (identified by microarray) following 7 days beta-adrenergic agonist treatment in ovine skeletal muscle (Dr Krystal Hemmings PhD Thesis) and were thus used as markers of metabolic gene expression herein (IDH2 = oxidative marker; Enolase 3 = glycolytic marker).

It was hypothesized that dynamic alterations in MyHC mRNA isoform expression would occur in response to Ractopamine and Reporcin administration, gradually replacing the slow isoforms with the type IIB MyHC isoform. Furthermore, it was predicted that metabolic gene expression would remain coupled with changes in MyHC gene expression.

## 4.1.2 MATERIALS AND METHODS

*A more detailed account of the techniques employed in this section can be found in Chapter 2 (Materials and Methods).*

### *4.1.2.1 Experimental design*

Growing pigs were exposed to a beta-adrenergic agonist (Ractopamine) in their feed or were administered recombinant growth hormone (Reporcin) via intramuscular injection every 2 days for up to 27 days to elucidate the effects of prolonged growth promoter administration on myosin heavy chain isoform expression in skeletal muscle.

### *4.1.2.2 Time course of growth promoter administration*

Approximately 5-month-old growing gilts (C23 X 337 progeny; obtained from PIC, UK), with a mean starting weight of 77kg ( $\pm 7$ kg), were fed Ractopamine HCL (20ppm; Elanco Animal Health, Grenfield, IN) or administered an intramuscular injection of Reporcin (Growth hormone; 10mg/pig/48 hours), for 1, 3, 7, 13 ( $n = 10$ ) or 27 days ( $n = 15$ ). Pigs were fed twice daily for 45 minutes (*ad libitum*) on a non-pelleted, 16.7% protein finisher feed (14MJ/kg). The trial was conducted in 3 batches (51, 51 and 63 pigs) over 6 months. All pigs were acclimatized in the animal housing facility for 7 days prior to treatment. Pigs were individually housed. Feed intake was measured every 2-3 days. Body weight was determined at the time of slaughter.

#### *4.1.2.3 Animal growth and tissue collection*

Following slaughter, a sample of the *Longissimus Dorsi* (LD) was isolated (from the 10<sup>th</sup> rib in each pig), immediately snap-frozen in liquid nitrogen and later stored at -80°C for subsequent RNA analysis. Following removal of organs, the carcass weight was determined. The *Vastus Lateralis* and *Semitendinosus* muscles were dissected from the left rear leg and weighed as an indicator of changes in muscle growth.

#### *4.1.2.4 Total RNA extraction and cDNA synthesis*

Total RNA was extracted from a 100mg sample of LD muscle using the Trizol method. RNA concentration was adjusted to 100ng/μl. First strand cDNA synthesis was carried out using a cDNA synthesis kit (Transcriptor First Strand cDNA Synthesis Kit, Roche, Burgess Hill, UK) as described in the Materials and Methods Chapter (Chapter 2).

#### *4.1.2.5 Quantitative-RT-PCR*

Real time PCR was conducted on a Lightcycler 480® (Roche, Burgess Hill, UK). Reactions were carried out in duplicate on 384 well plates (measuring the expression of 1 gene per plate). Details of the Q-RT-PCR are described in Chapter 2. Relative transcript abundance was calculated using the standard curve method and expression values were normalized to total cDNA in the PCR reaction (using the oligreen method).

#### 4.1.2.6 Myosin heavy chain primers

Myosin heavy chain primer sequences were obtained from Wimmers et al. (2008; see Table 4.1 below). Melt-curve analysis for all MyHC primer sets was conducted using pig muscle derived cDNA. Horizontal Agarose gel (1%) electrophoretic separation of the PCR amplicons was performed to ensure a) only one amplicon was being produced by the PCR, b) that the amplicon produced was of the correct length and c) that no primer-dimers were produced in the absence of template cDNA (see Figure 4.1 below). Annealing temperature for all porcine MyHC primers was 57°C (compared to 60°C for other primer sets) to improve the efficiency of detection of the type IIB MyHC mRNA isoform.

**Table 4.1** Oligonucleotide sequences for measuring porcine myosin heavy chain isoforms (from Wimmers et. 2008).

Gene	Forward primer	Reverse primer	Amplicon size
MyHC I	AAGGGCTTGAACGAGGAGTAGA	TTATTCTGCTTCCTCAAAGGG	115bp
MyHC IIA	GCTGAGCGAGCTGAAATCC	ACTGAGACACCAGAGCTTCT	137bp
MyHC IIX	AGAAGATCAACTGAGTGAAC	AGAGCTGAGAACTAACGTG	149bp
MyHC IIB	ATGAAGAGGAACACATTA	TTATTGCCTCAGTAGCTTG	166bp



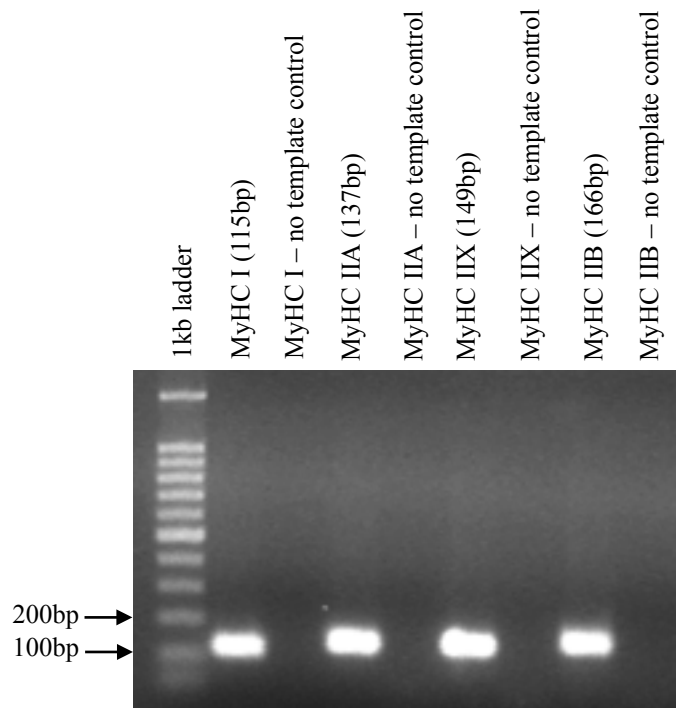


**Figure 4.1** Gel electrophoretic separation of the porcine MyHC isoform amplicons produced by Q-RT-PCR. The gel indicates single amplicons, of the correct length, were produced by the MyHC primer sequences published by Wimmers et al. (2008). In addition, no primer-dimers were formed in the absence of template cDNA.

#### 4.1.2.7 Other oligonucleotide primers

Oligonucleotide primers for the following genes were designed (by Dr Zoe Daniel or myself; see Table 4.2) using the current available pig genome (Sscfa9 – note that Sscrofa10.2 is now available and therefore sequences/annotations may vary). Six1 (ENSSSCT00000005607) and Eya1 (ENSSSCT00000006784) gene expression was measured as these genes were previously implicated in regulating a fast muscle phenotype (Grifone et al. 2004). Further, PGC-1a (ENSSSCT00000029467) and RIP140 (ENSSSCT00000028007) gene expression was measured as these transcriptional co-factors are known regulators of a slow muscle phenotype (Lin et al. 2002; Seth et al. 2007). MyoD (ENSSSCT00000014609) and

Myogenin (ENSSSCT00000016858) transcript abundance was measured as these myogenic regulatory factors are involved in the activation of muscle specific genes (Nabeshima et al. 1993; Hasty et al. 1993) and have also been shown to preferentially accumulate in fast and slow muscles respectively (Voytik et al. 1993; Hughes et al. 1993; Elmark et al. 2007). Enolase-3 (ENSSSCT00000019484) and IDH2 (ENSSSCT00000002075) transcript abundance was measured as a marker of glycolytic and oxidative gene expression, respectively. This laboratory previously monitored changes in expression of these genes (identified by microarray) following 7 days beta-adrenergic agonist treatment in ovine skeletal muscle (Dr Krystal Hemmings PhD Thesis).

**Table 4.2** Oligonucleotide sequences for measuring gene expression in porcine muscle

Gene	Forward primer	Reverse primer	Amplicon length
SIX1	AGGAAAGGGAGAACACCGAAA	CGAGTTCTGGTCTGGACTTTGG	137bp
EYA1	CCCTCACC GACTCGTGGTT	CAGTTTGTCGGGAGTGGAT	67bp
Enolase-3	CATGAGGATTGAGGAGGCTCTT	GGCCTTTGGGTTACGGAAC	70bp
IDH2	TTCATCAAGGAGAAGCTCATCCT	TGGTCTGGTCCCGGTTTG	85bp
PGC-1a	GCAGAAGAGCCGTCTCTACTTAAGA	TCTGGGTACTGAGACCACTGCAT	91bp
RIP140	GCTCGGACCTCTGTCATTGAA	GCTTTGGCCGATGCAAGTAG	83bp
MyoD	GAGGCGGAGAGCACTACAGC	AATCCATCATGCCGTCGG	75bp
Myogenin	TCCTGCAGTCCAGAATGGG	AGATGATCCCCTGGGTTGG	59bp

#### 4.1.2.8 SDS-PAGE separation of MyHC isoforms

Separation of the MyHC protein isoforms was attempted by SDS-PAGE. Unfortunately, successful separation of the porcine type II MyHC isoforms (IIA, IIX and IIB) was not possible with this method. Examples of successful separation of MyHC isoforms from other species (rat and sheep) are shown in the results section to highlight the difficulties in separating porcine MyHC isoforms using this method. Details of this technique are outlined in Chapter 2.

#### *4.1.2.9 Statistical analysis*

To determine whether there were significant differences between treatments across the 27-day time course, a two-way analysis of variance (ANOVA) was performed using GenStat statistical analysis software (Version 14). Statistical significance was accepted if  $p < 0.05$ .

Pearson correlation coefficient ( $r$ ) was conducted to assess the association between MyHC mRNA isoform expression with Enolase 3 and IDH2 gene expression.

### 4.1.3 RESULTS

#### 4.1.3.1 Growth performance

Starting body weight of pigs prior to the administration of treatments was not different within treatment or time-point groups (treatment:  $p = 0.894$ ; time:  $p = 0.521$ ; Figure 4.2). Final carcass weight increased with time ( $p < 0.001$ ) but was not influenced by treatment ( $p = 0.314$ ; Figure 4.2). The weight of the ST and Vlat muscles increased with time ( $p < 0.001$ ; Figure 4.3) but only the Vlat muscle weight was significantly responsive to treatment ( $p = 0.002$ ), being heavier in Ractopamine treated pigs at each time point studied.

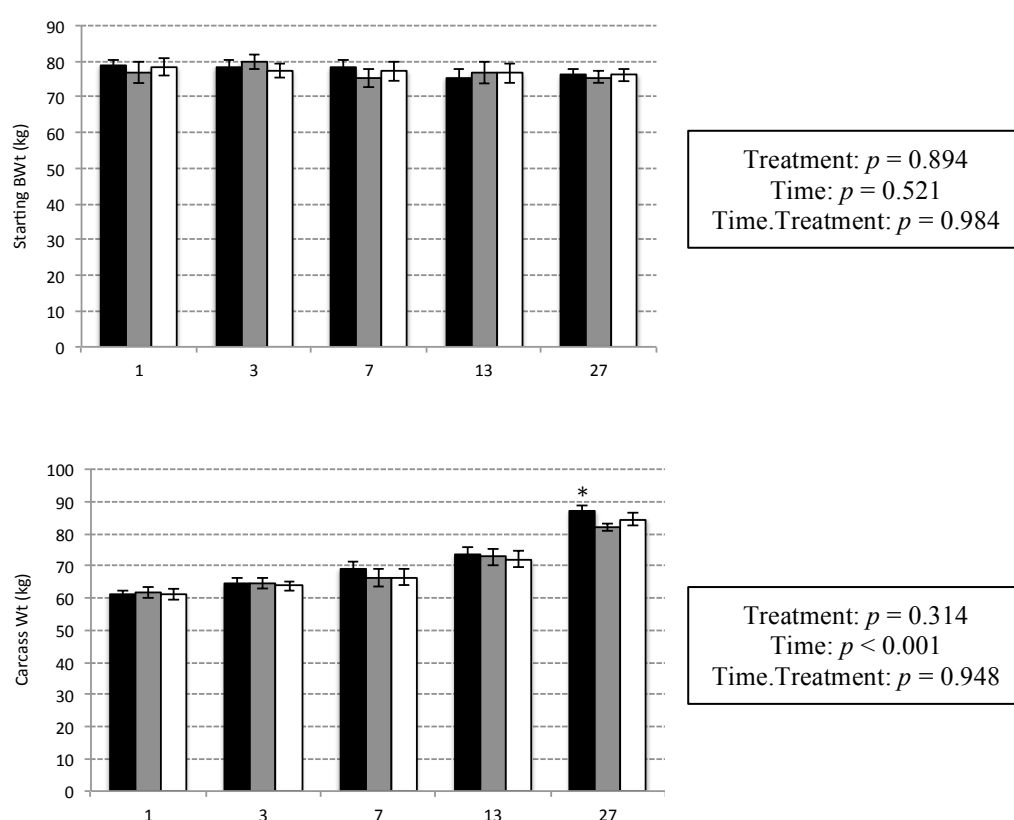


**Figure 4.2** Starting body weight and final carcass weight of non-treated pigs (grey bars) and pigs treated with Ractopamine (black bars) or Reporcin (white bars) for 1, 3, 7, 13 ( $n=10$ ) or 27 ( $n=15$ ) days. Data is displayed as mean  $\pm$  SEM. \* indicates significant difference relative to the control at the same time point ( $p = 0.034$ ).

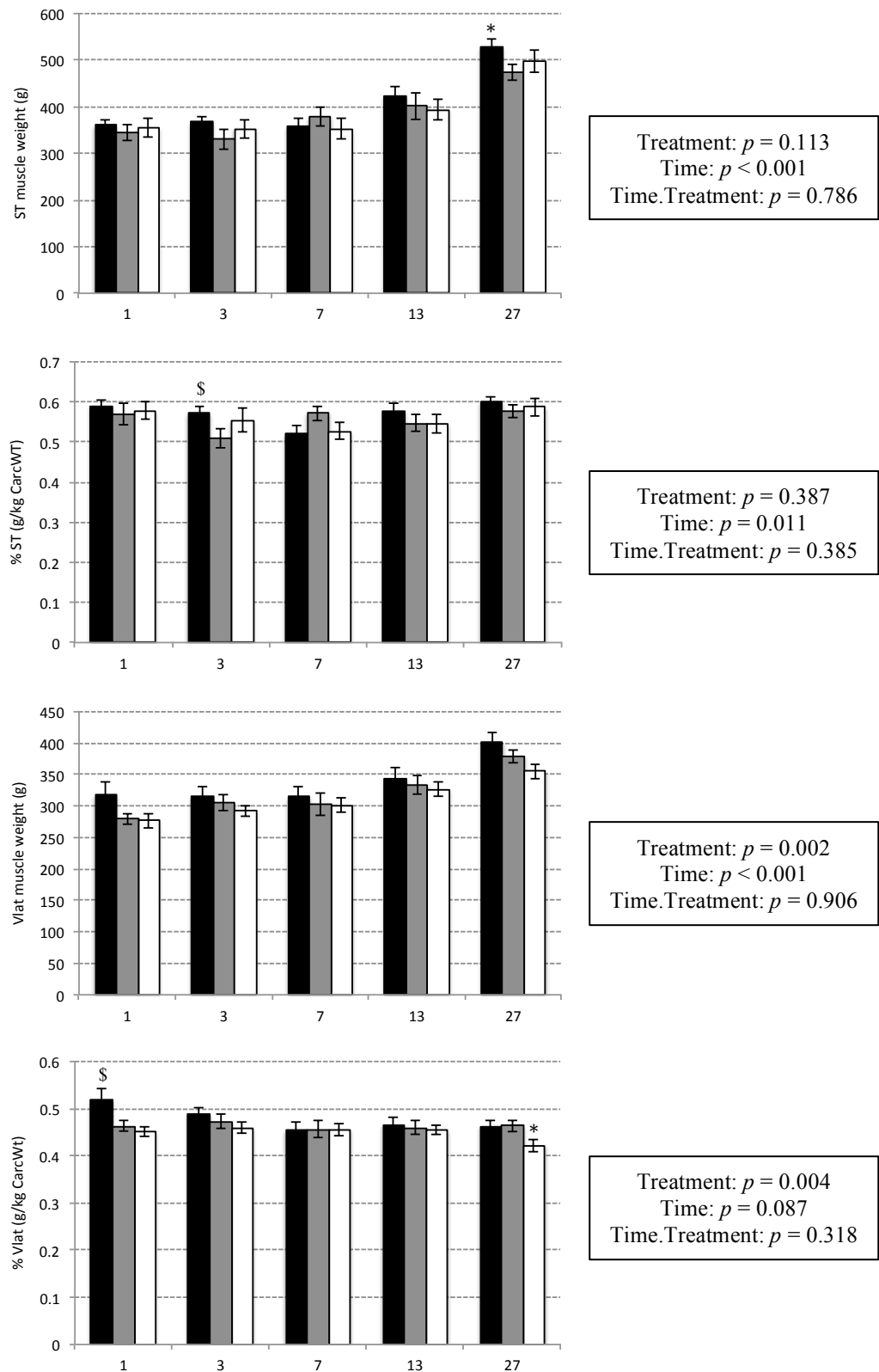


**Figure 4.3** Muscle weights (absolute and relative to carcass weight) of non-treated pigs (grey bars) and pigs treated with Ractopamine (black bars) or Reporcin (white bars) for 1, 3, 7, 13 ( $n=10$ ) or 27 ( $n=15$ ) days. Data is displayed as mean  $\pm$  SEM. \* indicates significant difference relative to the control at the same time point ( $p < 0.05$ ); \$ indicates a trend for a difference relative to the control at the same time point ( $p < 0.06$ ).

#### 4.1.3.2 Myosin heavy chain mRNA isoform expression

Myosin heavy chain (MyHC) isoform mRNA expression was measured in the LD muscle (a commercially relevant back muscle of the pig). Crossing point values and relative expression of MyHC mRNA isoforms are displayed in Table 4.3 and Figure 4.4, respectively. There was a significant treatment effect on mRNA expression of the type IIA, IIX and IIB MyHC isoforms ( $p < 0.001$ ,  $p = 0.021$  and  $p < 0.001$  respectively; Figure 4.4). There was no effect of treatment on the mRNA expression level of the type I MyHC isoform ( $p = 0.554$ ). Ractopamine treatment caused a chronic induction of the IIB MyHC isoform mRNA across the full 27-day time course relative to the control and growth hormone treated groups. This coincided with a modest reduction in mRNA expression of the type IIX MyHC isoform mRNA across the full 27-days of treatment with Ractopamine. MyHC IIA mRNA expression displayed a significant time-treatment interaction ( $p = 0.035$ ), with Ractopamine treatment inhibiting expression levels, reaching its largest reduction by day 7, and then returning to normal expression levels by day 27. Growth hormone treatment appeared to have no effect on the MyHC isoform mRNA expression profile in the LD muscle of treated pigs during the 27-day time course.

**Table 4.3** Crossing point values for porcine MyHC mRNA isoforms following 1-27 days treatment with beta-agonist (B), growth hormone (G) or control (C).

		MyHC I	MyHC IIA	MyHC IIX	MyHC IIB
Day 1	B	26.9	23.5	22.4	23.8
	C	27.2	23.5	22.7	25.1
	G	27.2	23.0	22.2	24.4
Day 3	B	27.1	24.0	22.3	23.1
	C	26.5	22.9	21.9	23.9
	G	27.4	23.2	22.5	24.0
Day 7	B	27.2	25.3	23.0	23.0
	C	26.7	22.9	22.1	25.7
	G	26.6	22.6	21.9	25.1
Day 13	B	27.5	23.9	23.0	23.8
	C	26.4	22.8	22.2	24.4
	G	26.6	22.6	22.0	24.8
Day 27	B	27.6	23.3	22.5	22.4
	C	27.9	23.4	22.3	23.7
	G	27.4	23.2	22.0	24.5

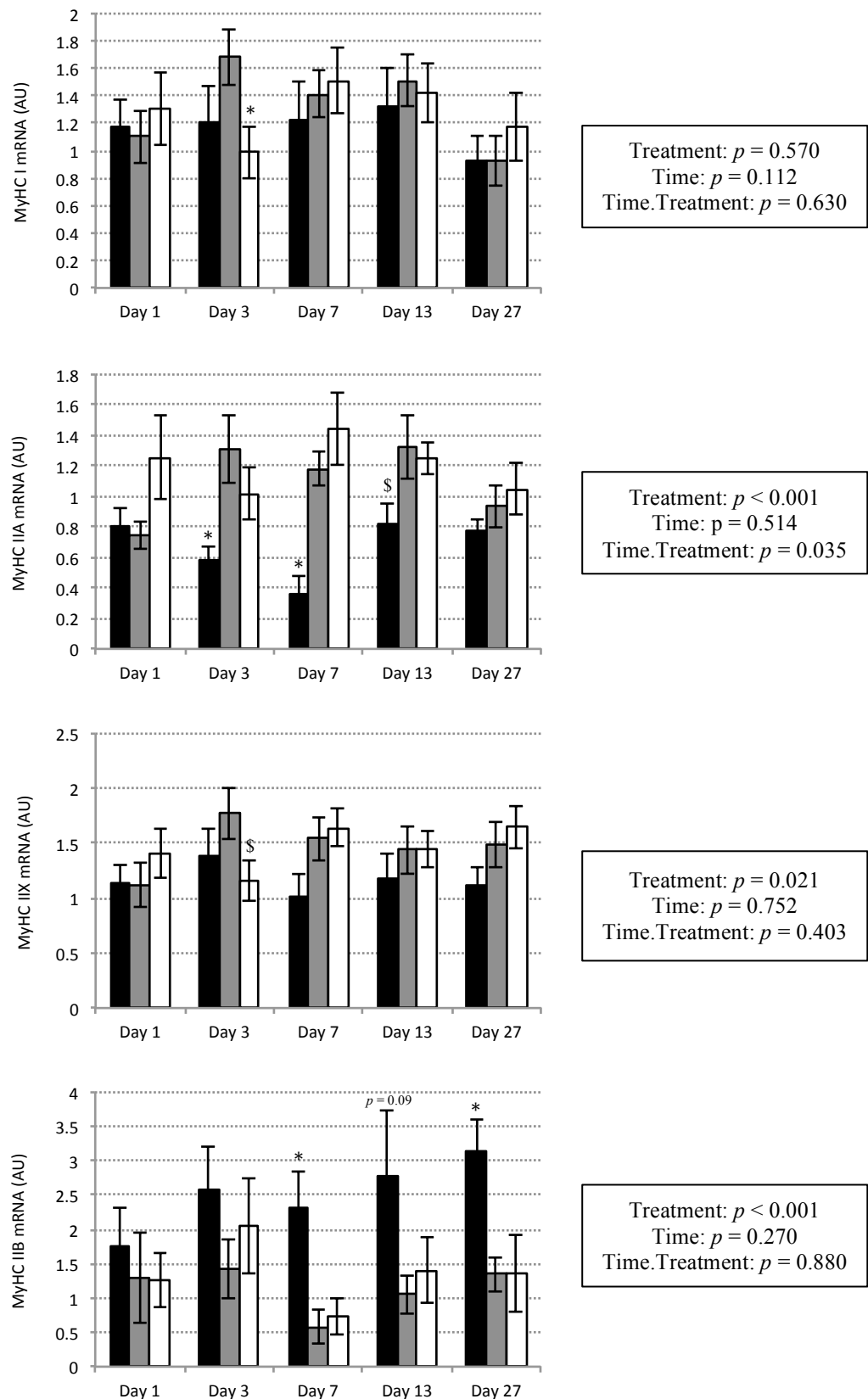


**Figure 4.4** Myosin heavy chain (MyHC) mRNA isoform expression in the LD muscle of non-treated pigs (grey bars) and pigs treated with Ractopamine (black bars) or Reporcin (white bars) for 1, 3, 7, 13 ( $n=10$ ) or 27 ( $n=15$ ) days. Data is displayed as mean  $\pm$  SEM. \* indicates significant difference relative to the control at the same time point ( $p < 0.05$ ); \$ indicates a trend for a difference relative to the control at the same time point ( $p < 0.06$ ).

#### 4.1.3.3 Myosin heavy chain protein expression

Separation of MyHC protein isoforms by SDS-PAGE was attempted but an inability to separate the porcine type II MyHC isoforms meant quantification of transitions in MyHC protein isoform expression was not possible. Methods used for the successful separation of rat and sheep MyHC isoforms by SDS-PAGE were only capable of separating the porcine type I MyHC isoform from the other isoforms (see Figure 4.5). Interestingly, the gel compositions used for separating MyHC protein isoforms were specific to the species being studied. In particular, the type II MyHC isoforms from different species display disparity in migration patterns by SDS-PAGE. It is unknown why these differences occur but may be due to very subtle differences in molecular weight of the MyHC isoforms or differences in relative charge placed on the MyHC isoforms during the electrophoresis.

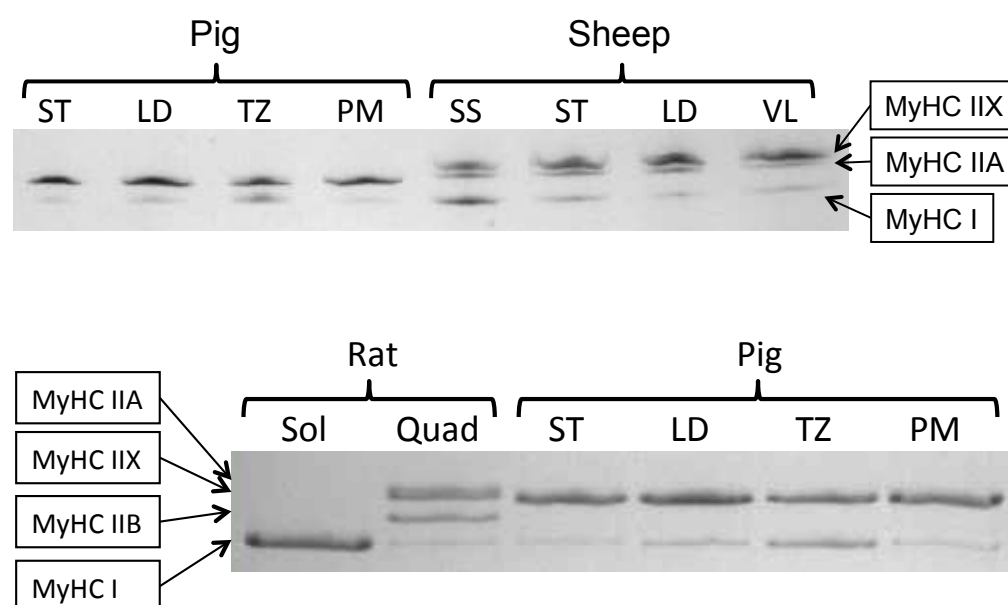


**Figure 4.5** Representative images of SDS-PAGE separation of myosin heavy chain protein isoforms. Note: gel compositions that successfully separated sheep or rat myosin heavy chain isoforms were unable to separate porcine type II myosin heavy chain isoforms.



#### 4.1.3.4 Metabolic gene expression

Transcript abundance of Enolase 3 and IDH2 were used as markers of glycolytic and oxidative gene expression, respectively (Figure 4.6). In response to Ractopamine treatment, Enolase-3 displayed a modest but chronic induction across the full 27-days of treatment ( $p < 0.001$ ). IDH2 mRNA expression, exhibited an initial reduction in expression levels in response to Ractopamine treatment, but returned to control levels by day 27 ( $p = 0.004$ ).

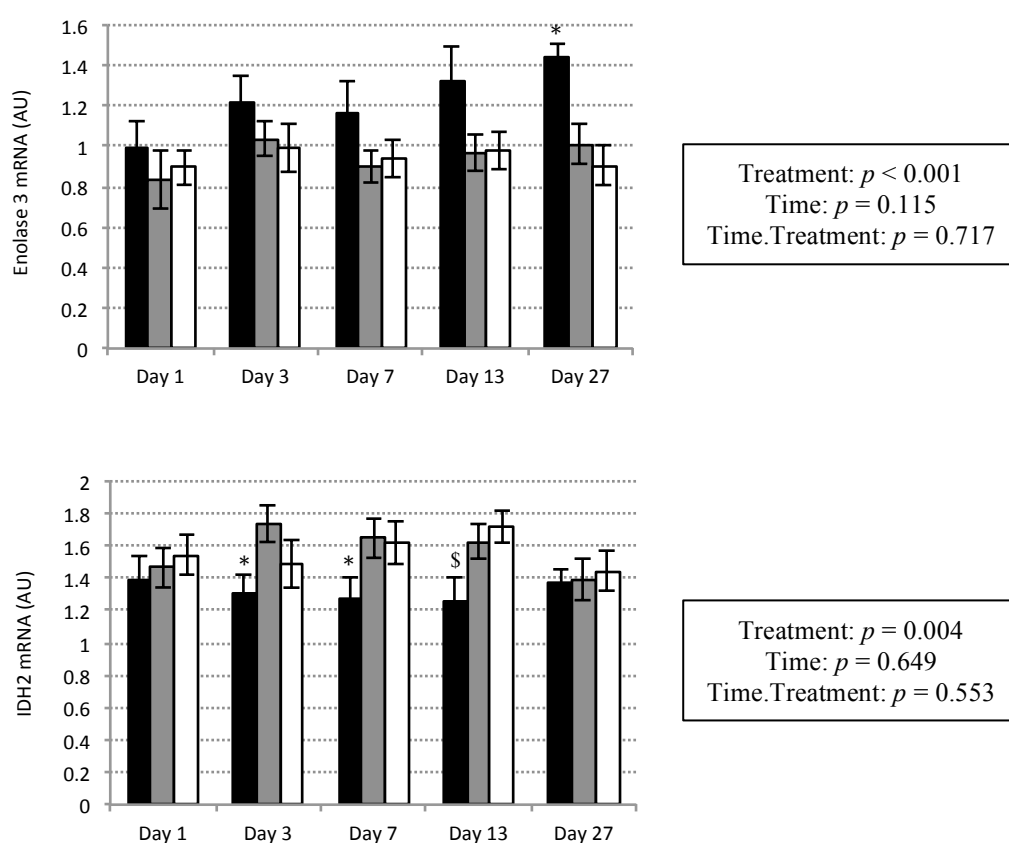


**Figure 4.6** Enolase 3 and IDH2 mRNA expression in the LD muscle of non-treated pigs (grey bars) and pigs treated with Ractopamine (black bars) or Reporcin (white bars) for 1, 3, 7, 13 ( $n=10$ ) or 27 ( $n=15$ ) days. Data is displayed as mean  $\pm$  SEM. \* indicates significant difference relative to the control at the same time point ( $p < 0.05$ ); \$ indicates a trend for a difference relative to the control at the same time point ( $p = 0.067$ ).

#### *4.1.3.5 Correlation between metabolic and MyHC expression*

Correlations were conducted between MyHC isoform and metabolic marker (Enolase 3 or IDH2) mRNA expression to assess whether contractile and metabolic gene expression were closely “coupled” (Figure 4.7 and 4.8). Enolase-3 and MyHC IIB mRNA expression displayed a very high level of correlation ( $r = 0.73$ ), a pattern that was not observed with the other MyHC isoforms (IIX:  $r = 0.32$ ; IIA:  $r = 0.17$ ; I:  $r = 0.24$ ). The correlation between IDH2 and type I MyHC mRNA was very strong ( $r = 0.77$ ). Correlations between IDH2 and the MyHC isoforms mRNA expression got progressively stronger with the slower contracting MyHC isoforms (IIB:  $r = 0.14$ ; IIX:  $r = 0.56$ ; IIA:  $r = 0.62$ ; type I:  $r = 0.77$ ). The large data set analyzed herein ( $n = 164$ ) reveals a close correlation between gene expression of metabolic and contractile components in porcine skeletal muscle.

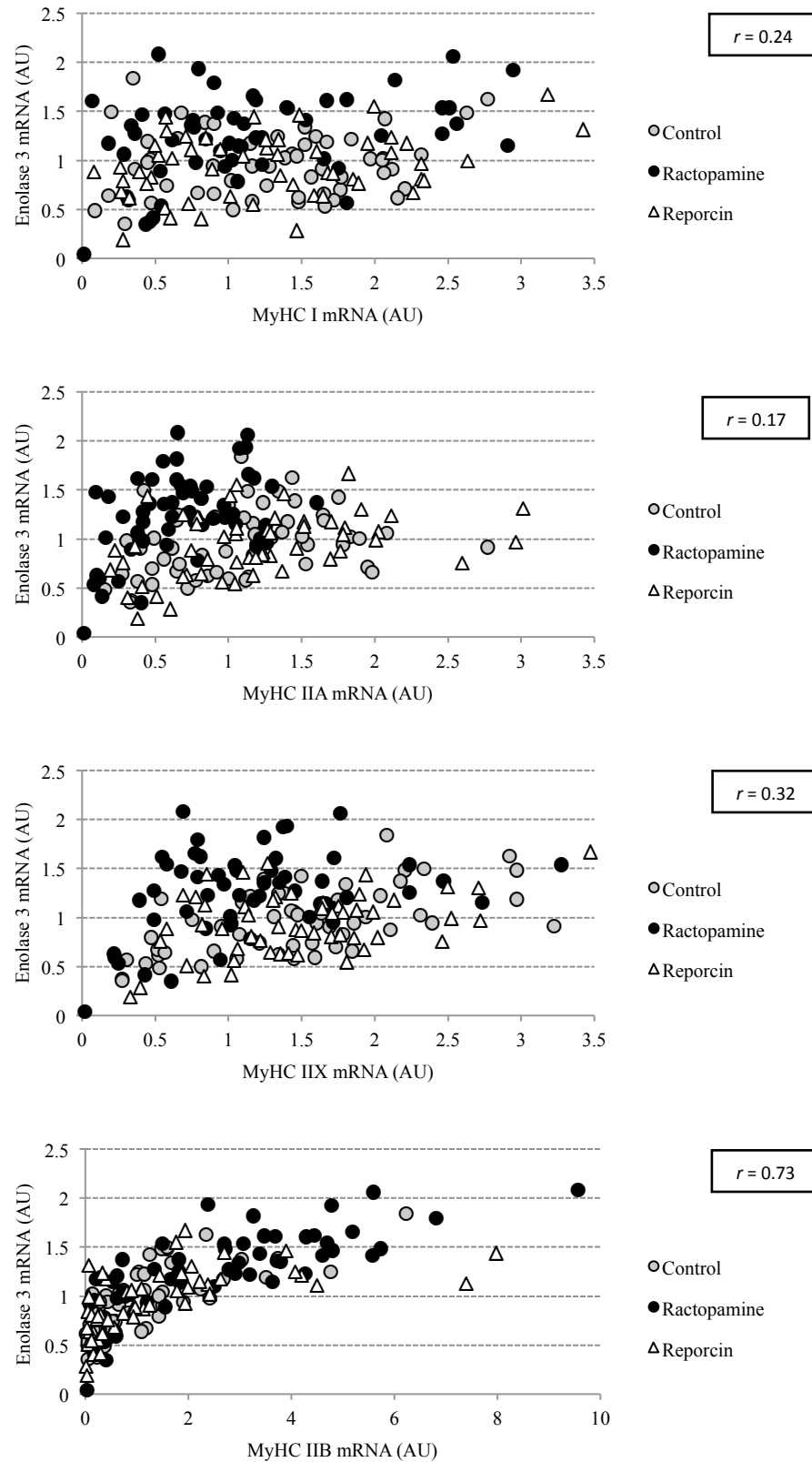


**Figure 4.7** Correlation between MyHC isoform and Enolase 3 mRNA expression. Pearson correlation coefficients are displayed in the corresponding boxes. Note that Enolase 3 and MyHC IIB display a very high correlation, whereas other isoforms did not correlate well.

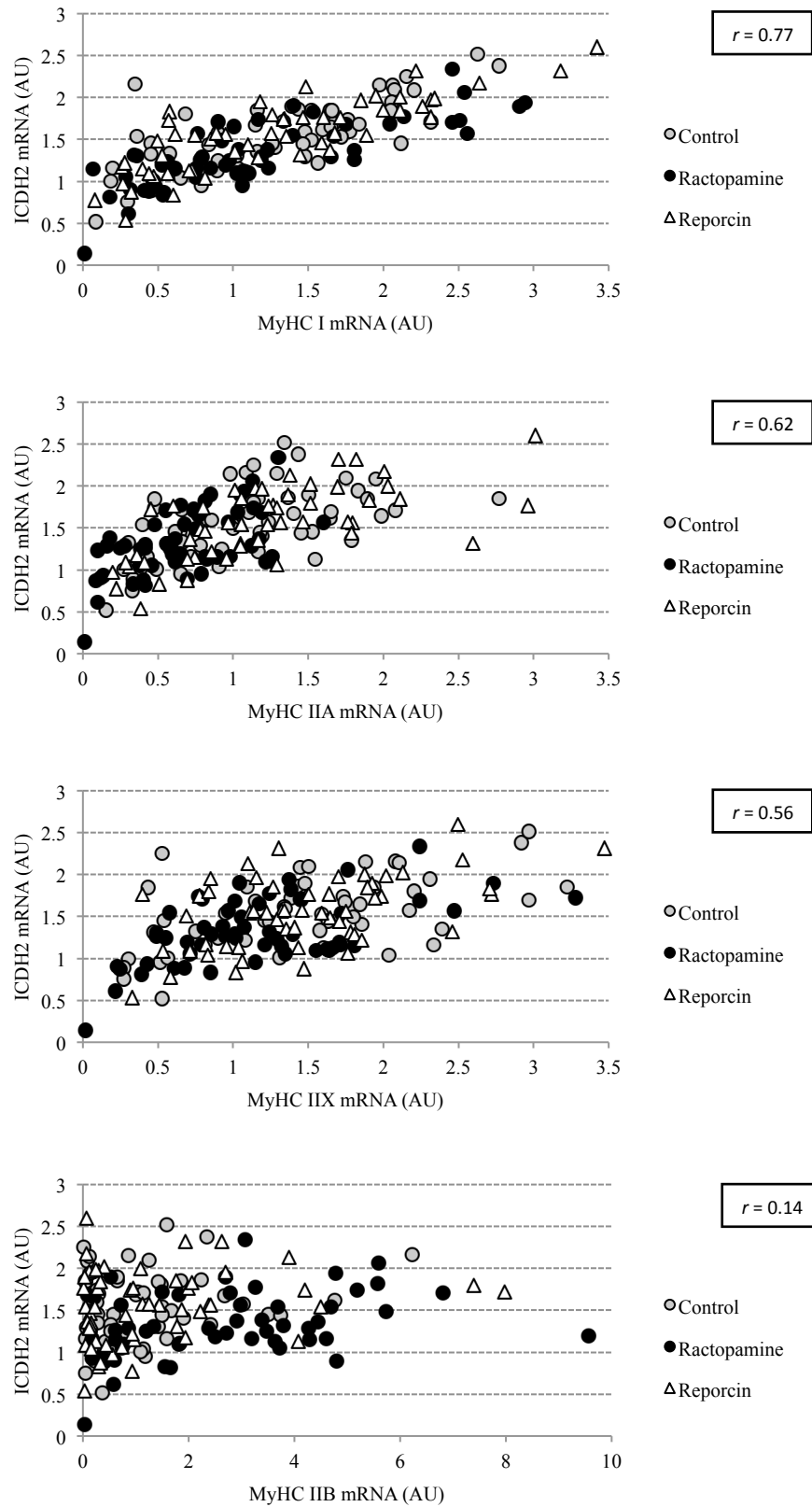


**Figure 4.8** Correlation between MyHC isoform and IDH2 gene expression. Pearson correlation coefficients are displayed in the corresponding boxes. Note that correlations between IDH2 and MyHC isoforms improved as the MyHC isoforms got slower.

#### 4.1.3.6 PGC-1 $\alpha$ and RIP-140 mRNA expression

Transcriptional co-regulatory factors implicated in remodeling towards a slower, more oxidative, muscle fibre type were measured at the mRNA level (Figure 4.9). No alterations in PGC-1 $\alpha$  or RIP140 gene expression were displayed in response to treatment ( $p = 0.068$  and  $p = 0.685$ , respectively) or time ( $p = 0.620$  and  $p = 0.246$ , respectively).

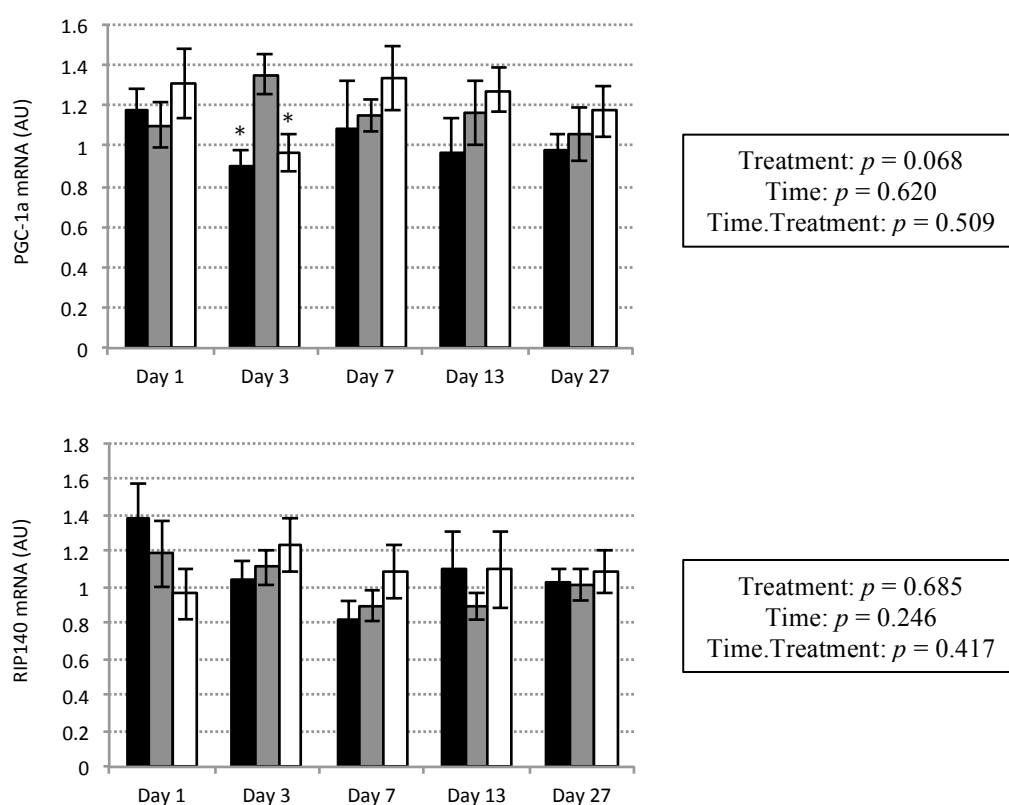


**Figure 4.9** PGC-1 $\alpha$  and RIP140 mRNA expression in the LD muscle of non-treated pigs (grey bars) and pigs treated with Ractopamine (black bars) or Reporcin (white bars) for 1, 3, 7, 13 ( $n=10$ ) or 27 ( $n=15$ ) days. Data is displayed as mean  $\pm$  SEM. \* indicates significant difference relative to the control at the same time point ( $p < 0.01$ ).

#### 4.1.3.7 Myogenic regulatory factor gene expression

Myogenic regulatory factor mRNA expression was utilized as a marker of myogenesis. Furthermore, these factors have also been associated with specific muscle fibre type composition and were thus of interest in the present study. Treatments elicited no effect on transcript abundance of myogenic regulatory factors, MyoD or myogenin ( $p = 0.382$  and  $p = 0.694$ , respectively; Figure 4.10).

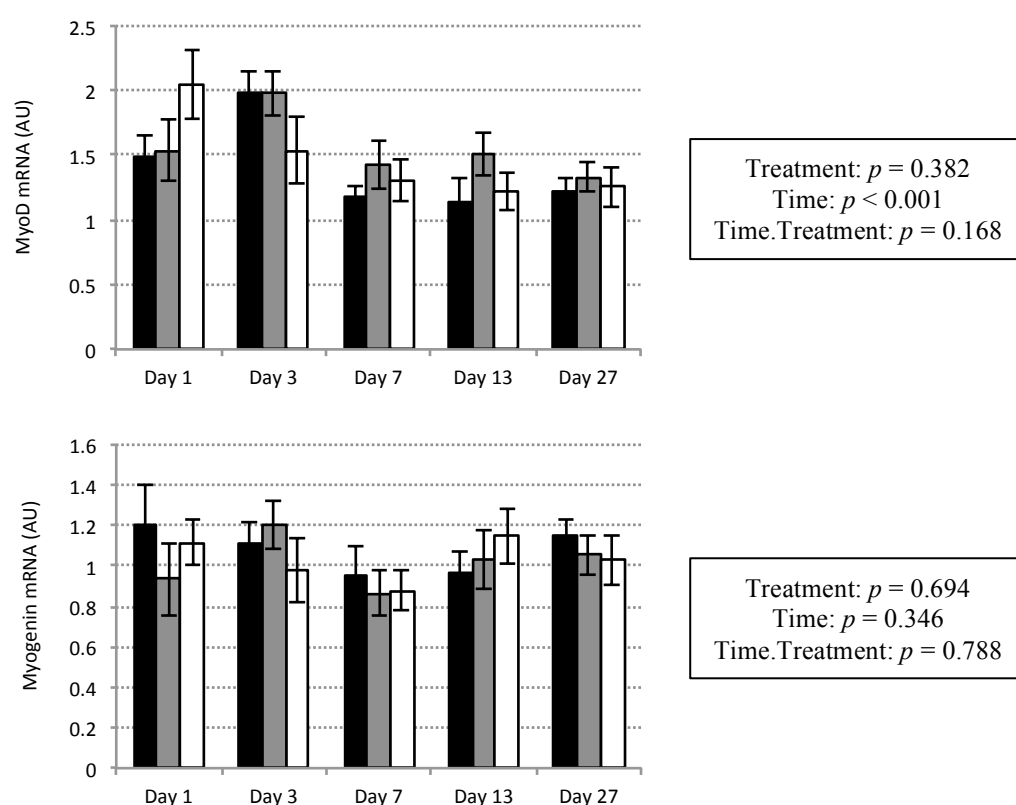


**Figure 4.10** MyoD and Myogenin mRNA expression in the LD muscle of non-treated pigs (grey bars) and pigs treated with Ractopamine (black bars) or Reporcin (white bars) for 1, 3, 7, 13 ( $n=10$ ) or 27 ( $n=15$ ) days. Data is displayed as mean  $\pm$  SEM.

#### 4.1.3.8 *Six1* and *Eya1* mRNA expression

*Six1* and *Eya1* have been associated with fast, glycolytic muscle fibres (Grifone et al. 2004). Transcript abundance of *Six1* and *Eya1* remained unaltered in response to treatments across the 27-day time course ( $p = 0.105$  and  $p = 0.406$ ; Figure 4.11).

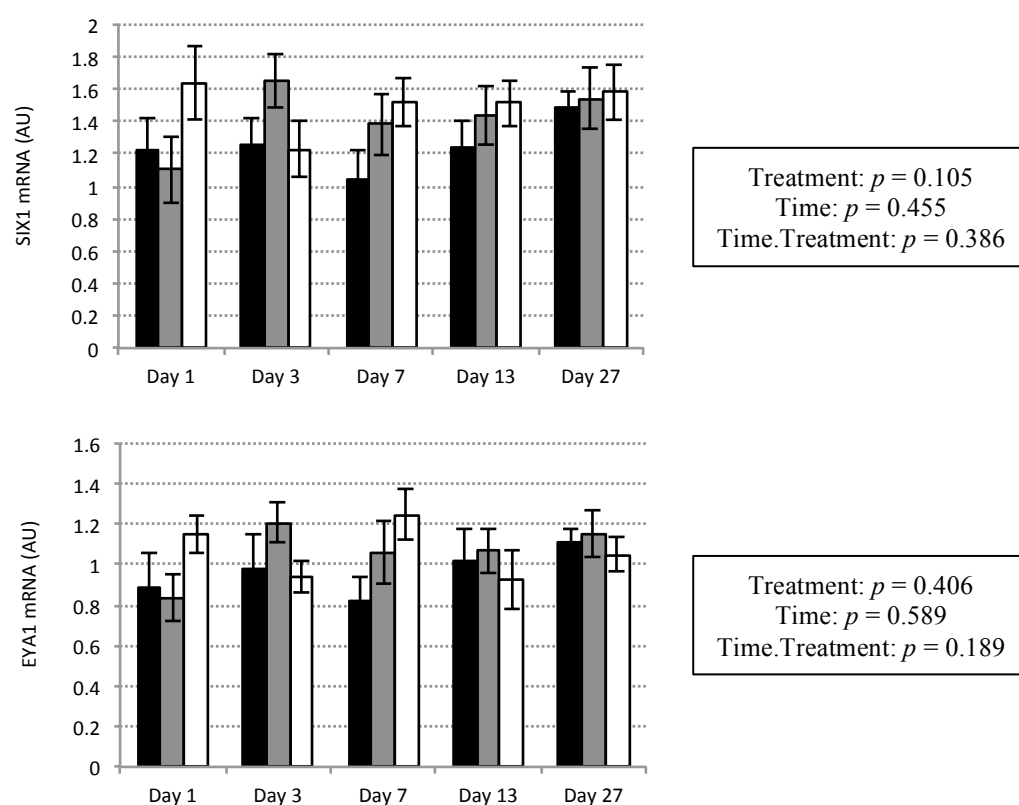


**Figure 4.11** *Six1* and *Eya1* mRNA expression in the LD muscle of non-treated pigs (grey bars) and pigs treated with Ractopamine (black bars) or Reporcin (white bars) for 1, 3, 7, 13 ( $n=10$ ) or 27 ( $n=15$ ) days. Data is displayed as mean  $\pm$  SEM.

#### 4.1.3.9 Summary of *in vivo* findings

To briefly summarize, 27 days of Ractopamine or Reporcin administration to growing pigs caused little or no change in the growth characteristics of the animal. There was, however, a significant transition in MyHC isoform gene expression in response to Ractopamine, but not Reporcin, treatment. Interestingly, the MyHC IIB isoform displayed a chronic induction across the full 27-day time course, whilst the MyHC IIA isoform exhibited an initial decline in expression before returning to expression levels comparable to the control group. In addition, the type IIX MyHC isoform displayed a modest reduction in expression throughout the 27-day treatment window. Taken together, this shows that beta-adrenergic agonist administration induces dynamic modulation in gene expression of the type II MyHC isoforms, with individual isoforms clearly being exclusively regulated, enabling remarkable plasticity of these genes in adult skeletal muscle.

Gene expression of factors previously implicated in muscle fibre type regulation displayed unaltered mRNA expression in response to treatments. Obviously, post-transcriptional modulation of these factors is possible and likely, but this data confirms no transcriptional alteration in expression of these regulatory factors in the fibre type switching model used herein.

These findings are discussed fully in Chapter 4.2 (below) to avoid repetition and to permit interesting comparisons of similar work conducted *in vivo* and *in vitro*.



## 4.2 BETA-ADRENERGIC AGONIST, RACTOPAMINE, ACTS DIRECTLY ON MUSCLE CELLS TO ACCELERATE THE INDUCTION OF THE MYOSIN HEAVY CHAIN IIB GENE DURING C2C12 MYOGENESIS

### 4.2.1 INTRODUCTION

Although growth hormone administration caused no effect on MyHC mRNA isoform expression in growing pigs (and will therefore no longer be examined in this thesis), beta-adrenergic agonist, Ractopamine, induced a chronic transition in MyHC mRNA isoform expression in growing pigs (Chapter 4.1). This dynamic transcriptional remodeling of the type II MyHC isoforms by beta-adrenergic receptor stimulation was further explored in C2C12 muscle cells. This approach would examine whether the altered mRNA expression of type II myosin heavy chain isoforms was a result of direct interaction of Ractopamine on muscle cells. Furthermore, *in vitro* examination of the effects of Ractopamine on cultured muscle cells would help elucidate a role of beta-adrenergic receptor stimulation on the induction of type II MyHC isoform genes during myogenic differentiation (explained below).

It was previously identified that the MyHC mRNA isoforms are expressed in two distinct cohorts during C2C12 myogenesis (Brown et al. 2012; Chapter 3.1), with the fast type II isoforms (IIA, IIX and IIB) being induced late in differentiation. This “delayed” induction of the type II MyHC isoforms in C2C12 myotubes provides an interesting model for studying the induction of type II MyHC isoforms during myogenesis. Since we and others (Baker et al. 2006; Bricout et al. 2004; Depreux et al. 2002; Oishi et al. 2002; Gunawan et al. 2007; Chapter 4.1) have shown beta-adrenergic agonists induce a strong induction of MyHC IIB expression *in vivo*, fusing C2C12 muscle cells, not yet

expressing the type II MyHC mRNA isoforms, were utilized to explore whether the beta-adrenergic agonist, Ractopamine, could accelerate the initial induction of the type II MyHC mRNA isoforms during myogenic differentiation. Interestingly, Ryall et al. (2010) previously reported that beta-1 and beta-2 adrenergic receptor mRNA expression increases during myoblast fusion (with expression peaking at day 2 of differentiation) and suggested a potential role of beta-adrenergic signaling during early myogenic fusion (see Figure 4.12). It was speculated herein that the appearance of beta-adrenergic receptor expression during this early stage of myogenic differentiation might be involved in the initial induction of the type II MyHC mRNA isoforms.

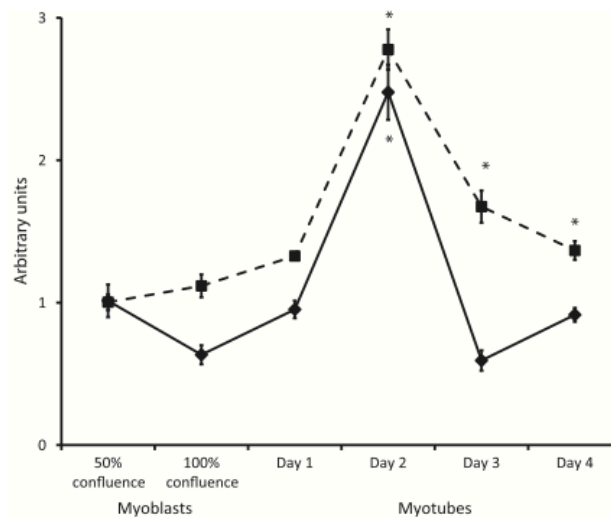


**Fig.** Quantitative real-time polymerase chain reaction was used to measure mRNA levels of *Adrb1* (◆) and *Adrb2* (■),  $\beta_1$ - and  $\beta_2$ -adrenoceptor genes, respectively, in C2C12 myoblasts at 50 and 100% confluency and in myotubes after 1, 2, 3 or 4 days of differentiation. Interestingly, levels of both *Adrb2* and *Adrb1* mRNA were markedly increased after 2 days in differentiation media. Data are the mean  $\pm$  SEM ( $n = 3$  samples/timepoint). \* $P < 0.05$  compared with 50% confluence.

**Figure 4.12** Figure (and description) taken from Ryall et al. (2010) showing relative mRNA expression of the Beta-1 and Beta-2 adrenergic receptors during early myogenic differentiation of C2C12 myoblasts. Ractopamine treatments in the present study were administered before and after the peak mRNA expression of the beta-receptors.

C2C12 muscle cells used herein were exposed to beta-adrenergic agonist, Ractopamine, before and after the peak in mRNA expression of the beta-receptors (Ryall et al. 2010), which also corresponded to the time of initial induction of the type II MyHC isoforms (Brown et al. 2012). Therefore, acute 48-hour windows of exposure to Ractopamine (1 $\mu$ M) were conducted during the early stages of myogenic differentiation to assess the role of beta-adrenergic receptor stimulation on the initial mRNA induction of the type II MyHC isoforms (see Figure 4.13). It was hypothesized that Ractopamine treatment would accelerate the initial induction of the type II MyHC mRNA isoforms (see the red arrows in Figure 4.13 below) and would be dependent on the timing window of administration.

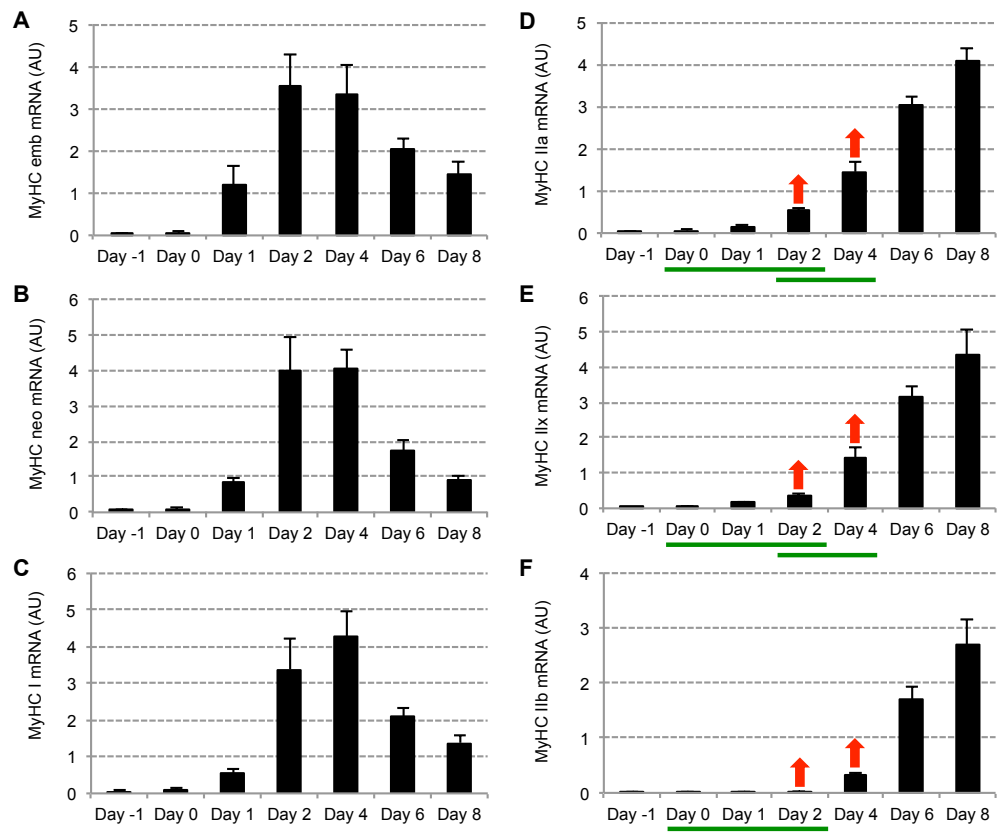


**Figure 4.13** Predicted effects (red arrows) of Ractopamine treatment (48 hour windows represented by green lines) on type II MyHC mRNA induction during myogenesis using the previously characterized C2C12 cell line (Figure from Chapter 3.1).

## 4.2.2 MATERIALS AND METHODS

### 4.2.2.1 Overview

C2C12 muscle cells were treated with Ractopamine during the early stages of myogenic differentiation to assess whether beta-adrenergic receptor stimulation causes changes in mRNA induction of the type II MyHC isoforms during myogenesis. A brief account of the experimental procedures is detailed below. A more detailed explanation of procedures used herein can be found in the Materials and Methods Chapter (Chapter 2).

### 4.2.2.2 Cell culture

C2C12 cells were grown in proliferation medium (DMEM, 10% FBS, 1% P/S) until ~90% confluent (day 0) at which point cells were encouraged to differentiate by changing to a low serum differentiation medium (DMEM, 2% HS, 1% P/S) and cultured for up to 4 days. All cultures were carried out on 6 well plates using 2 ml of culture medium per well. Representative images of the cells at days 0, 2 and 4 are provided in Figure 4.14.

### 4.2.2.3 Treatments

A 1mM solution of Ractopamine Hydrochloride (RAC; Sigma Aldrich, Poole, UK) was made in phosphate buffered saline (PBS; Sigma Aldrich, Poole, UK) containing 0.5% Dimethyl Sulfoxide (DMSO; Sigma Aldrich, Poole, UK), sterile filtered (0.2µm) and added to the differentiation medium (1:1000) to give a working concentration of 1µM. Previous literature suggested 1µM to be the most “responsive” dose *in vitro* (Anderson et al. 1990; Grant et al. 1990) and was thus used in the present study. The same dilution procedure of DMSO

only (i.e. without RAC) was carried out for use as a vehicle control (CON). Final DMSO concentration in the medium for RAC and CON treated cells was 0.0005%. Cells were treated with RAC or CON for 48 hours starting at day 0 (~90% confluence) or day 2 of differentiation. Nine separate wells were used per treatment, per time point (spread across 3 six-well plates) for mRNA analysis. In addition, six separate wells per treatment, per time point were used for creatine kinase, DNA and protein assays (spread across 2 six-well plates).

#### *4.2.2.4 Cell harvest for growth assays*

Following 48 hour treatments (finishing on day 2 or 4), culture medium was removed, cells were washed once with 1ml warm PBS, scraped into 500µl tri-sodium citrate buffer and stored in 1.5ml tubes at -20°C until use. Creatine kinase activity, DNA content and protein content were assayed as described in Chapter 2.

#### *4.2.2.5 Cell harvest for RNA extraction*

Following 48 hour treatments, culture medium was removed, cells were immediately scraped into 200µl RNase-free phosphate buffered saline (PBS), transferred to 1.5ml tubes, snap frozen on dry ice (solid CO<sub>2</sub>) and stored at -80°C until analysis. Total RNA was extracted using an RNA isolation kit (High Pure Isolation Kit for RNA isolation, Roche, Burgess Hill, UK). RNA concentrations were adjusted to 100ng/µl for cDNA synthesis.

#### 4.2.2.6 cDNA synthesis and Quantitative-RT-PCR

First strand cDNA synthesis was carried out using a Roche cDNA synthesis kit (Transcriptor First Strand cDNA Synthesis Kit, Roche, Burgess Hill, UK). Quantitative PCR was performed on a Lightcycler480 (Roche, Burgess Hill, UK). All reactions were carried out in triplicate on white 384 well plates, as described previously. Transcript abundance was determined using the standard curve method and subsequently corrected for total cDNA in the PCR reaction using the oligreen method (Rhinn et al. 2008; Brown et al. 2012).

#### 4.2.2.7 Quantitative-RT-PCR oligonucleotides primers

Oligonucleotide primers for detecting transcript abundance of the MyHC isoforms (I, IIa, IIx, IIb, embryonic and perinatal), MyoD and Myogenin were all tested previously and have been published (Brown et al. 2012). Myogenin mRNA expression was used as a marker of muscle cell differentiation (Brown et al. 2012). The primers in Table 4.3 were designed in house (by myself or Dr Zoe Daniel) to measure the same genes measured in porcine skeletal muscle (Chapter 4.1) to allow comparisons of responses *in vivo* and *in vitro*. The accession numbers for these genes are as follows: Six1 (ENSMUST00000050029), Eya1 (ENSMUST00000080664), Enolase-3 (ENSMUST00000108548), IDH2 (ENSMUST00000107384), PGC1-a (ENSMUST00000132734) and RIP140 (ENSMUST00000054178).

**Table 4.4** Oligonucleotide primer sets for Q-PCR analysis of gene expression

Gene	Forward primer	Reverse primer	Amplicon length
<i>SIX1</i>	AGGAAAGGGAGAACACCGAAA	CTTCCAGAGGAGAGAGTTGATTCTG	69bp
<i>EYA1</i>	ACAGCAGAGTACAGTACAATCCACAGT	AGCCGCTCGGAGTCAGTCT	65bp
<i>Enolase-3</i>	GCCTGCTCCTGAAGGTCAAC	TGCAAGTTTACAGGCCTGGAT	65bp
<i>IDH2</i>	TTGAGGCTGAGGCTGCTCAT	CCGGCCCTTCTGGTGTT	62bp
<i>PGC-1a</i>	TGCAGCGGTCTTAGCACTCA	CATGAATTCTCGGTCTTAACAATGG	89bp
<i>RIP140</i>	CGACTTCCAGACCCACAACA	GGCGCTCTTGGCATCGT	55bp

Melt-curve analysis was conducted for all primer sets to ensure a single amplicon of the correct length was produced in the PCR reaction, and that no primer dimers were produced in the presence or absence of template DNA. Serial dilutions of a pool of all cDNA samples were produced and tested to ensure the PCR was linear.

#### 4.2.2.8 Porcine 1kb MyHC IIB promoter-reporter

The *in vivo* experiments in Chapter 4.1 were conducted in porcine skeletal muscle and the present experiments (Chapter 4.2) are conducted in a mouse derived muscle cell line (C2C12 cells). Thus, to examine the effects of Ractopamine on MyHC IIB regulation during myogenic cell fusion, a pig MyHC IIB promoter-reporter construct was transfected into C2C12 cells to assess if the porcine specific MyHC IIB promoter sequence would elicit accelerated activity during C2C12 myogenesis following Ractopamine treatment *in vitro*. In addition, cells were treated with dbcAMP to increase intracellular cAMP levels in an attempt to mimic a beta-adrenergic response via an alternative method. A detailed explanation of how the porcine 1kb MyHC IIB promoter-reporter was generated and used is provided in Chapter 2 (*Molecular Biology Methods* section).

#### *4.2.2.9 Statistical analysis*

Statistical analysis was carried out on a single experiment with 9 biological replicates (per treatment, per time point) for quantitative-RT-PCR analysis and 6 biological replicates for creatine kinase activity and DNA content. To determine whether there were significant differences between treatments at either day 2 or 4, a one-way ANOVA was performed using GenStat statistical analysis software (Version 14). Comparisons across time were not conducted since treatments were administered as two discrete experiments. Data is displayed as mean  $\pm$  standard error of the mean (SEM). Significance was accepted if  $p < 0.05$ .



### 4.2.3 RESULTS

#### 4.2.3.1 Light microscopy

Representative images of the C2C12 cells at different stages of differentiation/treatment are shown in Figure 4.14. Cells treated from day 0 were proliferating myoblasts (~90% confluent) and received treatment until small, immature myotubes had formed (day 2). Cells beginning treatment on day 2 were treated until day 4 whereby significant myotube formation had occurred, differentiation was ceasing and myotubes were undergoing maturation. No visual differences in cell morphology were apparent in response to Ractopamine treatment.

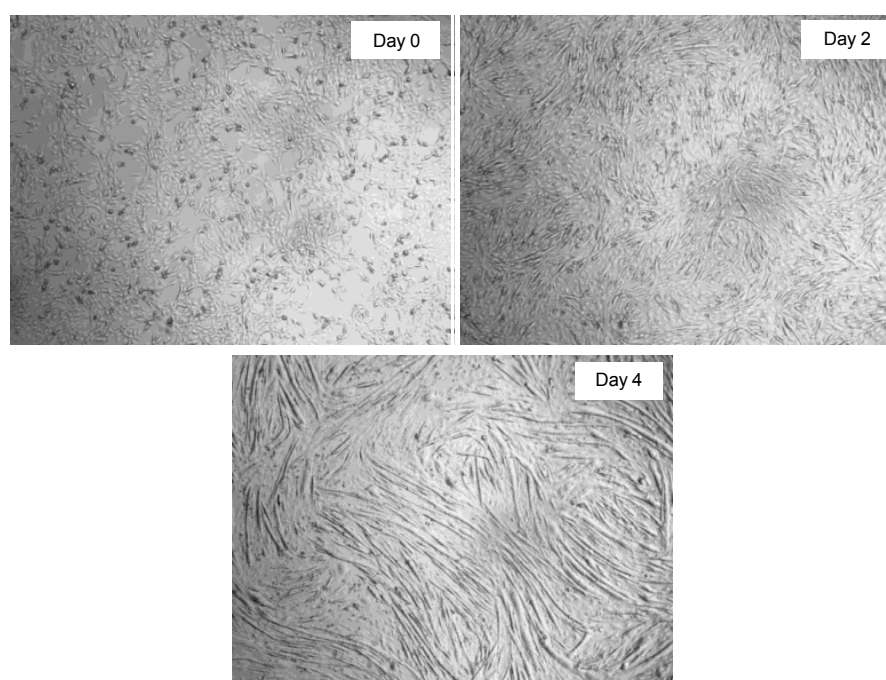


**Figure 4.14** Representative light microscopy (phase contrast) images of C2C12 cells at days 0, 2 and 4 during differentiation. Treatments were applied at either day 0 or 2 and harvested following 48 hours of Ractopamine treatment (at days 2 or 4). No visual differences between treated and non-treated cells was observed.

#### 4.2.3.2 Proliferation, differentiation and protein accretion

DNA content and creatine kinase activity were used as markers of proliferation and differentiation, respectively. Cells treated with Ractopamine at day 0-2 displayed a slight reduction in DNA content ( $p = 0.026$ ) whereas cells treated from day 2-4 displayed no change in DNA content ( $p = 0.677$ ; Figure 4.15). Creatine kinase activity remained unchanged in response to Ractopamine treatment from day 0-2 ( $p = 0.635$ ) and 2-4 ( $p = 0.983$ ; Figure 4.15). Protein:DNA ratio was determined as a marker of protein accretion (or cellular hypertrophy) and remained statistically unchanged following treatment from day 0-2 and 2-4 ( $p = 0.052$  and  $p = 0.407$ , respectively). The trend for increased protein:DNA ratio following treatment from day 0-2 ( $p = 0.052$ ) was likely due to a slight reduction in DNA content of Ractopamine treated cells.

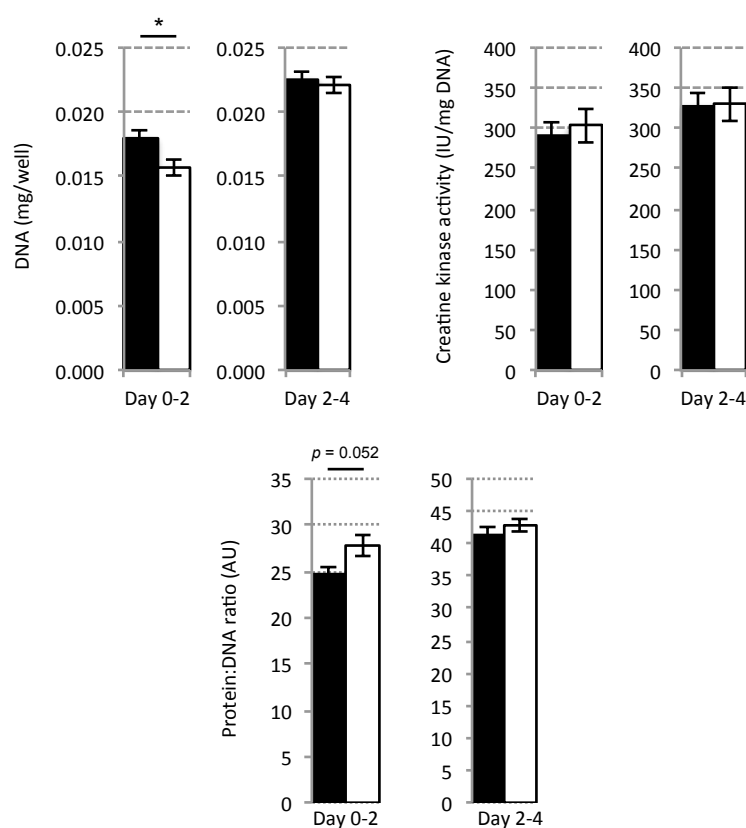


**Figure 4.15** DNA content, creatine kinase activity and protein:DNA ratio following 48 hours Ractopamine treatment finishing at either day 2 or 4. Solid bars = control; Open bars = Ractopamine treated (1 $\mu$ M). Significant differences between treated and non-treated groups are indicated by \* ( $p = 0.026$ ).

#### 4.2.3.3 Myogenic regulatory factor gene expression

MyoD and myogenin gene expression were measured as these genes are considered good markers of cellular differentiation (Brown et al. 2012). Expression of MyoD and myogenin mRNA exhibited no response to Ractopamine treatment at either day 0-2 ( $p = 0.564$  and  $p = 0.748$ , respectively) or 2-4 ( $p = 0.482$  and  $p = 0.509$ , respectively; Figure 4.16) and therefore support the lack of change in creatine kinase activity in response to Ractopamine treatment.

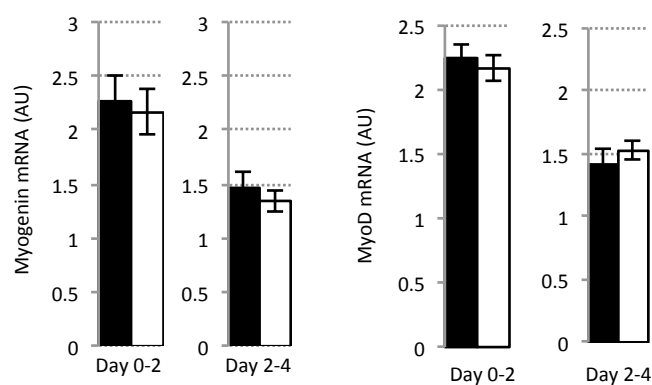


**Figure 4.16** mRNA expression of Myogenin and MyoD following 48 hours Ractopamine treatment finishing at either day 2 or 4. Solid bars = control; Open bars = Ractopamine treated (1 $\mu$ M).

#### 4.2.3.4 Myosin heavy chain mRNA isoform expression

Following 48 hours of Ractopamine treatment, MyHC IIB mRNA expression exhibited a 2.4-fold and 1.6-fold increase at days 0-2 and 2-4, respectively ( $p < 0.001$ ; Figure 4.17). Interestingly, mRNA expression of MyHC IIB was the only type II isoform that responded to Ractopamine treatment, with the IIA and IIX isoforms showing no change in mRNA expression following treatments at day 0-2 ( $p = 0.874$  and  $p = 0.140$ , respectively) or 2-4 ( $p = 0.337$  and  $p = 0.731$ , respectively).

Similarly, the mRNA expression of the adult type I and embryonic MyHC isoforms showed no response to Ractopamine treatment at day 0-2 ( $p = 0.818$  and  $p = 0.391$ , respectively) or 2-4 ( $p = 0.518$  and  $p = 0.174$ , respectively), whereas neonatal MyHC mRNA expression showed a small induction with Ractopamine treatment at the later treatment time point (day 2-4;  $p = 0.039$ ), but there was no change following 48 hours treatment from day 0 ( $p = 0.656$ ; Figure 4.17).

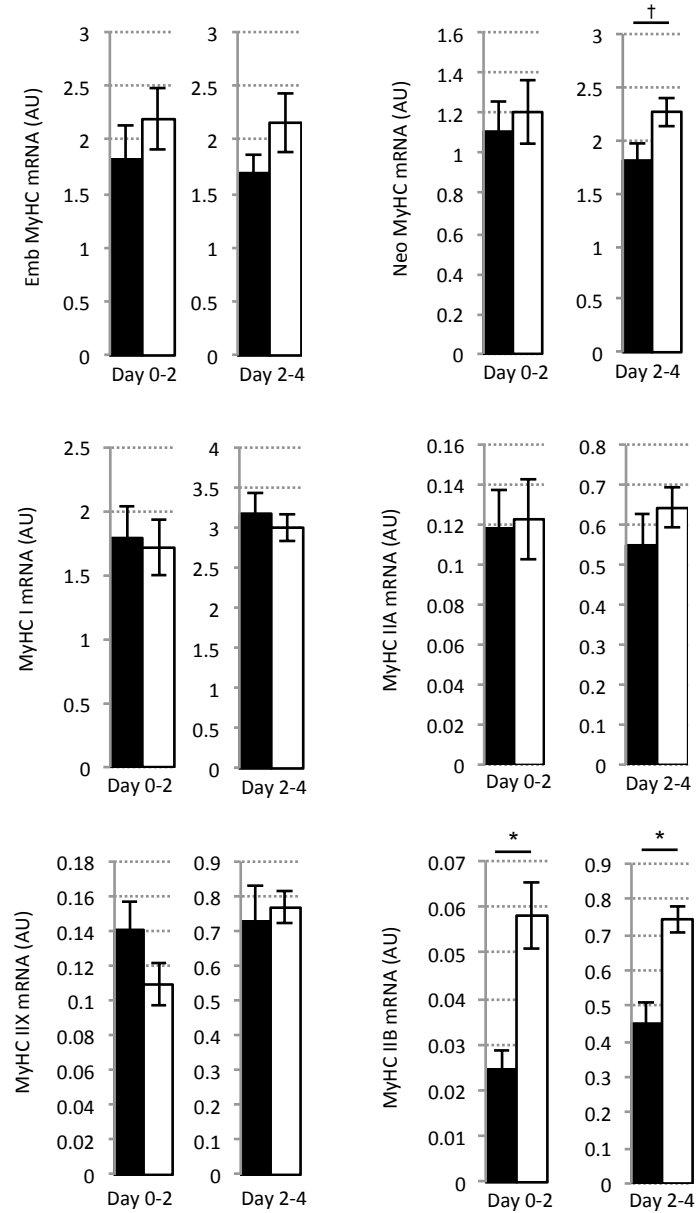


**Figure 4.17** mRNA expression of MyHC isoforms (embryonic, neonatal, I, IIA, IIX and IIB) following 48 hours Ractopamine treatment finishing at either day 2 or 4. Solid bars = control; Open bars = Ractopamine treated (1 $\mu$ M). Significant differences between treated and non-treated groups are indicated by \* ( $p < 0.001$ ) and † ( $p = 0.039$ ).

#### 4.2.3.5 Metabolic gene expression

Metabolic genes, Enolase-3 and IDH-2, were used as markers of glycolytic and oxidative gene expression respectively (as they closely correlated with the type I and type II MyHC isoforms respectively in Chapter 4.1)). No changes in mRNA expression of Enolase-3 or IDH-2 were observed in response to 48 hours Ractopamine treatment at either of the time points studied (Table 4.4). The transcriptional co-activators, PGC-1 $\alpha$  and RIP140, previously reported as master “regulators” of a slow oxidative muscle phenotype (Lin et al. 2002; Seth et al. 2007), displayed no change in mRNA expression in response to 48 hours Ractopamine treatment at either day 0-2 or 2-4 (Table 4.4).

**Table 4.5** Relative gene expression following 48 hours Ractopamine (1 $\mu$ M) treatment finishing at either day 2 or 4.

mRNA abundance (AU)	Day 0-2			Day 2-4		
	Control	Ractopamine	<i>P</i> -value	Control	Ractopamine	<i>P</i> -value
PGC1- $\alpha$	2.02 $\pm$ 0.14	2.36 $\pm$ 0.15	0.112	1.51 $\pm$ 0.08	1.50 $\pm$ 0.05	0.878
RIP140	2.50 $\pm$ 0.17	2.10 $\pm$ 0.12	0.068	1.38 $\pm$ 0.11	1.59 $\pm$ 0.09	0.142
Enolase 3	1.31 $\pm$ 0.07	1.22 $\pm$ 0.05	0.311	1.47 $\pm$ 0.09	1.62 $\pm$ 0.10	0.312
IDH2	2.29 $\pm$ 0.11	2.14 $\pm$ 0.09	0.339	1.23 $\pm$ 0.07	1.27 $\pm$ 0.08	0.693

#### 4.2.3.6 Beta-adrenergic receptor 2 (*Adrb2*) mRNA expression

Ryall et al. (2010) previously demonstrated a significant induction in beta-adrenergic receptor 2 (*Adrb2*) mRNA expression during the early stages of C2C12 differentiation. *Adrb2* mRNA expression was therefore measured herein to confirm the C2C12 cells utilized in this laboratory also express the transcripts encoding the *Adrb2* receptors. Indeed, *Adrb2* mRNA was expressed in C2C12 cells and showed a modest reduction ( $p = 0.011$ ) in expression with differentiation (from day 2 to 4; Figure 4.18). *Adrb2* mRNA expression in C2C12 cells remained statistically unaltered with Ractopamine treatments at both day 0-2 ( $p = 0.071$ ) and 2-4 ( $p = 0.288$ ; Figure 4.18).

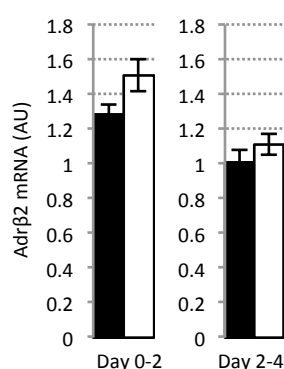


**Figure 4.18** Beta-adrenergic receptor 2 (*Adrb2*) mRNA expression following 48 hours Ractopamine treatment finishing at either day 2 or 4. Solid bars = control; Open bars = Ractopamine treated (1µM).

#### 4.2.3.7 *Six1* and *Eya1* mRNA expression

C2C12 cells treated with Ractopamine for 48 hours from the start of differentiation (day 0-2), exhibited a significant up-regulation of *Six1* and *Eya1* mRNA expression ( $p = 0.002$  and  $p < 0.001$ , respectively; Figure 4.19). However, this response in *Six1* and *Eya1* mRNA expression was not observed if Ractopamine treatment was administered later in differentiation (day 2-4;  $p = 0.925$  and  $p = 0.286$ , respectively).

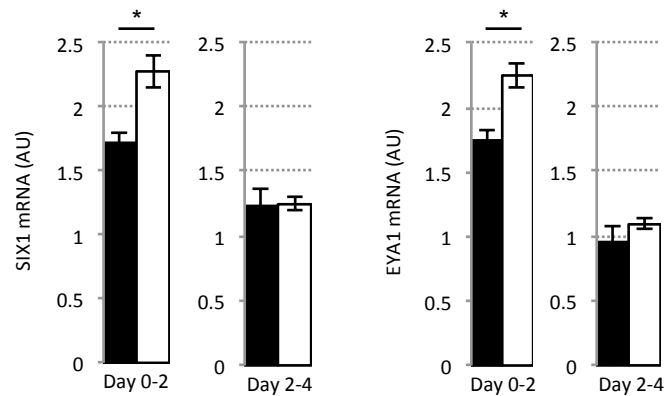


**Figure 4.19** mRNA expression of *Six1* and *Eya1* following 48 hours Ractopamine treatment finishing at either day 2 or 4. Solid bars = control; Open bars = Ractopamine treated (1 μM). Significant differences between treated and non-treated are indicated by \* ( $p < 0.01$ ) and \*\* ( $p < 0.001$ ).



#### 4.2.3.8 Porcine MyHC IIB promoter activation

In Chapter 4.1 it was shown that the beta-adrenergic agonist, Ractopamine, elicited a dynamic transition in type II MyHC mRNA isoforms in growing pigs, with a chronic induction of the type IIB MyHC mRNA isoform. Here (Chapter 4.2), Ractopamine was shown to specifically induce an early induction of the MyHC IIB gene *in vitro* during mouse C2C12 myogenesis. Therefore, the next step was to examine if the pig MyHC IIB promoter would also exhibit accelerated induction during C2C12 myogenesis following Ractopamine treatment *in vitro*. Indeed, there was a modest induction of the porcine 1kb MyHC IIB promoter following 4 days of Ractopamine treatment during C2C12 differentiation ( $p = 0.002$ ; Figure 4.20). This suggests this effect probably occurs in multiple species and that the increased MyHC IIB mRNA expression in C2C12 cells in response to beta-adrenergic agonist treatment is likely due to increased MyHC IIB promoter activity.

In addition, it was tested if increasing intracellular cAMP levels (as a downstream mediator of a beta-adrenergic response) using dbcAMP (1mM) would elicit a similar induction of the porcine MyHC IIB promoter during C2C12 myogenesis. dbcAMP treatment during the first 4 days of C2C12 differentiation caused an induction of the porcine MyHC IIB promoter ( $p = 0.002$ ) comparable to the Ractopamine induced promoter induction (Figure 4.20).

C2C12 cells were analyzed for porcine MyHC IIB promoter activity following 4 days of treatment because promoter activity was too low prior to this and was considered not quantifiable.

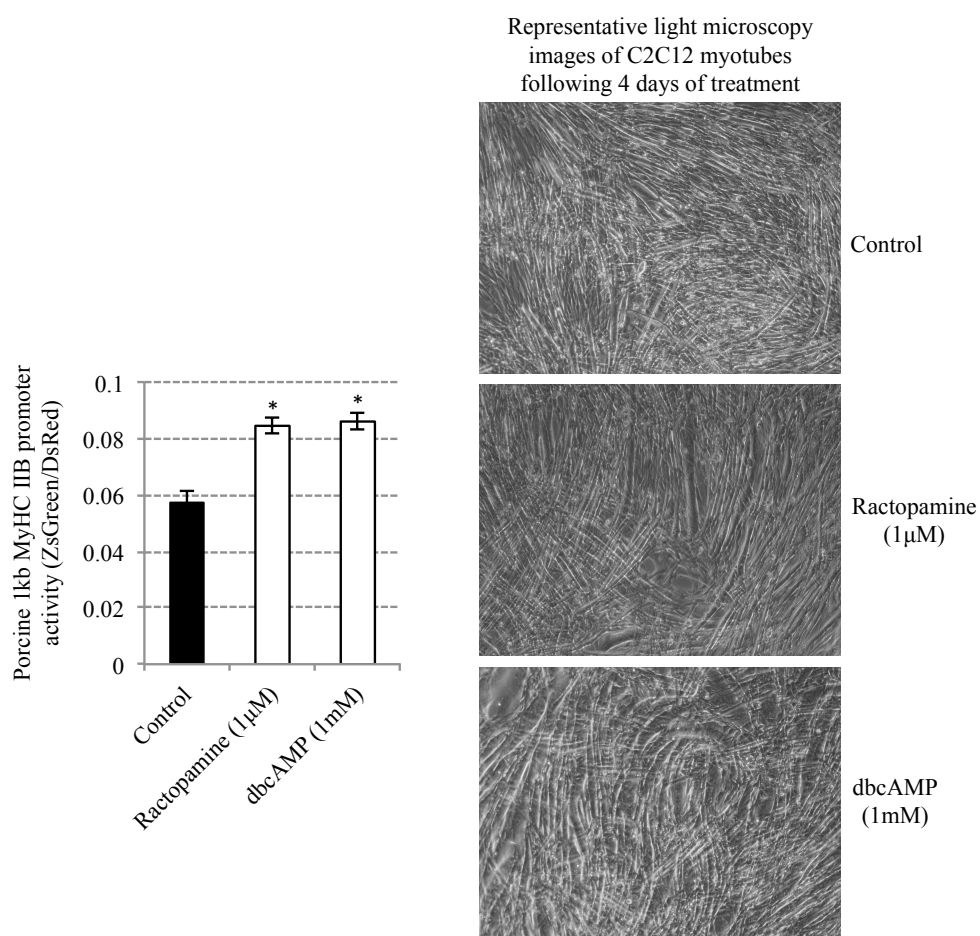


**Figure 4.20** Porcine 1kb myosin heavy chain IIB promoter activity in C2C12 myotubes following 4 days of treatment with Ractopamine or dbcAMP during differentiation. Promoter activity is displayed as mean  $\pm$  SEM. \* indicates a significant difference compared to the control group ( $p < 0.01$ ). Representative light microscopy images show visual differences in myotube morphology between treated and non-treated cells.

#### *4.2.3.9 Porcine 1kb MyHC IIB promoter lacks cAMP response elements (CRE)*

The porcine 1kb MyHC IIB promoter-reporter construct was responsive to Ractopamine and dbcAMP treatment in C2C12 cells. cAMP typically mediates its transcriptional effects by activating cAMP-response element binding proteins (also known as CREB's or ATF's). Interestingly, the 1kb mouse MyHC IIB promoter contained a consensus CREB/ATF binding site (identified by an online transcription factor search engine; TFSEARCH (<http://www.cbrc.jp/research/db/TFSEARCH.html>)) but the equivalent porcine promoter lacked any consensus response elements for CREB/ATF transcription factors (Figure 4.21). This suggests that the porcine MyHC IIB promoter can be induced during myogenic differentiation by beta-adrenergic or cAMP mediated signaling and moreover, this effect may occur independently of interactions at CREB/ATF consensus response elements.

TAGGTGACACACTTAGCGTGGACAGATTTGGCTGTTACATTAGCAGCAGCTGTGTCTGTGGCAAAACCCACAAAACCA  
ATTTACAAGCATCGTGGGCATATGTGATAGCCCCCTTATGTTCTCAACCCACAAAGAGTCCTGTGGGTATCACAATCTCT  
CCTCCCACCTTAAATAAAAAATACGTATTACCCACCTCATTAGAGCTACTGTCATGATCATGAGGATTTGGCTGTGAATACG  
GAATGCATATTGATGCCTCCTTCCATCATTACGGTAGAAAACACATAGAACATCACAGGCATCCTGCAGTCCCCG  
CAGTGAAAACATGTGAGCTCAAGACACCGCGAAGCTCTCCAGAAAAGGAAAAGAGTGTTCATCTATTTCTAAAT  
CCCTTATGGCTCCCCCACTGGTCTGTCAACCATGGCTTAGCCCCGAGAATCTGCCTAAACTTTCTCCTTCATGCTTAGTCT  
TTTAGACTTTAAAAAAATCTATCATCAGTATTTCTAAAAATCCAGACCAGGTCAGGAGTTTCTGCCTTTAATACCAATC  
ATGTTGTGCAGAGCTAAAACTCATCCGAGCTCCTCAATGGCCCTAAGCACTAAACAATCAATTAGTTCTCAACTCTCGT  
GTCTGCCTCATTCTGTGCGGACAATTTACAGCCAGGAGAGTAAGTGGGAAGCTGCCTTTTCAACTCAGTGAATGAATG  
GGAACAGCAAAGCTGGAGAAAATAGCCTTAGAAGCCCTGAATCTCCATCCCTATCAAAATGCCTCAAAGAACCCCTAGATG  
ATCCTCTGTCAAATTAATTTATAGGTGTCAAGAAATATTTCTAATTATATCCATTACAGCCACAGTCAGTGAATATTGT  
GCAAGAGATGTGCAAAAAAGGTTTGCCAAAGTAGGTTCCGAGCTGGGACAGCTGAGGTGGCTGCTGTGTTTGCAAAATG  
GCTCTATAAAAGTGAGCTGAGATGCCCTCTGTCTGCTGCTTCTCT

CAGGCCAGATCACAGGGACAGTTAGTAGTAGATTTCTGTGCATATTCAGCAACAGCTGTGCCTGTAACAAGTTAGTCAAA  
TCCAACCTCGGCCTTTCAAGGGCACCCTGGAGGCCGATCCACCACCTCTCTCTGCGGAGAGAGTTTTGTGGACAGC  
ATGCCCTTTCCTCCCACCTTTAAGTAAAGGTGTGATGACCAACCACCTCTCTGCGGTACCGCTAGCCTGAGCCTTTGCGCT  
TACCTTAGGAAATCTTGCTGTATCTCTCTCGTATGACGAGCAAAACATGCGGTATCACACAGCAGCTGCTTGCTGCC  
CTCGCAGTGCACGAGGGGACGCTCTATGACAAACCCCTCAGAAACGGGGCAGACAAGTTCTATCTCTGTCTGACTCCCT  
CTCCTCTTACTACCAACCCCTTCCACTGCCTAATCTGAGAATTCATTTCTCTCTCATGGTTAGACCTTCAGACTTTAG  
AAGAATCTATCACCAGTCTTTCTAAAATCCAGCCCTTGCTCAAGAAATTTTATCTTAATATCTGTCACTCGGTGCTCT  
CAGTCCAGTGTGCAGATCAAAAGTTACTCTCAGACTCCGTAATGGCTCTAAGCATAGCAGATTAATATGCTCCCACTGC  
CCCCACACCGGGCTCGTCTCCTGTGGGAAACAGCTTTATAGGCACGAGAGTAGTAGGAGCTGGCTTTGAATCTGTGTA  
GAATGATACAACACCCAAGCCGGGAGAAACAGCCTCCAAAAACCTGGATCTCCATTCCCTATCAGATGCTTATAAAGA  
ACCTAGATCATCCCTGATCAAAATTTATATAGTACGAGAAATATTTCTTAATATATCCATTCACAGCCACAGTCAG  
TGAATATTGTGTAAAGAGATTGCCAAAATGGTTTGGCAAGTAGGTTCCGACGTAGGACAGCTGAGGTGGCTGCTGTG  
TTTGACAACAGCCTCTATAAAAGTAGGCTGGGGTGCCTCTGCTCTGTCCTCTCCTCA

182

#### 4.2.4 DISCUSSION

Muscle fibre type transitions towards increasing the fast, glycolytic, type II muscle fibres is a phenomenon well documented to occur in animals exposed to beta-adrenergic stimulation (Baker et al. 2006; Bricout et al. 2004; Depreux et al. 2002; Oishi et al. 2002; Gunawan et al. 2007). This response was confirmed in growing gilts treated with Ractopamine and additionally explored *in vitro* to assess the effect of beta-adrenergic agonist administration directly to muscle cells and to specifically examine effects on MyHC regulation during early myogenic differentiation. Although cultured muscle cells do not form mature muscle fibres, they do express specific patterns of the contractile components that constitute the muscle fibre during myogenesis (Brown et al. 2012; Chapter 3.1). We utilized the C2C12 cell line, which exhibits a late induction of the type II MyHC isoforms, as a model to examine whether direct exposure of muscle cells to the beta-adrenergic agonist, Ractopamine, might accelerate the initial induction of the type II MyHC isoforms *in vitro*.

##### *4.2.4.1 Ractopamine induces differential regulation of MyHC isoforms in vivo compared to in vitro*

Dynamic alterations in transcript abundance of the MyHC isoforms occurred in pig skeletal muscle during 27 days of Ractopamine administration. More specifically, the MyHC IIB isoform mRNA displayed a chronic induction across the full 27-day treatment window, whilst the MyHC IIA isoform mRNA exhibited an initial decline in expression before returning to expression levels comparable to that of the control group. In addition, the type IIX MyHC isoform displayed a modest reduction in expression throughout the 27-day

treatment window. This drive towards increasing MyHC IIB expression, at the expense of the slower IIA and IIX isoforms, is a phenomenon previously documented to occur in response to beta-adrenergic treatment *in vivo*, using rats and pigs (Baker et al. 2006; Bricout et al. 2004; Depreux et al. 2002; Oishi et al. 2002; Gunawan et al. 2007). However, the data presented herein shows dynamic modulation in expression of the type II MyHC isoforms, with individual isoforms clearly being exclusively regulated (displaying differential expression profiles with duration of treatment), suggesting remarkable plasticity of these genes in adult skeletal muscle.

In contrast, 48-hour treatment of cultured C2C12 muscle cells with Ractopamine resulted in an exclusive up-regulation in mRNA expression of MyHC IIB, without altering the expression levels of the other adult type I or type II MyHC isoforms. Although there was a small induction in neonatal MyHC mRNA expression, the relative fold-induction was small compared with the dramatic increase in mRNA expression of the MyHC IIB isoform. The up-regulation of MyHC IIB mRNA in response to beta-adrenergic agonist treatment presented herein is consistent with a previous report *in vitro* (Shi et al. 2007), but this study used a mouse 1kb MyHC IIB promoter reporter construct and did not examine all MyHC isoforms. Importantly, this data indicates that beta-adrenergic signaling is capable of exclusively accelerating the initial induction of the MyHC IIB gene during C2C12 myotube formation. This response was not restricted to murine species as demonstrated by increased porcine 1kb MyHC IIB promoter-reporter activity in C2C12 muscle cells treated with Ractopamine. Furthermore, this suggests that the increased MyHC IIB transcript abundance is likely due to increased MyHC IIB promoter

activity. Although this drive towards increasing MyHC IIB expression is well documented to occur in response to beta-adrenergic receptor stimulation *in vivo* (Depreux et al. 2002; Gunawan et al. 2007), as shown in Chapter 4.1, this response is also normally characterized by an increase in MyHC IIB expression at the expense of the slower, more oxidative type II isoforms (IIA and IIX), albeit generally in response to a more chronic exposure (up to 28 days; Depreux et al. 2002; Baker et al. 2006; Gunawan 2007; Chapter 4.1). This “transition” in MyHC isoform expression did not occur during the 48-hour treatments employed herein using C2C12 muscle cells. Interestingly, Gunawan et al (2007) report that MyHC IIB is the earliest MyHC isoform to change in pigs treated with Ractopamine, increasing mRNA expression in just 12 hours, compared with 96 hours for the IIA and IIX isoforms. In the present *in vitro* experiments, the treatment time of 48 hours may not have been chronic enough to induce a “full transition” (i.e. an increase in IIB at the expense of another isoform). Thus, it seems likely that MyHC IIB may be the most responsive and/ or the earliest MyHC isoform to undergo altered levels of expression in response to beta-adrenergic stimulation.

It is interesting to speculate whether inter- and intra-genic mechanisms regulate the subsequent down-regulation in mRNA expression of the type IIA and IIX MyHC isoforms following an induction of the MyHC IIB mRNA isoform. For instance, after an increase in MyHC IIB gene expression by beta-adrenergic stimulation, it is plausible that miRNA transcripts within the MyHC IIB introns could co-regulate other MyHC isoforms (Van Rooij et al. 2009) or bi-directional promoters within the MyHC gene cluster could co-regulate subsequent MyHC isoform gene expression (Pandorf et al. 2006; Rinaldi et al.

2008). Such genomic mechanisms of gene regulation may also differ between species and developmental status (i.e. during myogenesis versus differentiated muscle). The data presented herein implicates MyHC IIB as the initial isoform targeted for up-regulation by beta-adrenergic signaling. Mechanisms controlling the coordinated regulation of the type IIA, IIX and IIB MyHC isoforms warrant exploration.

#### *4.2.4.2 Ractopamine altered in vivo but not in vitro metabolic gene expression*

Interestingly, chronic exposure (27 days) of pigs to Ractopamine (but not acute (48-hour) exposure in C2C12 muscle cells) altered mRNA expression of metabolic marker genes, Enolase 3 and IDH2. It is well documented that transitions towards increasing MyHC IIB isoform expression in response to beta-adrenergic agonist treatment is coupled with a concomitant shift from an oxidative to a more glycolytic muscle metabolism *in vivo*. This is evidenced by a reduced oxidative and increased glycolytic gene expression and enzyme activity in muscle (Gunawan et al. 2007; Vestergaard et al. 1994) and also a reduced muscle glycogen content (Vestergaard et al. 1994; Baker et al. 2006), all indicating a shift towards a more glycolytic metabolism in beta-agonist treated muscle *in vivo*. The disparity in response of metabolic gene expression presented herein may be due to differences in duration of treatment but also differences in the developmental status of the cells being studied (differentiated muscle versus differentiating cells). It is possible that transcriptional regulation of metabolic enzyme expression may occur secondary to alterations in contractile component gene expression and that a



more chronic treatment is required to see transcriptional alterations in metabolic gene expression in C2C12 muscle cells. Furthermore, as shown in Chapter 3.2, it is evident that C2C12 cells undergo significant metabolic remodeling during differentiation, which may over-ride the subtle Ractopamine induced alterations in metabolic gene expression.

Interestingly, the metabolic gene expression markers employed herein, Enolase 3 and IDH2, displayed remarkable correlation with the type IIB and type I MyHC mRNA isoforms *in vivo*, respectively, suggesting these genes may be excellent candidates for monitoring associated contractile-metabolic changes in skeletal muscle.

#### *4.2.4.3 Ractopamine increased Six1 and Eya1 mRNA expression in fusing muscle cells only*

The SIX and EYA gene family were originally identified as genes essential for eye development but certain family members (SIX 1, 4 and 5; Spitz et al. 1998 and EYA 1, 2 and 4; Grifone et al. 2004) have been shown to accumulate in skeletal muscle and have subsequently been implicated in regulating myogenesis (Heanue et al. 1999; Kawakami et al. 2000). SIX and SYA transcription factors co-operatively bind MEF3 response elements to drive expression of myogenic genes such as MyoD, myogenin and myosin heavy chain (Spitz et al. 1998; Heanue et al. 1999; Kawakami et al. 2000). The SIX1 and EYA1 family members were measured herein as they have previously been implicated to act in synergy to drive a fast, glycolytic muscle phenotype in mice (Grifone et al. 2004), similar to that induced by beta-adrenergic agonist treatment (Baker et al. 2006; Bricout et al. 2004).

For the first time, the data herein shows that 48 hours beta-adrenergic agonist administration can up-regulate mRNA expression of SIX1 and EYA1 in the mouse C2C12 muscle cells. However, induction of SIX1 and EYA1 mRNA expression was dependent on the timing of administration of the agonist. Firstly, Ractopamine administration *in vivo* did not influence SIX1 or EYA1 mRNA expression in fully differentiated adult skeletal muscle within a 27-day treatment window. However, Ractopamine administered for 48 hours *in vitro*, at the initiation of myoblast fusion (i.e. day 0-2 of differentiation), increased SIX1 and EYA1 mRNA expression, but there was no alteration in SIX1 and EYA1 mRNA expression when Ractopamine was administered later in differentiation (day 2-4 of differentiation). This suggests that the induction of SIX1 and EYA1 mRNA expression by beta-adrenergic receptor stimulation may occur in a myogenesis dependent manner, occurring only in the early stages of myoblast fusion. It is therefore interesting to speculate that beta-adrenergic signaling may be developmentally relevant during early myogenic differentiation.

The time dependent effect of Ractopamine administration on SIX1 and EYA1 gene expression and the accelerated induction of MyHC IIB mRNA expression in C2C12 cells suggest that beta-adrenergic signaling may play a role in regulating a fast type IIB muscle fibre phenotype specifically during the early stages of myotube development. The data presented herein also highlights the complexity of beta-adrenergic signaling during myogenesis, with downstream effects on gene expression differing depending on the stage of myogenesis.

*4.2.4.4 Increased MyHC IIB mRNA expression was independent of changes in cellular differentiation, growth and myogenic gene expression*

Ractopamine administration in growing pigs induced dramatic and chronic alterations in MyHC isoform expression, largely independent of changes in carcass and muscle growth characteristics (contradicting the typical porcine growth response to Ractopamine reported by others; Apple et al. 2007). Therefore, alterations in MyHC isoforms in response to Ractopamine treatment *in vivo* can occur independent of enhancements in muscle growth.

*In vitro*, an increased differentiation stimulus is a potential mechanism for inducing expression of the fast MyHC mRNA isoforms in C2C12 cells since this may effectively shift the induction of the type II MyHC isoforms to an earlier stage in differentiation (Brown et al. 2012). Differentiation status of C2C12 cells in the present study, indicated by creatine kinase activity, exhibited no change with Ractopamine treatment. Furthermore, no alterations in the mRNA expression of myogenin, a key regulatory factor known to drive myogenic differentiation (Nabeshima et al. 1993; Hasty et al. 1993), support the finding that differentiation status remained unchanged by Ractopamine treatment. Therefore, cellular differentiation was ruled out as a potential mechanism driving the induction of MyHC IIB mRNA expression in the present *in vitro* study.

Other *in vitro* models exploring the effects of beta-adrenergic agonist administration on muscle cell differentiation have proven inconclusive. Some studies report increased cell fusion in response to beta-adrenergic agonist treatments (Grant et al. 1990; McMillan et al. 1992), whilst others have seen

no effect (McMillan et al. 1992; McFarland et al. 1995). These studies used a variety of myogenic cell types from different species and also administered different classes of beta-adrenergic agonists. Clearly, variability in responsiveness of different cell types to different classes of beta-adrenergic receptor agonists exists and complicates comparisons between studies exploring beta-adrenergic agonists. To strengthen this notion, Wannenes et al (2012) recently reported that of four different beta-adrenergic agonists tested (Clenbuterol, Formoterol, Salbutamol and Salmeterol) on C2C12 cells, Clenbuterol was the only one that elicited a gene expression response. Thus it would appear that beta-adrenergic agonist pharmacology is likely complicating the understanding of beta-adrenergic signaling and its associated effects in muscle cells.

Myogenic regulatory factor MyoD, is a known regulator of myogenesis and an influential regulator of MyHC IIB expression (Allen et al. 2001; Harrison et al. 2011). In the present study, the Ractopamine induced increases in MyHC IIB mRNA in C2C12 cells and pig skeletal muscle occurred independent of changes in MyoD gene expression. This contradicts other *in vivo* studies reporting significant elevation in MyoD transcript abundance and/ or protein expression in response to beta-adrenergic agonist administration (Bricout et al. 2004; Jones et al. 2004; Koopman et al. 2010). However, Brown et al. (2012) have previously shown that mRNA expression of MyoD is similar throughout C2C12 myogenesis, suggesting that this myogenic regulatory factor can remain relatively unchanged at the mRNA level despite dramatic cellular changes. Although alterations in MyoD gene expression did not occur in the present study, it would be interesting to monitor MyoD phosphorylation status

by beta-adrenergic agonist treatment since de-phosphorylation of MyoD has been shown to increase MyHC IIB gene expression in soleus muscles of mice and rats (Ekmark et al. 2007).

#### 4.2.4.5 Conclusion

To summarise, Ractopamine administration to growing pigs caused a chronic induction of MyHC IIB with concomittent alterations in the slower IIA and IIX MyHC isoforms. In contrast, 48-hour Ractopamine treatment during the early stages of C2C12 myogenesis selectively accelerated MyHC IIB mRNA induction independent of alterations in expression of the other adult MyHC mRNA isoforms. Taken together, gene expression of the MyHC IIB isoform is dynamic and responsive, both *in vivo* and *in vitro*. The data presented herein (in Chapter 4) suggests expression of the MyHC IIB isoform mRNA elicits plasticity in developing myotubes and in fully differentiated adult muscle fibres. Despite the impressive and dynamic plasticity in expression of this very fast contracting myosin heavy chain isoform (MyHC IIB), mechanisms regulating its expression remain relatively elusive and will be explored further in Chapter 5.

# 5

## REGULATION OF THE MYOSIN HEAVY CHAIN IIB GENE IN PORCINE SKELETAL MUSCLE

---

*It was hypothesized that sequence variation in the myosin heavy chain IIB gene promoter dictates species differential expression of this gene in pigs and humans. Furthermore, it was hypothesized that the C2C12 skeletal muscle cell line would provide the dynamic myosin heavy chain IIB inducing environment required to examine this hypothesis in a cultured muscle cell model.*

## 5.1 TRANSCRIPTIONAL REGULATION OF THE MYOSIN HEAVY CHAIN IIB GENE IN PORCINE SKELETAL MUSCLE: *A COMPARISON OF PIG AND HUMAN GENE PROMOTER ACTIVITIES*

### 5.1.1 INTRODUCTION

Skeletal muscle is composed of a heterogeneous population of muscle fibres that display a broad spectrum of contractile and metabolic characteristics. The contractile capacity and ATP consumption of a muscle fibre is largely determined by the isotype of the components that constitute the sarcomere (Schiaffino and Reggiani 2011). In particular, maximal shortening velocity of a muscle fibre is dictated by the predominant Myosin Heavy Chain (MyHC) isoform expressed (Pellegrino et al. 2003) and increases in the order of MyHC I<IIA<IIIX<IIB. This crucial role of the MyHC isoform to influence the contractile performance of the muscle fibre has resulted in significant interest in understanding the regulation of different MyHC isoforms (Spangenburg and Booth 2003; Schiaffino 2010). In the previous chapters it was highlighted that the MyHC genes are a highly dynamic set of genes; displaying incredible plasticity in expression levels in response to a variety of stimuli. Although regulation of the slower (type I and IIA) MyHC isoforms is relatively well understood (Lin et al. 2002; Lunde et al. 2007; Narkar et al. 2008; Narkar et al. 2011), knowledge of the mechanisms regulating the gene expression of the faster contracting, type IIB MyHC isoform remains sparse and incomplete (Grifone et al. 2004; Ekmark et al. 2007).

Despite all mammals carrying the gene (MYH4) encoding MyHC IIB, extensive characterization has revealed a striking divide between large and small mammals with regard to MyHC IIB expression. Most small mammals

such as mice (Pellegrino et al. 2003), rats (Pellegrino et al. 2003), rabbits (Wada et al. 1995; Pellegrino et al. 2003), and guinea pigs (Gorza 1990; Tonge et al., 2010) express MyHC IIB but most larger mammals such as cows (Chikuni et al. 2004), sheep (Hemmings et al. 2009) horses (Rivero et al. 1999), goats (Arguello et al. 2001), cats (Talmadge et al. 1996; Lucas et al. 2000), dogs (Toniolo et al. 2007), baboons (Lucas et al. 2000) and humans (Smerdu et al., 1994, Pellegrino et al. 2003) do not express MyHC IIB. Interestingly, domesticated pigs remain an anomaly amongst the large mammals as they express high levels of MyHC IIB (Lefaucheur et al. 1998; Gunawan et al. 2007; Chapter 4.1), a phenotype likely exacerbated by the intensive selection pressure for enhanced muscle growth in these animals (Ruusunen and Puolanne 2004; Lefaucheur et al. 2004). This expression of MyHC IIB in pig skeletal muscle is associated with a dramatically faster and more glycolytic muscle phenotype compared to that of human skeletal muscle. Given the impact of MyHC isoform expression on the contractile and metabolic characteristics of the muscle fibre, it is interesting to explore the mechanisms dictating this unusually high expression of MyHC IIB in porcine skeletal muscle, which currently remains unknown.

Previous studies on the MyHC IIB promoter have elucidated several key regions of regulatory control (mAT 1/2/3, CArG-box and Ebox) but have predominantly been conducted on the mouse promoter sequence (a MyHC IIB expressing species; Takeda et al. 1992, 1995; Lakich et al. 1998; Swoap 1998; Wheeler et al. 1999; Allen et al. 2001, 2005). A recent study Harrison et al. (2011) extended this work to compare the activity of the human and mouse MyHC IIB promoter and revealed that a single base pair mismatch in the



human CArG-box sequence (-74bp relative to the TATA-box) inhibits binding of serum response factor (SRF) and results in reduced MyHC IIB promoter activity, relative to the equivalent mouse promoter.

Differences in the regulation of MyHC IIB expression between rodent species and humans might be expected as their muscle metabolism, and therefore their contractility characteristics, are different, probably reflecting the metabolic constraints caused by body size (Rennie et al. 2010). Pigs, on the other hand, are physiologically similar to humans and are increasingly being considered as a good animal model for studying a range of human diseases (Luo et al. 2012). Therefore it is important to determine what differences exist between these species in order to have confidence in the use of pig as a model. Given that pigs also have high expression of MyHC IIB, unlike humans and most large animals, we wished to determine whether the mechanisms by which this is achieved is also through variations in promoter sequence, as is the case in mice when compared to humans. We hypothesized that genomic differences in the MyHC IIB promoter of pigs and humans dictate the differential expression of MyHC IIB in these large mammals and that these differences may explain the different muscle phenotypes displayed in these otherwise physiologically similar mammals. Using an *in vitro* fluorescence based promoter-reporter system; we utilized approximately 1kb of the MyHC IIB promoter from a domestic pig and a human to elucidate the role of the promoter sequence in regulating the high expression of MyHC IIB in porcine skeletal muscle. Further, we examined stimuli capable of inducing both the pig and human MyHC IIB promoters during myogenesis.

### 5.1.2 MATERIALS AND METHODS

*The materials and methods presented here are a brief description only. For a more detailed explanation of the methods used herein, refer to the “Molecular Biology Methods” in the “Materials and Methods” chapter.*

#### 5.1.2.1 Cloning

Approximately 1kb of the pig and human myosin heavy chain IIB promoters (-961bp to +32bp, relative to the TATA box) was generated by polymerase chain reaction (PCR) and cloned into the pZsGreenI-I fluorescence-reporter plasmid (Clontech) for transfection studies in the C2C12 mouse myoblast cell line. All base pair numbering is relative to the TATA-box, as a discrepancy existed as to the location of the transcription start site between the two promoters. Accession numbers for the pig and human MyHC IIB gene (NM\_001123141.1 and ENSG00000264424.1, respectively) were used to locate the first exon and the 3' oligonucleotide primer was designed to span into the first exon to ensure inclusion of the transcription start site. All oligonucleotide sequences are displayed in the “Materials and Methods Chapter”.

Pig and human MyHC IIB promoters were subjected to 5' deletion analysis creating promoters of varying lengths (-961bp, -466bp, -231bp, -113bp, -67bp; promoter lengths are relative to the TATA-box). Site directed mutagenesis and site-specific deletions within the MyHC IIB promoters were introduced by PCR (specific base pair substitutions are described in the results section).

Chimeric MyHC IIB promoters (containing combinations of both distal and proximal regions of the pig and human MyHC IIB promoters) were produced

according to a design previously demonstrated (Harrison et al. 2011). A HindIII restriction site (2bp mutation; at -218bp and -217bp) was introduced to both the pig and human 1kb promoter allowing the proximal promoter regions to be swapped by restriction digest, generating chimeric promoters. Proximal promoter regions were also swapped with a minimal CMV promoter (84bp) to test for potential regulatory regions in the 5' distal region (~750bp) of each promoter, independent of the proximal promoter.

Full-length open reading frame MyoD cDNA (accession number: ENSMUST00000072514.1) was generated by RT-PCR, cloned into the pDsRed-Express-N1 plasmid (clontech) and over-expressed in C2C12 cells under the control of a CMV promoter. A pDsRed-Express-N1 plasmid lacking the CMV promoter was used as a vehicle transfection control.

#### *5.1.2.2 Electrophoretic mobility shift assay*

Protein-DNA interactions were assessed by incubating C2C12 myotube nuclear extracts with a 5' biotin labeled double-stranded probe for a 62bp region spanning (and inclusive of) the CArG-box and Ebox2 sequence (-93bp to -31bp relative to the TATA-box) from the pig MyHC IIB promoter (probe sequences are in the "Materials and Methods Chapter"). Three shorter unlabeled probes, from the same region (pig sequence), were used to compete for bound proteins and identify the specific regions within the 62bp probe interacting with nuclear protein(s). Three equivalent human unlabeled probes were used to assess whether the species-specific sequence variation in these regions impaired competition for the proteins bound to the pig 62bp labeled probe. Unlabeled competitor probes were designed to the following regions,

CAR<sub>G</sub>-box: -91bp to -60bp, mid-probe: -74bp to -51bp and E-box2 probe: -63bp to -31bp, all relative to the pig TATA-box.

EMSA's were conducted using the LightShift Chemiluminescent EMSA kit (Thermo Scientific). Protein-DNA binding conditions and detection of the biotin-labeled probes using the LightShift Chemiluminescent EMSA detection module (Thermo Scientific) are outlined in the Materials and Methods Chapter.

#### *5.1.2.3 Cell culture and transfections*

C2C12 mouse myoblasts were cultured in proliferation medium (DMEM, 10% FBS, 1% PS) and induced to differentiate at confluence by switching to differentiation medium (DMEM, 2% HS, 1% P/S) for up to 6 days. Medium was refreshed every 48 hours.

Myoblasts (at ~70% confluence) were transfected with the pig or human 1kb MyHC IIB pZsGreenI-I promoter-reporter plasmid using FugeneHD (Promega) transfection reagent at a ratio of 3:1 (FugeneHD:DNA). Each well was co-transfected with pDsRed-Express-N1 as a transfection efficiency control for normalizing ZsGreenI-I promoter-reporter fluorescence. MyHC IIB promoter activities (fluorescence output) were quantified following 5 or 6 days of differentiation using the Typhoon Trio+ (GE healthcare). MyoD over-expression plasmids (or pDsRed-Express-N1 plasmids lacking the CMV promoter) were transfected into myoblasts at the same time as the MyHC IIB promoter-reporter plasmids at a ratio of 1:1.

#### *5.1.2.4 dbcAMP treatments and myotube diameters*

Dibutyryl cyclic-AMP (dbcAMP; Sigma-Aldrich) or a vehicle control (water) was included in the differentiation medium of transfected cells and refreshed every 48 hours for up to 5 days. MyHC IIB promoter activities were quantified following 4 or 5 days of differentiation. Myotube diameters of MyHC IIB positive cells (as indicated by ZsGreen fluorescing myotubes) were measured on day 5 of differentiation. Myotube diameters were measured at 3 points (at 25%, 50% and 75% of the full myotube length to give an average myotube diameter) on 50 myotubes from 5 fields of view per well (n = 4 wells; a total of 200 myotubes per treatment). To remove bias, all images were blinded for analysis.

#### *5.1.2.5 Statistical analysis*

All fluorescence promoter-reporter assays were conducted on single experiments using 4 biological replicates (wells). The same promoter-reporter constructs were used in multiple experiments and confirmed reproducibility of results presented herein. Data is displayed as mean  $\pm$  standard deviation (SD). Statistical analysis was conducted using GenStat (version 15) and significance was accepted at  $p < 0.05$ .

## 5.1.3 RESULTS

### 5.1.3.1 The pig and human MyHC IIB promoter sequence

Alignment of the pig and human MyHC IIB promoter revealed very high similarity (1kb: 80% identical; proximal 200bp: 95% identical; see Figure 5.1).

```

Human -961 -----CTTAGAGTAGGTATATTTCTGCCATATTCAGTAACAGCTGTGTATGTA -913
Pig -961 TAGGTGACACACTTAGCGTGGACAGATTGCTGTACATTGATAGCCCCCTTATGT -902
          *****
Human -912 GCAAAACCATCAAAGCCAATTTATGAGTATTATGGGCATATGTGATGGCCCATCCATCT -853
Pig -901 GCAAAACCAACCAACCAATTTACAAGCATCGTGGGCATATGTGATAGCCCCCTTATGT -842
          *****
Human -852 TTTCAATCCACAGGGAATATCGTGGATACCATGACTTTCCTCCACCTTAAATAAAAA -793
Pig -841 TCTCAACCCACAA--AGAGTCCTGTGGGTATCACATCTCTCCTCCACCTTAAATAAAAA -784
          *
Human -792 TATGTGGTTCCCACTCATTAGAGCTATAGCTAGTCATGAGAGCTGCCCCATGAAGTAGG -733
Pig -783 TACGTATTACCCACCTCATTAGAGCTACTGCTAGTCATGAGGATTGCGCTGTGAAGTAGG -724
          *
Human -732 AATGCATGTTTGTGTCTCTTCCAT--TATGCAGAGGAAACATGCATGGAACATCACAC -676
Pig -723 AATGCATATTGATGCCTCCTTCCATCATTATGCGGTAGAAACACACATAGAACATCACAC -664
          *****
Human -675 AGCATCCTGTTGTTCTTCAGTGAACACATACAAGCTGGAGATATCCATGGAAGTCCTC -616
Pig -663 GGACTCCTGCAGTCCCCCAGTGAACACATGTAGCTCAAGACAGCCACGGCAAGCTCTC -604
          *
Human -615 CAGAAAAAGAACAGAAGTGTATATCTATTCTAAATCCCTTATGCCTCCCCCAGTGGTC -556
Pig -603 CAGAAAAGGAAAAGAAGTGTCTATCTATTCTAAATCCCTTATGGCTCCCCCACTGGTC -544
          *****
Human -555 CATCACCCTGCCTAATCTGAGAATTC-----ACTTTCACCTTCATATTTAGACTTTCA -502
Pig -543 TGTCAACCATGGCTTAGCCCGAGAATCTGCCTAACTTTCTCCTTCATGCTTAGTCTTTTA -484
          *****
Human -501 GACTTTAAAGAATCTATCGCCAGTCTTTCTAAATCCAGACTGTGGCTAGGAATGTTGT -442
Pig -483 GACTTTAAAAAATCTATCATCAGTATTCTAAATCCAGCCAGGCTAGGA--GTTTT -426
          *****
Human -441 CTTAAATCCATCGCTCACTGCTTCCAATCATAGTGTGAGGCTCTAAATTCATCCAGAG -382
Pig -425 CT-----GCTT--TAATACCAATCATGTTGTGAGAGCTAAACTCATCCAG-C -380
          *
Human -381 TCCTTAATGGCTCTAAGAACCAACAAATTAATTAATCCTAAATCCTCACATCAGACTCA -322
Pig -379 TCCTCAATGGCCCTAAGCACTAACAATCAATTAGTTCTCAACTCCTCGTGTCTGGCTCA -320
          *****
Human -321 TTCTGTTGGACCAATTTTATAGGCAGAGAGTAAGTGGGAATCTGGCTTTGAATTTCTGTG -262
Pig -319 TTCTGTGCGGACCAATTTTACAGGCAGGAGAGTAAGTGGGAACCTGGCTTTCAACTCAGTG -260
          *****
Human -261 ATGAATGATGCAACAGCCAACTGGAGAAACAGTGTTAGAAGCCCTGAATCCCCATCCCC -202
Pig -259 ATGAATGATGGAACAGCAAGCTGGAGAAATAGCCTTAGAAGCCCTGAATCTCCATCCC- -201
          *****
Human -201 TATCAAATGCCTATAAAGAACCTAGATCATCCTCTGTAAATTATTTATGGGTGTCAAG -142
Pig -200 TATCAAATGCCTCAAAGAACCCTAGATGATCCTCTGTCAAATTATTTATAGGTGTCAAG -141
          *****
Human -141 AAATATTTCTAATTATATCCATTACAGCCACAGTCAGTGAATATTGTGCAAGAGATTG -82
Pig -140 AAATATTTCTAATTATATCCATTACAGCCACAGTCAGTGAATATTGTGCAAGAGATTG -81
          *****
Human -81 CCAAAAACGGTTTGGCCAAGTAGGTTCCAGCTAGGACAGCTGAGGTGGCTGCTGTGTTT -22
Pig -80 CCAAAAAGGTTT-GCCAAGTAGGTTCCAGCTGGGACAGCTGAGGTGGCTGCTGTGTTT -22
          *****
Human -21 GCAGAATGGTCTCTATAAAGTGGAGCTGAGATGCCTCTTTCCCATCCTTCCT +32
Pig -21 GCAAAATGGTCTCTATAAAGTGGAGCTGAGATGCCTCTGCTCCTTCCTTCCT +32
          *****

```

**Figure 5.1** Alignment of ~1kb of the pig and human MyHC IIB promoters. Base pair numbering is relative to the TATA-box (+1). Regions highlighted in grey represent areas of known regulatory importance. \* Indicates matching bases between the pig and human sequences.

#### *5.1.3.2 Pig and human MyHC IIB promoter activity*

Following transfection into mouse C2C12 muscle cells, activity of the 1kb pig and human MyHC IIB promoters was restricted to differentiated myotubes (indicated by ZsGreen fluorescence), unlike a CMV-driven ZsGreen control, which was expressed in myoblasts and myotubes; see Figure 5.2A). Despite both promoters being active in differentiated C2C12 myotubes, the 1kb pig MyHC IIB promoter had higher activity than the equivalent human promoter, which was only mildly active (Figure 5.2A and 5.2B;  $p = 0.006$ ). Figure 5.2C shows a representative output of the ZsGreen-reporter and DsRed-co-reporter using the Typhoon Trio+ (used to quantify fluorescence output).

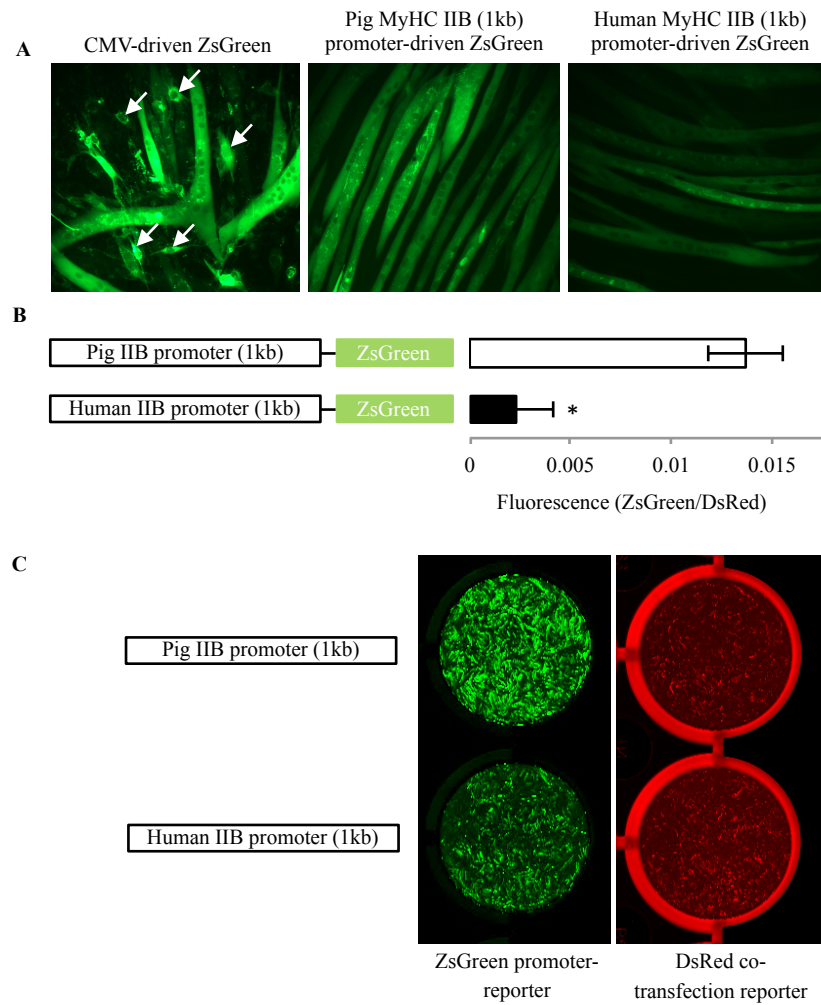


**Figure 5.2** (A) Representative fluorescence images show 1kb MYHC IIB promoter-reporter constructs are differentiation specific. (B) 1kb pig and human MyHC IIB promoter activity in day 6 differentiated C2C12 myotubes (mean  $\pm$  SD). \* Indicates 1kb human MyHC IIB promoter activity was significantly different to the 1kb pig MyHC IIB promoter activity ( $p < 0.05$ ). Open bar = pig promoter; closed black bar = human promoter. (C) Representative fluorescence output of transfected myotubes using the Typhoon Trio+.



#### *5.1.3.3 MyoD activates the pig and human MyHC IIB promoter*

Due to the disparity in MyHC IIB promoter induction during myogenesis, we asked whether MyoD, a myogenic regulatory factor known to induce MyHC IIB expression (Wheeler et al. 1999; Allen et al. 2001; Ekmark et al. 2007; Harrison et al. 2011), was activating the pig, but not human MyHC IIB promoter during C2C12 myogenesis. Over-expression of mouse MyoD during C2C12 differentiation was capable of inducing both the pig and human MyHC IIB promoters by ~3 and ~4-fold respectively (Figure 5.3A;  $p < 0.01$ ). Fluorescence microscopy revealed that MyHC IIB promoter activity was still restricted to differentiated myotubes in the presence of MyoD over-expression (Figure 5.3B). Although both the pig and human MyHC IIB promoters were induced by a myogenic signal (MyoD), the absolute capacity for induction of the human MyHC IIB promoter was restricted in comparison to the pig MyHC IIB promoter activity. It was therefore postulated that response elements within the human MyHC IIB promoter were limiting the capacity to fully activate the promoter and that the pig MyHC IIB promoter contained response elements that permitted a much greater potential for activation during myogenic differentiation.

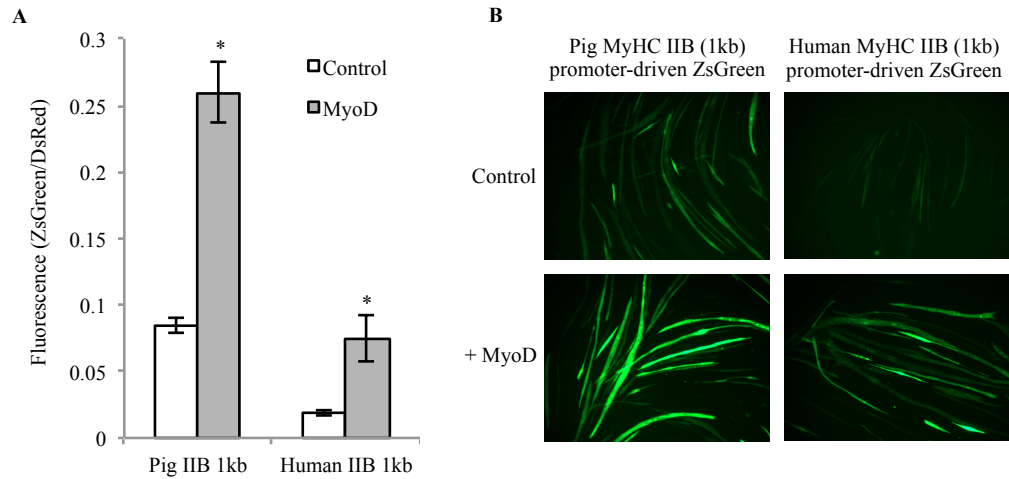


**Figure 5.3** (A) 1kb pig and human MyHC IIB promoter activity in response to (mouse) MyoD over expression in day 5 differentiated C2C12 myotubes (mean  $\pm$  SD). \* Indicates MyHC IIB promoter activity was significantly different to the control transfection ( $p < 0.05$ ). (B) Representative fluorescence-reporter images showing MyHC IIB promoter induction by MyoD over-expression in day 6 differentiated C2C12 myotubes.

#### 5.1.3.4 Five prime deletion of the pig and human MyHC IIB promoter

In order to locate regulatory regions controlling the differential activity of the pig and human 1kb MyHC IIB promoters, we conducted equivalent 5' deletion analysis of both promoters. Disparity in pig and human MyHC IIB promoter activity persisted with decreasing promoter length (from -961bp to -113bp) and declined similarly for promoters from both species (Figure 5.4). Removal (by 5' deletion) of ~120bp, between -231bp to -113bp, essentially removing the AT-rich regions (AT 1, 2 and 3), caused the largest reduction in promoter activity for both the pig and human MyHC IIB promoters (84% and 82% respectively). Deletions at the 5' end of the pig and human MyHC IIB promoters from -961bp to -466bp caused a 26% and 37% reduction, respectively, and deletion from -466bp to -231bp caused a 50% and 58% reduction, respectively. The largest disparity in promoter activity between the

pig and human MyHC IIB promoters existed in the -231bp promoters (~5-fold difference;  $p < 0.001$ ), indicating that response elements controlling high and low MyHC IIB promoter activity likely resided downstream of -231bp.

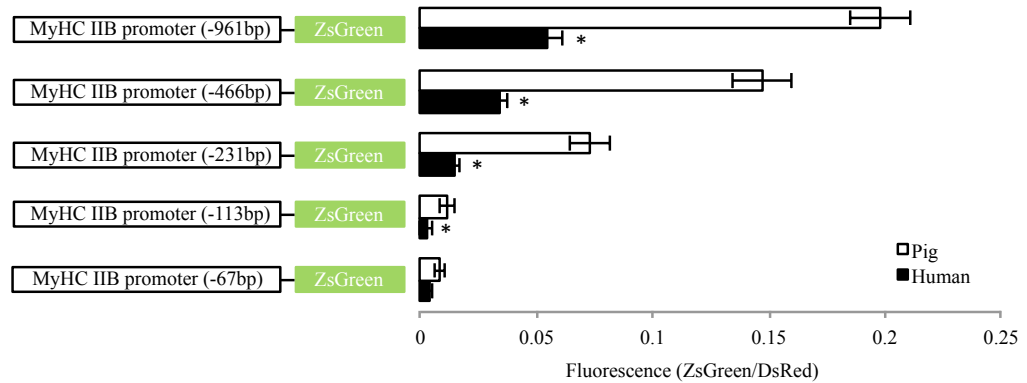


**Figure 5.4** Equivalent 5' deletion analysis of the pig and human MyHC IIB promoters. Promoter activities in Day 6 differentiated C2C12 myotubes (mean  $\pm$  SD). \* Indicates Human MyHC IIB promoter activity was significantly different to the equivalent length pig promoter ( $p < 0.05$ ).

#### 5.1.3.5 Chimeric MyHC IIB promoters

To confirm the role of the proximal promoter sequence in dictating high and low MyHC IIB promoter activity, we produced chimeric MyHC IIB promoters (generated by swapping the proximal region (-218bp to +32bp) of the pig and human promoters). When the proximal region of the pig 1kb MyHC IIB promoter was replaced with the equivalent human proximal promoter, activity was reduced ( $p < 0.001$ ) to the same level as the human 1kb MyHC IIB promoter (Figure 5.5A;  $p = 0.627$ ). When the proximal region of the human 1kb MyHC IIB promoter was replaced by the equivalent pig proximal promoter, activity was increased ( $p < 0.001$ ) and interestingly exhibited an almost 2-fold greater activity than the 1kb pig MyHC IIB promoter ( $p =$

0.005). The chimeric promoters confirmed that sequence differences in the proximal promoter regions (totaling 14bp differences) dictate the high and low MyHC IIB promoter activities. For completeness, the pig and human proximal MyHC IIB promoters (-218bp to +32bp) were replaced by an 84bp minimal CMV promoter which revealed that the 5' distal human ( $p < 0.001$ ), but not pig ( $p = 0.135$ ), MyHC IIB promoter region was capable of increasing the basal promoter activity of the minimal CMV promoter (Figure 5.5B). This highlighted that the proximal MyHC IIB promoter region contains the key response elements required to elicit differential promoter activity between pigs and humans.

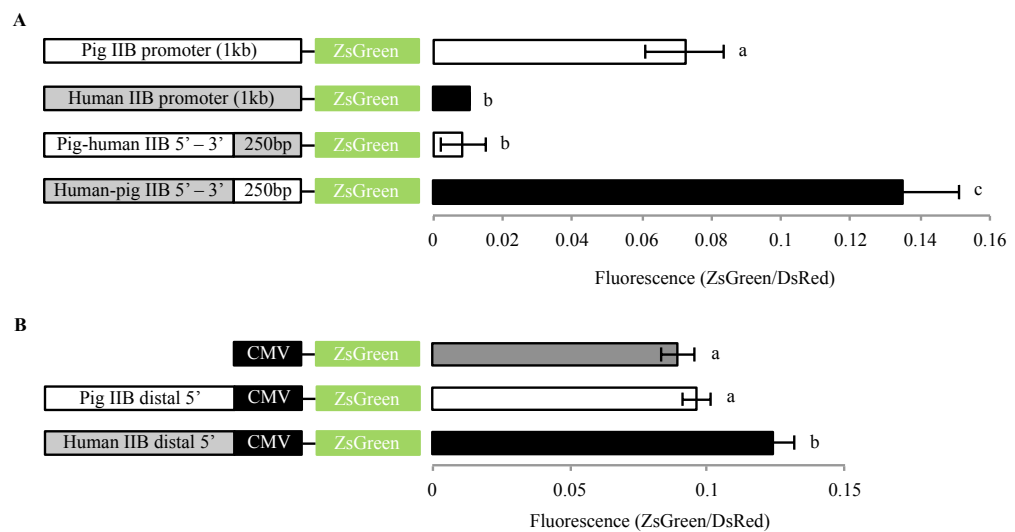


**Figure 5.5** (A) Pig-human and human-pig (5' to 3') chimeric MyHC IIB promoters were constructed to assess the role of the proximal 250bp of each promoter within the context of a 1kb promoter. (B) The distal (~750bp) of the pig and human MyHC IIB promoters were cloned upstream of a minimal CMV promoter (84bp) to assess whether this region elicits enhancer activity independent of the proximal (~250bp) MyHC IIB promoter (mean  $\pm$  SD). Differing letters (a,b,c) constitute a significant difference between promoter activities ( $p < 0.05$ ).

#### *5.1.3.6 Site directed mutagenesis of the human MyHC IIB promoter*

To identify the specific sequence differences responsible for the differential pig and human MyHC IIB promoter activities, we analyzed the effects of site directed mutagenesis on promoter activities in C2C12 myotubes. Site directed mutagenesis within the AT rich regions (mAT2 and mAT3) of the human 1kb MyHC IIB promoter (making base pair alterations to match the equivalent pig promoter), had no impact on MyHC IIB promoter activity (Figure 5.6). However, a single base pair alteration within the human CArG-box (at -74bp), was sufficient to increase promoter activity by ~2.5-fold ( $p = 0.001$ ), but promoter activity remained lower than the 1kb pig MyHC IIB promoter ( $p = 0.007$ ; Figure 5.6).



#### *5.1.3.7 Site directed mutagenesis (round 2) of the human MyHC IIB promoter*

Further site directed mutagenesis downstream of the CArG-box in the human MyHC IIB promoter highlighted a group of 3bp mutations required to increase promoter activity to the same level as the pig MyHC IIB promoter (Figure 5.7). A single base pair mutation within the human CArG-box sequence (at -74bp) increased promoter activity ( $p < 0.001$ ) but remained lower than the activity of the 1kb pig MyHC IIB promoter ( $p < 0.001$ ). Removal of a single nucleotide (at -68bp) from the human MyHC IIB CArG-box mutant promoter resulted in a further increase in promoter activity, compared to the CArG-box mutant promoter ( $p < 0.001$ ), but this level of activity still remained lower than the 1kb pig MyHC IIB promoter ( $p = 0.023$ ). Finally, a combination of the CArG-box mutation (at -74bp), with the removal of a single nucleotide (at -68bp), and a single base pair change in the E-box2 (at -48bp) caused an increase in human MyHC IIB promoter activity ( $p < 0.001$ ) to a level equal to the 1kb pig MyHC IIB promoter ( $p = 0.895$ ).

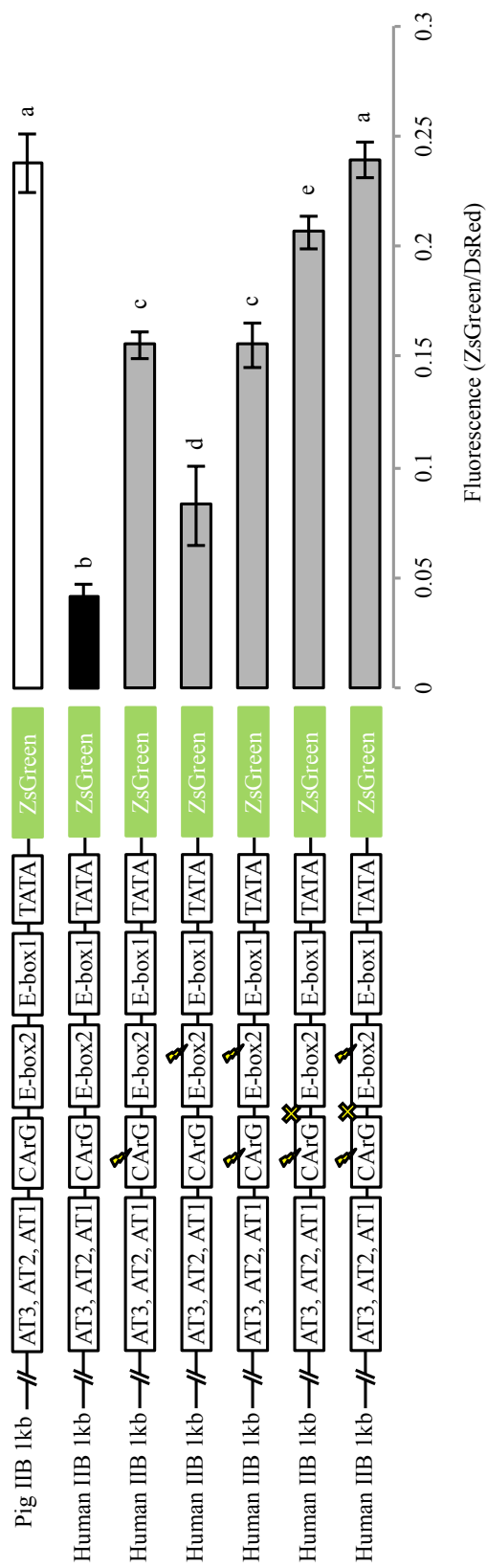


**Figure 5.7** Site directed mutagenesis within the CArG-box and E-box of the 1kb human MyHC IIB promoter. A “bolt” indicates a single base pair mutation and a “cross” indicates a single base pair removal. Promoter activities were measured in day 6 differentiated C2C12 myotubes (mean  $\pm$  SD). abcde = differing letters constitute a significant difference between promoter activities ( $p < 0.05$ ). Open bar = pig promoter; black bar = human promoter; grey = mutant human promoter.



#### *5.1.3.8 Electrophoretic mobility shift assay of the CArG/Ebox region*

Electrophoretic mobility shift assays were conducted to determine whether the 3bp mismatch, responsible for the disparity in promoter activity between the pig and human MyHC IIB promoters, caused differential nuclear protein binding to this region (Figure 5.8). Two protein-DNA complexes (labeled A and B) formed with the pig 62bp probe (spanning and inclusive of the CArG-box and Ebox2 (-93bp to -31bp)). To identify specific regions of the 62bp probe bound by protein(s), 200-fold molar excess of shorter, un-labeled competitor probes were included in the binding reactions. The un-labeled pig CArG-box probe (29bp in length) bound the proteins forming both complexes A and B with the 62bp pig probe, as both bands were lost/reduced (Figure 5.8). The un-labeled pig mid-probe and Ebox2 probes, however, were unable to compete for proteins bound to the 62bp probe, as there were no effects on either band. Interestingly, proteins bound to the pig CArG-box sequence were sensitive to the species-specific differences in the pig and human CArG-box sequences (2bp mismatch). The un-labeled human CArG-box competitor probe was capable of competing with the pig 62bp probe for proteins forming complex A, but not B. Like the equivalent pig competitor probes, the human mid-probe and Ebox2 probes were also unable to compete for proteins bound to the 62bp pig probe. Therefore, the 2bp mismatch in the pig and human CArG-box probes resulted in differential protein-DNA interactions.

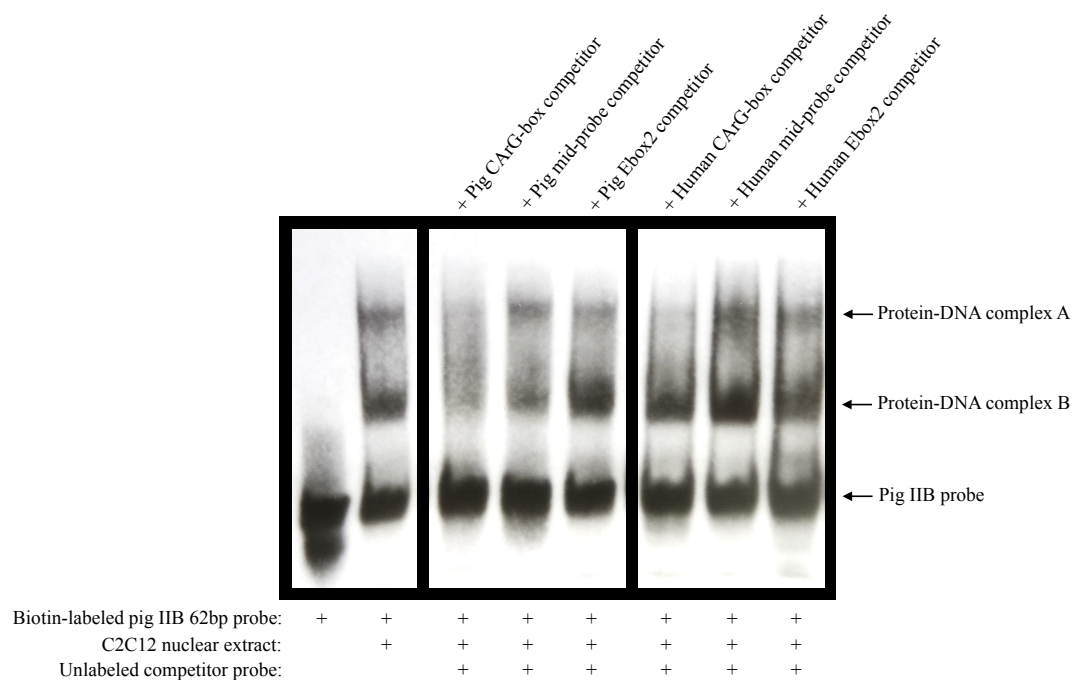


**Figure 5.8** Electrophoretic mobility shift assay using a 62bp biotin labeled probe (spanning the pig CArG and Ebox2 region; -91bp to -31bp relative to the TATA-box). Probes were incubated with C2C12 myotube nuclear extracts. Cross-species competition for bound proteins was conducted using shorter un-labeled pig and human probes. The human CArG-box is unable to bind proteins forming complex B with the pig CArG-box. EMSA assays were repeated 3 times to confirm the result.

#### 5.1.3.9 Deletion of the CArG-box promoter response element

Finally, to confirm that sequence variation in the CArG-box region did not convert this region from an activating to a repressive response element in the human compared to pig 1kb MyHC IIB promoter, the CArG-box region (-63bp to -84bp; inclusive of the two mismatches at -74bp and -68bp) was deleted from both promoters. Deletion of the pig CArG-box region reduced MyHC IIB promoter activity ( $p < 0.001$ ; Figure 5.9) to the same level as the 1kb human MyHC IIB promoter ( $p = 0.134$ ). Despite sequence differences in this region, removal of the CArG-box from the 1kb human MyHC IIB promoter also moderately reduced promoter activity ( $p < 0.001$ ; Figure 5.9). These data confirm that the CArG-box region presents an activating, not repressive, response element in the both MyHC promoters.

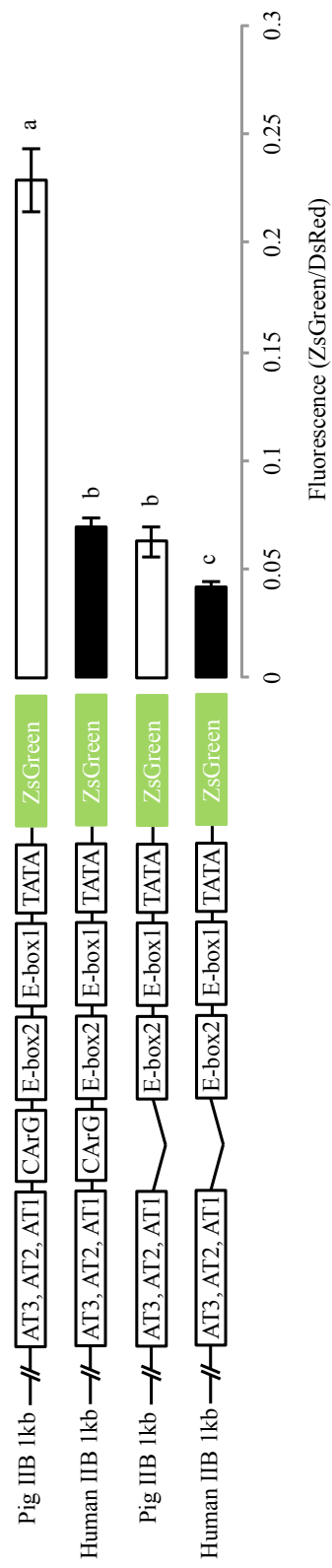
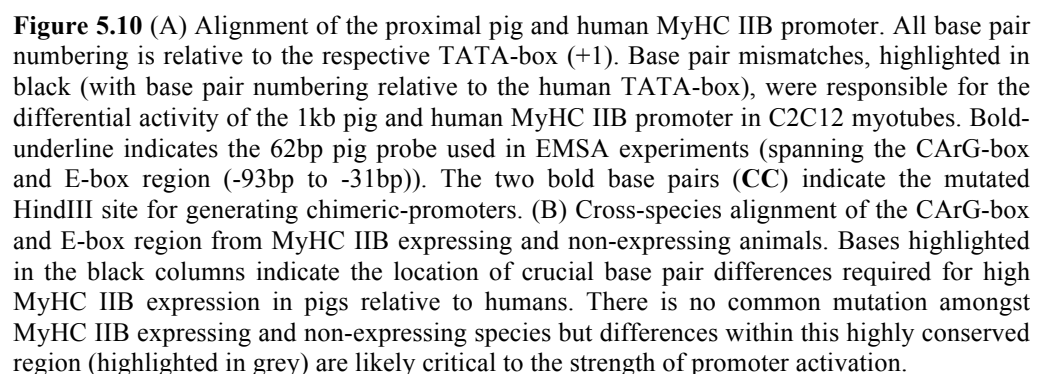


**Figure 8** Removal of the CArG-box (total of 22bp removed) from the 1kb pig and human MyHC IIB promoters. Promoter activities were measured in Day 6 differentiated C2C12 myotubes (mean  $\pm$  SD). abc = differing letters constitute a significant difference between promoter activities ( $p < 0.05$ ).

An alignment of the proximal pig and human MyHC IIB promoter (Figure 5.10A) highlighted the close proximity of the 3bp mismatches in the CArG-box region that are responsible for the high level activity of the porcine MyHC IIB promoter. An additional alignment of this CArG-box region from multiple MyHC IIB expressing and non-expressing species (Figure 5.10B) identified that there is no common variation in sequence that is responsible for the differential expression of MyHC IIB, but sequence variation within this region does exist between species.



#### 5.1.3.11 Induction of MyHC IIB promoter-reporters with cAMP

We next treated C2C12 cells with an analog of cAMP (dbcAMP) as a downstream mediator of a beta-adrenergic response (a stimulus known to drive a fast muscle phenotype in MyHC IIB expressing species *in vivo*; Baker et al. 2006; Bricout et al. 2004; Depreux et al. 2002; Oishi et al. 2002; Gunawan et al. 2007). dbcAMP treatment during the first 5 days of C2C12 differentiation induced a modest increase ( $p < 0.05$ ) in 1kb pig and human MyHC IIB promoter activities (Figure 5.11A, 5.11D), whilst also inducing an ~2-fold increase in myotube diameters ( $p < 0.001$ ; Figure 5.11B, 5.11C, 5.11E, 5.11F). We were concerned that the ZsGreen protein was being diluted as myotubes grew larger with dbcAMP treatments, thus masking or reducing the magnitude of change in fluorescence-reporter intensity in response to dbcAMP treatments. Using a CMV-driven ZsGreen plasmid (pZsGreenI-NI), which would not be expected to respond to dbcAMP treatment, we observed a decline in fluorescence output ( $p = 0.001$ ; Figure 5.11G) when myotube diameters were increased ( $p < 0.001$ ; Figure 5.11I) in response to dbcAMP, confirming that increased myotube diameters can reduce ZsGreen fluorescence intensity of transfected myotubes. This shows that the human MyHC IIB promoter can be induced by dbcAMP treatment but the absolute capacity for promoter induction remained blunted in comparison to the equivalent pig promoter. This also highlights a limitation of the use of fluorescence promoter-reporters when cell size/volume is likely to change with the intervention of interest.

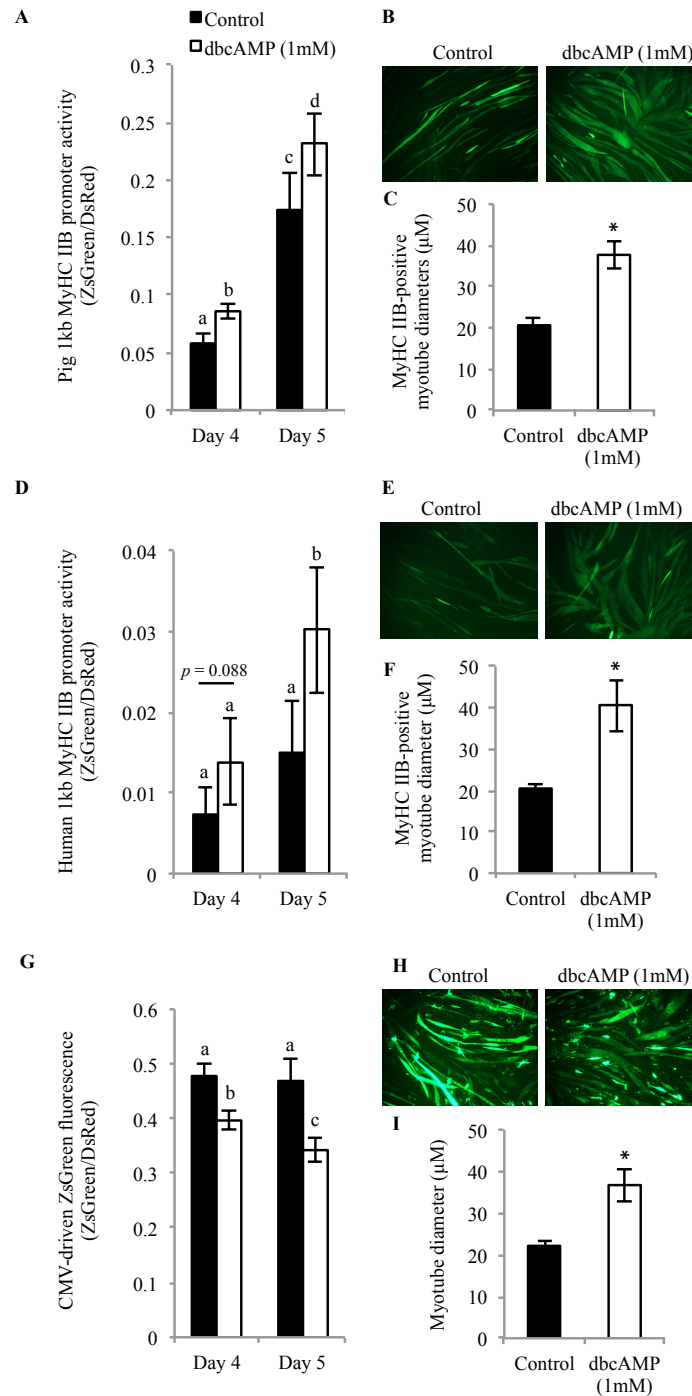


**Figure 5.11** (A) Pig and (D) human MyHC IIB promoter activity and (G) CMV-driven ZsGreen fluorescence output in C2C12 myotubes in response to 4 and 5 days exposure to 1mM dbcAMP treatment (mean  $\pm$  SD). Average day 5 myotube diameters of myotubes with (C) pig or (F) human MyHC IIB or (I) CMV promoter activity (ZsGreen fluorescent). Representative images of day 5 differentiated C2C12 myotubes treated with dbcAMP (or vehicle control) expressing ZsGreen controlled by the 1kb (B) pig or (E) human MyHC IIB promoter or (H) CMV promoter. \* or differing letters (a,b,c,d) indicate a significant difference between promoter activities, myotube diameters or mRNA expression ( $p < 0.05$ ).

#### 5.1.4 DISCUSSION

Myosin heavy chain (MyHC) isoform expression is a key determinant of the contractile performance of the muscle fibre, with maximal shortening velocity increasing in the order of MyHC I<IIA<IIX<IIB (Pellegrino et al. 2003). Mechanisms regulating the expression of the different MyHC isoforms in skeletal muscle have therefore been of significant interest within the scientific community (Spangenburg and Booth 2003; Schiaffino 2010). Interestingly, extensive characterization has revealed species-specific expression of the fastest contracting isoform, MyHC IIB, lending to vastly different muscle phenotypes between species. Of particular interest, domestic pigs express very high levels of MyHC IIB (Ruusunen and Puolanne 2004; Lefaucheur et al. 1998; 2004), unlike most large mammals (which do not normally express MyHC IIB), and exhibit a faster and more glycolytic muscle phenotype in comparison. We examined the role of the MyHC IIB promoter sequence in dictating the expression of MyHC IIB in pigs, compared to humans, which do not express MyHC IIB (Smerdu et al., 1994, Pellegrino et al. 2003). Due to its similarity to humans, the pig is increasingly being considered as an animal model for a range of human diseases (Luo et al. 2012) and it is therefore useful to understand the mechanisms responsible for the physiological differences between these species. We identify the genomic differences within the MyHC IIB promoter of pigs and humans that dictate differential promoter activity during myogenesis and postulate that these genomic differences partly explain the vastly different muscle phenotypes displayed in these otherwise physiologically similar mammals.

We previously reported that the C2C12 cell line is a dynamic MyHC IIB expressing environment, with mRNA expression increasing throughout the later stages of myogenic differentiation (Brown et al. 2012; Chapter 3.1). This cell line was selected for transfection studies of the pig and human MyHC IIB promoter-reporter constructs, providing a common and non-biased MyHC IIB inducing environment for testing both promoters. In this environment, 1kb of the pig MyHC IIB promoter elicited very strong activity that is consistent with the very high level of endogenous MyHC IIB expression observed in pigs (Lefaucheur et al. 1998; Gunawan et al. 2007). In contrast, the human 1kb MyHC IIB promoter was only mildly active during C2C12 myogenic differentiation. We were slightly surprised by the extent of the human MyHC IIB promoter activity in C2C12 cells given that humans do not normally express MyHC IIB transcripts *in vivo* (Smerdu et al. 1994; Pellegrino et al. 2003), suggesting that this promoter can display mild activity given the appropriate environment. In support of this, Harrison et al. (2011) previously reported expression of the MyHC IIB transcript in cultured human fetal primary myotubes, but not in adult human muscle biopsy samples, suggesting that the human MyHC IIB promoter may only be active during myogenesis. Despite being active during C2C12 myogenesis, the human MyHC IIB promoter activity remains blunted in comparison to equivalent promoters from MyHC IIB expressing species, such as pigs (data presented herein) or mice (Harrison et al. 2011). Taken together, this suggests that the MyHC IIB promoter sequence plays a critical role in dictating the strength of MyHC IIB promoter induction during myogenesis and that this disparity in promoter activity can occur independent of nerve innervation in muscle cells.



Furthermore, we also show that although both the pig and human MyHC IIB promoters are responsive to known MyHC IIB inducing stimuli, such as MyoD over-expression (Ekmark et al. 2007; Allen et al. 2001; Harrison et al. 2011) and beta-adrenergic signaling (Baker et al. 2006; Bricout et al. 2004; Depreux et al. 2002; Oishi et al. 2002; Gunawan et al. 2007), the absolute capacity to activate the human MyHC IIB promoter was limited in comparison to the equivalent pig promoter, suggesting that sequence differences between the two promoters dictate the capacity for induction during myogenesis.

We proceeded to elucidate the specific genomic sequence variation responsible for the differential MyHC IIB promoter activities during myogenesis. Surprisingly, a cluster of just 3bp mismatches in the proximal CArG and Ebox region (at -74bp, -68bp and -48bp) was responsible for the disparity in pig and human MyHC IIB promoter activities during myogenesis. The nucleotide mismatch at -74bp was located in the AT-rich region of a proximal CArG-box (consensus sequence: CC(A/T)<sub>6</sub>GG), resulting in the human CArG-box being a non-consensus CArG-box (CCAAAAAcGG), unlike the equivalent consensus CArG-box in the pig MyHC IIB promoter (CCAAAAAaGG). This single bp difference was partly responsible for the differential pig and human MyHC IIB promoter activities during myogenesis. The CArG-box is a response element that is typically (but probably not exclusively) bound by serum response factor (SRF) and is instrumental for activating many muscle specific genes, particularly genes encoding contractile and structural components of muscle (Groisman et al. 1996; Miano 2003). By deleting the CArG-box region (inclusive of mismatch sites -74bp and -68bp) from the MyHC IIB promoters, we report a critical role of the CArG-box in regulating transcriptional

activation of MyHC IIB during myogenesis. Furthermore, by mutating the species-specific mismatches (-74bp and -68bp) in the CArG-box region, we confirm that these subtle sequence variations within the CArG-box region are crucial to the species-specific strength of MyHC IIB promoter induction during myogenesis. This is in agreement with the findings of Harrison et al. (2011) who also report that a single bp mutation in the same location (-74bp) of the AT rich region of the proximal CArG-box is instrumental in dictating the strong induction of the mouse MyHC IIB promoter. Interestingly, we show that the human non-consensus CArG-box was still partially functional, as removal of this element was sufficient to moderately reduce promoter activity. Therefore, we speculated that binding of nuclear protein(s) to the human CArG-box is likely impaired but perhaps not completely eliminated. Alternatively, as shown by Catala et al. (1995), an intact CArG-box may have been required for the binding of nearby myogenic regulatory factors, thus impairing promoter activation in the absence of the CArG-box. We report differential protein-DNA interactions at the pig and human CArG-box site (with a 2bp difference) and show that only 1 of the 2 complexes that form with the pig CArG-box are capable of forming with the human CArG-box. We therefore suggest that the genomic sequence variation between pigs and humans at this location (-74bp and -68bp) improves the stability of factors binding the CArG-box region of the porcine MyHC IIB promoter and that this causes stronger induction of the porcine MyHC IIB promoter during myogenesis.

It is also interesting to speculate whether the close proximity of the 3bp mismatches identified herein may permit, or restrict, co-operative interactions

between factors binding CArG-boxes and E-boxes, since such factors have been shown to physically interact and form trimeric heterodimers (Groisman et al. 1996). Furthermore, sequence variation within CArG-boxes has been reported to influence promoter trans-activation by myogenic regulatory factors that bind nearby E-boxes (Catala et al. 1995), suggesting co-operation between SRF and the myogenic regulatory factors is likely. We show that the removal of a single nucleotide at -68bp (from the human CArG-mutant MyHC IIB promoter), which effectively reduces the gap between the CArG-box and the E-box2, resulted in an increase in promoter activity that, although speculative, may be facilitated by co-operative binding at these two response elements. Indeed, others have shown that spacing between E-boxes can be critical to the transcriptional regulation of the Myosin Light Chain 1A gene (Catala et al. 1995) and made similar speculations of interactions between CArG and E-boxes. Therefore, we speculate that species-specific differences in the CArG/E-box2 region, rather than within a specific response element, likely influence co-operative protein-DNA interactions to facilitate a strong induction of the MyHC IIB promoter. It is important to note that the specific promoter sequence mismatches identified herein between pigs and human are unlikely to account for the lack of MyHC IIB expression in other non-expressing species (see Figure 8B). For example, the MyHC IIB promoters of cows and sheep contain a consensus CArG-box sequence (in the equivalent location) yet still display a lack of MyHC IIB expression. These species do however show mismatches (relative to MyHC IIB expressing species) within the highly conserved CArG/E-box2 region, supporting our speculation that sequence variation within this region is likely a critical mechanism underlying

differential MyHC IIB promoter activation. Further work investigating the complexities of protein-DNA interactions occurring in the CArG/E-box region, between MyHC IIB-expressing and non-expressing species, would be informative for muscle biology research.

In summary, for the first time, we identify a genomic mechanism responsible for the very high expression of MyHC IIB in domesticated pigs, explaining the vastly different muscle phenotypes between pigs and humans. We therefore extend the work of Harrison et al. (2011) and conclude that the sequence of the CArG-box and its immediate flanking regions, are not only critical for MyHC IIB expression in small mammals, but is also a region whereby critical sequence variation can permit or restrict MyHC IIB expression in large mammals as well. We also demonstrate that the human MyHC IIB promoter is responsive to stimuli (i.e. MyoD and cAMP) known to increase MyHC IIB expression, but the capacity for induction is severely limited by the 3bp genomic mutation identified herein. This work furthers our understanding of genomic mechanisms dictating expression of the fast contracting MyHC IIB isoform in mammalian skeletal muscle cells. Further work should be conducted to investigate the complexities of protein-DNA interactions between the CArG- and E-box response elements to investigate their role in controlling muscle specific gene expression.

# 6

## CONCLUSIONS AND FUTURE WORK

---

## **6.1 FINAL CONCLUSIONS AND DIRECTIONS FOR FUTURE WORK**

Traditionally, research investigating muscle fibre type regulation has been conducted *in vivo*, analyzing global changes at a whole muscle level. The body of work presented herein aimed to utilize molecular and cell biology-based approaches to improve our understanding of the regulation of myosin heavy chain (MyHC) isoform expression, as an indicator of muscle fibre composition. Firstly, the C2C12 cell line was fully characterized to establish its suitability for conducting *in vitro* examination of MyHC regulation. Specifically, the dynamics of endogenous and induced MyHC isoform expression were explored and compared to *in vivo* situations. Secondly, the C2C12 cell line was utilized as a host environment for the molecular analysis of the mechanisms regulating the very high level expression of the MyHC IIB isoform in porcine skeletal muscle. Particular emphasis was placed on investigating the regulation of the type IIB MyHC isoform since the regulatory mechanisms dictating expression of this isoform remain poorly understood. Improving our understanding of the fundamental biology controlling MyHC isoform expression is important since these proteins are key determinants of the contractile and metabolic characteristics of the muscle fibre; influencing locomotion, metabolism and age related musculoskeletal diseases (Schiaffino and Reggiani 2011). Furthermore, establishing whether muscle fibre type research can be conducted using molecular and cell biology-based approaches, as explored herein, may encourage more extensive work to be conducted by such methods and advance our molecular understanding of muscle fibre type regulation.

### *6.1.1 Characterization and exploration of MyHC isoform gene expression*

Despite the common use of the C2C12 mouse muscle cell line in muscle biology laboratories across the world, when this work was conducted very little information was available regarding the induction of the MyHC isoforms during myogenesis. Therefore, a comprehensive characterization of gene expression during C2C12 myogenesis was conducted, describing the mRNA profiles of MyHC isoforms, myogenic regulatory factors and metabolic enzymes throughout myogenesis. An objective of this characterization was to establish whether muscle fibre “type” research could be conducted *in vitro* using the C2C12 cell and to establish a series of biomarkers to reflect the differentiation status of the C2C12 cells, providing useful information for future experiments conducted using this commonly used cell line.

It is well documented that during muscle cell differentiation, genes encoding contractile proteins, such as the MyHC's, are activated and expressed (Silberstein et al. 1986; Weydert et al. 1987; Miller 1990). Data presented in this thesis advanced the understanding of MyHC isoform gene expression and showed, for the first time, that the activation of MyHC genes during C2C12 myogenesis are not all activated at the same time, nor in the same pattern. Specifically, MyHC mRNA isoforms are expressed in two distinct cohorts, denoted as “early” and “late” expressed isoforms, transitioning from the embryonic, neonatal and type I to the fast, type II MyHC isoforms. This detailed analysis provides important information regarding the expression profiles of MyHC isoform genes in what is likely the most commonly used muscle cell line for muscle biology research. In particular, this thesis reports

that the C2C12 cell line mimics developing fast-twitch muscle fibres, information that should be taken into consideration by scientists utilizing this cell line. Furthermore, the detection of MyHC expression is often used as a biomarker of differentiation status of cultured muscle cells. Thus, the identification herein of two distinct cohorts of “early” and “late” expressed MyHC isoforms, provides a comprehensive set of MyHC biomarkers for a more precise indication of differentiation status of C2C12 muscle cells using MyHC mRNA expression. This characterization of muscle specific gene expression during C2C12 myogenesis therefore provides useful information for scientists utilizing the C2C12 cell line, as evidenced by a number of authors having already cited this research for its intended purpose (An et al. 2013; Elkalaf et al. 2013; Yang et al. 2013; Ryan et al. 2014; Wright et al. 2014).

In addition to identifying the endogenous transitions in mRNA expression of the MyHC isoforms during C2C12 myogenesis, the research presented in this thesis demonstrates the dynamic plasticity of these genes. In particular, beta-adrenergic agonist administration, both in fully differentiated adult pig muscle and during C2C12 myogenesis *in vitro*, induced alterations in MyHC isoform gene expression. Specifically however, MyHC IIB was the only isoform to elicit a similar response to treatment in the two developmentally distinct muscle cell types (i.e. adult muscle and differentiating muscle cells). Due to the consistency in responsiveness of MyHC IIB gene expression to beta-adrenergic receptor stimulation, both *in vivo* and *in vitro*, expression of the MyHC IIB gene may be a useful end-point biomarker to screen for novel beta-adrenergic agonists using cultured muscle cells (as demonstrated herein using a



1kb MyHC IIB promoter-reporter plasmid in C2C12 cells). Furthermore, the plasticity of the MyHC IIB gene, as demonstrated by the endogenous induction during late myogenesis and by beta-adrenergic receptor stimulation *in vitro*, demonstrate that expression of the MyHC IIB gene is highly responsive to factors not regulated by neural innervation.

Future work should focus on investigating the proteins interacting with the MyHC IIB promoter in response to beta-adrenergic receptor stimulation. Investigating protein-DNA interactions on the MyHC IIB promoter in response to beta-adrenergic receptor stimulation, perhaps utilizing ChIP-seq and EMSA approaches, could elucidate the specific transcriptional regulators involved in this now well-characterized response to beta-adrenergic signaling. Furthermore, it should be determined whether beta-adrenergic signaling influences DNA methylation within the type II MyHC gene cluster to subsequently influence transitions in the expression of the type II MyHC genes. Similar experiments could be conducted on the MyHC IIB promoter during the early and late phases of myogenic differentiation to elucidate the transcriptional regulators inducing this gene during myogenesis.

#### *6.1.2 Metabolic gene expression of proliferating and differentiated C2C12 cells*

Following the identification of a dramatic transition in MyHC isoform mRNA expression during C2C12 myogenesis, to a predominantly type II MyHC expressing profile, it was speculated that cellular metabolism would likely be very glycolytic to support the contractile machinery being expressed. By

comparing the metabolic gene expression profile of fully differentiated C2C12 myotubes, expressing type II MyHC mRNA isoforms, against proliferating myoblasts, an interesting and novel observation was made. It was shown, for the first time, that a dramatic restructuring of metabolic gene expression occurred during the switch from proliferating to differentiated C2C12 muscle cells. Specifically, the changes in metabolic gene expression suggest that post-mitotic muscle cells might redirect glucose carbons into ATP generating pathways and away from macromolecule biosynthesis. The work generated in this thesis highlights that continued research is needed to elucidate whether myogenic differentiation can be regulated by specific metabolic profiles, an idea recently reviewed by Ryall (2013). Indeed, it has been shown that proliferating cancer cells display a dramatic metabolic remodeling to support mitotic cell growth (Possemato et al. 2011; Tong et al. 2009). Furthermore, it was recently shown that specific metabolic pathways could act as novel regulators of myogenic differentiation with some interesting results (Bracha et al. 2010), emphasizing that this area of muscle biology is an exciting and relatively unexplored scientific niche. Therefore, further work should be conducted, perhaps by over-expression and/or knockdown of specific metabolic genes, or by pharmacological inhibition of metabolic intermediates, to elucidate the role of cellular metabolism in myogenesis. Metabolic targets need to be carefully selected, with a strong hypothesis, and the use of high throughput methods for screening metabolic targets could accelerate the identification of key metabolic regulators of myogenesis.

### *6.1.3 Regulation of the MyHC IIB gene in porcine skeletal muscle*

Utilizing the C2C12 cell line as a host environment, a molecular mechanism was identified that is responsible for the unusually high expression of the MyHC IIB isoform in porcine skeletal muscle. Pigs are physiologically similar to humans and are therefore increasingly being considered as a good animal model for studying a range of human diseases (Luo et al. 2012). However, the high level expression of MyHC IIB in porcine skeletal muscle, which is associated with a dramatically faster and more glycolytic muscle phenotype compared to that of human skeletal muscle, presents a major limitation of the pig for use as a model of human skeletal muscle biology. Therefore it is important to determine what differences exist between these species in order to have confidence in the use of the pig as a model. Furthermore, the fundamental biology responsible for the expression of the MyHC IIB gene in porcine skeletal muscle is not only physiologically interesting but also has potential implications for livestock production, growth performance and meat quality. At the initiation of the work presented herein, no mechanisms had been highlighted with regard to the species-specific expression of MyHC isoforms. However, after commencing this work, Harrison et al. (2011) reported that a single base pair difference in the mouse MyHC IIB promoter was responsible for differences in expression of MyHC IIB between mice and humans. Work presented in this thesis, comparing the pig and human MyHC IIB promoters, was continued to elucidate if a similar mechanism was responsible for the high level expression of MyHC IIB in pigs. Data presented in this thesis shows, for the first time, that a genetic difference of 3bp in the proximal MyHC IIB

promoters of pigs and humans is critical in determining the differential expression of this gene between these otherwise physiologically similar mammals. Specifically, the porcine MyHC IIB promoter is likely “hyper-responsive” (relative to humans) to factors interacting with the CArG-Ebox promoter response element region, as demonstrated by differential protein-DNA interactions in this region between the pig and human MyHC IIB promoters. The genomic mechanisms reported herein advance our biological understanding of the mechanisms dictating a physiological difference in muscle phenotype between pigs and humans. In particular, a genomic mechanism was identified controlling the expression of the MyHC IIB gene in porcine skeletal muscle, a gene that is not normally expressed in the muscles of large mammals. Data presented in this thesis therefore advances the work of Harrison et al. (2011) by elucidating a genomic mechanism regulating the MyHC IIB gene in a species that was previously unexplored. Taken together, with the work of Harrison et al. (2011), the CArG-Ebox promoter-response element region of the MyHC IIB promoter is critical in determining the strength of MyHC IIB promoter activity across multiple species, including both small rodents and large mammals. Finally, this work has provided an understanding of a mechanism responsible for a major limitation of the pig as a model of human skeletal muscle biology.

It is also noteworthy that the subtle differences in promoter sequence responsible for the large disparity in MyHC IIB promoter activity between pigs and humans highlight the potential impact of single nucleotide polymorphisms (SNP's) in non-coding, promoter regions of DNA on subsequent gene expression. Thus it is evident that SNP's in important promoter response

elements may be critical in determining the “end-point” physiology within an animal and that sequence variation in promoter regions could be causative to certain pathologies.

Future work should be focused on identifying the transcriptional regulators differentially binding at the CArG-Ebox region, which are considered fundamental to the strength of the pig and human MyHC IIB promoter activity. Unfortunately, due to technical difficulties and limited time, it was not possible to identify the specific proteins interacting with this region of DNA in this thesis. As discussed in Chapter 5, it is postulated that multiple proteins, likely involving serum response factor (SRF) and myogenic regulatory factors (MRF's), are differentially interacting in the region identified and warrants further exploration. Such a body of work (which would be technically demanding and time consuming) could elucidate binding activities of transcriptional regulators co-operatively interacting at CArG and E-boxes to further establish their complex role in regulating muscle specific gene expression and in particular, the regulation of the MyHC IIB gene.

#### *6.1.4 Final summary of novel findings from this thesis*

In conclusion, this body of work has shown, for the first time, the following:

1. The distinct mRNA expression profiles of six MyHC isoform genes during C2C12 myogenesis and importantly, that the C2C12 cell line mimics developing fast-twitch muscle fibres. These results provide useful information for future research conducted using this cell line.
2. The dynamic plasticity of the MyHC IIB gene in response to beta-adrenergic receptor stimulation in both fully differentiated adult muscle and differentiating muscle cells, highlighting a role for beta-adrenergic signaling in MyHC IIB transcriptional regulation during two developmental distinct stages of muscle growth.
3. A dramatic restructuring of metabolic gene expression during the switch from proliferating to fully differentiated C2C12 muscle cells, highlighting the requirement for future work to investigate the role of metabolism in regulating myogenic differentiation.
4. A genomic mechanism dictating the high level expression of the MyHC IIB gene in porcine skeletal muscle, identifying a molecular mechanism regulating a major physiological difference in the muscle phenotype between pigs and humans (which is important for understanding the pig as a model of human muscle biology research).

## 7. REFERENCES

- Agbulut, O., Noirez, P., Beaumont, F. and Butler-Browne, G. (2003) Myosin heavy chain isoforms in postnatal muscle development of mice. *Biol Cell* 95, 399–406
- Allen, D.L., Sartorius, C.A., Sycuro, L.K. and Leinwand, L.A. (2001) Different Pathways Regulate Expression of the Skeletal Myosin Heavy Chain Genes. *J Biol Chem* 276 (47), 43524–43533
- Allen, D.L., Weber, J.N., Sycuro, L.K. and Leinwand, L.A. (2005) Myocyte Enhancer Factor-2 and Serum Response Factor Binding Elements Regulate Fast Myosin Heavy Chain Transcription *in Vivo*. *J Biol Chem* 280 (17), 17126–17134
- Always, S.E., Degens, H., Lowe, D.A. and Krishnamurthy, G. (2002) Increased myogenic repressor Id mRNA and protein levels in hindlimb muscles of aged rats. *Am J Physiol Regul Integr Comp Physiol* 282, 411–422
- An, C.I., Ganio, E. and Hagiwara, N. (2013) Trip12, a HECT domain E3 ubiquitin ligase, targets Sox6 for proteasomal degradation and affects fiber type-specific gene expression in muscle cells. *Skeletal muscle* 3(11)
- Andersen, J.L. and Aagaard, P. (2000) Myosin heavy chain IIX overshoot in human skeletal muscle. *Muscle Nerve* 23(7), 1095–1104
- Anderson, P.T., Helferich, W.G., Parkhill, L.C., Merkel, R. and Bergen, W.G. (1990) Ractopamine Increases Total and Myofibrillar Protein Synthesis in Cultured Rat Myotubes. *J Nutr* 120, 1677–1683
- Apple, J.K., Rincker, P.J., McKeith, F.K., Carr, S.N., Armstrong, T.A. and Matzat, P.D. (2007) Review: Meta-Analysis of the Ractopamine Response in Finishing Swine. *Pro Anim Sci* 23, 179–196
- Arguello, A., Lopez-Fernandez, J. and Rivero, J.L. (2001) Limb Myosin Heavy Chain Isoproteins and Muscle Fiber Types in the Adult Goat (*Capra hircus*). *Anat Rec* 264, 284–293
- Ausoni, S., Gorza, L., Schiaffino, S., Gundersen, K. and Lomo, T. (1990) Expression of myosin heavy chain isoforms in stimulated fast and slow rat muscles. *J Neurosci* 10(1), 153–160
- Baker, D.J., Constantin-Teodosiu, D., Jones, S.W., Timmons, J.A. and Greenhaff, P.L. (2006) Chronic Treatment with the B2-Adrenoceptor Agonist Prodrug BRL-47672 Impairs Rat Skeletal Muscle Function by Inducing a Comprehensive Shift to a Faster Muscle Phenotype. *J Pharmacol Exp Ther* 319, 439–446
- Barany, M. (1967) ATPase activity of myosin correlated with speed of muscle shortening. *J Gen Physiol* 50, 197–218

- Beitzel, F., Gregorevic, P., Ryall, J.G., Plant, D.R., Sillence, M.N. and Lynch, G.S. (2004) Beta-2-Adrenoceptor agonist fenoterol enhances functional repair of regenerating rat skeletal muscle after injury. *J Appl Physiol* 96, 1385-1392
- Beitzel, F., Sillence, M.N. and Lynch, G.S. (2007) Beta-Adrenoceptor signaling in regenerating skeletal muscle after beta-agonist administration. *Am J Physiol Endocrinol Metab* 293, 932-940
- Bentzinger, C.F., Wang, Y.X. and Rudnicki, M.A. (2012) Building muscle: molecular regulation of myogenesis. *Cold Spring Harbor perspectives in biology* 4(2), a008342
- Bracha, A.L., Ramanathan, A., Huang, S., Ingber, D.E. and Schreiber, S.L. (2010) Carbon metabolism-mediated myogenic differentiation. *Nature chem biol* 6(3), 202-204
- Braun, T., Rudnicki, M.A., Arnold, H.H. and Jaenisch, R. (1992) Targeted inactivation of the muscle regulatory gene Myf-5 results in abnormal rib development and perinatal death. *Cell* 71, 369–382
- Bricout, V.A., Serrurier, B.D. and Bigard, A.X. (2004) Clenbuterol treatment affects myosin heavy chain isoforms and MyoD content similarly in intact and regenerated soleus muscles. *Acta Physiol Scand* 180, 271–280
- Brown, D.M., Parr, T. and Brameld, J.M. (2012) Myosin heavy chain mRNA isoforms are expressed in two distinct cohorts during C2C12 myogenesis. *J Muscle Res Cell Motil* 32, 383-390
- Buller, A.J., Eccles, J.C. and Eccles, R.M. (1960) Interactions between motoneurons and muscles in respect of the characteristic speeds of their responses. *J Physiol* 150, 417–439
- Burke, R.E., Levine, D.N. and Zajac, F.E. (1971) Mammalian motor units: physiological-histochemical correlation in three types in cat gastrocnemius. *Science* 174, 709 –712
- Caiozzo, V.J., Haddad, F., Baker, M.J., Herrick, R.E., Prietto, N. and Baldwin, K.M. (1996) Microgravity-induced transformations of myosin isoforms and contractile properties of skeletal muscle. *J Appl Physiol* 81(1), 123-132
- Catala, F., Wanner, R., Barton, P., Cohen, A., Wright, M. and Buckingham, M. (1995) A Skeletal Muscle-Specific Enhancer Regulated by Factors Binding to E and CArG Boxes Is Present in the Promoter of the Mouse Myosin Light-Chain 1A Gene. *Mol Cell Biol* 15, 4585–4596
- Cerny, L.C. and Bandman, E. (1986) Contractile activity is required for the expression of neonatal myosin heavy chain in embryonic chick pectoral muscle cultures. *J Cell Biol* 103 (6), 2153-2161



- Chikuni, K., Muroya, S. and Nakajima, I. (2004) Myosin heavy chain isoforms expressed in bovine skeletal muscles. *Meat Sci* 67, 87-94
- Chung, S., Arrell, D.K., Faustino, R.S., Terzic, A. and Dzeja, P. (2010) Glycolytic network restructuring integral to the energetics of embryonic stem cell cardiac differentiation. *J Mol Cell Cardio*, 48: 725–734
- Clower, C.V., Chatterjee, D., Wang, Z., Cantley, L.C., Vander Heiden, M.G. and Krainer, A.R. (2010) The alternative splicing repressors hnRNP A1/A2 and PTB influence pyruvate kinase isoform expression and cell metabolism. *Proc Natl Acad Sci* 107(5), 1894-1899
- D'Antona, G., Lanfranconi, F., Pellegrino, M.A., Brocca, L., Adami, R., Rossi, R., et al. (2006) Skeletal muscle hypertrophy and structure and function of skeletal muscle fibres in male body builders. *J Physiol* 570.3, 611–627
- Da costa, N., Edgar, J., Ooi, P.T., Su, Y., Meissner, J.D. and Chang, K.C. (2007) Calcineurin differentially regulates fast myosin heavy chain genes in oxidative muscle fibre type conversion. *Cell Tissue Res* 329, 515-527
- David, C.J., Chen, M., Assanah, M., Canoll, P. and Manley, J.L. (2010) HnRNP proteins controlled by c-Myc deregulate pyruvate kinase mRNA splicing in cancer. *Nature* 463(7279), 364–368
- Davis, R.L., Weintraub, H. and Lassar, A.B. (1987) Expression of a single transfected cDNA converts fibroblasts to myoblasts. *Cell* 51, 987–1000
- Delbono, O. (2010) Myosin – still a good reference for skeletal muscle fibre classification? *J Physiol* 588.1, 9
- Demirel, H.A., Powers, S.K., Naito, H., Hughes, M. and Coombes, J. S. (1999) Exercise-induced alterations in skeletal muscle myosin heavy chain phenotype: dose-response relationship. *J Appl Physiol* 86(3), 1002-1008
- Depreux, F.F.S., Grant, A.L., Anderson, D.B. and Gerrard, D.E. (2002) Paylean alters myosin heavy chain isoform content in pig muscle. *J Anim Sci* 80, 1888-1894
- Ekmark, M., Rana, Z.A., Stewart, G., Hardie, D.G. and Gundersen, K. (2007) De-phosphorylation of MyoD is linking nerve-evoked activity to fast myosin heavy chain expression in rodent adult skeletal muscle. *J Physiol* 584(2), 637–650
- Elkalaf, M., Anděl, M. and Trnka, J. (2013) Low Glucose but Not Galactose Enhances Oxidative Mitochondrial Metabolism in C2C12 Myoblasts and Myotubes. *PloS one* 8(8), e70772
- Fahey, A.J., Brameld, J.M., Parr, T. and Buttery, P.J. (2005) Ontogeny of factors associated with proliferation and differentiation of muscle in the ovine fetus. *J Anim Sci* 83, 2330–2338

Gambke, B., Lyons, G.E., Haselgrove, J., Kelly, A.M. and Rubinstein, N.A. (1983) Thyroidal and neural control of myosin transitions during development of rat fast and slow muscles. *FEBS Lett* 156, 335–339

Gatenby, R.A. and Gillies, R.J. (2004) Why do cancers have high aerobic glycolysis? *Nat Rev Cancer* 4, 891–899

Gayraud-Morel, B., Chrétien, F., Flamant, P., Gomès, D., Zammit, P.S. and Tajbakhsh, S. (2007) A role for the myogenic determination gene *Myf5* in adult regenerative myogenesis. *Dev Biol* 312, 13–28

Giger, J., Qin, A.X., Bodell, P.W., Baldwin, K.M. and Haddad, F. (2007) Activity of the  $\beta$ -myosin heavy chain antisense promoter responds to diabetes and hypothyroidism. *Am J Physiol Heart Circ Physiol* 292, 3065–3071

Gorza, L. (1990) Identification of a Novel Type 2 Fiber Population in Mammalian Skeletal Muscle by Combined Use of Histochemical Myosin ATPase and Anti-myosin Monoclonal Antibodies. *J Histochem Cytochem* 38, 257–265

Grant, A.L., Helferich, W.G., Merkel R.A. and Bergen, W.G. (1990) Effects of phenethanolamines and propranolol on the proliferation of cultured chick breast muscle satellite cells. *J Anim Sci* 68, 652–658

Grifone, R., Laclef, C., Spitz, F., Lopez, S., Demignon, J., Guidotti, J., Kawakami, K., Xu, P., Kelly, R., Petrof, B.J., Daegelen, D., Concordet, J. and Marie, P. (2004) *Six1* and *Eya1* Expression Can Reprogram Adult Muscle from the Slow-Twitch Phenotype into the Fast-Twitch Phenotype. *Mol Cell Biol* 24, 6253–6267

Groisman, R., Masutani, H., Leibovitch, M., Robin, P., Soudant, I., Trouche, D. and Harel-Bellan, A. (1996) Physical Interaction between the Mitogen-responsive Serum Response Factor and Myogenic Basic-Helix-Loop-Helix Proteins. *J Biol Chem* 271, 5258–5264

Gunawan, A.M., Richert, B.T., Schinckel, A.P., Grant, A.L. and Gerrard, D.E. (2007) Ractopamine induces differential gene expression in porcine skeletal muscles. *J Anim Sci* 85, 2115–2124

Haddad, F., Qin, A.X., Bodell, P.W., Jiang, W., Giger, J.M. and Baldwin, K.M. (2008) Intergenic transcription and developmental regulation of cardiac myosin heavy chain genes. *Am J Physiol -Heart C* 294(1), H29–H40

Harrison, B.C., Allen, D.L. and Leinwand, L.A. (2011) *IIf* or not *IIf*? Regulation of myosin heavy chain gene expression in mice and men. *Skeletal Muscle* 1(5), 1–9

Hasty, P., Bradley, A., Morris, J.H., Edmondson, D.H., Venuti, J.M., Olson, E.N. and Klein, W.H. (1993) Muscle deficiency and neonatal death in mice with a targeted mutation in the myogenin gene. *Nature* 364, 501–506

- Heanue, T.A., Reshef, R., Davis, R.J, Mardon, G., Oliver, G. and Tomarev, S. (1999) Synergistic regulation of vertebrate muscle development by Dach2, Eya2, and Six1, homologs of genes required for Drosophila eye formation. *Genes Dev* 13, 3231-3243
- Hemmings, K.M., Parr, T., Daniel, Z.C.T.R., Picard, B., Buttery, P.J. and Brameld, J.M. (2009) Examination of myosin heavy chain isoform expression in ovine skeletal muscles. *J. Anim. Sci.* 87, 3915–3922
- Hill, A.V. (1950) The dimensions of animals and their muscular dynamics. *Sci Prog* 38, 209–230
- Hughes, S.M., Taylor, J.M., Tapscott, S.J., Gurley, C.M., Carter, W.J. and Peterson, C.A. (1993) Selective accumulation of MyoD and Myogenin mRNAs in fast and slow adult skeletal muscle is controlled by innervation and hormones. *Development* 118, 1137-1147
- Hurley, M.S., Flux, C., Salter, A.M. and Brameld, J.M. (2006) Effects of fatty acids on skeletal muscle differentiation *in vitro*. *Br J Nutr* 95, 623-630
- Jang, Y.N. and Baik, E.J. (2013) JAK-STAT pathway and myogenic differentiation. *JAK-STAT*, 2(2)
- Jones, S.W., Baker, D.J., Gardiner, S.M., Bennett, T., Timmons, J.A. and Greenhaff, P.L. (2004) The Effect of the Beta-2-Adrenoceptor Agonist Prodrug BRL-47672 on Cardiovascular Function, Skeletal Muscle Myosin Heavy Chain, and MyoD Expression in the Rat. *J Pharm Exp Therap* 311(3), 1225-1231
- Kawakami, K., Sato, S., Ozaki, H. and Ikeda, K. (2000) Six family genes - structure and function as transcription factors and their roles in development. *BioEssays* 22, 616-626
- Kitzmann, M., Carnac, G., Vandromme, M., Primig, M., Lamb, N.J.C. and Fernandez, A. (1998) The Muscle Regulatory Factors MyoD and Myf-5 Undergo Distinct Cell Cycle-specific Expression in Muscle Cells. *J Cell Biol* 142(6), 1447–1459
- Kline, W.O., Panaro, F.J., Yang, H. and Bodine, S.C. (2007) Rapamycin inhibits the growth and muscle-sparing effects of clenbuterol. *J Appl Physiol* 102, 740-747
- Klitgaard, H., Mantoni, M., Schiaffino, S., Ausoni, S., Gorza, L., Laurent-Winter, C., Schnohr, P., Saltin, B. (1990) Function, morphology and protein expression of ageing skeletal muscle: a cross-sectional study of elderly men with different training backgrounds. *Acta Physiol Scand* 140, 41–54

- Konopka, A.R., Trappe, T.A., Jemiolo, B., Trappe, S.W. and Harber, M.P. (2011) Myosin heavy chain plasticity in aging skeletal muscle with aerobic exercise training. *The Journals of Gerontology Series A: Biological Sciences and Medical Sciences* 66(8), 835-841
- Koopman, R., Gehrig, S.M., Leger, B., Trieu, J., Walrand, S., Murphy, K.T. et al. (2010) Cellular mechanisms underlying temporal changes in skeletal muscle protein synthesis and breakdown during chronic  $\beta$ -adrenoceptor stimulation in mice. *J Physiol* 588, 4811-4823
- Lakich, M.M., Diagana, T.T., North, D.L. and Whalen, R.G. (1998) MEF-2 and Oct-1 Bind to Two Homologous Promoter Sequence Elements and Participate in the Expression of a Skeletal Muscle-specific Gene. *J Biol Chem* 273 (24), 15217–15226
- Langley, B., Thomas, M., Bishop, A., Sharma, M., Gilmour, S. and Kambadur, R. (2002) Myostatin inhibits myoblast differentiation by down-regulating MyoD expression. *J Biol Chem* 277(51), 49831-49840
- Larsson, L., Müller, U., Li, X. and Schiaffino, S. (1995) Thyroid hormone regulation of myosin heavy chain isoform composition in young and old rats, with special reference to IIX myosin. *Acta Physiol Scand* 153(2), 109-116
- Lefaucheur, L. (2010) A second look into fibre typing – Relation to meat quality. *Meat Sci* 84, 257-270
- Lefaucheur, L., Hoffman, R.K., Gerrard, D.E., Okamura, C.S., Rubinstein, N. and Kelly, A. (1998) Evidence for Three Adult Fast Myosin Heavy Chain Isoforms in Type II Skeletal Muscle Fibers in Pigs. *J Anim Sci* 76, 1584–1593
- Lefaucheur, L., Milan, D., Ecolan, P. and Le Callennec, C. (2004) Myosin heavy chain composition of different skeletal muscles in Large White and Meishan pigs. *Anim Sci* 82, 1931-1941
- Lin, J., Wu, H., Tarr, P.T., Zhang, C., Wu, Z., Boss, O., Michael, L.F., Puigserver, P., Isotani, E., Olson, E.N., Lowell, B.B., Bassel-Dubyk, R. and Spiegelman, B.M. (2002) Transcriptional co-activator PGC-1 $\alpha$  drives the formation of slow-twitch muscle fibres. *Nature* 418, 797-801
- Loughna, P.T., Izumo, S., Goldspink, G. and Nadal-Ginard, B. (1990) Disuse and passive stretch cause rapid alteration in expression of developmental and adult contractile protein genes in skeletal muscle. *Development* 109, 217–23
- Lucas, C.A., Kang, L.H.D. and Hoh, J.F.Y. (2000) Monospecific Antibodies against the Three Mammalian Fast Limb Myosin Heavy Chains. *Biochem Bioph Res Co* 272, 303-308

- Lunde, I.G., Ekmark, M., Rana, Z.A., Buonanno, A. and Gundersen, K. (2007) PPAR $\delta$  expression is influenced by muscle activity and induces slow muscle properties in adult rat muscles after somatic gene transfer. *J Physiol* 582.3, 1277–1287
- Lunt, S.Y. and Vander Heiden, M.G. (2011) Aerobic Glycolysis: Meeting the Metabolic Requirements of Cell Proliferation. *Annu Rev Cell Dev Biol* 27, 441-464
- Luo, Y., Lin, L., Bolund, L., Jensen, T.G. and Sorensen, C.B. (2012) Genetically modified pigs for biomedical research. *J Inherit Metab Dis* 35, 695-713
- Luther, H.P., Haase, H., Hohaus, A., Beckmann, G., Reich, J. and Morano, I. (1998) Characterization of Naturally Occurring Myosin Heavy Chain Antisense mRNA in Rat Heart. *J Cell Biochem* 70, 110–120
- Lyons, G.E., Ontell, M., Cox, R., Sassoon, D. and Buckingham, M. (1990) The expression of myosin genes in developing skeletal muscle in the mouse embryo. *J Cell Biol* 111, 1465–76
- Lyssiotis, C.A., Anastasiou, D., Locasale, J.W., Vander Heiden, M.G., Christofk, H.R. and Cantley, L.C. (2012) Cellular Control Mechanisms that Regulate Pyruvate Kinase M2 Activity and Promote Cancer Growth. *Biomed Res* 23, SI 213-217
- Matsakas, A., Mouisel, E., Amthor, H. and Patel, K. (2010) Myostatin knockout mice increase oxidative muscle phenotype as an adaptive response to exercise. *J Muscle Res Cell Motil* 31, 111-125
- McCall, G.E., Haddad, F., Roy, R.R., Zhong, H., Edgerton, V.R. and Baldwin, K.M. (2009) Transcriptional regulation of the myosin heavy chain IIb gene in inactive rat soleus. *Muscle Nerve* 40(3), 411-419
- McFarland, D.C., Pesall, J.E., Gilkerson, K.K., Ye, W.V., Walker, J.S., Wellenreiter, R. (1995) Comparison of *in vitro* properties of satellite cells derived from the pectoralis major and biceps femoris muscles of growing turkeys. *Basic Appl Myol* 95(1), 27-31
- McMillan, D.N., Noble, B.S. and Maltin, C.A. (1992) The effect of the beta-adrenergic agonist clenbuterol on growth and protein metabolism in rat muscle cell cultures. *J Anim Sci* 70, 3014-3023
- Miano, J.M. (2003) Serum response factor: toggling between disparate programs of gene expression. *J Mol Cell Cardiol* 35, 577-593
- Miller, J.B. (1990) Myogenic programs of mouse muscle cell lines: expression of myosin heavy chain isoforms, myoD1, and myogenin. *J Cell Biol* 111, 1149-1159

Nabeshima, Y., Hanaoka, K., Hayasaka, M., Esumi, E., Li, S., Nonaka, I. and Nabeshima, Y.I. (1993) Myogenin gene disruption results in perinatal lethality because of severe muscle defect. *Nature* 364, 532-535

Narkar, V.A., Downes, M., Yu, R.T., Embler, E., Wang, Y., Banayo, E., Mihaylova, M.M., Nelson, M.C., Zou, Y., Juguilon, H., Kang, H., Shaw, R.J. and Evans, R.M. (2008) AMPK and PPAR $\alpha$  Agonists Are Exercise Mimetics. *Cell* 134, 405-415

Narkar, V.A., Fan, W., Downes, M., Yu, R.T., Jonker, J.W., Alaynick, W.A., Banayo, E., Karunasiri, M.S., Lorca, S. and Evans, R.M. (2011) Exercise and PGC-1 $\alpha$ -Independent Synchronization of Type I Muscle Metabolism and Vasculature by ERR $\alpha$ . *Cell Metab* 13, 283-293

Needham, D.M. (1926) Red and white muscles. *Physiol Rev* 6, 1-27

Oishi, Y., Imoto, K., Ogata, T., Taniguchi, K., Matsumoto, H. and Roy, R.R. (2002) Clenbuterol induces expression of multiple myosin heavy chain isoforms in rat soleus fibres. *Acta Physiol Scand* 176, 311-318

Pandorf, C.E., Haddad, F., Roy, R.R., Qin, A.X., Edgerton, V.R. and Baldwin, K.M. (2006) Dynamics of Myosin Heavy Chain Gene Regulation in Slow Skeletal Muscle - Role of Natural Antisense RNA. *J Biol Chem* 281(50), 38330-38342

Pellegrino, M.A., Canepari, M., Rossie, R., D'Antona, G., Reggiani, C. and Bottinelli, R. (2003) Orthologous myosin isoforms and scaling of shortening velocity with body size in mouse, rat, rabbit and human muscles. *J Physiol* 546.3, 677-689

Pfeiffer, T., Schuster, S. and Bonhoeffer, S. (2001) Cooperation and Competition in the Evolution of ATP-Producing Pathways. *Science* 292, 504-507

Possemato, R., Mark, K.M., Shaul, Y.D., Pacold, M.E., Kim, D., Birsoy, K., et al. (2011) Functional genomics reveal that the serine synthesis pathway is essential in breast cancer. *Nature* 476(7360), 346-350

Powers, S.K. and Howley, E.T. (2007) *Exercise Physiology: Theory and Application to Fitness and Performance*. Sixth Edition. Mc Graw Hill, New York

Ranvier, L. (1874) De quelques faits relatifs a l'histologie et a la physiologie des muscles stries. *Archives de Physiologie normale et Pathologique* 6, 1-15

Rennie, M.J., Selby, A., Atherton, P., Smith, K., Kumar, V., Glover, E.L. and Philips, S.M. (2010) Facts, noise and wishful thinking: muscle protein turnover in aging and human disuse atrophy. *Scand J Med Sci Sports* 20, 5-9

- Rhinn, H., Scherman, D. and Escric, V. (2008) One-step quantification of single-stranded DNA in the presence of RNA using Oligreen in a real-time polymerase chain reaction thermocycler. *Anal Biochem* 372, 116-118
- Rinaldi, C., Haddad, F., Bodell, P.W., Qin, A.X., Jiang, W. and Baldwin, K.M. (2008) Intergenic bidirectional promoter and cooperative regulation of the IIX and IIB MHC genes in fast skeletal muscle. *Am J Physiol –Reg I* 295(1), R208-R218
- Rivero, J.L., Serrano, A.L., Barrey, E., Valette, J.P. and Jouglin, M. (1999) Analysis of myosin heavy chains at the protein level in horse skeletal muscle. *J Muscle Res Cell Motil* 20, 211-221
- Rudnicki, M.A., Braun, T., Hinuma, S. and Jaenisch, R. (1992) Inactivation of MyoD in mice leads to up-regulation of the myogenic HLH gene Myf-5 and results in apparently normal muscle development. *Cell* 71, 383–390
- Rudnicki, M.A., Schnegelsberg, P.N., Stead, R.H., et al. (1993) MyoD or Myf-5 is required for the formation of skeletal muscle. *Cell* 75, 1351–1359
- Russell, S.D., Cambon, N., Nadal-Ginard, B. and Whalen, R.G. (1988) Thyroid hormone induces a nerve-independent precocious expression of fast myosin heavy chain mRNA in rat hindlimb skeletal muscle. *J Biol Chem* 263(13), 6370-6374
- Ruusunen, M. and Puolanne, E. (2004) Histochemical properties of fibre types in muscles of wild and domestic pigs and the effect of growth rate on muscle fibre properties. *Meat Sci* 67, 533-539
- Ryall, J.G. (2013) Metabolic reprogramming as a novel regulator of skeletal muscle development and regeneration. *FEBS J* 280(17), 4004-4013
- Ryall, J.G., Gregorevic, P., Plant, D.R., Sillence, M.N. and Lynch, G.S. (2002) Beta-2-Agonist fenoterol has greater effects on contractile function of rat skeletal muscles than clenbuterol. *Am J Physiol Regul Integr Comp Physiol* 283, 1386-1394
- Ryall, J.G., Plant, D.R., Gregorevic, P., Sillence, M.N. and Lynch, G.S. (2004) Beta-2-Agonist administration reverses muscle wasting and improves muscle function in aged rats. *J physiol* 555(1), 175-188
- Ryan, K.J., Daniel, Z.C.T.R., Craggs, L.J., Parr, T. and Brameld, J.M (2013) Dose-dependent effects of vitamin D on transdifferentiation of skeletal muscle cells to adipose cells. *J Endocrinol* 217(1), 45-58
- Sabourin, L.A. and Rudnicki, M.A. (2000) The molecular regulation of myogenesis. *Clin Genet* 57(1), 16–25

Sabourin, L.A., Girgis-Gabardo, A., Seale, P., Asakura, A. and Rudnicki, M.A. (1999) Reduced Differentiation Potential of Primary MyoD <sup>-/-</sup> Myogenic Cells Derived from Adult Skeletal Muscle. *J Cell Biol* 144 (4), 631–643

Schiaffino, S. (2010) Fibre types in skeletal muscle: a personal account. *Acta Physiol* 199, 451–463

Schiaffino, S. and Reggiani, C. (2011) Fibre Types in Mammalian Skeletal Muscles. *Physiol Rev* 91, 1447-1531

Shanely, R.A., Zwetsloot, K.A., Childs, T.E., Lees, S.J., Tsika, R.W. and Booth, F.W. (2009) IGF-I activates the mouse type IIb myosin heavy chain gene. *Am J Physiol -Cell Ph* 297(4), C1019-C1027

Sharples, A.P., Al-Shanti, N. and Stewart, C.E. (2010) C2 and C2C12 murine skeletal myoblast models of atrophic and hypertrophic potential: relevance to disease and ageing? *Journal of cellular physiology* 225(1), 240-250

Shi, H., Zeng, C., Ricome, A., Hannon, K.M., Grant, A.L. and Gerrard, D.E. (2007) Extracellular signal-regulated kinase pathway is differentially involved in beta-agonist-induced hypertrophy in slow and fast muscles. *Am J Physiol Cell Physiol* 292, 1681-1689

Shyh-Chang, N., Daley, G.Q. and Cantley, L.C. (2013) Stem cell metabolism in tissue development and aging. *Dev* 140, 2535-2547

Silberstein, L., Webster, S.G., Travis, M. and Blau, H.M., (1986) Developmental progression of myosin gene expression in cultured muscle cells. *Cell* 46(7), 1075-1081

Sillence, M.N. (2004) Technologies for the control of fat and lean deposition in livestock. *Vet J* 167, 242-257

Smerdu, V., Karsch-Mizrachi, I., Campione, M., Leinwand, L. and Schiaffino, S. Type IIx myosin heavy chain transcripts are expressed in type IIb fibers of human skeletal muscle. *Am J Physiol* 267, 1723-1728

Spangenburg, E.E. and Booth, F.W. (2003) Molecular regulation of individual skeletal muscle fibre types. *Acta Physiol Scand* 178, 413–424

Spitz, F., Demignon, J., Porteu, A., Kahn, A., Concordet, J.P., Daegelen, D., et al. (1998) Expression of myogenin during embryogenesis is controlled by Six/sine oculis homeoproteins through a conserved MEF3 binding site. *Dev Biol* 95, 14220-14225

Stephenson, G.M., (2001) Hybrid skeletal muscle fibres: a rare or common phenomenon? *Clin Exp Pharmacol P* 28, 692–702

Swoap, S.J. (1998) *In vivo* analysis of the myosin heavy chain IIB promoter region. *Am J Physiol* 274, 681–687



- Takeda, S., North, D.L., Diagana, T., Miyagoe, Y., Lakich, M.M. and Whalen, R.G. (1995) Myogenic regulatory factors can activate TATA-containing promoter elements via an E-box independent mechanism. *J Biol Chem* 270, 15664-15670
- Takeda, S., North, D.L., Lakich, M.M., Russell, S.D. and Whalen, R.G. (1992) A possible regulatory role for conserved promoter motifs in an adult-specific muscle myosin gene from mouse. *J Biol Chem* 267(24), 16957-16967
- Talmadge, R.J., Grossman, E.J. and Roy, R.R. (1996) Myosin heavy chain composition of adult feline (*Felis catus*) limb and diaphragm muscles. *J Exp Zool* 15, 413-420
- Thomas, M., Langley, B., Berry, C., Sharma, M., Kirk, S., Bass, J. and Kambadur, R. (2000) Myostatin, a negative regulator of muscle growth, functions by inhibiting myoblast proliferation. *J Biol Chem* 275(51), 40235-40243
- Tong, X., Zhao, F., Mancuso, A., Gruber, J.J. and Thompson, C.B. (2009) The glucose-responsive transcription factor ChREBP contributes to glucose-dependent anabolic synthesis and cell proliferation. *Proc Natl Acad Sci* 106(51), 21660-21665
- Tonge, D.P., Jones, S.W., Bardsley, R.G. and Parr, T. (2010) Methodology article Characterisation of the sarcomeric myosin heavy chain multigene family in the laboratory guinea pig. *BMC Mol Biol* 11(52)
- Toniolo, L., Maccatrozzo, L., Patrino, M., Pavan, E., Caliaro, F., Rossi, R., Rinaldi, C., Canepari, M., Reggiani, C. and Marscarello, F. (2007) Fiber types in canine muscles: myosin isoform expression and functional characterization. *Am J Physiol Cell Physiol* 292, 1915-1926
- Ustanina, S., Carvajal, J., Rigby, P. and Braun, T. (2007) The Myogenic Factor Myf5 Supports Efficient Skeletal Muscle Regeneration by Enabling Transient Myoblast Amplification. *Stem Cells* 25, 2006 –2016
- Van Rooij, E., Liu, N. and Olson, E. N. (2008) MicroRNAs flex their muscles. *Trends Genet* 24(4), 159-166
- Van Rooij, E., Quiat, D., Johnson, B.A., Sutherland, L.B., Qi, X., Richardson, J.A. and Olson, E.N. (2009) A family of microRNAs encoded by myosin genes governs myosin expression and muscle performance. *Dev cell* 17(5), 662-673
- Vestergaard, M., Henckel, P., Oksbjerg, N. and Sejrsen, K. (1994) The effect of cimaterol on muscle fiber characteristics, capillary supply, and metabolic potentials of longissimus and semitendinosus muscles from young Friesian bulls. *J Anim Sci* 72, 2298-2306

- Voytik, S.L., Przyborski, M., Badylak, S.F. and Konieczny, S.F. (1993) Differential Expression of Muscle Regulatory Factor Genes in Normal and Denervated Adult Rat Hindlimb Muscles. *Dev Dynam* 198, 214-224
- Wada, M., Hamalainen, N. and Pette, D. (1995) Isomyosin patterns of single type IIB, IID and IIA fibres from rabbit skeletal muscle. *J Muscle Res Cell Motil* 16, 237-242
- Wang, Y., Zhang, C., Yu, R.T., Cho, H.K., Nelson, M.C., Bayuga-Ocampo, C.R., et al. (2004) Regulation of Muscle Fiber Type and Running Endurance by PPAR $\delta$ . *PLoS Biol* 2(10), 1532-1539.
- Weiss, A. and Leinwand, L.A. (1996) The Myosin Heavy Chain Gene Family. *Annu Rev Cell Dev Biol* 12, 417-39
- Weiss, A., Schiaffino, S. and Leinwand, L.A. (1999) Comparative sequence analysis of the complete human sarcomeric myosin heavy chain family: Implications for functional diversity. *J Mol Biol* 290, 61-75
- Weydert, A., Barton, P., Harris, J.A., Pinset, C. and Buckingham, M. (1987) Developmental pattern of mouse skeletal myosin heavy chain gene transcripts *in vivo* and *in vitro*. *Cell* 49, 121-29
- Wheeler, M.T., Snyder, E.C., Patterson, M.N. and Swoap, S.J. (1999) An E-box within the MHC IIB gene is bound by MyoD and is required for gene expression in fast muscle. *Am J Physiol* 276, 1069-1078
- Wimmers, K., Ngu, N.T., Jennen, D.G.J., Tesfaye, D., Murani, E., Schellander, K. and Ponsuksili, S. (2008) Relationship between myosin heavy chain isoform expression and muscling in several diverse pig breeds. *J Anim Sci* 86, 795-803
- Wright, C.R., Brown, E.L., Della-Gatta, P.A., Ward, A.C., Lynch, G.S. and Russell, A.P. (2014) G-CSF does not influence C2C12 myogenesis despite receptor expression in healthy and dystrophic skeletal muscle. *Front in physiol* 5, 170
- Wright, W.E., Sassoon, D.A. and Lin, V.K. (1989) Myogenin, a factor regulating myogenesis, has a domain homologous to myoD. *Cell* 56, 607-617
- Yaffe, D. (1968) Retention of differentiation potentialities during prolonged cultivation of myogenic cells. *Proc Natl Acad Sci* 61, 477-483
- Yang, M., Wei, D., Mo, C., Zhang, J., Wang, X., Han, X., Wang, Z. and Xiao, H. (2013) Saturated fatty acid palmitate-induced insulin resistance is accompanied with myotube loss and the impaired expression of health benefit myokine genes in C2C12 myotubes. *Lipids Health Dis* 12, 104
- Zhou, Y., Liu, D. and Kaminski, H.J. (2010) Myosin Heavy Chain Expression in Mouse Extraocular Muscle: More Complex Than Expected. *Invest Ophthalmol Vis Sci* 51 (12), 6355-6363

Zu, X.L. and Guppy, M. (2004) Cancer metabolism: facts, fantasy, and fiction.  
Biochem Bioph Res Co 313, 459-465